A Convex Decomposition Perspective on Dynamic Bandwidth Allocation and Applications

Ph.D. Dissertation by

Antoni Morell Pérez
E-mail: antoni.morell@uab.cat

Thesis Advisor: Dr. Gonzalo Seco Granados
Department of Telecommunications and Systems Engineering
Universitat Autònoma de Barcelona (UAB)

7 July, 2008

Universitat Politècnica de Catalunya (UPC)
Departament de Teoria del Senyal i Comunicacions (TSC)

To my parents and Eva,

To Pau and Kim,

"Imagination is more important than knowledge",
Albert Einstein

Abstract

Traditionally, multiple access schemes in multi-user communications systems have been designed either connection-oriented or traffic-oriented. In the first ones, the goal was to provide as many orthogonal channels as possible, each one serving a different connection. That is the motivation of the so-called FDMA, TDMA and CDMA solutions. On the other hand, random access techniques, which started with the so-called ALOHA protocol, aim to statistically multiplex a shared communication medium by means of exploiting the random and bursty nature of transmission needs in data networks. Most of the multiple access solutions can be interpreted according to that classification or as a combination of those approaches. Notwithstanding, modern systems, such as the digital satellite communications standard DVB-RCS or the broadband wireless access WiMAX, have implemented a multiple access technique where users request for transmission opportunities and receive grants from the network, therefore requiring dynamic bandwidth allocation techniques.

The concept of dynamic bandwidth allocation is wide and involves a number of physical and link layer variables, configurations and protocols. In this Ph.D. dissertation we first explore the mathematical foundation that is required to coordinate the distinct layers of the OSI protocol stack and the distinct nodes within the network. We talk about decomposition techniques focused on the resolution of convex programs, which have elegantly solved many problems in the signal processing and communications fields during the last years. Known schemes are reviewed and a novel decomposition methodology is proposed. Thereafter, we compare the four resulting strategies, each one having its own particular signalling needs, which results in distinct cross-layer interactions or signalling protocols at implementation level. The results in terms of iterations required to converge are favourable to the proposed method, thus opening a new line of research.

Finally, we contribute with two practical application examples in the DVB-RCS and WiMAX systems. First, we formulate the dynamic bandwidth allocation problem that is derived from the multiple access schemes of both systems. Thereafter, the resulting Network Utility Maximization (NUM) based problem is solved by means of the previous decomposition mechanisms. The goal is to guarantee fairness among the users at the same time that Quality of Service (QoS) is preserved. In order to achieve that, we choose adequate utility functions that allow to balance the allocation towards the most priority traffic flows under a common fairness framework. We show that in the scenarios considered, the novel proposed coupled-decomposition method reports significant gains since it reduces significantly the iterations required (less iterations implies less signalling) or it reduces the time needed to obtain the optimal allocation when it is centrally computed (more users can be managed). We further show the advantages of cross-layer interactions with the physical and upper layers, which allow to benefit from more favourable adjustments of the transmission parameters and to consider the QoS requirements at upper layers.

In general, an efficient implementation of dynamic bandwidth allocation techniques in Demand Assignment Multiple Access (DAMA) schemes may report significant performance gains but it requires proper coordination among system layers and network nodes, which is attained thanks to decomposition techniques. Each new scenario and system adds another optimization challenge and, as far as we are able to coordinate all the variables in the system towards that optimal point, the highest will be the revenue.

Resumen

Tradicionalmente, las técnicas de acceso múltiple en sistemas comunicaciones multi-usuario han sido desarrolladas o bien orientadas a conexión o bien orientadas al tráfico. En el primer caso, el objetivo es establecer tantos canales ortogonales como sea posible con el fin de asignarlos a los usuarios. Esta idea motivó el diseño de las estrategias más conocidas, como son FDMA, TDMA y CDMA. Por otro lado, los métodos de acceso aleatorio que tuvieron sus inicios en el famoso ALOHA pretenden compartir estadísticamente un mismo medio de comunicación sacando provecho de la necesidad de transmitir la información en ráfagas, caso habitual en las redes de datos. De este modo, muchos de los sistemas actuales se pueden enmarcar dentro de dicha clasificación si además tenemos en cuenta posibles soluciones híbridas. No obstante, sistemas modernos como el DVB-RCS en el entorno de las comunicaciones digitales por satélite o WiMAX en el acceso terrestre de banda ancha han implementado mecanismos de petición y asignación de recursos, los cuales requieren de una gestión dinámica de éstos en el sistema (a lo que llamamos distribución dinámica del ancho de banda en sentido amplio).

El concepto anterior incluye múltiples variables, configuraciones y protocolos tanto de capa física como de capa de enlace. En esta tesis se exploran en primer lugar las bases matemáticas que permiten coordinar las distintas capas de la división OSI de los sistemas y los diferentes nodos dentro de la red. Nos referimos a las técnicas de descomposición centradas en problemas de descomposición convexos, los cuales han aportado, durante los últimos años, soluciones elegantes a muchos problemas dentro de los campos del procesado de la señal y las comunicaciones. Revisamos los esquemas conocidos y proponemos una nueva metodología. Acto seguido, se comparan las distintas posibilidades de descomposición, cada una de las cuales implica distintas formas de establecer la señalización. En la práctica, son dichas descomposiciones las que dan lugar a las diferentes interacciones entre capas o los protocolos de control entre los elementos de red. Los resultados en cuanto a número de iteraciones necesarias para llegar a la solución óptima son favorables al método propuesto, el cual abre nuevas líneas de investigación.

Finalmente, se contribuye también con ejemplos de aplicación, en DVB-RCS y en WiMAX. Planteamos el problema de gestión de recursos resultante del acceso múltiple dispuesto en cada uno de los sistemas como un problema de maximización de utilidad de red (conocido como NUM en la bibliografía) y los solucionamos aplicando las técnicas anteriores. El objetivo será garantizar la equidad entre los usuarios y preservar, al mismo tiempo, su calidad de servicio. Para conseguirlo se deben seleccionar funciones de utilidad adecuadas que permitan balancear la asignación de recursos hacia los servicios más prioritarios. Mostraremos como en los escenarios considerados, el uso del método propuesto conlleva ganancias significativas en términos de iteraciones necesarias en el proceso (y por lo tanto, menos señalización) o bien menos tiempo de cálculo en un enfoque centralizado (que se traduce en la posibilidad de incluir más usuarios). También se muestran las ventajas de considerar interacciones entre capas, ya que se pueden

ajustar los parámetros de capa física con el objetivo de favorecer los tráficos más prioritarios o bien extraer los requerimentos de servicio de valores típicamente disponibles en capas superiores.

En general, la implementación eficiente de técnicas de gestión dinámica de recursos en el acceso múltiple de los sistemas puede aportar ganancias importantes pero necesita de una buena coordinación entre capas y elementos de red. La herramienta matemática que lo hace posible está en las técnicas de descomposición. Cada nuevo escenario y sistema introduce un nuevo reto de optimización y la capacidad de guiar las variables del sistema hacia el punto óptimo de trabajo es lo que determinará su rendimiento global.

Resum

Tradicionalment, les tècniques d'accés múltiple en sistemes de comunicacions multi-usuari han estat desenvolupades o bé orientades a la connexió o bé orientades al tràfic. En el primer cas, l'objectiu és establir tants canals ortogonals com sigui possible per tal d'assignar-los als usuaris. Aquesta idea va motivar el disseny de les estratègies més conegudes, com són FDMA, TDMA i CDMA. Per altra banda, però, els mètodes d'accés aleatori que s'iniciaren amb el conegut ALOHA pretenen compartir estadísticament un mateix medi de comunicació aprofitant la necessitat de transmetre la informació a ràfegues que s'origina en les xarxes de dades. Així, molts dels actuals sistemes es poden encabir dins d'aquest esquema si a més a més, tenim en compte combinacions d'aquestes. No obstant, sistemes moderns com el DVB-RCS en l'entorn de comunicacions digitals per satèl·lit o el WiMAX en l'accés terrestre de banda ampla implementen mecanismes de petició i assignació de recursos, els quals requereixen una gestió dinàmica d'aquests en el sistema (és el que s'anomena distribució dinàmica de l'amplada de banda en un sentit ampli).

L'anterior concepte inclou múltiples variables, configuracions i protocols tant de capa física com de capa d'enllaç. En aquesta tesi s'exploren en primer lloc les bases matemàtiques que permeten coordinar les diferents capes de la divisió OSI dels sistemes i els distints nodes dins la xarxa. Ens referim a les tècniques de descomposició focalitzades en problemes d'optimització convexa, els quals han aportat, durant els últims anys, solucions elegants a molts problemes dins dels camps del processament del senyal i les comunicacions. Revisarem els esquemes coneguts i proposarem una nova metodologia. Acte seguit, es comparen les diferents possibilitats de descomposició, cadascuna de les quals implica diferents maneres d'establir la senyalització. A la pràctica, són aquestes diverses opcions de descomposició les que infereixen les diferents interaccions entre capes o els protocols de control entre elements de la xarxa. Els resultats en quant a nombre d'iteracions requerides per a convergir a la solució òptima són favorables al nou mètode proposat, la qual cosa obra noves línies d'investigació.

Finalment, es contribueix també amb dos exemples d'aplicació, en DVB-RCS i en WiMAX. Formulem el problema de gestió de recursos resultant de l'accés múltiple dissenyat per cadascun dels sistemes com un problema de maximització d'utilitat de xarxa (conegut com a NUM en la bibliografia) i el solucionarem aplicant les tècniques anteriors. L'objectiu serà garantir l'equitativitat entre els usuaris i preservar, al mateix temps, la seva qualitat de servei. Per aconseguir-ho, cal seleccionar funcions d'utilitat adequades que permetin balancejar l'assignació de recursos cap als serveis més prioritaris. Mostrarem que en els escenaris considerats, l'ús del mètode proposat comporta guanys significatius ja que requereix menys iteracions en el procés (i per tant, menys senyalització) o bé menys temps de càlcul en un enfoc centralitzat (que es tradueix en la possibilitat d'incloure més usuaris). També es mostren els avantatges de considerar interaccions entre capes, ja que es poden ajustar els paràmetres de capa física per tal d'afavorir els tràfics més prioritaris o bé extreure els requeriments de servei de valors típicament

disponibles en capes superiors.

En general, la implementació eficient de tècniques de gestió dinàmica de recursos treballant en l'accés múltiple dels sistemes pot aportar guanys significatius però implica establir una bona coordinació entre capes i elements de xarxa. L'eina matemàtica que ho possibilita són les tècniques de descomposició. Cada nou escenari i sistema introdueix un nou repte d'optimització i la capacitat que tinguem de coordinar totes les variables del sistema cap al punt òptim en determinarà el rendiment global.

Acknowledgements

I would like to take this occasion to acknowledge all the people that has helped me through this Ph.D. dissertation. First of all, I must thank my advisor, Dr. Gonzalo Seco-Granados, for his tremendous motivation, support and useful discussions. I also want to thank Prof. Ana I. Pérez-Neira for introducing me to the world of research and for being a helpful guide during my first steps in the field. Finally, I should also acknowledge all the people who took part in my education from the very beginning. Without them, I would have been a different person.

Fortunately, not everything in life is work and research. During all these years I have experienced multitude of sensations and feelings, I have shared good and bad moments, I have felt the wonder of nature and I have enjoyed in most of the activities I took part in. Most of the things in this incomplete and ever-growing list would have been not possible without the presence of all my friends and my family. Thank you very much for being there.

Last but not least, I would like to dedicate a few words to a very special person, Pau Barrios Bosch, who left us in July 2005 while climbing one of the most exciting and impressing routes in the old continent: the Mont-Blanc Integral Peuterey Ridge (in the Alps). With his friendly and courageous character, his way of viewing and loving life and his huge human side, he has served as a very valuable example to all of us. As my father once said (in catalan): "El Pau no et podia caure malament". From these words, I want to express my heartfelt condolences to the family and friends. At the same time, I am convinced that Pau has lived more in 26 years of existence than many others in a whole and long life.

In memory of Pau, an excellent human being and mountaineer.

Contents

Notation

Boldface upper-case letters denote matrices, boldface lower-case letters denote column vectors, upper-case italics denote sets, and lower-case italics denote scalars.

$\mathbb{N}, \mathbb{R}, \mathbb{C}$	The set of natural, real and complex numbers, respectively.
$\mathbb{R}_{++}$	The set of real and strictly positive numbers.
$\mathbb{R}_{+}$	The set of real and positive numbers.
dom f	The domain of function f.
$\log x$	The natural logarithm of x.
$\boldsymbol{A}^T$	The transpose of matrix $\boldsymbol{A}$.
$\boldsymbol{x} \preceq \boldsymbol{y}$	Component-wise inequality between vectors $\boldsymbol{x}$ and $\boldsymbol{y}$.
$\boldsymbol{x} \succeq \boldsymbol{y}$	Component-wise inequality between vectors $\boldsymbol{x}$ and $\boldsymbol{y}$.
$\boldsymbol{x} \prec \boldsymbol{y}$	Component-wise strict inequality between vectors $\boldsymbol{x}$ and $\boldsymbol{y}$.
$\boldsymbol{x} \succ \boldsymbol{y}$	Component-wise strict inequality between vectors $\boldsymbol{x}$ and $\boldsymbol{y}$.
bd $\mathcal{Y}$	The boundary of the subset $\mathcal{Y}$.
int $\mathcal{Y}$	The interior of the subset $\mathcal{Y}$.
inf $\mathcal{Y}$	The infimum of the subset $\mathcal{Y}$.
sup $\mathcal{Y}$	The supremum of the subset $\mathcal{Y}$.
card $\{\mathcal{M}\}$	The cardinality of the subset $\mathcal{M}$.
$rank(\boldsymbol{A})$	Rank of matrix $\boldsymbol{A}$.
$diag(\boldsymbol{A})$	Main diagonal of matrix $\boldsymbol{A}$.
$length(\boldsymbol{b})$	Number of elements in vector $\boldsymbol{b}$.
$\mathbf{0}$	A vector with null elements.
$\mathbf{1}$	A vector with unit elements.

$\boldsymbol{y} \overset{M}{\succ} \boldsymbol{x}$	Majorization of vector $\boldsymbol{y}$ with respect to vector $\boldsymbol{x}$.
$\lceil a \rceil$	The nearest integer higher than or equal to a.
$\lfloor b \rfloor$	The nearest integer lower or equal to b.
$\|\boldsymbol{a}\|$	Square-norm of vector $\boldsymbol{a}$.
$\boldsymbol{a} \times \boldsymbol{b}$	The scalar product of vectors $\boldsymbol{a}$ and $\boldsymbol{b}$.
$\sim$	Distributed as. Used to make equivalences between random variables and the pdf's that generate them.

Acronyms

3G	Third Generation.
ACM	Adaptive Coding and Modulation.
ATM	Asynchronous Transfer Mode.
AVBDC	Absolute VBDC.
BS	Base Station.
CDMA	Code Division Multiple Access.
CRA	Constant Rate Assignment.
CS	Convergence Sublayer.
CSMA	Carrier Sense Multiple Access.
CSMA/CA	Carrier Sense Multiple Access/Collision Avoidance.
DAMA	Demand-Assignment Multiple Access.
DBA	Dynamic Bandwidth Allocation.
DCA	Dynamic Channel Assignment.
DiffServ	Differentiated Services.
DLL	Data link layer layer of the OSI model.
DSL	Digital Subscriber Line.
DVB-RCS	Digital Video Broadcasting - Return Channel Satellite.
DVB-S	Digital Video Broadcasting - Satellite.
DVB-S2	Second generation of DVB-S.
e-mail	Electronic mail.
FCA	Free Capacity Assignment.
FCT	Frame Composition Table.
FDMA	Frequency-Division Multiple Access.
FTP	File Transfer Protocol.
GEO	Geostationary Earth Orbit.
GSM	Global System for Mobile Communications.
HTTP	HyperText Transfer Protocol.
i.i.d.	Independent and identically distributed.

IP	Internet Protocol.
KKT	Karush-Kuhn-Tucker.
LAN	Local Area Network.
LOS	Line of Sight.
MAC	Medium access control sublayer of the OSI model.
MAN	Metropolitan Area Network.
MF-TDMA	Multi-Frequency Time-Division Multiple Access.
MPEG	Moving Picture Experts Group.
MVC	Mean Value Cross.
NBS	Nash Bargaining Solution.
NCC	Network Center Controller.
NET	Network layer of the OSI model.
NLOS	Non-Line of Sight.
NUM	Network Utility Maximization.
OFDM	Orthogonal Frequency Division Multiplexing.
OFDMA	Orthogonal Frequency Division Multiple Access.
OSI	Open Systems Interconnection.
pdf	Probability density function.
PDU	Packet Data Unit.
PHY	Physical layer of the OSI model.
PMP	Point-to-Multipoint
QoS	Quality of service.
RBDC	Rate-Based Dynamic Capacity.
RRM	Radio Resource Management.
RTT	Round Trip Time.
SAC	Satellite Access Control.
S-ALOHA	Slotted ALOHA.
SDMA	Spatial Division Multiple Access.
SDU	Service Data Unit.
SMS	Short Message Service.
SMTP	Simple Mail Transfer Protocol.
SP	Service Provider.
SS	Subscriber Station.
TBTP	Terminal Burst Time Plan.
TCP	Transmission Control Protocol.
TCT	Time Composition Table.

TDMA	Time-Division Multiple Access.
UMTS	Universal Mobile Telecommunications Systems.
VBDC	Volume-Based Dynamic Capacity.
WiMAX	Worldwide Interoperability for Microwave Access.
WLAN	Wireless Local Area Network.

Chapter 1

Introduction

1.1 Motivation

Since the irruption of modern wireless communications with the first generation of mobile telephony, one of the major issues to be solved in the design of these systems was the management of multiple users accessing to the system at the same time. At the very beginning, the design was strongly influenced by the connection-oriented philosophy that prevailed in the switched core networks. Note that at the time, all the effort was devoted to the provision of voice services and thus, the idea of establishing a dedicated and permanent end-to-end connection was meaningful, since the connection would be, in principle, used during the most of the call duration. In that sense, the goal was to define multiple 'virtual channels' within the air interface so that the access network could work similarly to the core network. Depending on the available research and technology at each time, that virtual channelization has been achieved in basically three different ways (from oldest to newest): i) assign part of the radio-frequency spectrum to each user, ii) allocate a different portion of the time to each user and iii) transmit all the time using all the available spectrum but differentiating users thanks to orthogonal modulations. A brief review on those topics is provided in Chapter 2.

However, the introduction of a novel network philosophy, i.e. packet-oriented, changed things completely. Assuming services with large inactivity periods (as for example web browsing or e-mail), it made no sense to create permanent and dedicated connections. The new approach was to organize the information in packets of bits and to share the links in the network in order to transport packets from different users. Each packet must contain the destination address so that it can be correctly routed through the nodes in the network. Nowadays, the widely spread Transfer Control Protocol (TCP) in combination with the Internet Protocol (IP) and multiple works that discuss about the convergence of systems at an IP-like level is a contrasting proof about the interest on packet networks. This new philosophy also influenced the access networks and some multiple-access protocols performed a contention-based statistical multiplexing of the

wireless link in order to adapt the access technique to the packetized and bursty nature of the traffic. A pioneering example of traffic-based multiple access protocols is the well-known ALOHA network developed in the Hawaiian islands in 1970.

Notwithstanding, both multiple access techniques have its pros and cons. In one hand, in connection-oriented solutions, one can dimension the 'virtual channels' within the system in order to provide the desired level of Quality of Service (QoS) to the end-users. However, in case that a single connection is intended to support multiple services with different QoS requirements, there may be over-provisioning of resources as far as the design must necessarily accommodate the most demanding services (note that other services do not take advantage of the extra resource allocation). Moreover, a dedicated connection strategy is also inefficient when it manages traffic types that have long non-activity periods, which leads to a waste of resources, too. Furthermore, it is unfair since some users may be blocked whereas others do not take full advantage of their own connections. On the other hand, in contention-based solutions, users try to access the channel at the time that they have information to be sent and hence, they are statistically multiplexed. However, it is known that such mechanisms lead to a poor utilization of the multi-user channel and do not asses well the issues of fairness among users and QoS management. Dynamic Bandwidth Allocation (DBA) techniques can interpreted as hybrid solutions between connection-based and contention-based strategies and they are good candidates to exploit the bandwidth of the system, supporting QoS requirements and guaranteeing fairness among users.

In the last years, many problems within the communications and signal processing fields have been expressed as convex programs and elegantly solved thanks to the well-established convex optimization theory. Motivated by the advantages that convex optimization provides, this work explores the implementation of DBA strategies in the framework of convex programming. Furthermore, since the performance metrics under study depend, in the most general case, on parameters that are either spread over the network elements or over distinct variables within the same element (that may belong to different layers in the protocol stack), the development of distributed optimization techniques plays a very important role. In the first case, for example when we try to find the optimal rates of service flows within a given network, distributed techniques avoid gathering information at a central node (which implies excessive network signalling). In the second case, when we further try to jointly adjust the capacity of each link (that depends on parameters in the physical layer), distributed techniques guide us in the process of establishing the required messaging between layers on the protocol stack. Therefore, exploring the universe of decomposition possibilities within the convex programming framework has also been part of the motivation of the following work.

1.2 Outline of the Dissertation

In this Ph.D. dissertation we study Dynamic Bandwidth Allocation as a technique that allows us to dynamically allocate radio resources in response to the current transmission needs of users accessing a given system. The concept of bandwidth is interpreted in a wide sense throughout this work (analogue to radio resource) and it does not necessarily mean a portion of the radio-frequency spectrum. For example, from a network perspective, it just means a portion of the total rate capacity of a given link (assumed fixed) and it does not take into account any dynamic adjustment of the transmission parameters. In a wider view that includes communication issues, DBA also tunes the parameters at the physical layer in order to attain a more favourable allocation. Throughout this text, DBA is framed as a convex optimization problem and, as motivated in the previous section, we are interested in solutions that are distributed and, if possible, efficient in terms of computational time. The text is organized as follows.

In Chapter 2 we review multiple access techniques and we introduce all the theoretical issues that will be considered later on in the specific DBA schemes. Those issues are cross-layer design, fairness formulation and the Network Utility Maximization (NUM) framework. Thereafter, we detail a literature review on the DBA-related works in two systems aiming to support multimedia applications: the Digital Video Broadcasting (DVB)-Return Channel Satellite (RCS) as a multimedia satellite platform and the Worldwide Interoperability for Microwave Access (WiMAX) as the terrestrial wireless solution for the broadband access in the mid-range.

Chapter 3 includes theoretical work about convex decomposition techniques to solve the NUM problem, which allow us to attain distributed algorithms in practice. We begin the chapter by reviewing some basics in convex optimization and thereafter, we present known decomposition techniques. The first ones, primal and dual decomposition, have been widely used in many research papers. On the contrary, the third one, which is the Mean Value Cross (MVC) decompositions method, has been recently introduced in the wireless community and proposes a combination of primal and dual decompositions in a single approach. Finally, we introduce our proposed method, the coupled-decompositions method. It also combines primal and dual decompositions as the MVC decomposition method but using a radically different structure. We compare our scheme with the previous strategies and it shows significant advantage in terms of iterations required to reach the solution.

In Chapter 4 we analyze how the multiple access is defined in DVB-RCS and we propose an specialized framework to organize the standardized Multi Frequency (MF)-Time Division Multiple Access (TDMA) frame. Thanks to the application of the previous decomposition results we derive a computationally efficient solution. Even given that the DVB-RCS scenario allows us to perform a centralized optimization, the proposed method is still superior when compared to known efficient techniques such as the bisection method. We further show that our solution

allows a proper bandwidth utilization when we take into account cross-layer information from the physical layer in the resource allocation process. Finally, we exemplify that the resulting solution responds to a fairness criteria and that it provides mechanisms to balance resources towards the most priority services.

Chapter 5 contains another application of the results in Chapter 3 to the computation of a DBA multiple access in the uplink of a WiMAX system. Within the general DBA model described in Section 2.4.2, we focus on the flow control part, thus assuming fixed link capacities in the network. Resources are distributed, as in the previous case, according to requests and to services priorities. The main difference is in the network topology considered. Whereas in the DVB-RCS case we assumed a Point-to-MultiPoint (PMP) network, in this case we consider a tree-deployed structure, which is a particular case of a WiMAX mesh network. Using the coupled-decomposition method, it is possible to globally solve the flow allocation problem using reduced inter-node signalling. Indeed, it is only required inside the sub-pieces in which we divide the whole network. Furthermore, the resulting strategy is in accordance with the definition of centralized scheduling in the standard document.

Finally, Chapter 6 ends this Ph.D. dissertation with a summary of the work and some conclusions. We also outline some open issues to be dealt with in future research.

1.3 Research Contributions

This thesis collects all the work that has been carried during the last three years. Most of the results have been published in one book chapter, one international journal and some international conference papers. In the following we list the contributions at each chapter.

Chapter 3

Part of the results within the chapter have been published in the following international conference papers:

- A. Morell, G. Seco-Granados, M.A. Vázquez-Castro, "Computationally Efficient Cross-Layer Algorithm for Fair Dynamic Bandwidth Allocation", in Proceedings of the 16th International Conference on Computer Communications and Networks 2007, ICCCN'07, pp.13-18, August 2007.
- A. Morell and G. Seco-Granados, "Distributed Algorithm for Uplink Scheduling in WiMAX Networks", to appear in Proceedings of IEEE Broadnets 2008.
- G. Seco-Granados, M.A. Vázquez-Castro, A. Morell and F. Vieira, "Algorithm for Fair

Bandwidth Allocation with QoS Constraints in DVB-S2/RCS", in Proceedings of the IEEE Global Telecommunications Conference 2006, GLOBECOM'06, pp.1-5, November 2006.

Chapter 4

The results within the chapter have been published in the following book chapter, international journal and international conference papers:

- T. Pecorella, G. Mennuti (chapter editors), N. Celandroni, F. Davoli, E. Ferro, A. Gotta, S. Karapantazis, A. Morell, G. Seco-Granados, P. Todorova and M.A. Vázquez-Castro (authors in alphabetical order), "Dynamic Bandwidth Allocation", chapter in Resource Management in Satellite Networks: Optimization and Cross-Layer Design, edited by G. Giambene, ISBN 0-387-36897-3, Springer Science+Bussiness Media, 2007.

- A. Morell, G. Seco-Granados and M.A. Vázquez-Castro, "Cross-Layer Design of Dynamic Bandwidth Allocation in DVB-RCS", IEEE Systems Journal, Volume 2, Number 1, pp. 62-73.

- A. Morell, G. Seco-Granados and M.A. Vázquez-Castro, "Enhanced Dynamic Resource Allocation for DVB-RCS: a Cross-Layer Operational Framework", in Proceedings of Military Communications Conference 2007, MILCOM'07, Orlando, October 2007.

- M. Luglio, F. Zampognaro, A. Morell and F. Vieira, "Joint DAMA-TCP protocol optimization through multiple cross layer interactions in DVB RCS scenario", in Proceedings of the International Workshop on Satellite and Space Communications, IWSSC'07, pp. 13-14, September 2007.

- A. Morell, G. Seco-Granados, M.A. Vázquez-Castro, "Joint Time Slot Optimization and Fair Bandwidth Allocation for DVB-RCS Systems", IEEE Global Telecommunications Conference 2006, GLOBECOM'06, pp.1-5, November 2006.

- A. Omari, G. Seco-Granados, M.A. Vázquez-Castro, A. Morell, A. Lyhyaoui and N. Raissouni, "Analysis of the Efficiency and Delay of Bandwidth Request Algorithms in DVB-RCS", in Proceedings International Workshop on Satellite and Space Communications, IWSSC'06, pp. 165-169, September 2006.

Chapter 5

The results within the chapter have been published in the following international conference paper. Furthermore, an international journal paper has been submitted.

- A. Morell, G. Seco-Granados and J.L. Vicario, "Fair Adaptive Bandwidth and Subchannel Allocation in the WiMAX Uplink", submitted to the special issue on "Fairness in Radio Resource Management for Wireless Networks" of the EURASIP Journal on Wireless Communications and Networking.
- A. Morell and G. Seco-Granados, "Distributed Algorithm for Uplink Scheduling in WiMAX Networks", to appear in Proceedings of IEEE Broadnets 2008.

Other Research Contributions

The author of this Ph.D. dissertation has contributed as the main author in other research contributions whose content is not included in the present document. These contributions are:

- A. Morell, A. Pascual-Iserte and Ana I. Pérez-Neira, "Fuzzy Inference Based Robust Beamforming", Elsevier Signal Processing, Volume 85, pp. 2014-2029, October 2005.
- A. Morell, A. Pascual-Iserte, A.I. Pérez-Neira and M.A. Lagunas, "Robust Scheduling in MIMO-OFDM Multi-User Systems Based on Convex Optimization", in Proceedings of the 1st IEEE International Workshop on Computational Advances in Multi-Sensor Adaptive Processing (CAMSAP), pp. 13-15, December 2005.
- A. Morell, A.I. Pérez-Neira and N. Martin, "Fuzzy-Inference-Based Robust Beamforming", in Proceedings of the Information Processing and Management of Uncertainty in Knowledge-Based Systems 2004, IPMU'04, pp. 1627-1634, Perugia (Italy), July 2004.

Finally, other research works where the author has contributed are:

- A.I. Pérez-Neira, M.A. Lagunas, A. Morell and J. Bas, "Neuro-Fuzzy Logic in Signal Processing for Communications: from Bits to Protocols", chapter in Lecture Notes in Computer Science, ISBN 3-540-31257-9, pp. 10-36, ed. Springer Verlag Berlin Heidelberg, 2005.
- J.L. Vicario, A. Morell, A. Bel and G. Seco-Granados, "Optimal Power Allocation in Opportunistic Relaying with Outdated CSI", in Proceedings of IEEE Sensor Array and Multichannel Signal Processing Workshop (SAM), 2008.
- J. Albiol, J.M. Alins, J.M. Cebrián, J. Mata, A. Morell, C. Morlet, G. Seco-Granados, M.A. Vázquez-Castro and F. Vieira, "IP-Friendly Cross-Layer Optimization of DVB-S2/RCS", in Proceedings of the ESA Workshop on Signal Processing for Space Communications, 2006.

Chapter 2

Dynamic Bandwidth Allocation

Dynamic Bandwidth Allocation (DBA), as considered in this work, is a relatively recent concept closely connected to the development of new communication services and systems. It is the natural evolution of the old Dynamic Channel Assignment (DCA) schemes that date from the early 70s, where the goal was to dynamically allocate system channels to the base stations so as to adapt to varying channel, interference and traffic conditions [And73]. By those days (and more or less until the early 90s), the list of accessible telecommunication services (excluding broadcast radio and television) by most of the population in developed countries was monopolized by the phone voice service. It was in that time when the wireless segment began to complement the wired telephone network and when the Internet started to be used. Those were two great technical steps forward at the end of the past century, with great social and economical repercussion. As mobile phones became more and more popular, one of the main concerns of system designers was to enable the coexistence of as many radio signals as possible in the wireless channel. Therefore, the distinct strategies should provide some type of orthogonality between signals so as to be able to distinguish them. In market terms, this increased revenue for the companies that operated the service because more users (clients) would use the network and pay for that. However, there was very little concern on the service itself because the interest was only in a single one: the voice. So much so that when Europe designed the second generation of mobile telephony, the Global System for Mobile Communications (GSM), still in use, the Short Message Service (SMS) was added without expecting the popularity it finally reached.

In parallel, Internet arrived to the home user and the broadband access was enabled thanks to the family of Digital Subscriber Line (DSL) or cable technologies. Much attention has been paid to DSL (using OFDM modulation) since it allows us to take advantage of the available bandwidth in the old copper pairs without substituting them whereas the cable solution has an important deployment cost. Moreover, the third generation of mobile telephony, known as Universal Mobile Telecommunications Systems (UMTS), provides potential broadband access to IP services such as Voice over IP (VoIP), videoconference or simple web browsing. Therefore,

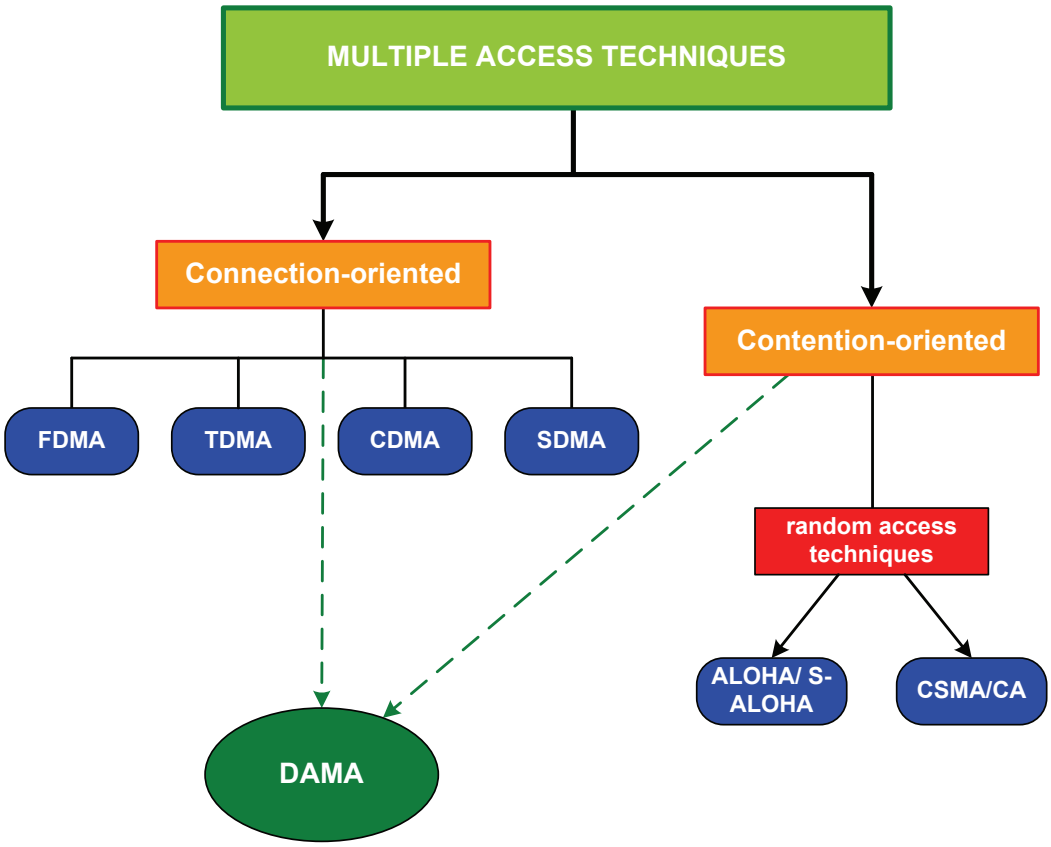

Figure 2.1: Classification of multiple access strategies.

voice is no longer the only service of interest and a new challenge appears: how to effectively manage the set of present and future services that may have different network requirements. Note, for example, that a latency of about a second does not bother the potential user that is surfing the Internet but will definitely exasperate an individual talking over VoIP. Roughly speaking, we identify two big problems in the new scenario, namely: i) the classical one, which is to boost the capacity of the network and ii) the efficient management of services with distinct requirements from the network.

Let us now review the mechanisms that communication systems use to enable the coexistence of the users in the network, i.e. the so-called multiple access techniques. We classify them into connection-oriented and contention-oriented multiple access techniques. In connection-oriented mechanisms, the concern is about how to coordinate the transmission of the multiple users without taking into account the nature of the transported traffic and the services within. It is for example the case in most still in use wireless telephony systems, such as GSM in Europe or cdmaOne in the United States, where the goal is to enable as many simultaneous connections (calls) as possible. On the other hand, contention-oriented techniques are designed responding to the nature of the traffic in datagram packet networks [Cer78], e.g. Internet Protocol (IP). See the classification in Figure 2.1.

Among the connection-oriented techniques, we distinguish:

- Frequency Division Multiple Access (FDMA): In this case, orthogonality among signals is granted by transmitting them in distinct frequency bands, the subchannels. In general, each user accessing the network is assigned a subchannel where it transmits. Due to technological impairments in the transceiver equipment, e.g. subchannel selection filters, it is necessary to keep some guard interval between adjacent subchannels, which introduces inefficiency in bandwidth utilization. It is possible to counteract such inefficiency using the Orthogonal Frequency Division Multiplexing (OFDM) modulation principles in the so-called Orthogonal Frequency Division Multiple Access (OFDMA) technique [Kof02]. The idea is to allow adjacent subchannels to overlap but keeping the orthogonality of the transmitted signals. The implementation of OFDM and OFDMA has not been possible until the digital age.

- Time Division Multiple Access (TDMA): In TDMA, all users transmit using the whole available bandwidth in the system. In order to keep orthogonality among signals, only one user accesses the channel at a given time. Time is divided in TDMA in frames and the time within each frame into slots. In general, one users employs one time slot per frame to complete its transmission, so that it uses a portion of the total. As in FDMA, it is necessary to fix a time guard interval between adjacent time slots in order to avoid collisions.

- Code Division Multiple Access (CDMA): In CDMA all users benefit from the whole system

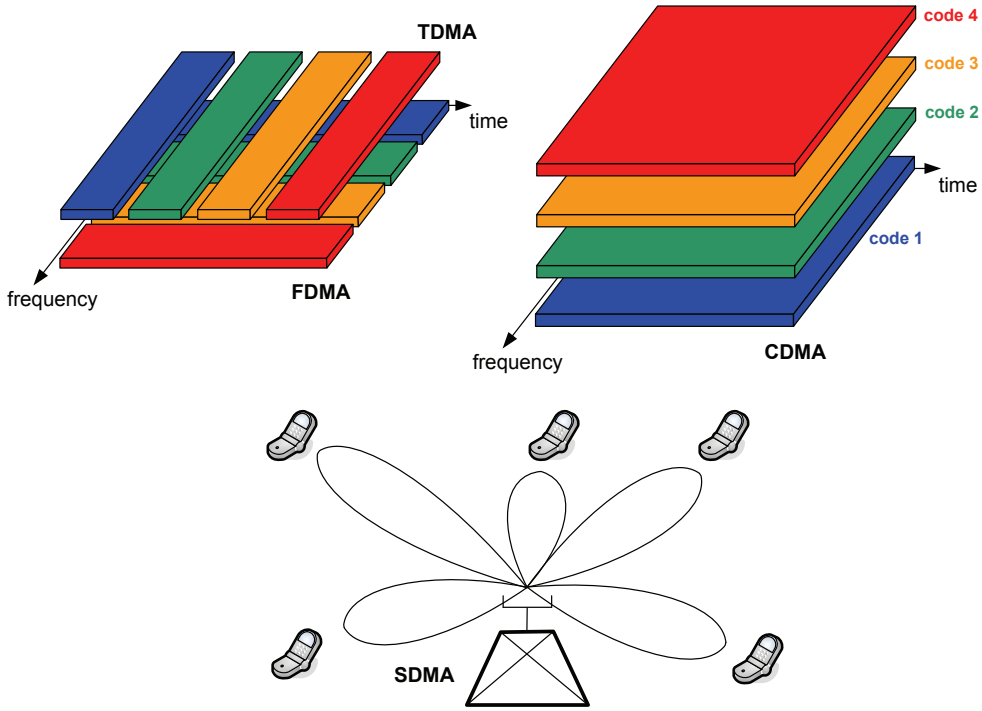

Figure 2.2: Connection-oriented multiple access. Top left: FDMA and TDMA. Top right: CDMA. Bottom: SDMA.

bandwidth and transmit during all the time [Pic82]. Orthogonality is attained thanks to the code signals that modulate the user waveform. Each user has its own code and it is orthogonal to the codes employed by the other users. This option is more efficient than the previous ones but its implementation in real systems is also more difficult since it requires in general finer synchronization and good power control mechanisms.

- Spatial Division Multiple Access (SDMA): The development of multiple antennas techniques [Pau97] introduced an extra dimension also in the multiple access problem since mobile users in a wireless network can be separated depending on their spatial position. In this way, simultaneous transmission in the same bandwidth, time and code is possible if the users are spatially spread out. Therefore, SDMA has to be applied in combination with the other techniques (hybrid strategies are also possible) rather than as a stand-alone solution.

Figure 2.2 summarizes the connection-oriented multiple access techniques. Note that the goal in all the previous approaches is to organize the transmitting resources in order to provide as many connections as possible. In general, the larger the resource subspace is, the better the system performance may be. Therefore, adding the code and space dimensions to the classic time and frequency resources provides better usage of the radio-frequency spectrum.

However, connection-oriented access techniques do not match well to the bursty nature of the packets in data networks. Note that it makes no sense to reserve resources and to establish a connection that is going to be used only during some intervals of time. The previous approaches may be dramatically inefficient and contention-oriented techniques (also refereed to as random access solutions) are designed to better accommodate such type of packetized traffic [Gol05, Sec. 14.3].

Random access techniques began with the pioneering work of Norman Abramson at the University of Hawaii in 1970. A novel packet radio network was deployed to communicate the university campuses using the ALOHA protocol. The idea was pretty simple and intuitive: any transmitter in the network was allowed to transmit a radio packet as soon as it became available. When the traffic load in the system is low, this simple strategy performs well because the wireless channel is used by a single transmission with high probability. As the load increases, the probability that two packets from different transmitters collide increases. In that case, the collided transmitter waits for a random time to retransmit the packet. Note that when the traffic load is significantly high, this mechanism will cause system starvation. It is known that the maximum achievable throughput in a network using ALOHA is only 18%. In other words, the data rate in the network is the 18% of the data rate that a single user would achieve on the system [Gol05, Sec. 14.3]. The ALOHA protocol was upgraded with its slotted version or S-ALOHA. Time is divided into slots and a transmitter is allowed to transmit only at the beginning of each slot. In this way, the throughput of the system is doubled since the probability of having a collision is reduced. However, it is still less than 40%.

Another performance upgrade in the ALOHA protocol was achieved by the so-called Carrier Sense Multiple Access (CSMA) solution, which is nowadays widely used. Within this approach, terminals sense the channel to identify when it is busy. If the result is affirmative (busy), all the terminals wait a random backoff period before retrying transmission. This random waiting time is crucial to avoid all terminals to transmit after the current packet in the channel is completely sent. CSMA is used as the access protocol in wired LANs. It is also used in wireless LANs with some modifications that adapt to the particularities of the wireless channel. It is the CSMA/Collision Avoidance (CSMA/CA) technique [Gol05, Sec. 14.3].

However, the actual convergence trends of the different traffic types into a single IP-based network requires modifications of the multiple access techniques in order to give an adequate solution to the new situation. Note that CSMA has acceptable performance in traditional LAN services such as web browsing, File Transfer Protocol (FTP) or Simple Mail Transfer Protocol (SMTP) applications but it may not capture the more stringent Quality of Service (QoS) requirements of services like Voice over IP (VoIP) or video streaming, which demand for more regular transmission opportunities. As an example, assume a congested LAN where one terminal wishes to establish a VoIP conference. In principle, there is no mechanism that guarantees the regular

transmission of the VoIP packets since the multiple access is contention-based and the other players have the same chances to access the channel. The Demand Assignment Multiple Access (DAMA) constitutes a recent methodology that takes into account this new paradigm. As depicted in Figure refDBAfigOverview, it can be regarded as an evolution of both contention-based and connection-based mechanisms. The interested reader can find in [Zan97, Sai97] two general scope communications that discuss the need of good Radio Resource Management (RRM) techniques in modern wireless networks to provide a certain degree of QoS.

DAMA may be interpreted from a functional perspective as an intermediate point between the two previous basic strategies as well. The idea is that terminals request resources to the network depending on the traffic in their MAC queues. Thereafter, the network allocates resources using a certain distribution criterion. Potentially, it is possible to set up a 'virtual' connection when the traffic type requires it, as it is the case of VoIP or videoconference or, on the contrary, it is also possible to perform statistical multiplexing of data packets as in random access solutions. Maybe the first occurrences of DAMA techniques in the literature can be associated to the DCA implementations [Rap79] that date from the 70s. A wider and modern vision of the concept is described in [Hac00], where several DAMA protocols are analyzed in the context of ATM wireless networks. In this thesis, we focus on DAMA strategies that are implemented by means of Dynamic Bandwidth Allocation (DBA) techniques and we do it from a mathematical optimization perspective.

2.1 Cross-Layer and Dynamic Bandwidth Allocation

As stated before, a DAMA strategy is adequate to preserve the QoS requirements of the service flows within the system. In many cases, these QoS definitions are not explicitly available at the MAC layers of the network elements, where DBA techniques usually run. For example, when we have IP implementing DiffServ (Differentiated Services), the requirements about QoS are found in the different classes in which the traffic is divided at the third Open Systems Interconnection (OSI) layer [Zim80]. Hence, potential interactions between the MAC and the higher layers in the system in order to obtain this information are of interest. An specific example about DAMA with DiffServ, from the satellite field, is found in [Ada02]. Other interactions may be useful, too, as it is the case of information exchange from PHY to MAC layer and viceversa in systems that use adaptive PHY layers. Without considering such interaction, dynamic bandwidth allocation manages the fixed link rate capacities seen from the MAC layers of the terminals in order to optimize a certain network performance metric. But if it is possible to adjust also the PHY layers of the terminals, then the network may attain some extra performance because PHY and MAC layers are jointly optimized according to the traffic conditions in the network. See those relations in Figure 2.3.

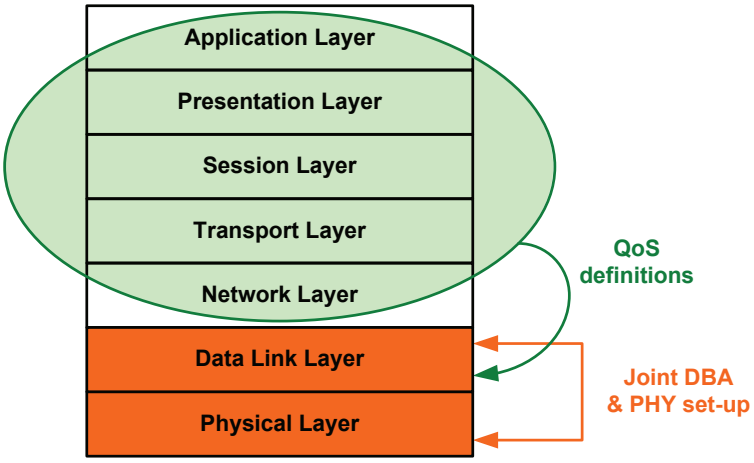

Figure 2.3: Potential cross-layer interactions in DBA.

All these interactions among OSI layers having the objective of optimizing a given system performance metric appear in the literature under the so-called nomenclature of cross-layer interactions and cross-layer optimization [Ber04, Sha03]. The need of breaking the traditional layering of systems, which so good results had shown, emerged with the new era of mobile wireless communications. As discussed in [Sha03], communications links in old wired networks were seen as bit pipes that provided a constant data rate with some seldom random errors. Therefore, the mission of communication engineers was to provide the best possible data pipes, ideally getting close to the Shannon limit [Sha48]. The job was in part attained with the discover of turbo decoding by Berrou et al. in 1993 [Ber93]. On the other hand, network engineers handled the allocation of packets into the bit pipes or, in other words, packet scheduling. Relevant issues were, among others, traffic balancing or QoS provision. The situation changed with the introduction of mobility in the networks, mainly due to two big differences between fixed and wireless channels:

- The short-term channel variation: because of the multi-path component in most wireless scenarios, communication links are not well modelled with the pipe-like vision. The channel induces fast variations over time, frequency and location. To exemplify it with numbers, coherence times [Gol05, Sec. 3.3.3] in wireless channels can be in the order of few milliseconds.

- The large-scale channel variation: when the channel is measured in mean value, it may happen that some users are favoured (from the point of view of channel gain) in front of the others if they are in better locations or if they are not in hostile interference scenarios, for example. A global view of any communication system that aims to provide certain QoS to its users should take this fact into account and respond with an adequate balancing of network resources.

In the following, we exemplify the utility of cross-layer solutions with two illustrative works in the literature. In the first one, the performance of the Transmission Control Protocol (TCP) applied over wireless links is studied [Sha03]. The problem is focused on the congestion control mechanism of TCP, which is based on a measure of the packet losses in order to estimate the congestion status of the routers through the network. Whereas TCP works well for wired networks, where losses are mainly due to congestion, it fails in the wireless environment since the nature of the channel also causes packet losses. The result is a significant reduction in system throughput [Xyl99]. A possible solution is to apply good channel encoders in combination with an Automatic Repeat reQuest (ARQ) [Lin84] strategy with the objective of smoothing the variations of the channel. However, further improvement is achieved by distinguishing the nature of packet losses, i.e. wether they are due to congestion in the internet or they respond to a bad channel status. The authors in [Kun03] asses the performance of the previous approach using Explicit Congestion Notification (ECN) in TCP. Finally, a review on cross-layer approaches that interact with layers below TCP for wireless scenarios can be found in [Tia05, Gia06].

A second example is a pioneering cross-layer work from Knopp and Humblet, which is described in [Kno95]. The scenario is the uplink of a single cell multi-user communications system. The authors obtain the optimal power control of the users in the cell under a total power constraint. The goal is to maximize the sum-rate capacity and as a result, it is found that only the user with the best channel condition should transmit using the whole available bandwidth. Therefore, the multiple access of the system is implicitly derived from a PHY layer design and a practical implementation requires the knowledge of the channel condition of all users at the MAC layer. However, the previous solution has an important fairness drawback. Because of the large-scale channel variation, it is reasonable to consider the situation where a user is permanently in bad channel condition during a long period of time. The solution is terribly unfair respect to the other users, although a global system view in terms of sum-rate capacity is maximized. In order to avoid that situation, some definitions of fairness have been adopted by the scientific community. In the next section, we review them motivated by the fact that part of the work in this thesis is aimed to provide fair dynamic bandwidth allocation (alternatively scheduling) mechanisms.

2.2 Fairness and Dynamic Bandwidth Allocation

In general, formal fairness definitions are necessary to explicitly say how competing users are assumed to share the resources available in a given system, as it is the case in scheduling or DBA. The results we present in this section have an important contribution from the work of Kelly, who introduced the concept of proportional fairness [Kel98] and also discussed about the differences with max-min fairness [Kel97], which was the most common criterion at the time. Both works

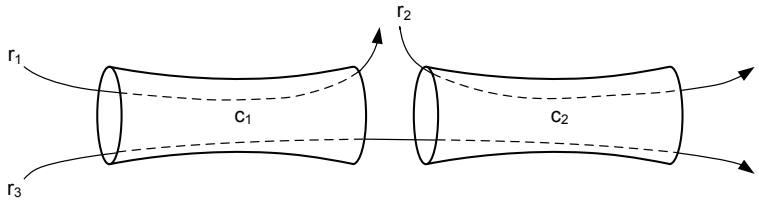

Figure 2.4: Network example.

are devoted to the optimization of the end-to-end rates in a fixed wired network achieving fairness among users. Later on, the concept was generalized in [Mo00] with the definition of $(\boldsymbol{p}, \alpha)$-proportional fairness.

Let us consider the problem of end-to-end rate control of N users over the internet. As proposed in [La02], the problem can be formulated as

$$\begin{array}{ll} \max\limits_{\{r_i\}} & \sum_{i=1}^{N} U_i(r_i) \\ s.t. & \boldsymbol{A}\boldsymbol{r} \leq \boldsymbol{c} \\ & r_i \geq 0 \end{array} , \tag{2.1}$$

where $\boldsymbol{r} = [r_1, \ldots, r_N]^T$ is the vector that contains the rates of all users. The functions $U_i(r_i)$ aim to measure the utility perceived by the i^{th} user when it is allocated a rate r_i. Finally, the bottlenecks in the network are explicitly considered in the matrix A, whose entries are either 0 or 1. Each row in the matrix reveals which user flows share the available capacity in the bottleneck. The vector $\boldsymbol{c}$ groups those available network capacities. A simple example from [La02] is depicted in Figure 2.4 with 3 users and 2 bottlenecks. Note that users 1 and 3 share the link capacity c_1 whereas users 2 and 3 share the link capacity c_2, so that

$$\begin{bmatrix} 1 & 0 & 1 \\ 0 & 1 & 1 \end{bmatrix} \begin{bmatrix} r_1 \\ r_2 \\ r_3 \end{bmatrix} \leq \begin{bmatrix} c_1 \\ c_2 \end{bmatrix}. \tag{2.2}$$

A rate allocation $\boldsymbol{r}^{\triangleright}$ is said to be max-min fair [Ber87, Sec. 6.5] if it is feasible, i.e. it attains the constraints imposed by the network ($r_i \geq 0$ and $\boldsymbol{A}\boldsymbol{r} \leq \boldsymbol{c}$ in the previous formulation), and if it is not possible to increase any of the rates within $\boldsymbol{r}^{\triangleright}$, say $r_j^{\triangleright}$, without decreasing another rate $r_p^{\triangleright} < r_j^{\triangleright}$. The max-min fairness approach tends to allocate more resources to flows with smaller rates. Note that any increase in one of the rates within $\boldsymbol{r}^{\triangleright}$, even a large one, will not be attained under a max-min fair criterion if it implies a reduction of another rate, even if the reduction is small. In the network of Figure 2.4, if the capacity vector is fixed to $\boldsymbol{c} = [c_1, c_2]^T = [1, 1]^T$, then the max-min solution is $\boldsymbol{r} = [\frac{1}{2}, \frac{1}{2}, \frac{1}{2}]^T =$ and the total throughput in the network is $\frac{3}{2}$. In that situation, a relaxation of the max-min criterion, i.e. if we allow a certain reduction in r_3, involves an increase in network throughput because the reduction in r_3 implies the same increase in both r_1 and r_2. Note that the maximum network performance is achieved with $r_3 = 0$ and a total throughput of 2, but then the solution is totally unfair.

Motivated by this trade-off between fairness and throughput, Kelly introduced in [Kel97] the proportional fairness criterion in order to attain the desired compromise. A vector $\boldsymbol{r}^{\dagger}$ is said to be proportionally fair if it is feasible and if for any other feasible rate allocation $\boldsymbol{r}^{\ddagger}$, the sum of relative changes is not positive. In other words, $\boldsymbol{r}^{\dagger}$ (feasible) is proportionally fair when it attains

$$\sum_{i=1}^{N} \frac{r_i^{\ddagger} - r_i^{\dagger}}{r_i^{\dagger}} \leq 0, \qquad \forall \boldsymbol{r}^{\ddagger} \; s.t. \; r_i^{\ddagger} \geq 0, \boldsymbol{A}\boldsymbol{r}^{\ddagger} \leq \boldsymbol{c}. \tag{2.3}$$

If we use this new fairness vision with the previous example, we realize that the optimal flow allocation is now $\boldsymbol{r} = [\frac{2}{3}, \frac{2}{3}, \frac{1}{3}]^T =$ and that the network throughput is $\frac{5}{3}$. Therefore, an intermediate solution between max-min fairness and maximum sum-rate is achieved.

From a practical point of view, in connection with the formulation in (2.1), it is desirable to find explicit expressions of the utility functions that allow us to find the optimal fair allocation of resources within the network by means of solving the mathematical programming problem. Kelly proved in [Kel97] that using the following utility functions in (2.1),

$$U_i(r_i) = \log(r_i), \tag{2.4}$$

the proportionally fair solution is attained. Note that with this utility functions, the objective of the optimization problem considered is the aggregation of the logarithms of the rates. An equivalent problem is found by replacing that with the product of the rates as

$$\begin{array}{ll} \max\limits_{\{r_i\}} & \prod_{i=1}^{N} r_i \\ s.t. & \boldsymbol{A}\boldsymbol{r} \leq \boldsymbol{c} \\ & r_i \geq 0 \end{array}, \tag{2.5}$$

since the transformation of the objective function in (2.5) with a monotone increasing one does not change the point $\boldsymbol{r}$ where the optimum value is attained [Boy03, Sec. 4.1.3]. In this case, transforming $\prod_{i=1}^{N} r_i$ with the logarithm function gives (2.1) in combination with (2.4) as a result (since the feasible rates are positive, the value within the logarithm is always positive and the transformation is well-defined). Furthermore, it is known from game theory [Mut99] results that the maximization of the product of competing resources attains the so-called Nash Bargaining Solution (NBS) [Maz91, Yaï00] and hence, it verifies the axioms of linearity, irrelevant alternatives and symmetry of the solution. Therefore, we can conclude that NBS is equivalent to the proportional fair approach.

Finally, the authors in [Mo00] generalize the proportional fairness criterion to $(\boldsymbol{p}, \alpha)$-proportional fairness. They also contribute with analytical expressions of the corresponding utility functions to attain it. A feasible rate vector $\boldsymbol{r}^{\dagger}$ is said to be $(\boldsymbol{p}, \alpha)$-proportionally fair (where $\boldsymbol{p} = [p_1, \ldots, p_N]^T$ and α are positive real numbers) if, given any other feasible rate vector $\boldsymbol{r}^{\ddagger}$, it holds that

$$\sum_{i=1}^{N} p_i \frac{r_i^{\ddagger} - r_i^{\dagger}}{(r_i^{\dagger})^{\alpha}} \leq 0, \qquad \forall \boldsymbol{r}^{\ddagger} \; s.t. \; r_i^{\ddagger} \geq 0, \boldsymbol{A}\boldsymbol{r}^{\ddagger} \leq \boldsymbol{c}. \tag{2.6}$$

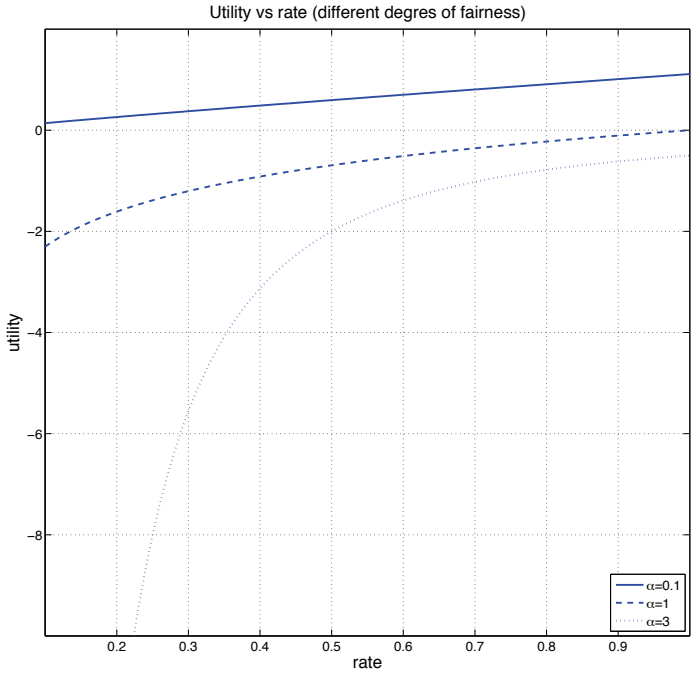

Figure 2.5: Different degrees of fairness in the definition of utility functions.

Note that for $\boldsymbol{p} = [1, \ldots, 1]^T$ and $\alpha = 1$, the criterion reduces to proportional fairness. The utility functions in this case are defined as

$$U_i(r_i; p_i, \alpha) = \begin{cases} p_i \log(r_i), & \alpha = 1 \\ p_i \frac{r_i^{(1-\alpha)}}{1-\alpha}, & \alpha \neq 1 \end{cases} . \tag{2.7}$$

When $\boldsymbol{p} = [1, \ldots, 1]^T$ and $\alpha \longrightarrow \infty$, it is shown in [Mo00] and [Kel97] that the resulting optimal rate allocation after solving (2.1) tends to the max-min fair rate vector. On the other hand, when $\alpha \longrightarrow 0$, problem (2.1) formulates a maximum sum-rate approach. Therefore, it is the convexity of the utility functions what fixes the degree of fairness of the solution. See in Figure 2.5 three different plots of $U_i(r_i; p_i, \alpha)$ for $\alpha = 0.1$, $\alpha = 1$ and $\alpha = 3$ (always with $p_i = 1$). Note in the figure that as α increases, the utility attained at low rates diminishes more severely and therefore, much attention is required to avoid that low-rate situations. It is thus in accordance with the max-min fairness criterion. On the other hand, the concavity of the functions reveals that at the high-rate regime, lower utility gains are achieved for a fixed increase in rate, so that the maximization of the aggregate of utilities in (2.1) forces the distribution of resources, as it is expected in a fair approach. This is true in general except for low α values, where the utility function tends to be linear in the rate. The criterion is then to allocate as much rate as possible to the flows regardless any fairness consideration in order to operate at the maximum network throughput point.

In summary, there is no unique criterion to define fairness, but a series of them are explicitly characterized with the utility functions in (2.7). Furthermore, some flows can be prioritized in front of the others within a specific fairness framework (fixed by α) by particular adjustment of the scale thanks to the parameters $\{p_i\}$. In general, proportional fairness ($\alpha = 1$) provides a nice trade-off between fairness and resource utilization (network throughput).

2.3 DBA in Relation with Network Utility Maximization and Distributed Computation

Our work about DBA throughout this thesis is mathematically modelled using the Network Utility Maximization (NUM) framework. It is a nomenclature recently adopted to refer to the type of problems that arise, in general, in network resource allocation. A basic NUM formulation has been introduced in (2.1) and the philosophy is to maximize the aggregated utility of the users (that measure their satisfaction) given the physical limitations imposed by the current system (constraints in the optimization problem). Traditionally, the interest was to provide distributed solutions that allow to compute the optimal resource allocation without the need of gathering all the information in a central node in the network. The motivation is to reduce signalling requirements and to provide scalable approaches that may operate also with large networks. The reader can fin examples of that in [Low99, Mo00, La02, Low03].

Most of the works in the extensive NUM literature achieve distributed solutions by means of managing the dual version of the problem, or in other words, making a dual decomposition, which we review in Section 3.2.2. The motivation is that it attains a fully decoupled approach in the sense that each node in the network is configured with only local information. An example of that can be found in [Low99], where the authors demonstrate the viability of that type of approach in static and slow time-varying network conditions. Dual-based techniques are often indistinctly called price-based strategies because dual variables can be interpreted as prices under a resource-price framework, whereas resources are identified with primal variables. We also discuss this issue in the next chapter. Another interesting example is found in [Low03], where it is shown that the TCP protocol that controls the end-to-end rates in the network can be viewed as a pure dual decomposition of a NUM problem.

The works of Palomar and Chiang in [Pal06, Pal07] review and expand the number of available decomposition possibilities, always from a convex decomposition perspective. They show that primal decomposition, reviewed in Section 3.2.1, has to be considered in addition to dual decomposition. Moreover, hybrid approaches that combine both techniques in a multi-level decomposition strategy are also feasible. For example, one can split the main NUM problem into several subproblems with a dual decomposition and then use a second problem splitting (for instance primal decomposition) in order to solve each of the subproblems at the highest level. In

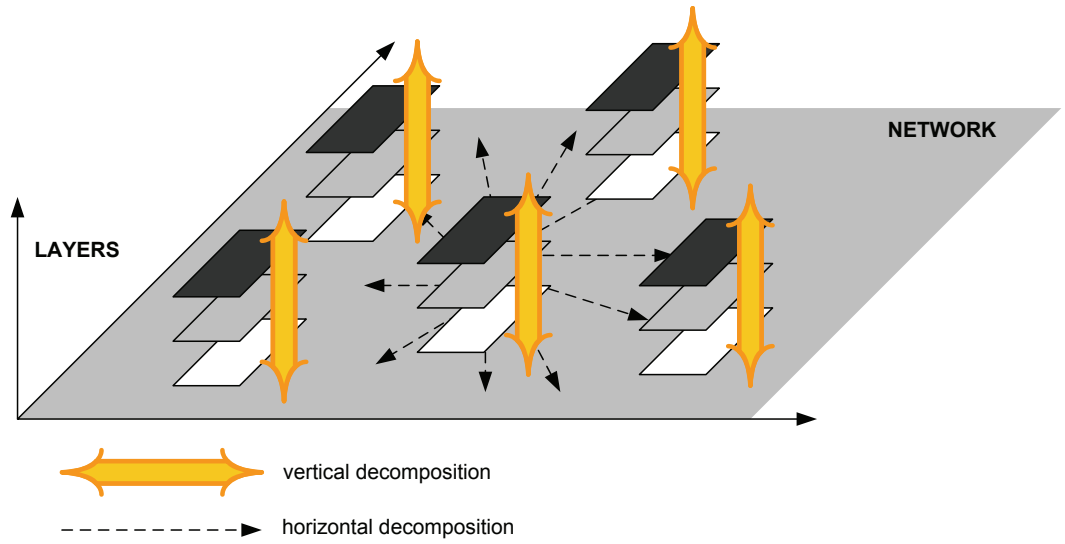

Figure 2.6: Vertical and horizontal decompositions.

[Pal07] they also contribute with application examples of more sophisticated NUM formulations, all of them solved with the multi-decompositions perspective. In those formulations, they include issues such as power control, multipath routing or QoS. Specifically, the first one assumes that the network is power-limited and that the capacities of the links depend on the power allocated to them. Therefore, optimization takes into account two groups of variables: rates and powers. It is a good example of a joint optimization of parameters that belong to distinct OSI layers in order to attain a common goal, which is the system performance measured as aggregated utility.

There are a number of works that extend the NUM formulation to obtain a joint optimization of several system parameters in a cross-layer design [Xia04, Zha06, Joh06]. A recent paper by Chiang et al. [Chi07] takes into account both cross-layer system design and distributed optimization among the elements in the network in a quite ambitious approach. The basic idea is to generalize the NUM formulation including the relevant parameters in all layers as variables having a common performance objective. Thanks to decomposition techniques, the global problem is distributed among layers (vertical decomposition) and among network elements (horizontal decomposition), as Figure 2.6 depicts, with several subproblems. The signalling required to coordinate such decompositions will show the adequate interfaces among layers and among network elements. It is thus a reverse engineering view of the traditional layering of systems. The paper contains a good summary of existing examples, key methodologies and future challenges.

In this thesis, we review the known decomposition methods: primal and dual decompositions (and hybrid techniques) [Pal06] and also a combined primal-dual approach known as Mean Value Cross (MVC) decomposition (introduced in the NUM context in [Joh06]). We also develop a novel solution to decompose the NUM problem in a mixed primal-dual scheme, which is different

to the MVC decomposition and provides significant gains in terms of computational efficiency. Note that each strategy induces different control protocols and different signalling requirements from the reverse engineering point of view in [Chi07] and therefore, our contribution provides an additional exploration path in the design.

Up to this point we have motivated the use of dynamic bandwidth allocation in combination with a DAMA technique to provide an adequate response to modern traffic characteristics and QoS requirements. Furthermore, we have reviewed the pieces that have a significative role in our work, namely: distributed NUM, fairness definitions and cross-layer solutions. Since we will propose DBA solutions in the context of Digital Video Broadcasting (DVB)-Return Channel Satellite (RCS) and Worldwide Interoperability for Microwave Access (WiMAX) standards in Chapters 4 and 5, respectively, next we make a literature review of existing DBA solutions therein.

2.4 Applications of Dynamic Bandwidth Allocation

2.4.1 DBA in Digital Video Broadcasting-Return Channel Satellite

Dynamic Bandwidth Allocation has been considered in the satellite return channel of the DVB standard [ETS05a, ETS03c] as a potential measure to efficiently distribute the valuable spectrum and to provide adequate QoS according to traffic requirements. The authors in [Ibn04] review available technologies and open issues in the design of high-speed mobile communications. Among others, they identify the interest in good dynamic bandwidth allocation techniques as part of the resource management. Two particularities appear in the design of DBA strategies for DVB-RCS in contraposition to other existing systems. First, the satellite channel varies in time even in fixed scenarios, which is basically due to the phenomena that take place at the Earth's troposphere (rain, snow, ...). Although it is not as aggressive as in most wireless terrestrial systems that operate in rich scattering environments, it is important to take it into account since it directly reports on the effective transmission rates of the ground station to satellite links. DVB-RCS uses adaptive coding to counteract the channel variability and therefore, each coding rate fixes a different bit rate. We will assume that once the coding rate is correctly set-up, the channel can be considered quasi-error-free. Second, there is a large propagation delay when transmitting to a Geostationary Earth Orbit (GEO) satellite, which implies about half a second of Round Trip Time (RTT). It is quite large if we compare it with terrestrial systems and, as we discuss later, it also influences the DBA design.

Regarding satellite bandwidth allocation in general, two main philosophies are distinguished in the literature, namely: i) static allocation and ii) dynamic allocation [Cel03, Pie05]. The DVB-RCS standard document [ETS05a] includes both. Within a static approach, terminals receive a

certain amount of resources, which remain constant during the connection's lifetime. However, note that each terminal can dynamically manage its portion of bandwidth (depending on the information flows that use the static link) without involving the sub-satellite network. In other words, DBA techniques can still be used in this case for scheduling issues within each terminal. On the other hand, a dynamic approach focuses the already described process whereby users request resources (in the DVB-RCS scenario we consider a central node in the network which is referred to as Network Central Controller or NCC that collects those demands) and receive grants indicating the allocation. Note that the information available at the NCC to compute the allocation is the collection of requests from all the terminals and the available resources (known since all the information is centralized). Furthermore, we can differentiate three possible strategies within dynamic allocation. From less flexible to more flexible solutions:

- Fixed allocation, where each terminal requests a rate capacity to be able to transmit at its maximum source rate. If the satellite capacity can not satisfy all requests, then the capacity is somehow shared. The most simple way to do it is by means of performing a proportional allocation, although more elaborate decisions can be taken. In general, we consider that the validity period of each allocation is large when compared to more flexible solutions. As it will be discussed in Chapter 4, radio resources are organized in DVB-RCS in a Multi Frequency-Time Division Multiple Access (MF-TDMA) frame. The work in [Kifl06] contributes with a number of strategies to attain an efficient frame utilization under a fixed-like allocation approach.

- Mixed DBA and fixed allocation techniques, when part of the satellite capacity is dedicated to perform a fixed allocation whereas the remaining part is used to statistically multiplex the flows of the users. Operating in shorter time-scales, this DBA part is intended to absorb the traffic burstiness.

- Full DBA techniques, aiming to exploit the whole satellite capacity in order to attain both good tracking of traffic variation and efficient utilization of radio resources. Examples of full DBA strategies using different performance criteria and different ways to solve the underlying optimization problem can be found in [Lee04, Alo05, Cel06, Ros06].

In real life, a mixed strategy seems to be the most adequate solution since both the fixed allocation and the full DBA have its pros and cons. A fixed allocation is clearly inefficient from the point of view of resource utilization because significant amounts of satellite capacity are lost in the silent periods. On the contrary, it has advantage in terms of delay and signalling. Since there is no need to negotiate a resource allocation before a transmission occurs, this extra delay is avoided. Note that this delay is at least the RTT, which is a relatively high value in GEO satellites. Furthermore, the request-grant process involves signalling and it is avoided using a fixed allocation. Therefore, a compromise solution might be to use a fixed allocation for traffic

types that require stringent QoS provisioning and that generate traffic in a periodic basis and to statistically multiplex traffic types that are more bursty in nature. Note that bandwidth utilization is not severely compromised because we do not squander the fixed allocation portion. DVB-RCS defines several ways to request capacity (detailed in Chapter 4) and among them, Constant Rate Assignment (CRA) can be explicitly employed for fixed allocation purposes. The multiplexing task is then associated to the remaining types of request.

However, related research lines in the literature do not exclusively focus their attention on the best possible way to react to the requests emitted by the terminals. Some of them also consider how requests are generated [Chi04b, Pri04, Pie05] and how this generation influences the system behaviour. In order to help the explanation, let us consider in Figure 2.7 a generic architecture of a DVB-RCS terminal implementing Internet Protocol (IP) with differentiated services, which has been inspired by [Pie05]. The IP data flow to be transmitted through the satellite is classified and regulated, which results in various queues that map distinct IP service or priority classes. The IP packets within the queues are then scheduled and segmented into MAC layer units in order to be conveyed at this lower layer. Without loss of generality, a number of queues at the MAC layer are defined as well to represent the priority classes at that level. Finally, the MAC scheduler makes an ordered selection (following a given criterion) of the contents in the queues to be sent to the air interface.

Note that each terminal drains its queues depending on the amount of PHY layer resources it can use to transmit, which definitely configures its link capacity. Thanks to a DAMA technique implemented by means of a DBA solution, the satellite spectrum (or part of it) is statistically shared among users. As depicted in the figure, it is necessary to gather information about the MAC queues (basically length and priority) at a DBA control module, who requests capacity to the NCC and receives the assignments in the Terminal Burst Time Plan (TBTP) table. The works in [Pri04, Pie05] show that the intuitive solution of requesting just the length in the queues works well for non-congested states, i.e. when the satellite capacity is able to fulfill all the requests. Notwithstanding, the average queue length can be reduced if control theoretic mechanisms are implemented to track a reference queue length value. The result is that in congested states, the requests are computed as the input rate plus an extra demand that depends on the queue length. The authors also propose a modification on their scheme to cope with free capacity assignments, which are capacity grants that have not been previously requested (this occurs when some satellite capacity is left unused). However, as discussed in [Nea01], free capacity assignments must be carefully studied in combination with the Transfer Control Protocol (TCP) since they may introduce unexpected degradation.

Finally, we can further distinguish within DBA techniques between reactive and proactive strategies. Note that all the solutions that we have introduced up to this point, which are classified as reactive techniques, aim to respond to the current status of the queues but they

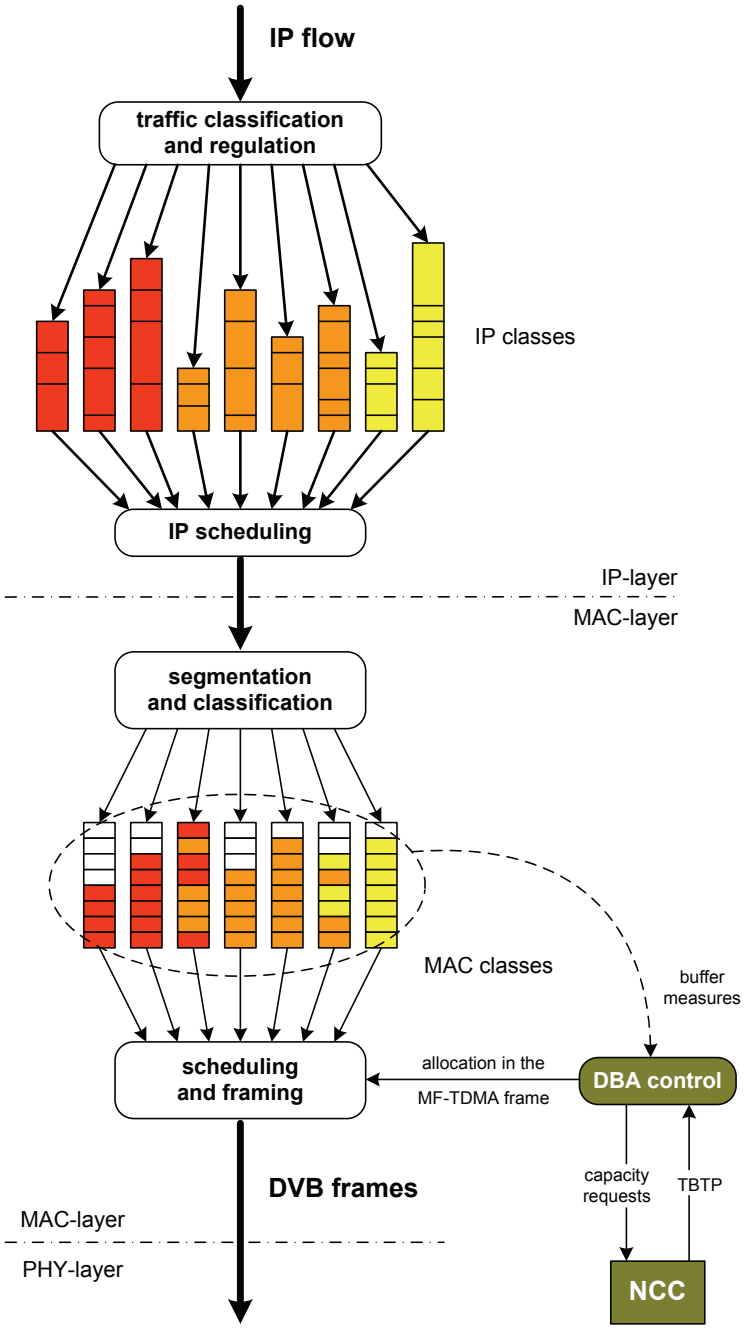

Figure 2.7: Generic terminal architecture.

do not try to anticipate to traffic dynamics. A major drawback of reactive approaches with GEO satellites is that, due to the high RTT value, the requests may not represent the actual QoS needs. Free capacity assignments are intended to counteract this fact and they can be useful, for example, to send an HyperText Transfer Protocol (HTTP) request without waiting for the completion of a resource request/allocation phase [Nea01]. In general, proactive schemes try to anticipate to future traffic requirements to paliate the RTT problem. In [Chi04b] the authors introduce an adaptive traffic predictor implemented with a Recursive Least Squares (RLS) adaptation scheme [Hay96, Ch. 13] that adjusts the parameters of the Auto-Regressive (AR) model [Hay96, Ch. 2] proposed for the input traffic flow.

Our DBA proposal for DVB-RCS in Chapter 4 is focused on how the resources available in the MF-TDMA of the satellite are distributed for a given resources request. We do not consider how requests are generated and we concentrate our attention in supplying a DBA framework that provides a proper set-up of the shared spectrum taking into account the PHY layer configuration of the satellite terminals and allowing to balance the resulting allocation towards the most prioritized flows under a global fairness criterion. A mathematical representation of the situation as a NUM problem and the novel decomposition technique developed in Section 3.3 allows us to attain the optimal allocation and to obtain it efficiently (in terms of computational time).

2.4.2 Distributed Scheduling in WiMAX Networks

Similarly to what happens in DVB-RCS, the multiple access in the WiMAX [IEE04, IEE06] uplink also responds to a DAMA solution, where there is a process of requesting and granting transmission opportunities. The interested reader can find a good review on the PHY and MAC layer aspects of WiMAX in [And07, Ch. 8, Ch.9]. Notwithstanding, we notice that the WiMAX scenario is more rich due to the following issues: i) the network topology and ii) the PHY layer reconfigurability.

Regarding network topology, a Point-to-MultiPoint (PMP) structure is always assumed in the DVB-RCS satellite subnetwork. In any case, satellite terminals may distribute their capacity among various users to which are connected, for example, through a Local Area Network (LAN) or a Wireless LAN (WLAN). WiMAX, as the broadband wireless solution for the medium distance, also considers PMP and optionally, a mesh network configuration. In mesh mode, terminals do not need to communicate directly to the Base Station (BS) as they do in PMP mode. Therefore, a global optimal network operation (given some performance metric) requires in general a more complex formulation and practical strategies to attain it, which implies searching for adequate distributed solutions. Finally, we want to remark the interest in tree-deployed topologies. They are an intermediate case between PMP and general mesh networks and have been considered in WiMAX deployments that build the backhaul transport network [Lee06b,

Hin07].

The WiMAX standard includes four different PHY layers that are based on a single carrier, an Orthogonal Frequency Division Modulation (OFDM) or an Orthogonal Frequency Division Multiple Access (OFDMA) architecture. All the solutions offer different reconfiguration possibilities and thus, it is possible to send information at a number of distinct rates. Since WiMAX is envisaged for both fixed and wireless scenarios working at the microwave band, where channel fluctuations may be significant, PHY layer reconfigurability allows to track those variations and to make the best possible channel use (almost reaching Shannon capacity [Sha48]). Among others, the standard includes adaptive coding and modulation, power control, subcarrier allocation in OFDM/OFDMA [Won99, Kiv03] or Multiple-Input-Multiple-Output (MIMO) [Ale08] techniques. Always in relation with the multiple access in the system, DBA is found in the literature according to two distinct interpretations (possibly mixed): i) assuming fixed link capacities, the goal is to distribute the bandwidth among the information flows in order to sustain the QoS definitions and ii) considering non-empty MAC queues to be drained, the goal is to operate the network at a proper multi-user rate point in the network capacity region [Cov91, Ch. 14] in order, for example, to achieve maximum network throughput.

If we search for an integrated QoS provisioning, one approach does not exclude the other. In fact, the goal is to balance the available bit rate at each link towards the most priority flows and, at the same time, to select a feasible rate point in the network that allocates more resources to the links transporting such priority flows. It is a joint vision of DBA that responds to the previously discussed vertical decomposition of [Chi07] and, in general, to cross-layer designs. In this joint direction goes the work in [Sol06] for a single-carrier WiMAX network. The authors use a NUM formulation similar to (2.1) and extend it to a proper selection of the link capacities as

$$\begin{array}{cc} \max\limits_{\{r_i\},\boldsymbol{c}} & \sum_{i=1}^{N} U_i(r_i) \\ s.t. & \boldsymbol{A}\boldsymbol{r} \leq \boldsymbol{c} \\ & \boldsymbol{c} \in \mathcal{C} \\ & r_i \geq 0 \end{array} , \tag{2.8}$$

where r_i is the rate of the i^{th} flow, $\boldsymbol{A}$ is the routing matrix and $\mathcal{C}$ is the set of all feasible link rates, i.e. the capacity region of the network. The authors divide the problem into a flow allocation problem (solving $\{r_i\}$ for fixed $\boldsymbol{c}$) and a scheduling problem that updates the link rates in order to find the optimal value of (2.8). They make use of the Mean Value Cross (MVC) decomposition method (described in Section 3.2.3) to attain a vertically distributed solution.

The works about DBA in WiMAX that have appeared in the literature can be understood as particular solutions to smaller problems considering parts of the aspects included in the general framework in (2.8). Depending on the PHY-layer considered and on the network topology, researchers put more stress on some network issues than in others. For example, the works in

[Erw06, Niy07] put the emphasis on the flow control part of two distinct network topologies. In particular, [Niy07] assumes a mesh topology and formulates the flow control using game theory and attaining a Nash bargaining solution. Papers [AY07, Mak07] provide algorithms to optimize the sum-rate in a single-cell OFDMA WiMAX system by allocating subcarriers to users in the OFDM modulation and by performing bit and power allocation. On the other hand, the concern in [Tao05, Wei05, Du07] is to find a proper routing tree and scheduling in mesh mode in order to minimize interference among transmissions (possibly allowing concurrent transmission), which allows us to enhance the network throughput or to reduce the length of the scheduling cycle. We define the length of the scheduling cycle as the number of time slots required to complete all pending transmissions.

In summary, the challenge is to be able to provide practical mechanisms that allow us to jointly optimize as many system variables as possible (i.e. including scheduling, flow control, power allocation, ...). Therefore, we need to cope with general formulations that include these variables in the PHY and MAC layers (and possibly higher layers), as it is the case in (2.8). In that context, distributed computation techniques are crucial to split the optimization into the distinct layers and network elements and hence, to define future cross-layer interactions and protocols. In our DBA contribution in Chapter 5, we concentrate on the flow control problem (as an important piece in more sophisticated formulations) in PMP and tree-deployed WiMAX mesh networks. More precisely, we show that it is possible to attain a fully distributed and time efficient computation thanks to the coupled-decomposition method described in Sec. 3.3.

Chapter 3

Unified Decompositions Framework in Convex Programming

This chapter is devoted to the main theoretical contribution of this thesis: a framework to formulate and efficiently solve DBA problems. The results herein have been derived using a special mixture of two distinct lines of thought in the mathematical optimization community, namely convex optimization theory and mathematical decomposition theory. The former defines an important type of problems in optimization with many real application examples in engineering (see for example [Boy03, Part II], [Dat99, Ch. 5] and [Ger05, Ch. 8]). The latter provides some results that allow us to split some specific optimization problems into several smaller (and more tractable) problems (from now on the subproblems). We review both theories before describing our proposed method.

3.1 Review of Convex Optimization Theory

In order to write a formal definition of a convex optimization problem (or convex program), consider first the following representation of a general optimization problem,

$$\begin{array}{ll} \min\limits_{\boldsymbol{x}} & f_0(\boldsymbol{x}) \\ s.t. & f_i(\boldsymbol{x}) \leq 0 \quad 1 \leq i \leq m \\ & h_i(\boldsymbol{x}) = 0 \quad 1 \leq i \leq p \end{array} , \tag{3.1}$$

where $\boldsymbol{x} \in \mathbb{R}^n$ are the optimization variables and $f_0(\boldsymbol{x})$ is the objective function. The problem is constrained through the functions f_i and h_i on the variables in $\boldsymbol{x}$. The first ones are called inequality constraints while the second ones are the equality constraints. In case there were none of them, the problem is said to be unconstrained and it is a classic problem in the optimization literature, strongly related to the numerical resolution of nonlinear equations. A good reference can be found in [Den83].

A particularization of (3.1) conducts to the definition of a convex optimization problem.

More precisely, if the functions $f_0 \dots f_m$ are convex functions of the variables and the functions $h_1 \dots h_p$ are affine (linear) functions, then the problem is said to be convex. A function $f : \mathbb{R}^n \longrightarrow \mathbb{R}$ is convex if, for any two points in its domain, $\boldsymbol{x}$ and $\boldsymbol{y}$, and any scalar $\theta \in [0, 1]$, it holds: i) the domain of the function is a convex set, i.e. $\theta\boldsymbol{x} + (1-\theta)\boldsymbol{y} \in \text{dom } f$ and ii) $f(\theta\boldsymbol{x} + (1-\theta)\boldsymbol{y}) \leq \theta f(\boldsymbol{x}) + (1-\theta)f(\boldsymbol{y})$. That is, the value of the function at any point within the line segment between $\boldsymbol{x}$ and $\boldsymbol{y}$ is always under the segment that connects the points $f(\boldsymbol{x})$ and $f(\boldsymbol{y})$. Note that some well-studied problems in the literature fall or can be arranged into a convex representation. For example, when all the functions f_i and h_i are affine (linear), we talk about linear programs (LP), or when the objective function is quadratic and the constraint functions are linear, it is a quadratic program (QP).

The goal in convex optimization problems (and in all optimization problems in general) is to find the optimal solution to the problem, which we denote as $\boldsymbol{x}^*$. The optimal solution is the point in the domain of the optimization problem that attains the minimum possible value of the objective function, i.e., $p^* = f(\boldsymbol{x}^*)$, and accomplishes all (equality and inequality) constraints. A formal definition of the domain of the problem is the set of points where the objective and constraint functions are defined, i.e.,

$$D = \bigcap_{i=0}^{m} \text{dom } f_i \cap \bigcap_{i=1}^{p} \text{dom } h_i \tag{3.2}$$

A subset of the domain of the problem is the feasible set and it contains all the feasible points of the optimization problem. A feasible point is a point in D that accomplishes all the constraints. On the contrary, an unfeasible point belongs to D but does not satisfy at least one constraint. Therefore, the optimal solution is always inside the feasible set. In the case the feasible set is empty, we say that the optimal value of the problem $p^* = +\infty$. Regarding inequality constraints, we distinguish between those that are satisfied with equality in a given point inside the feasible set and those that are not. We call active constraints to the first ones and inactive constraints to the second ones.

Such convex optimization problems have attracted much attention in the last decades with many application examples. See some of them in [Boy03, Part II]. Also in the communications community, the convex way of representing and solving problems has inspired lots of works and it has been the tool to deal with problems that had not been solved previously. A good example, among others, is the work of D.P. Palomar [Pal03].

From a practical point of view, we have good numerical procedures to compute convex problems. This implies that if it is possible to write a given problem in convex form, we can say that it is readily solved. Many works that can be found in the literature are devoted to transforming original non-convex problems to their equivalent convex representations. This is not always possible and there is not a systematical procedure to do so, requiring some handcrafted

work.

3.1.1 Numerical Algorithms to Solve Convex Problems

Convex problems can be sometimes solved analytically thanks to the optimality conditions of the solution. These are well defined in the so-called Karush-Kuhn-Tucker (KKT) conditions, which we review later. In this section, we want present an overview of the numerical algorithms that are used in convex problems, and maybe the most famous ones are the family of interior point methods. They were initially proposed for linear programming by Karmarkar in 1984 and generalized for convex problems in [Nes94]. As one of the major contributions of this thesis is a novel algorithm specialized in a particular case of convex problems, a brief idea of interior-point methods will give the reader some perspective about the topic.

In the sequel, a basic interior-point method, the barrier method, is presented. Further details to the ones exposed next can be found in [Boy03, Sec. 11.3]. Notwithstanding, other representative methods that we do not review here are the primal-dual interior-point methods [Boy03, Sec 11.7], [Ber99, Sec. 4.4.4] and the cutting plane methods [Ber99, Sec. 6.3.3]. Let us consider now a reformulation of (3.1) that implicitly includes the inequality constraints in the objective function:

$$\begin{array}{ll} \min\limits_{\boldsymbol{x}} & f_0(\boldsymbol{x}) + \sum_{i=1}^{m} I^-(f_i(\boldsymbol{x})) \\ s.t. & \boldsymbol{A}\boldsymbol{x} = \boldsymbol{b} \end{array} , \tag{3.3}$$

where $\boldsymbol{A} \in \mathbb{R}^{p \times n}$ with $rank(\boldsymbol{A}) = p < n$, the functions f_i $(i = 0 \dots m)$ are assumed to be twice differentiable and $I^- : \mathbb{R} \longrightarrow \mathbb{R}$ is the indicator function for the non-positive real numbers:

$$I^-(u) = \begin{cases} 0 & u \leq 0 \\ \infty & u > 0 \end{cases} . \tag{3.4}$$

Note that the indicator functions enforce to search the optimal solution inside the feasible set and also to keep the objective function of the redefined problem equal to $f_0(\boldsymbol{x})$ in the feasible set.

The logarithmic barrier method approximates the indicator function as

$$\hat{I}^-(u) = (-\frac{1}{t}) \log(-u) \tag{3.5}$$

which is twice differentiable and a smooth functions of the variable u. The reader can find in Figure 3.1 two different plots of the indicator function for two values of the parameter t, namely $t = 0.5$ and $t = 2$. Note that as the value of t increases, the approximation resembles more and more the indicator function.

The basic idea of the method is quite simple and intuitive. Assuming that good numerical methods to solve unconstrained convex problems are available and well studied (e.g. Newton-like methods[Boy03, Fle80]), the idea of the barrier method is to solve a sequence of unconstrained

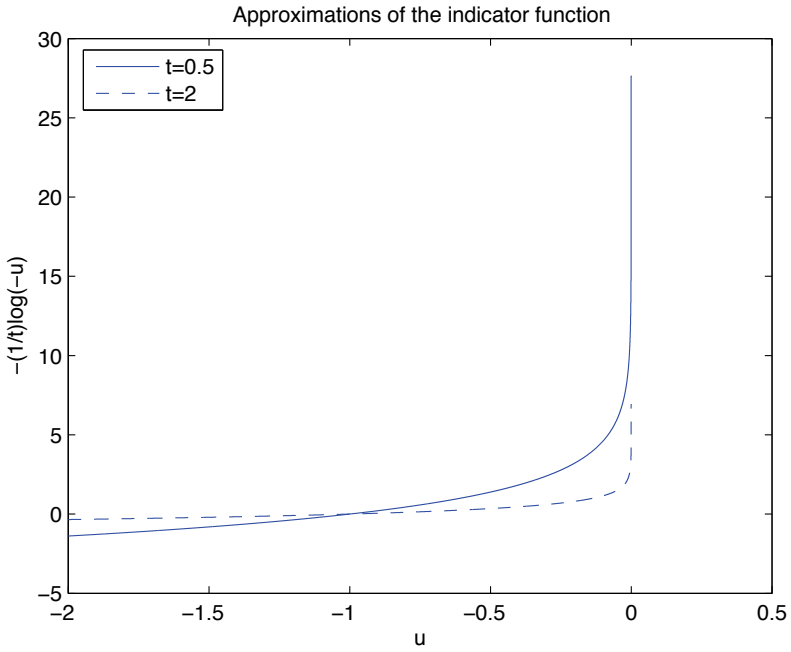

Figure 3.1: Approximations of the indicator function.

minimization problems in such a way that, in the last iterations, the problem resembles as much as desired the original problem. In practical terms, the method first uses a non-accurate approximation of $I^-(u)$, i.e. with a low value for t and computes the solution. This is used as the initial guess to solve the next unconstrained problem, that uses an increased value of t. The equivalent problem to (3.3) that is solved at each iteration (from [Boy03])

$$\begin{array}{ll} \min & t\, f_0(\boldsymbol{x}) + \phi(\boldsymbol{x}) \\ s.t. & \boldsymbol{A}\boldsymbol{x} = \boldsymbol{b} \end{array} \tag{3.6}$$

where $\phi(\boldsymbol{x}) = -\sum_{i=1}^{m} \log\left(-f_i(\boldsymbol{x})\right)$ with $\mathbf{dom}\phi = \{\boldsymbol{x} \in \mathbb{R}^n | f_i(\boldsymbol{x}) < 0, i = 1, \ldots, m\}$ is called the logarithmic barrier of the problem. The name of the method comes from the use of those mathematical barriers that avoid to find a solution outside the feasible set and that slightly modify the objective function inside the set (assuming a high value for the parameter t).

Then a summary of the method is [Boy03]:

---

given an strictly feasible $\boldsymbol{x}$, $t := t^0$ and $\mu > 1$

repeat

1. Compute $\boldsymbol{x}^*(t)$ by solving (3.6) with initial guess $\boldsymbol{x}$
2. Update $\boldsymbol{x} = \boldsymbol{x}^*(t)$
3. Stopping criterion: quit if the optimal solution is found

4. Increase t, $t := \mu t$

In numerical optimization, the stopping criterion defines when the optimal solution has been found so that the iterations can be stopped. Typical stopping criteria decide to finish the iterative procedure when $\frac{|f_0(\boldsymbol{x}^{n+1})-f_0(\boldsymbol{x}^n)|}{|f_0(\boldsymbol{x}^{n+1})|} < \epsilon$ or $\frac{||\boldsymbol{x}^{n+1}-\boldsymbol{x}^n||}{||\boldsymbol{x}^{n+1}||} < \epsilon$ or both. However, depending on the operating principles of each particular method, other criterions can be designed. In the previous examples, n indexes iterations and ϵ is the tolerance of the method.

After this brief review of a particular case of an interior point method, note that the method is clearly dependent on the parameters t and μ, which are defined arbitrarily (the interested reader can find some guide on the design of the parameters in [Boy03]). Furthermore, the performance in speed of convergence of the algorithm is affected by a proper or improper choice. This fact is not an exclusive feature of the barrier method and it is quite common among numerical optimization procedures (in interior point methods and even in Newton-like methods). Although it is something unavoidable in most cases, that dependance on user-defined parameters is not desirable. An interesting issue from that point of view is to contribute with methods that are non-parameter dependant. We achieve this with the novel method proposed in this thesis.

3.1.2 Duality Theory in Convex Optimization

Once convex problems have been formally defined and once some flavour about how to solve them numerically (using interior-point methods) has been given, it is the turn now to introduce a different (but related) perspective to look at optimization problems in general. In this occasion, duality theory is introduced. It is not specific to convex optimization problems and allows to formally formulate any optimization problem using an alternative representation. In that sense, the reader can think about the possibility of having two versions of the same problem, namely the primal and the dual problem (hence the name of dual). The primal problem is already defined in (3.1) and the dual problem is derived using the Lagrange dual function. Thanks to duality theory applied to convex problems, many useful optimality conditions have been derived. These are summarized in the so-called KKT conditions, which have provided most of the analytical or semi-analytical solutions to convex problems in many areas of interest.

Consider again the problem in (3.1) and define the Lagrangian function of the problem as

$$L(\boldsymbol{x}, \boldsymbol{\lambda}, \boldsymbol{\nu}) = f_0(\boldsymbol{x}) + \sum_{i=1}^{m} \lambda_i f_i(\boldsymbol{x}) + \sum_{i=1}^{p} \nu_i h_i(\boldsymbol{x}) \tag{3.7}$$

with $\operatorname{dom} L = D \times \mathbb{R}^m \times \mathbb{R}^p$. The set of variables $\boldsymbol{\lambda}$ and $\boldsymbol{\nu}$ are the Lagrange multipliers associated to the constraints. More precisely, λ_i is associated to $f_i(\boldsymbol{x}) \leq 0$ and ν_i is associated to $h_i(\boldsymbol{x}) = 0$. Note that the Lagrangian function is the objective function of the original problem additively augmented by the constraints of the problem (each one scaled by its corresponding multiplier).

From the Lagrangian function, the Lagrange dual function (or just dual function) is defined as the minimizer of $L(\boldsymbol{x}, \boldsymbol{\lambda}, \boldsymbol{\nu})$ over the variables in $\boldsymbol{x}$. Hence, $g : \mathbb{R}^m \times \mathbb{R}^p \longrightarrow \mathbb{R}$,

$$g(\boldsymbol{\lambda}, \boldsymbol{\nu}) = \inf_{\boldsymbol{x} \in D} L(\boldsymbol{x}, \boldsymbol{\lambda}, \boldsymbol{\nu}) = \inf_{\boldsymbol{x} \in D} \left(f_0(\boldsymbol{x}) + \sum_{i=1}^{m} \lambda_i f_i(\boldsymbol{x}) + \sum_{i=1}^{p} \nu_i h_i(\boldsymbol{x}) \right) \tag{3.8}$$

In the case the Lagrangian is unbounded below in $\boldsymbol{x}$, the dual function takes the value $-\infty$. We say that the values $(\boldsymbol{\lambda}, \boldsymbol{\nu})$ with $\boldsymbol{\lambda} \succeq 0$ and $g(\boldsymbol{\lambda}, \boldsymbol{\nu}) > -\infty$ are dual feasible.

Both the Lagrangian in (3.7) and the dual function in (3.8) are not exclusive definitions of convex problems. They are valid for all type of problems. However, some useful results appear when convex problems are considered. A key point now is that the dual function is a concave function of the dual variables ($\boldsymbol{\lambda}$ and $\boldsymbol{\nu}$), even if the original problem is not convex, as it is the point-wise minimum of a family of affine functions of $(\boldsymbol{\lambda}, \boldsymbol{\nu})$ [Boy03].

Proof. Consider that $f_1(\boldsymbol{\lambda})$ and $f_2(\boldsymbol{\lambda})$ are two concave functions over the variable $\boldsymbol{\lambda}$ and define

$$f(\boldsymbol{\lambda}) = \min \{ f_1(\boldsymbol{\lambda}), f_2(\boldsymbol{\lambda}) \} \tag{3.9}$$

with $\mathbf{dom} f = \mathbf{dom} f_1 \cap \mathbf{dom} f_2$. We want to prove first that $f(\boldsymbol{\lambda})$ is also a concave function of $\boldsymbol{\lambda}$. This fact is easily verified form the definition of concavity. For any two given points in $\mathbf{dom}\, f$, $\boldsymbol{\lambda}_1$, $\boldsymbol{\lambda}_2$, and any scalar θ, $0 \leq \theta \leq 1$, we already know

$$f_i(\theta \boldsymbol{\lambda}_1 + (1-\theta)\boldsymbol{\lambda}_2) \geq \theta f_i(\boldsymbol{\lambda}_1) + (1-\theta) f_i(\boldsymbol{\lambda}_2), \qquad i = 1, 2 \tag{3.10}$$

The definition is also verified with the function f as

$$\begin{aligned} f(\theta \boldsymbol{\lambda} + (1-\theta)\boldsymbol{\lambda}) &= \min \{ f_1(\theta \boldsymbol{\lambda}_1 + (1-\theta)\boldsymbol{\lambda}_2), f_2(\theta \boldsymbol{\lambda}_1 + (1-\theta)\boldsymbol{\lambda}_2) \} \\ &\geq \min \{ \theta f_1(\boldsymbol{\lambda}_1) + (1-\theta) f_1(\boldsymbol{\lambda}_2), \theta f_2(\boldsymbol{\lambda}_1) + (1-\theta) f_2(\boldsymbol{\lambda}_2) \} \\ &\geq \theta \min \{ f_1(\boldsymbol{\lambda}_1), f_2(\boldsymbol{\lambda}_2) \} + (1-\theta) \min \{ f_1(\boldsymbol{\lambda}_1), f_2(\boldsymbol{\lambda}_2) \} = \theta f(\boldsymbol{\lambda}_1) + (1-\theta) f(\boldsymbol{\lambda}_2) \end{aligned} \tag{3.11}$$

Note also that $\min \{ f_1(\boldsymbol{\lambda}), f_2(\boldsymbol{\lambda}), f_3(\boldsymbol{\lambda}) \} = \min \Big\{ \min \{ f_1(\boldsymbol{\lambda}), f_2(\boldsymbol{\lambda}) \},\ f_3(\boldsymbol{\lambda}) \Big\}$. Recursively applying this result, it is derived that the point-wise minimum of any number of concave functions is also concave. The dual function is then a family of affine functions of $\boldsymbol{\lambda}$ and $\boldsymbol{\nu}$ (indexed by all the points $\boldsymbol{x} \in D$) and hence, concave. ■

Example 1: Consider the problem

$$\begin{array}{ll} \min & 3(x-2)^2 - \log y \\ s.t. & x + y \leq 1 \end{array} \tag{3.12}$$

with primal variables x and y and $D = \mathbb{R} \times \mathbb{R}_{++}$. In Figure 3.2 the reader can find a plot of the objective function (left) and a contour plot of the same function together with the constraint $x+y = 1$ (right). Note that the optimal values of the problem (x^*, y^*) can be obtained graphically in this small example.

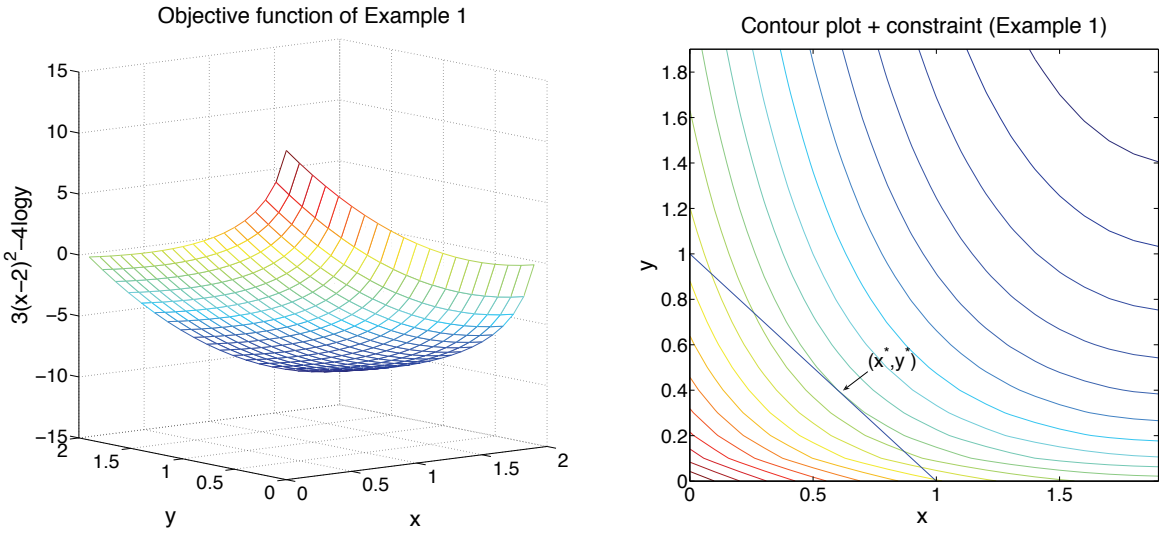

Figure 3.2: Objective function and contour plot + constraint for Example 1.

The Lagrangian function of the problem is

$$L(x, y, \lambda) = 3(x-2)^2 - \log y + \lambda(x + y - 1) \tag{3.13}$$

Forcing the partial derivative of $L(x, y, \lambda)$ with respect to x (or y) equal to zero, we obtain the following minimizers of the Lagrangian, which are functions of the multiplier λ:

$$x^*(\lambda) = \frac{12 - \lambda}{6}, \quad y^*(\lambda) = \frac{1}{\lambda} \tag{3.14}$$

Finally, the substitution into the Lagrangian gives the dual function, which in this case is:

$$g(\lambda) = \frac{-\lambda^2}{12} + \log \lambda + \lambda + 1 \tag{3.15}$$

It is easily verified that the dual function is concave. In Figure 3.3, $g(\lambda)$ is represented and the maximum value of the function is marked as λ^*.

An important property of the dual function is that it is a lower bound of the optimal value of the problem p^*. That is, for any $\boldsymbol{\lambda} \succeq 0$ and any $\boldsymbol{\nu}$, it holds that

$$g(\boldsymbol{\lambda}, \boldsymbol{\nu}) \leq p^*. \tag{3.16}$$

Given a feasible point $\boldsymbol{x}^{\triangleright}$ for the problem in (3.1) and $\boldsymbol{\lambda} \succeq 0$, then

$$L(\boldsymbol{x}^{\triangleright}, \boldsymbol{\lambda}, \boldsymbol{\nu}) = f_0(\boldsymbol{x}^{\triangleright}) + \sum_{i=1}^{m} \lambda_i f_i(\boldsymbol{x}^{\triangleright}) + \sum_{i=1}^{p} \nu_i h_i(\boldsymbol{x}^{\triangleright}) \leq f_0(\boldsymbol{x}^{\triangleright}), \tag{3.17}$$

since $\sum_{i=1}^{p} \nu_i h_i(\boldsymbol{x}^{\triangleright}) = 0$ for a feasible $\boldsymbol{x}$ and $\sum_{i=1}^{m} \lambda_i f_i(\boldsymbol{x}^{\triangleright}) \leq 0$ for a feasible $\boldsymbol{x}$ and $\boldsymbol{\lambda} \succeq 0$. It is also true that

$$g(\boldsymbol{\lambda}, \boldsymbol{\nu}) = \min_{\boldsymbol{x} \in D} L(\boldsymbol{x}, \boldsymbol{\lambda}, \boldsymbol{\nu}) \leq L(\boldsymbol{x}^{\triangleright}, \boldsymbol{\lambda}, \boldsymbol{\nu}) \leq f_0(\boldsymbol{x}^{\triangleright}) \tag{3.18}$$

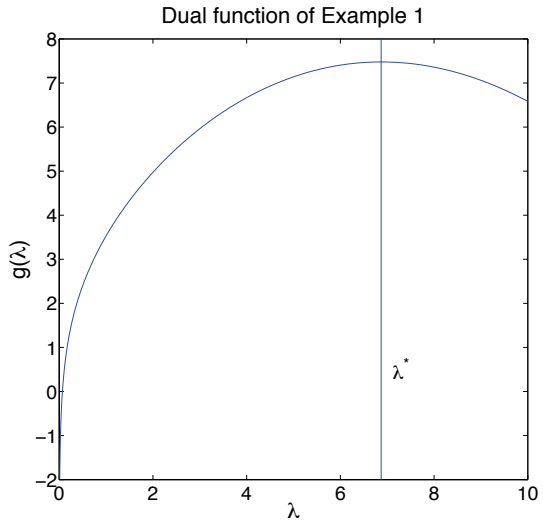

Figure 3.3: Dual function for Example 1.

since the dual function chooses a minimizer of the Lagrangian in the set D, that includes the feasible set. And as (3.18) is valid for every feasible point, it also holds for $f_0(\boldsymbol{x}^*) = p^*$.

In the light of the previous result and as the dual function is concave, it makes sense to find the best under-estimator of p^* from a dual point of view. We refer to it as d^* and it is obtained as the solution of the following convex optimization problem

$$\begin{array}{lll} d^* = & \max\limits_{\boldsymbol{\lambda},\boldsymbol{\nu}} & g(\boldsymbol{\lambda},\boldsymbol{\nu}) \\ & s.t. & \boldsymbol{\lambda} \succeq 0 \end{array} \tag{3.19}$$

Note that the constraints are convex and that to maximize a concave function $g(\boldsymbol{\lambda},\boldsymbol{\nu})$ is equivalent to minimize $-g(\boldsymbol{\lambda},\boldsymbol{\nu})$, which is convex. We have shown that

$$d^* \leq p^*. \tag{3.20}$$

We refer to the quantity $|p^* - d^*|$ as the duality gap. When the duality gap is zero, we say that strong duality holds. Otherwise, we have weak duality.

All the results discussed up to now about Lagrange duality hold even when the problem under study is not convex. When the previous analysis is applied to convex problems, we reach a central result of great importance in convex optimization. It establishes that, under some technicalities (usually called constraint qualifications), the duality gap reduces to zero [Boy03]. A simple version of the constraint qualifications is Slater's condition, that is satisfied if the problem in (3.1) has at least one strictly feasible point (if $f_i(\boldsymbol{x}^\dagger) < 0$, $i = 1, \ldots, m$ and $h_i(\boldsymbol{x}^\dagger) = 0$, $i = 1, \ldots, p$, then $\boldsymbol{x}^\dagger$ is strictly feasible). Constraint qualifications are not hard to accomplish and most convex problems exhibit strong duality.

Assuming that strong duality holds, convex problems can be solved by minimizing the primal problem in (3.1) or, equivalently, one can solve the dual problem in (3.19). In other words, given the optimal values for the dual, $\boldsymbol{\lambda}^*$ and $\boldsymbol{\nu}^*$, the primal optimal point $\boldsymbol{x}^*$ is readily found as the minimizer of the Lagrangian.

Let us suppose that we have both primal ($\boldsymbol{x}^*$) and dual ($\boldsymbol{\lambda}^*, \boldsymbol{\nu}^*$) optimal values and that we have strong duality. Then,

$$\begin{array}{c} d^* = g(\boldsymbol{\lambda}^*, \boldsymbol{\nu}^*) = L(\boldsymbol{x}^*, \boldsymbol{\lambda}^*, \boldsymbol{\nu}^*) \\ = f_0(\boldsymbol{x}^*) + \sum_{i=1}^m \lambda_i^* f_i(\boldsymbol{x}^*) + \sum_{i=1}^p \nu_i^* h_i(\boldsymbol{x}^*) = p^* = f_0(\boldsymbol{x}^*), \end{array} \tag{3.21}$$

and as $\sum_{i=1}^p \nu_i h_i(\boldsymbol{x}) = 0$ for any feasible point (also for x^*), it must hold that

$$\lambda_i^* f_i(\boldsymbol{x}^*) = 0, \qquad i = 1, \ldots, m \tag{3.22}$$

since $\lambda_i \geq 0$ and $f_i(x) \leq 0$ in the feasible set. The set of conditions in (3.22) are called complementary slackness conditions. From slackness conditions, we know that if $\lambda_i > 0$, then the i^{th} inequality constraint is active, i.e. $f_i(\boldsymbol{x}) = 0$. Conversely, if the optimal solution is not bounded by the i^{th} inequality constraint, then $\lambda_i = 0$ and the Lagrange function is not augmented by $f_i(\boldsymbol{x})$.

Note also from (3.21) that $d^* = p^* = g(\boldsymbol{\lambda}^*, \boldsymbol{\nu}^*)$. Taking into account the definition of the dual function in (3.8), we can conclude that the gradient of the Lagrangian must vanish at $(\boldsymbol{x}^*, \boldsymbol{\lambda}^*, \boldsymbol{\nu}^*)$. With that last condition and grouping previous results, we can formulate the KKT conditions for convex problems (whenever strong duality holds):

$$\begin{array}{rcll} f_i(\boldsymbol{x}^*) & \leq & 0, & i = 1, \ldots, m \\ h_i(\boldsymbol{x}^*) & = & 0, & i = 1, \ldots, p \\ \lambda_i^* & \geq & 0, & i = 1, \ldots, m \\ \lambda_i^* f_i(\boldsymbol{x}^*) & = & 0, & i = 1, \ldots, m \\ \nabla f_0(\boldsymbol{x}^*) + \sum_{i=1}^m \lambda_i^* \nabla f_i(\boldsymbol{x}^*) + \sum_{i=1}^p \nu_i^* \nabla h_i(\boldsymbol{x}^*) & = & 0. & \end{array} \tag{3.23}$$

In practical terms, KKT conditions are very useful to find analytical solutions to convex problems.

3.2 Review on Decomposition Methods

The philosophy under decomposition methods [Ber99, Las02] is very simple: the idea is to split an optimization problem into several smaller problems, which are usually called *the subproblems*, and let a *master problem* to be in charge of coordinating all the subproblems so as to achieve the global optimum. Therefore, all decomposition techniques require some signalling between the subproblems and the master problem.

This approach is advantageous in many cases since it is easier to solve each of the subproblems separately than to attack the original problem as a whole. There are, however, additional motivations in some application examples within the communications area, where decomposition methods have attracted much attention in the recent years due to the fact that distributed solutions have been used to cope with some problems that are still of interest. A good example of that can be found in the works of Chiang [Chi07] and Palomar (see [Pal07] and references therein).

In the sequel, two basic decomposition methods are revisited, namely primal decomposition (also known as *decomposition by right-hand side allocation* [Ber99]) and dual decomposition (also referred to as *Lagrangian relaxation of the coupling constraints* or *decomposition using a pricing mechanism* [Ber99, Las02]). Finally, a more recent approach that combines both primal and dual decompositions, the Mean Value Cross (MVC) decomposition method, is revisited [VR83, Hol92, Hol97, Hol06].

3.2.1 Primal Decomposition

A primal decomposition strategy is adequate for separable problems of the form

$$\begin{array}{lll} \min\limits_{\{\boldsymbol{y}_j,\boldsymbol{x}_j\}} & \sum_{j=1}^{J} f_j(\boldsymbol{x}_j) & \\ s.t. & \boldsymbol{x}_j \in \mathcal{X}_j, & j=1,\ldots,J \\ & \boldsymbol{A}_j\boldsymbol{x}_j \preceq \boldsymbol{y}_j, & j=1,\ldots,J \\ & \sum_{j=1}^{J} \boldsymbol{y}_j \preceq \boldsymbol{b} & \end{array} \tag{3.24}$$

with variables $\{\boldsymbol{x}_j, \boldsymbol{y}_j\}$. Here, $f_j : \mathbb{R}^{n_j} \longrightarrow \mathbb{R}$ and $\mathcal{X}_j$ are subsets in $\mathbb{R}^{n_j}$. Furthermore, $\boldsymbol{A}_j$ is a $r \times n_j$ matrix with real entries and $\boldsymbol{b}, \{\boldsymbol{y}_j\} \in \mathbb{R}^r$.

Note that for fixed values of $\{\boldsymbol{y}_j\}$, the problem is fully separable. A primal decomposition technique makes use of this fact. Equivalently to (3.24), we can write

$$\begin{array}{lll} \min\limits_{\{\boldsymbol{y}_j\}} & \sum_{j=1}^{J} & \min\limits_{\substack{\boldsymbol{x}_j \in \mathcal{X}_j \\ \boldsymbol{A}_j\boldsymbol{x}_j \preceq \boldsymbol{y}_j}} f_j(\boldsymbol{x}_j) \\ s.t. & \sum_{j=1}^{J} \boldsymbol{y}_j \preceq \boldsymbol{b}, \ \boldsymbol{y}_j \in \mathcal{Y}_j, & j=1,\ldots,J \end{array} \tag{3.25}$$

where the subsets $\mathcal{Y}_j$ take into account that the inner minimization problem,

$$p(\boldsymbol{y}_j) = \begin{array}{ll} \min & f_j(\boldsymbol{x}_j) \\ s.t. & \boldsymbol{A}_j\boldsymbol{x}_j \preceq \boldsymbol{y}_j, \quad \boldsymbol{x}_j \in \mathcal{X}_j \end{array} \tag{3.26}$$

has at least one feasible solution. The inner minimization problems are usually called the subproblems, and they depend on the values taken by the variables $\boldsymbol{y}_j$ with $\mathbf{dom}\, p_j = \mathcal{Y}_j$.

Using this definition, the original problem in (3.24) is rewritten as

$$\begin{array}{ll} \min & \sum_{j=1}^{J} p_j(\boldsymbol{y}_j) \\ s.t. & \sum_{j=1}^{J} \boldsymbol{y}_j \preceq \boldsymbol{b}, \ \boldsymbol{y}_j \in \mathcal{Y}_j, \quad j=1,\ldots,J \end{array} \tag{3.27}$$

and is usually called the master problem. Note that with this approach, the master problem fixes the variables $\boldsymbol{y}_j$ so as to achieve the optimum of the problem given the coupling constraint. Using these values, the subproblems fix, at their turn, the local variables $\boldsymbol{x}_j$. Often in the literature a resource allocation interpretation is given to this strategy. Imagine that the total quantity of available resources is $\boldsymbol{b}$ and that it has to be distributed among some entities, the subproblems. Under this point of view, the master problem decides the allocation of the available resources while the subproblems are in charge of achieving the highest revenue with the granted values of the shared means.

Up to this point, no convexity assumptions have been made, so the discussion above is valid for all kind of problems in the form of (3.24). However, from a practical point of view, the interest is in finding the optimal solutions to the problem. In the sequel, a pretty simple numerical method, the subgradient method, is reviewed to attain the optimal solution when the subsets $\mathcal{X}_j$ are convex and the functions $f_j(\boldsymbol{x}_j)$ are also convex.

The subgradient method is in fact an adaptation of the gradient projection method [Ber99, Sec. 2.3] to the problem in (3.27). In short, the gradient projection method iteratively finds the solution to the problem by: i) moving the current solution towards a descent direction (the opposite of the gradient) and ii) projecting the solution onto the feasible set. In the case under study, a deeper insight into the functions $p_j(\boldsymbol{y}_j)$ is required. We need to certify that the subsets $\mathcal{Y}_j$ are convex, which is required by the gradient projection method. Another issue is to define and to be able to numerically evaluate a gradient (or a similar function) of $p_j(\boldsymbol{y}_j)$ at any point in $\mathcal{Y}_j$. Note that, in general, any descent-type method will find local solutions to the problem under study. However, if the problem is convex, a local solution is also global [Ber99, Prop. 2.1.1]. Since it is assumed that $f_j(\boldsymbol{x}_j)$ are convex, it is also important to establish the convexity of $p(\boldsymbol{y}_j)$.

In order to answer the questions above, let us rewrite the j^{th} subproblem in (3.26) in a more general form [Ber99, Sec. 5.4.4] (subindex j is omitted in the subsequent analysis).

$$p(\boldsymbol{y}) = \min_{\substack{\boldsymbol{x} \in \mathcal{X} \\ g_i(\boldsymbol{x}) \leq y_i,\ i = 1, \ldots, r}} f(\boldsymbol{x}). \tag{3.28}$$

with $\mathbf{dom}\, p = \mathcal{Y}$ as above. The functions $g_i(\boldsymbol{x})$ are convex and define the feasible set of the problem for a given[1] $\boldsymbol{y}$. Note that we can interpret that representation as a perturbation on the general representation of a convex problem, with tightened or loosened constraints. That is, if $y_i > 0$, then we are loosening the i^{th} constraint; otherwise, when $y_i < 0$, we are tightening the i^{th} constraint. When $\boldsymbol{y} = \mathbf{0}$, the problem resembles to the initial formulation in (3.1).

[1] They shall not be confused with the dual function $g(\boldsymbol{x})$.

Lemma 1 *Given the problem in (3.28), i holds that: i) the subset $\mathcal{Y}$ is a convex subset and ii) the function $p(\boldsymbol{y})$ is convex over $\mathcal{Y}$.*

Proof. See [Ber99]. To verify it, take any two points inside $\mathcal{Y}$, $\boldsymbol{y}_1$ and $\boldsymbol{y}_2$, any scalar $\alpha \in [0,1]$ and $\epsilon > 0$. Then choose any two points inside $\mathcal{X}$, i.e. $\boldsymbol{x}_1, \boldsymbol{x}_2 \in \mathcal{X}$, that satisfy: i) $\boldsymbol{g}(\boldsymbol{x}_i) \preceq \boldsymbol{y}_i,\ i = 1,2$ and ii) $f(\boldsymbol{x}_i) \leq p(\boldsymbol{y}_i) + \epsilon,\ i = 1,2$. Assuming convexity of $\mathcal{X}, f$ and $\{g_i\}$, it holds that [Ber99]

$$p\left(\alpha \boldsymbol{y}_1 + (1-\alpha)\boldsymbol{y}_2\right) \leq \alpha p(\boldsymbol{y}_1) + (1-\alpha)p(\boldsymbol{y}_2) + \epsilon. \tag{3.29}$$

Since $p\left(\alpha \boldsymbol{y}_1 + (1-\alpha)\boldsymbol{y}_2\right) < +\infty$, $\alpha \boldsymbol{y}_1 + (1-\alpha)\boldsymbol{y}_2 \in \mathcal{Y}$ and $\mathcal{Y}$ is a convex set. And taking the limit $\epsilon \longrightarrow 0$, (3.29) converts into the definition of a convex function, so the primal subproblems are convex functions with convex domains. ■

To finally complete the subgradient method, a gradient of the primal subproblems at any point inside the corresponding domains is required. In the general case, the subproblems are convex but non-differentiable, so the existence of a gradient is not guaranteed. However, it is possible to resort to a more general definition of the concept, the subgradient. It does not require differentiability and suits for our purposes. From [Las02, Appendix 2], a vector $\boldsymbol{s}(\boldsymbol{x}^0)$ is said to be a subgradient of f at the point $\boldsymbol{x}^0$ if it holds

$$f(\boldsymbol{x}) \geq f(\boldsymbol{x}^0) + \boldsymbol{s}(\boldsymbol{x}^0)^T(\boldsymbol{x} - \boldsymbol{x}^0) \tag{3.30}$$

and thus, the subgradient is the slope of a supporting hyperplane of f at $\boldsymbol{x}^0$, even if the function is non-differentiable. When f is differentiable at any point $\boldsymbol{x}$, then it holds that $\boldsymbol{s}(\boldsymbol{x}) = \nabla f(\boldsymbol{x})$. See Figure 3.4. Note in the figure that it is possible to define other subgradients at $\boldsymbol{x}^0$ accomplishing (3.30).

We assume now that strong duality holds in the problem (3.28) and that a dual optimum is attained at the point $\boldsymbol{\lambda}^*$ for the unperturbed problem (i.e., $\boldsymbol{y} = \boldsymbol{0}$). Take any feasible point $\boldsymbol{x}$ for the perturbed problem (i.e., $\boldsymbol{g}(\boldsymbol{x}) = [g_1(\boldsymbol{x}), \ldots, g_r(\boldsymbol{x})]^T \preceq \boldsymbol{y}$) and it holds

$$p(\boldsymbol{0}) = g(\boldsymbol{\lambda}^*) \leq f(\boldsymbol{x}) + \sum_{i=1}^{r} \lambda_i^* g_i(\boldsymbol{x}) \leq f(\boldsymbol{x}) + \boldsymbol{\lambda}^{*T}\boldsymbol{y} \tag{3.31}$$

since the dual function is always an under-estimator of the optimum value of the problem and $\boldsymbol{\lambda} \succeq \boldsymbol{0}$. And since $\boldsymbol{x}$ can be any point in $\mathcal{X}$, we can choose the one that gives the optimum value, $p(\boldsymbol{y})$. We finally get

$$p(\boldsymbol{0}) \leq p(\boldsymbol{y}) + \boldsymbol{\lambda}^{*T}\boldsymbol{y} \tag{3.32}$$

from where (together with (3.30)) we see that $-\boldsymbol{\lambda}^*$ is a subgradient of p at the point $\boldsymbol{y} = \boldsymbol{0}$. The result is easily extensible to any value of $\boldsymbol{y}$, $\boldsymbol{y}^{\triangleright}$, after the application of the change of variables $\boldsymbol{y}' = \boldsymbol{y} - \boldsymbol{y}^{\triangleright}$ to the perturbed problem in (3.28) and the previous derivation in (3.31)-(3.32). Therefore, we can establish that:

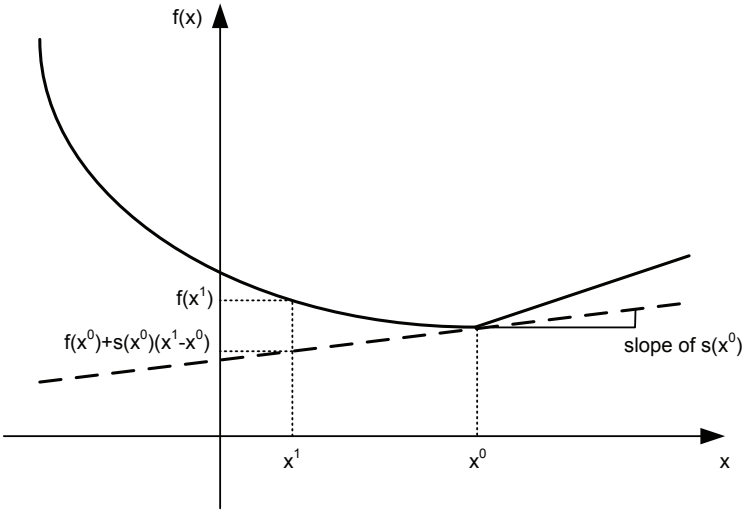

Figure 3.4: Illustration of the subgradient concept.

$-\boldsymbol{\lambda}^*(\boldsymbol{y}^\triangleright)$ is a subgradient of $p(\boldsymbol{y})$ at the point $\boldsymbol{y} = \boldsymbol{y}^\triangleright$.

Using the subgradient, problem (3.27) can be iteratively solved using the conditional gradient method [Ber99, Sec. 2.2] by just replacing the gradient with the subgradient. Therefore, it is of interest to find the subgradient of the objective function of the problem, i.e. $\sum_{j=1}^{J} p_j(\boldsymbol{y}_j)$. Using the previous relation between the subgradient and the Lagrange multipliers, it is readily established that a subgradient of the function at the point $[\boldsymbol{y}_1, \ldots, \boldsymbol{y}_J]^T$ is:

$$\underset{[\boldsymbol{y}_1,\ldots,\boldsymbol{y}_J]^T}{\boldsymbol{s}} \left(\sum_{j=1}^{J} p_j(\boldsymbol{y}_j) \right) = -[\boldsymbol{\lambda}_1^*(\boldsymbol{y}_1), \ldots, \boldsymbol{\lambda}_J^*(\boldsymbol{y}_J)]^T \tag{3.33}$$

from what the updates of the subgradient method are given by the equation (k indexes iteration number)

$$\boldsymbol{y}^{k+1} = [\boldsymbol{y}^k - \alpha^k \boldsymbol{s}^k]^\dagger \tag{3.34}$$

where $[\cdot]^\dagger$ denotes the projection on the constraint set $\left\{ \boldsymbol{y} = [\boldsymbol{y}_1, \ldots, \boldsymbol{y}_J]^T \,|\, \sum_{j=1}^{J} \boldsymbol{y}_j = \boldsymbol{b}, \boldsymbol{y}_j \in \mathcal{Y}_j \right\}$ and α^k is a positive step size. The projection of a given point on a set finds out the point in the set that is closer to the given point (in any defined distance function). Note that in the case where the point is already in the set, the projection is the same point. For more information about projections on sets, please refer to [Boy03, Sec. 8.1].

Resorting to the results on the gradient projection methods [Ber99, Sec. 2.3], there are several possibilities to set up the step size in a manner that convergence of the algorithm is guaranteed. Maybe the most used ones in practice are the constant step size, the constant step length and the diminishing step size [Pal07]. In the constant step size,

$$\alpha^k = \alpha, \qquad k = 0, 1, \ldots \tag{3.35}$$

whereas in the constant step length,

$$\alpha^k = \frac{\alpha}{\|\boldsymbol{s}^k\|}, \qquad k = 0, 1, \dots \tag{3.36}$$

For the diminishing step size, we set up α^k such that

$$\alpha^k \longrightarrow 0, \ \sum_{k=0}^{\infty} \alpha^k = \infty, \tag{3.37}$$

for example [Pal07]

$$\alpha^k = \frac{1+m}{k+m} \qquad k = 0, 1, \dots \tag{3.38}$$

where m is fixed and nonnegative. Note that in all cases the speed of convergence will depend on a user-defined parameter (α^k), which is generally not optimized to guarantee the maximum speed of the algorithm. Therefore, it is desirable to avoid such procedures when possible so as not to slow down the obtention of solutions.

3.2.2 Dual Decomposition

A dual decomposition strategy is adequate for separable problems of the form

$$\begin{array}{ll} \min\limits_{\{\boldsymbol{x}_j\}} & \sum_{j=1}^{J} f_j(\boldsymbol{x}_j) \\ s.t. & \boldsymbol{x}_j \in \mathcal{X}_j, \qquad j = 1, \dots, J \\ & \sum_{j=1}^{J} \boldsymbol{h}_j(\boldsymbol{x}_j) \preceq \boldsymbol{b}. \end{array} \tag{3.39}$$

Here, $\boldsymbol{h}_j : \mathbb{R}^{n_j} \longrightarrow \mathbb{R}^r$ and $b \in \mathbb{R}^r$.

Different to a primal decomposition, in this occasion the problem is separated thanks to a Lagrangian relaxation of the coupling constraint [Ber99, Sec. 6.4.1]. The corresponding dual function is

$$q(\boldsymbol{\mu}) = \sum_{j=1}^{J} \min_{\boldsymbol{x}_j \in \mathcal{X}_j} \left\{ f_j(\boldsymbol{x}_j) + \boldsymbol{\mu}^T \boldsymbol{h}_j(\boldsymbol{x}_j) \right\} - \boldsymbol{\mu}^T \boldsymbol{b} \tag{3.40}$$

Note that the dual function is separable, each part associated to a different $\boldsymbol{x}_j$. Taking this into account we define the subproblems, that are expressed as $q_j(\boldsymbol{\mu})$, where

$$q_j(\boldsymbol{\mu}) = \min_{\boldsymbol{x}_j \in \mathcal{X}_j} \left\{ f_j(\boldsymbol{x}_j) + \boldsymbol{\mu}^T \boldsymbol{h}_j(\boldsymbol{x}_j) \right\} \tag{3.41}$$

It is assumed at this point that it exists a vector $\boldsymbol{x}_j$ for all j and $\boldsymbol{\mu}$ that attains the minimums above. We refer to those vectors as $\boldsymbol{x}_j^*(\boldsymbol{\mu})$ and replacing them in the equation above, the dual subproblems are finally rewritten as

$$q_j(\boldsymbol{\mu}) = f_j(\boldsymbol{x}_j^*(\boldsymbol{\mu})) + \boldsymbol{\mu}^T \boldsymbol{h}_j(\boldsymbol{x}_j^*(\boldsymbol{\mu})) \tag{3.42}$$

and the dual master problem becomes

$$\begin{array}{ll} \max\limits_{\boldsymbol{\mu}} & q(\boldsymbol{\mu}) = \sum_{j=1}^{J} q_j(\boldsymbol{\mu}) - \boldsymbol{\mu}^T \boldsymbol{b} \\ s.t. & \boldsymbol{\mu} \succeq \mathbf{0} \end{array} \tag{3.43}$$

As in the primal decomposition, we can numerically solve the dual master using a subgradient method. To do so, the subgradient of the dual subproblem $q_j(\boldsymbol{\mu})$ at the point $\boldsymbol{\mu}$ is required. Consider now one of the subproblems, $q_k(\boldsymbol{\mu})$, and for any value of $\boldsymbol{\mu}$, $\boldsymbol{x}_k^*(\boldsymbol{\mu})$ is the minimizer of (3.41). Note that $q_k(\boldsymbol{\mu})$ is the dual function of the following optimization problem

$$\begin{array}{ll} \min\limits_{\boldsymbol{x}_k \in \mathcal{X}_k} & f_k(\boldsymbol{x}_k) \\ s.t. & \boldsymbol{h}_k(\boldsymbol{x}_k) \preceq \mathbf{0} \end{array} \tag{3.44}$$

From the definition of the dual function, it is verified that

$$\begin{array}{rcl} q_k(\boldsymbol{\mu}) & \leq & f_k(\boldsymbol{x}_k^*(\boldsymbol{\mu}^0)) + \boldsymbol{\mu}^T \boldsymbol{h}_k(\boldsymbol{x}_k^*(\boldsymbol{\mu}^0)) \\ & = & f_k(\boldsymbol{x}_k^*(\boldsymbol{\mu}^0)) + \boldsymbol{\mu}^{0^T} \boldsymbol{h}_k(\boldsymbol{x}_k^*(\boldsymbol{\mu}^0)) + (\boldsymbol{\mu} - \boldsymbol{\mu}^0)^T \boldsymbol{h}_k(\boldsymbol{x}_k^*(\boldsymbol{\mu}^0)) \\ & = & q_k(\boldsymbol{\mu}^0) + (\boldsymbol{\mu} - \boldsymbol{\mu}^0)^T \boldsymbol{h}_k(\boldsymbol{x}_k^*(\boldsymbol{\mu}^0)) \end{array} \tag{3.45}$$

where the inequality holds since the dual function chooses the point in $\mathcal{X}_k$ that minimizes the Lagrangian in (3.41) and so, any other point will attain the same value or higher.

Since (3.45) is valid for any $\boldsymbol{\mu}^0 \in \mathbb{R}^r$, we can conclude that $\boldsymbol{h}_k(\boldsymbol{x}_k^*(\boldsymbol{\mu}^0))$ is a subgradient of the dual subproblem k at $\boldsymbol{\mu}^0$, which is readily verified from the subgradient definition in (3.30), and therefore

$$\boldsymbol{s}_{\boldsymbol{\mu}^0,k}\ q_k = \boldsymbol{h}_k(\boldsymbol{x}_k^*(\boldsymbol{\mu}^0)), \qquad q_k(\boldsymbol{\mu}) \leq q_k(\boldsymbol{\mu}^0) + (\boldsymbol{\mu} - \boldsymbol{\mu}^0)^T \boldsymbol{s}_{\boldsymbol{\mu}^0,k} \tag{3.46}$$

With this last result, it is easy to compute a subgradient for the dual master and to finally determine the subgradient method for dual decomposition. A subgradient of the dual master at a point $\boldsymbol{\mu}^0$, $\boldsymbol{s}_{\boldsymbol{\mu}^0}$, is given by

$$\boldsymbol{s}_{\boldsymbol{\mu}^0} = \sum_{j=1}^{J} \boldsymbol{s}_{\boldsymbol{\mu}^0,j} - \boldsymbol{b} \tag{3.47}$$

and the iterates of the method use an updating equation that resembles the one in primal decomposition,

$$\boldsymbol{\mu}^{k+1} = [\boldsymbol{\mu}^k + \alpha^k \boldsymbol{s}^k]^+ \tag{3.48}$$

where k indexes iterations. Note that the projection on the feasible set is easier this time since the master dual problem only requires $\boldsymbol{\mu} \succeq \mathbf{0}$. Therefore, the projection is readily solved by fixing the negative values of $\boldsymbol{\mu}^k + \alpha^k \boldsymbol{s}^k$ to 0. More formally,

$$[a]^+ = \begin{cases} a, & a > 0 \\ 0, & a \leq 0 \end{cases} \tag{3.49}$$

Finally, α^k is the step size of the method as in primal decomposition and the same results and conclusions can be drawn.

3.2.3 Mean Value Cross Decomposition

In this section we review the cross decomposition method developed by Holmberg and Kiwiel and described in their relatively recent paper [Hol06] when applied to convex programs. Previous steps of this mixed proposal for other types of problems can be found in [VR83, Hol92, Hol97]. The technique is designed to solve some special types of convex problems with a wider framework than in primal or dual decompositions, and thus, problems suiting such strategies can also be embedded in the Mean Value Cross (MVC) decomposition method. Conceptually speaking, the philosophy of the technique is quite different from the preceding solutions due to two main reasons:

- The way the problem is separated is different (as will be seen in the problem formulation).
- The idea is to update primal and dual variables at the same time while information among primal and dual visions of the problem is interchanged. Note that in primal decomposition, the goal is to iteratively move towards the optimal values for the primal variables, whereas in dual the decomposition the goal is the equivalent in the dual domain of the problem.

Consider the following problem formulation,

$$\begin{array}{ll} \min\limits_{\boldsymbol{x},\boldsymbol{y}} & c(\boldsymbol{x}) + d(\boldsymbol{y}) \\ s.t. & \boldsymbol{A}_1(\boldsymbol{x}) + \boldsymbol{B}_1(\boldsymbol{y}) \preceq \boldsymbol{b}_1 \\ & \boldsymbol{A}_2(\boldsymbol{x}) + \boldsymbol{B}_2(\boldsymbol{y}) \preceq \boldsymbol{b}_2 \\ & \boldsymbol{x} \in \mathcal{X} \\ & \boldsymbol{y} \in \mathcal{Y} \end{array} \tag{3.50}$$

where $c : \mathbb{R}^{n_1} \longrightarrow \mathbb{R}$, $d : \mathbb{R}^{n_2} \longrightarrow \mathbb{R}$, $\boldsymbol{A}_1 : \mathbb{R}^{n_1} \longrightarrow \mathbb{R}^{m_1}$, $\boldsymbol{B}_1 : \mathbb{R}^{n_2} \longrightarrow \mathbb{R}^{m_1}$, $\boldsymbol{A}_2 : \mathbb{R}^{n_1} \longrightarrow \mathbb{R}^{m_2}$ and $\boldsymbol{B}_2 : \mathbb{R}^{n_2} \longrightarrow \mathbb{R}^{m_2}$ are convex functions. The sets $\mathcal{X}$ and $\mathcal{Y}$ are also convex and compact. It is further assumed that strong duality holds.

Note that all the functions in (3.50) depend only on one subset of primal variables, either $\boldsymbol{x}$ or $\boldsymbol{y}$. If, for example, we define $\boldsymbol{x} = [\boldsymbol{x}_1^T, \ldots, \boldsymbol{x}_J^T]^T$, $A_1(\boldsymbol{x}) = \boldsymbol{A}\boldsymbol{x}$, $\boldsymbol{B}_1(\boldsymbol{y}) = -\boldsymbol{y}$, $\boldsymbol{b_1} = \boldsymbol{0}$ and $A_2(\boldsymbol{x}) = \boldsymbol{B}_2(\boldsymbol{y}) = \boldsymbol{b_2} = \boldsymbol{0}$, [2] then we have a primal decomposition-type structure but without explicit separation of the variables within $\boldsymbol{x}$. Similarly, if we set $A_1(\boldsymbol{x}) = \sum_{j=1}^{J} \boldsymbol{h}_j(\boldsymbol{x}_j)$, $\boldsymbol{B}_1(\boldsymbol{y}) = \boldsymbol{0}$, $\boldsymbol{b_1} = \boldsymbol{b}$ and $A_2(\boldsymbol{x}) = \boldsymbol{B}_2(\boldsymbol{y}) = \boldsymbol{b_2} = \boldsymbol{0}$, then the structure coincides with the one suitable for a dual decomposition.

Construct now the partial Lagrangian function of the problem (3.50) as

$$L(\boldsymbol{x}, \boldsymbol{y}, \boldsymbol{\mu}) = c(\boldsymbol{x}) + d(\boldsymbol{y}) + \boldsymbol{\mu}^T(\boldsymbol{A}_1(\boldsymbol{x}) + \boldsymbol{B}_1(\boldsymbol{y}) - \boldsymbol{b}_1) \tag{3.51}$$

[2] The set of constraints $\sum_{j=1}^{J} \boldsymbol{y}_j \preceq \boldsymbol{b}$ is included in $\mathcal{Y}$.

and minimize it over the variable $\boldsymbol{x}$, including the constraints that have not been taken into account in the Lagrangian definition, to obtain the function $K(\boldsymbol{y}, \boldsymbol{\mu})$,

$$\begin{array}{rlc} K(\boldsymbol{y}, \boldsymbol{\mu}) = & \min\limits_{\boldsymbol{x}} & L(\boldsymbol{x}, \boldsymbol{y}, \boldsymbol{\mu}) \\ & s.t. & \boldsymbol{A}_2(\boldsymbol{x}) \leq \boldsymbol{b}_2 - \boldsymbol{B}_2(\boldsymbol{y}) \\ & & \boldsymbol{x} \in \mathcal{X} \end{array} \tag{3.52}$$

Note that the problem is convex given that $\boldsymbol{\mu} \succeq \boldsymbol{0}$ and that for a fixed value of $\boldsymbol{y}$, it coincides with the definition of the dual function of (3.50) according to the Lagrangian definition in (3.51). Therefore, as stated in [Hol06], it is intuitively true that $K(\boldsymbol{y}, \boldsymbol{\mu})$ is a convex function of $\boldsymbol{y}$ given $\boldsymbol{\mu}$ and a concave function of $\boldsymbol{\mu}$ given $\boldsymbol{y}$. Primal and dual subproblems, as defined by Holmberg and Kiwiel, make use of this fact.

The primal subproblem is defined as

$$\begin{array}{rlc} p(\boldsymbol{y}) = & \max\limits_{\boldsymbol{\mu}} & K(\boldsymbol{y}, \boldsymbol{\mu}) \\ & s.t. & \boldsymbol{\mu} \succeq \boldsymbol{0} \end{array} \tag{3.53}$$

whereas the dual subproblem is defined as

$$\begin{array}{rlc} d(\boldsymbol{\mu}) = & \min\limits_{\boldsymbol{y}} & K(\boldsymbol{y}, \boldsymbol{\mu}) \\ & s.t. & \boldsymbol{y} \in \mathcal{Y} \end{array} \tag{3.54}$$

Since strong duality holds and since the primal subproblem (for a fixed value of $\boldsymbol{y}$) can be interpreted in terms of the maximization of a dual function (i.e., it is in fact a dual problem for a fixed $\boldsymbol{y}$), it is possible to attain the same optimal value by solving the corresponding primal problem, which is

$$\begin{array}{rlc} p(\boldsymbol{y}) = & \min\limits_{\boldsymbol{x}} & c(\boldsymbol{x}) + d(\boldsymbol{y}) \\ & s.t. & \boldsymbol{A}_1(\boldsymbol{x}) \leq \boldsymbol{b}_1 - \boldsymbol{B}_1(\boldsymbol{y}) \\ & & \boldsymbol{A}_2(\boldsymbol{x}) \leq \boldsymbol{b}_2 - \boldsymbol{B}_2(\boldsymbol{y}) \\ & & \boldsymbol{x} \in \mathcal{X} \end{array} \tag{3.55}$$

The complete expression for the dual subproblem for a fixed value of $\boldsymbol{\mu}$ is (by substitution)

$$\begin{array}{rlc} d(\boldsymbol{\mu}) = & \min\limits_{\boldsymbol{x},\boldsymbol{y}} & c(\boldsymbol{x}) + d(\boldsymbol{y}) + \boldsymbol{\mu}^T(\boldsymbol{A}_1(\boldsymbol{x}) + \boldsymbol{B}_1(\boldsymbol{y}) - \boldsymbol{b}_1) \\ & s.t. & \boldsymbol{A}_2(\boldsymbol{x}) + \boldsymbol{B}_2(\boldsymbol{y}) \leq \boldsymbol{b}_2 \\ & & \boldsymbol{x} \in \mathcal{X} \\ & & \boldsymbol{y} \in \mathcal{Y} \end{array} \tag{3.56}$$

Once the subproblems (primal and dual) are fully described, a possibility to solve the whole problem is to define the master problems associated to the subproblems. In that way, we finally have to options: i) solve from a primal-only perspective or ii) solve from a dual-only perspective. The master problems are defined as:

$$\begin{array}{rlc} p^* = & \min\limits_{\boldsymbol{y}} & p(\boldsymbol{y}) \\ & s.t. & \boldsymbol{y} \in \mathcal{Y} \end{array} \tag{3.57}$$

for the primal and

$$d^* = \begin{array}{ll} \max\limits_{\boldsymbol{\mu}} & d(\boldsymbol{\mu}) \\ s.t. & \boldsymbol{\mu} \succeq \mathbf{0} \end{array} . \tag{3.58}$$

Both are convex optimization problems [Hol06] that verify $p^* = d^*$ due to strong duality. When evaluated not in the optimum, the primal subproblem is an over-estimator of the optimum and the dual subproblem is an under-estimator of it [Hol06]. In other words, it holds that

$$d(\boldsymbol{\mu}) \leq d^* = p^* \leq p(\boldsymbol{y}) \tag{3.59}$$

and the result is consistent with the duality results in Section 3.1.2.

Note that this approach is conceptually the same as in primal or dual decompositions with some important differences regarding the structure of the problem: in the MVC decomposition method, the separability of the problem in some subgroups of variables (except for a coupling constraint or a coupling variable) is not exploited as it happens with the previous techniques. Although the formulation is in principle more general (in the sense that more types of convex programs fulfill the MVC decomposition approach), it lacks for specialization (a distributed solution is not naturally derived as in primal/dual decompositions). As it will be discussed later, primal and dual decomposition techniques are suitable for parallel computing as the subproblems can operate independently with some signalling with the master problem, which coordinates the global problem. Such parallelization is sometimes an important feature, since it enables to perform distributed solutions. These are very interesting in application problems where centralizing operations needs great effort. The works within network optimization are an example of this issue [Pal07].

Consider again the master problems in (3.57) and (3.58). Now, instead of keeping the same philosophy as in primal or dual decompositions, the MVC decomposition method proposes to skip the usage of master problems and to update primal ($\boldsymbol{y}$) and dual ($\boldsymbol{\mu}$) variables among primal (3.55) and dual (3.56) subproblems. That is, once the primal subproblem in (3.55) is solved (for a given value of $\boldsymbol{y}$), the dual variables $\boldsymbol{\mu}$, related to the constraint $\boldsymbol{A}_1(\boldsymbol{x}) \leq \boldsymbol{b}_1 - \boldsymbol{B}_1(\boldsymbol{y})$, are readily found. These are then used (with some modifications) as an input to the dual subproblem in (3.56). Once it is solved, the primal variables $\boldsymbol{y}$ are obtained at no cost as its minimizers. And finally, the circle is closed by feeding again the primal subproblem with the new values of $\boldsymbol{y}$ (with some modifications).

As noted, primal and dual variables are not directly passed between subproblems and instead, it is required to average a new value with all past results previously to the exchange. More formally,

$$\bar{\boldsymbol{\mu}}^k = \frac{1}{k}\sum_{i=0}^{k-1} \boldsymbol{\mu}^{k-1} \qquad \text{and} \qquad \bar{\boldsymbol{y}}^k = \frac{1}{k}\sum_{i=0}^{k-1} \boldsymbol{y}^{k-1} \tag{3.60}$$

where k indexes iterations. Note that the method implicitly defines an step-size ($\frac{1}{k}$) for each new contribution to the mean value, and it diminishes as the number of iterations increase. The

same problems that primal and dual decomposition methods had, related to the choice of the step-size also appear in this case. In practical terms, the smoothing approach slows down the speed of convergence of the technique (it is further discussed later on in this chapter).

To end this review of the method, let us summarize it in an algorithmic form:

Take starting points $\boldsymbol{\mu}^0 \succeq \mathbf{0}$ and $\boldsymbol{y}^0 \in \mathcal{Y}$ and let $k = 1$.

Repeat

1. Let $\bar{\boldsymbol{\mu}}^k = \frac{1}{k}\sum_{i=0}^{k-1} \boldsymbol{\mu}^{k-1} = \frac{1}{k}\,\boldsymbol{\mu}^{k-1} + \frac{k-1}{k}\,\bar{\boldsymbol{\mu}}^{k-1}$ and compute $d(\bar{\boldsymbol{\mu}}^k)$ as in (3.56). Get $\boldsymbol{y}^k$ as an inner minimizer of $d(\bar{\boldsymbol{\mu}}^k)$.
2. Let $\bar{\boldsymbol{y}}^k = \frac{1}{k}\sum_{i=0}^{k-1} \boldsymbol{y}^{k-1} = \frac{1}{k}\,\boldsymbol{y}^{k-1} + \frac{k-1}{k}\,\bar{\boldsymbol{y}}^{k-1}$ and compute $p(\bar{\boldsymbol{y}}^k)$ as in (3.55). Get $\boldsymbol{\mu}^k$ as the inner Lagrange multiplier of $p(\bar{\boldsymbol{y}}^k)$.
3. $k = k + 1$.

Until $p(\bar{\boldsymbol{y}}^k) - d(\bar{\boldsymbol{\mu}}^k) < \epsilon$.

Note that the stopping criterion of the method is defined using a measure of the duality gap, that is, the difference between the primal and dual versions of the problem. It is assumed that the duality gap is zero since strong duality holds. For further details on the MVC decomposition method, please refer to [Hol06].

3.3 Proposed Coupled-Decomposition Method

Once the decomposition methods in the literature have been reviewed, it is now turn to develop the coupled-decomposition method that we propose in this thesis, which is our major theoretical contribution. Conceptually speaking, it can be classified in between primal/dual decomposition methods and the MVC decomposition method. From the former, we get the way the problem is separated (in a master problem with several subproblems). From the latter, the idea of combining both primal and dual decompositions in a single method is shared[3].

Note that, as it has already been discussed in the previous chapter, it is also possible to create several decomposition layers within certain types of problems. To exemplify it, imagine that the primal or dual subproblems derived through decomposition of the original optimization problem, at their turn (and whenever it is possible), are solved by performing a second decomposition (primal or dual) running at a lower level. The idea, well exposed in [Pal07], should not be confused with our proposal here, where both decompositions intertwine as in the MVC decomposition

[3]The idea of the coupled-decomposition method was autonomously conceived. We related it to the works in [VR83, Hol92, Hol97, Hol06] when a reviewer mentioned them.

method. Moreover, the decomposition we propose here can replace either the primal or the dual decomposition (if the formulation of the problem suits) in a multi-layer decomposition strategy. In that sense, it is not an excluding technique and the benefits of the method must be interpreted not only as an isolated procedure but also in combination with others.

3.3.1 Description of the Method

Consider now the following convex problem formulation

$$\begin{array}{lll} \min\limits_{\{\boldsymbol{x}_j\},\boldsymbol{y}} & \sum_{j=1}^{J} f_j(\boldsymbol{x}_j) & \\ s.t. & \boldsymbol{x}_j \in \mathcal{X}_j, & j = 1,\ldots,J \\ & h_j(\boldsymbol{x}_j) \leq y_j, & j = 1,\ldots,J \\ & \boldsymbol{A}\boldsymbol{y} \preceq \boldsymbol{c} & \\ & \boldsymbol{y} \in \mathcal{Y}, & \mathcal{Y} = \mathcal{Y}_1 \times \ldots \times \mathcal{Y}_J \end{array} \tag{3.61}$$

where $f_j : \mathbb{R}^{n_j} \longrightarrow \mathbb{R}$ and $h_j : \mathbb{R}^{n_j} \longrightarrow \mathbb{R}$ are convex functions of $\boldsymbol{x}_j$, $\mathcal{X}_j$ and $\mathcal{Y}$ are convex and compact subsets, $\boldsymbol{A} = [\boldsymbol{a}_1, \ldots, \boldsymbol{a}_r]^T$ is a $r \times J$ ($r \leq J$) matrix with entries $a_{k,l} \in \{0, 1\}$ and $rank(\boldsymbol{A}) = r$ and $\boldsymbol{c} \in \mathbb{R}^J$. The subsets $\mathcal{Y}_j$ are defined as the images of the subsets $\mathcal{X}_j$ through the functions $h_j(\boldsymbol{x}_j)$, i.e. $h_j : \mathcal{X}_j \longrightarrow \mathcal{Y}_j,\ \forall j$. Note that the constraint $\boldsymbol{y} \in \mathcal{Y}$ is redundant since $\mathcal{Y}$ collapses the information already available in the subsets $\mathcal{X}_j$. Notwithstanding, it is necessary to derive the proposed method and hence, we include it in (3.61). We further assume that strong duality holds, i.e., for every point $\boldsymbol{y}$ in the domain, there exists a point $\boldsymbol{x}_j$ in the interior of $\mathcal{X}_j$ that attains $h_j(\boldsymbol{x}_j) < y_j$ for every $j = 1, \ldots, J$ with $\boldsymbol{A}\boldsymbol{y} \prec \boldsymbol{c}$ and $\boldsymbol{y}$ in the interior of $\mathcal{Y}$.

In short, the coupled-decomposition method intertwines the primal/dual subproblems that would be obtained with a primal/dual decomposition. However, the connection is not direct and we need to introduce the novel dual/primal projection elements instead. A complete block diagram of the method can be found in Figure 3.5. We do not define at this moment the variables that appear in the figure because they will be next introduced while we describe all the steps within the proposed strategy.

From Primal Projection to Dual Projection: the Primal Subproblems

Assume now that the values of $\boldsymbol{y}$ are fixed in (3.61), with $\boldsymbol{y} \in \mathcal{Y}$ ($\hat{\boldsymbol{y}}$ in Figure 3.5). Then, the problem clearly decouples into J subproblems depending on the variables $\boldsymbol{x}_j$,

$$\begin{array}{lll} \min\limits_{\boldsymbol{x}_j} & f_j(\boldsymbol{x}_j) & \\ s.t. & \boldsymbol{x}_j \in \mathcal{X}_j, & \cdot \\ & h_j(\boldsymbol{x}_j) \leq y_j & \end{array} \tag{3.62}$$

We refer to this subproblems as the primal subproblems for the coupled-decomposition method. The corresponding optimal solutions $\boldsymbol{x}_j^{p*}(y_j)$ can be attained in the general case using numerical

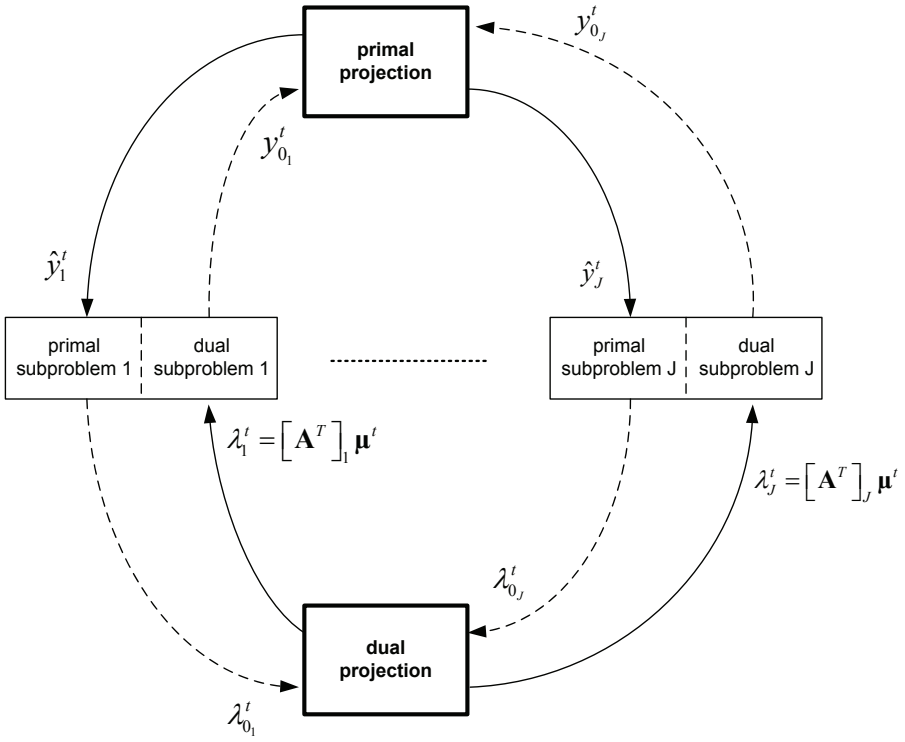

Figure 3.5: Block diagram of the coupled-decomposition method.

methods (e.g. interior point methods, see Section 3.1.1). However, in some cases, they can also be found analytically using the KKT conditions in (3.23).

As stated before, there is certain similarity in formulation between the subproblems in pure primal decomposition and the subproblems in the proposed technique. However, there are slight differences in the way we use them. In the first case, the interest was in extracting information from the subproblems in (3.26) in order to coordinately advance towards the optimal solution in the master problem of (3.27). More precisely, a subgradient [4] for the master problem was readily computed from the subgradients extracted from the subproblems, which were obtained at no cost given the Lagrange multipliers related to the constraints $\boldsymbol{A}_j\boldsymbol{x}_j \preceq \boldsymbol{y}_j$; c.f. (3.33). In the cross decompositions method, the goal is to use that dual information provided by the primal subproblems to optimize the original problem in (3.61) from a dual perspective. In that sense, the method resembles the MVC decomposition method. However, the interchange of information from primal to dual and viceversa differs from the smoothing mean value applied there.

Assume now that the minimizers of the primal subproblems (3.62) are attained at the points $\boldsymbol{x}_j^{p*}(y_j)$ and let us represent the subsets $\mathcal{X}_j$ by an arbitrary number K_j of constraints of the type

[4] A subgradient is a generalization of the gradient concept also valid for non-differentiable functions: a vector $\boldsymbol{s}(\boldsymbol{x_0})$ is said to be a subgradient of the function f at the point $\boldsymbol{x}_0$ if, given any point $\boldsymbol{x} \in \mathrm{dom} f$, it is true that $f(\boldsymbol{x}) = f(\boldsymbol{x}^0) + \boldsymbol{s}(\boldsymbol{x}^0)^T(\boldsymbol{x} - \boldsymbol{x}^0)$.

$\boldsymbol{g}_j(\boldsymbol{x}_j) \preceq \mathbf{0}$, where $\boldsymbol{g}_j : \mathbb{R}^{n_j} \longrightarrow \mathbb{R}$. Then, the application of the KKT conditions in (3.23) forces the following equalities and inequalities to the dual variables,

$$\begin{array}{rcll} \lambda_j & \geq & 0, & \\ \upsilon_j^k & \geq & 0, & k = 1, \ldots, K_j, \\ \lambda_j(h_j(\boldsymbol{x}_j^{p*}) - y_j) & = & 0, & \\ \upsilon_j^k g_j^k(\boldsymbol{x}_j^{p*}) & = & 0, & \\ \nabla f_j(\boldsymbol{x}_j^{p*}) + \lambda_j \nabla h_j(\boldsymbol{x}_j^{p*}) + \sum_{k=1}^{K_j} \upsilon_j^k \nabla g_j^k(\boldsymbol{x}_j^{p*}) & = & 0, & \end{array} \tag{3.63}$$

where $\boldsymbol{\upsilon}_j = [\upsilon_1, \ldots, \upsilon_{K_j}]^T$ are the dual Lagrange variables associated to the set of constraints $\boldsymbol{g}_j(\boldsymbol{x}_j) \preceq \mathbf{0}$ and λ_j is the dual variable associated to $h_j(\boldsymbol{x}_j^{p*}) \leq y_j$, being $\boldsymbol{\lambda} = [\lambda_1, \ldots, \lambda_J]^T$. From the previous equations, the values of λ_j can be computed, either analytically or numerically. These are labelled as $\boldsymbol{\lambda}_0^t$ in Figure 3.5. Note that the slackness constraint $\lambda_j(h_j(\boldsymbol{x}_j^{p*}) - y_j) = 0$ forces $\lambda_j = 0$ if the constraint is not active, i.e. $h_j(\boldsymbol{x}_j^{p*}) < y_j$. We say then that the j^{th} value of $\boldsymbol{\lambda}$ is not active. Furthermore, the values of $\boldsymbol{\lambda}$ are classified accordingly into two subsets: the active and the non-active ones.

From Dual Projection to Primal Projection: the Dual Subproblems

It is also possible to decouple the problem in (3.61) from a dual perspective using the ideas from a pure dual decomposition strategy. For that purpose, a partial Lagrangian for (3.61) is constructed by relaxing only the constraints $\boldsymbol{A}\boldsymbol{y} \leq \boldsymbol{c}$ with associated dual variables $\boldsymbol{\mu}$,

$$L(\{\boldsymbol{x}_j\}, \boldsymbol{y}, \boldsymbol{\mu}) = \sum_{j=1}^{J} f_j(\boldsymbol{x}_j) + \boldsymbol{\mu}^T(\boldsymbol{A}\boldsymbol{y} - \boldsymbol{c}). \tag{3.64}$$

From this Lagrangian definition, the dual function of the problem can be derived. The constraints not explicitly included in the Lagrangian are now implicitly taken into account. The resulting dual function is

$$q(\boldsymbol{\mu}) = \begin{array}{c} \min \\ \{\boldsymbol{x}_j\}, \boldsymbol{y} \\ \boldsymbol{x}_j \in \mathcal{X}_j, \forall j \\ h_j(\boldsymbol{x}_j) \leq y_j, \forall j \\ y_j \in \mathcal{Y}_j, \forall j \end{array} L(\{\boldsymbol{x}_j\}, \boldsymbol{y}, \boldsymbol{\mu}) \tag{3.65}$$

and finally, substitution of (3.64) into (3.65) attains

$$q(\boldsymbol{\mu}) = \left(\sum_{j=1}^{J} \begin{array}{c} \min \\ \boldsymbol{x}_j, y_j \\ \boldsymbol{x}_j \in \mathcal{X}_j \\ h_j(\boldsymbol{x}_j) \leq y_j \\ y_j \in \mathcal{Y}_j \end{array} f_j(\boldsymbol{x}_j) + y_j([\boldsymbol{A}^T]_j\, \boldsymbol{\mu}) \right) - \boldsymbol{\mu}^T \boldsymbol{c} \tag{3.66}$$

since $\boldsymbol{\mu}^T(\boldsymbol{A}\boldsymbol{y}-\boldsymbol{c}) = \boldsymbol{y}^T\boldsymbol{A}^T\boldsymbol{\mu} - \boldsymbol{\mu}^T\boldsymbol{c} = (\sum_{j=1}^{J} y_j\,[\boldsymbol{A}^T]_j\,\boldsymbol{\mu}) - \boldsymbol{\mu}^T\boldsymbol{c}$. We define $[\boldsymbol{M}]_j$ to be the j^{th} file of matrix $\boldsymbol{M}$.

This result clearly decouples the dual function into several dual subproblems, $q_j(\boldsymbol{\mu})$, where

$$q_j(\boldsymbol{\mu}) = \begin{array}{c} \min \\ \boldsymbol{x}_j, y_j \\ \boldsymbol{x}_j \in \mathcal{X}_j \\ h_j(\boldsymbol{x}_j) \leq y_j \\ y_j \in \mathcal{Y}_j \end{array} \quad f_j(\boldsymbol{x}_j) + y_j([\boldsymbol{A}^T]_j\,\boldsymbol{\mu}), \qquad j = 1, \ldots, J \tag{3.67}$$

and

$$q(\boldsymbol{\mu}) = \sum_{j=1}^{J} q_j(\boldsymbol{\mu}) \; - \boldsymbol{\mu}^T\boldsymbol{c}. \tag{3.68}$$

The dual converse to extracting the dual variables $\boldsymbol{\lambda}$ from fixed values of $\boldsymbol{y}$ applies now. Using the dual subproblems and fixing a value $\boldsymbol{\mu} \succeq \boldsymbol{0}$, the optimal values of $\boldsymbol{x}_j$ and y_j are obtained. We call these values $\boldsymbol{x}_j^{d*}(\boldsymbol{\mu})$ and $y_j^{d*}(\boldsymbol{\mu})$, respectively.

Let us consider now a full Lagrangian of (3.61),

$$\begin{array}{rl} L(\{\boldsymbol{x}_j, \boldsymbol{\upsilon}_j\,\gamma_j, \delta_j\}, \boldsymbol{y}, \boldsymbol{\mu}) & = \sum_{j=1}^{J} f_j(\boldsymbol{x}_j) + \sum_{j=1}^{J}\sum_{k=1}^{K_j} \upsilon_j^k g_j^k(\boldsymbol{x}_j) \\ & + \sum_{j=1}^{J} \lambda_j h_j(\boldsymbol{x}_j) + \boldsymbol{\mu}^T(\boldsymbol{A}\boldsymbol{y} - \boldsymbol{c}) \\ & + \sum_{j=1}^{J} \gamma_j(y_j - \sup \mathcal{Y}_j) - \sum_{j=1}^{J} \delta_j(y_j - \inf \mathcal{Y}_j) \end{array} . \tag{3.69}$$

If we assume that the local constraints in $\mathcal{Y}_j$ are not active at the optimal y_j values, then it is true that $\gamma_j = \delta_j = 0$ (due to the slackness constraints). Under this hypothesis, the application of the KKT conditions imposes the following subset of constraints,

$$\frac{\partial}{\partial y_j}\Big\{ y_j\,([\boldsymbol{A}^T]_j\,\boldsymbol{\mu}) + \lambda_j(h_j(\boldsymbol{x}_j) - y_j)\Big\}\Big|_{y_j = y_j^*} = 0, \qquad j = 1, \ldots, J \tag{3.70}$$

and hence we verify that

$$\lambda_j = [\boldsymbol{A}^T]_j\,\boldsymbol{\mu} \tag{3.71}$$

when the local constraints on y_j are not active. Furthermore, if $[\boldsymbol{A}^T]_j\,\boldsymbol{\mu} > 0$, then $\lambda_j > 0$ and the slackness constraints impose $y_j^* = h_j(\boldsymbol{x}_j^*)$.

Again, the values $y_j^{d*}(\boldsymbol{\mu})$ provide the necessary information to obtain a subgradient of $q(\boldsymbol{\mu})$ and one could proceed as in a pure dual decomposition. Once more, the idea now is to interchange that primal information with the primal subproblems in order to coordinately reach the optimal solution. Note that, due to strong duality, the optimal values of $\boldsymbol{\mu}$ for the general problem applied to the dual subproblems return the optimal values of $\boldsymbol{x}_j$ and y_j. The converse is also true: given the optimal values of y_j to the primal subproblems, the optimal values of x_j and $\lambda_j = [\boldsymbol{A}^T]_j\,\boldsymbol{\mu}$, derived from (3.71), are found.

However, a direct interconnection between primal and dual subproblems is not possible unless an adequate treatment of data in both directions is performed. Checking whether the KKT conditions hold or not with the sole use of primal and dual subproblems reveals that something else is required. An example supporting the discussion is found in the MVC decomposition method, where a key point was to perform a time average of the successive updates from primal and dual subproblems.

We keep in background by the moment the task of analyzing the KKT conditions of the original problem in (3.61) in order to finally conclude the method. The interest now is on studying the dependencies between primal and dual subproblems, that is, how the variables y_j are related to the Lagrange multipliers $\lambda_j = [\boldsymbol{A}^T]_j \, \boldsymbol{\mu}$.

Primal-dual Relationship in Subproblems

Take now the j^{th} primal subproblem in (3.62) and assume that the constraint $h_j(\boldsymbol{x}_j)$ is active between the values y_j^1 and y_j^2, i.e. $h_j(\boldsymbol{x}_j) = y_j, y_j \in [y_j^1, y_j^2]$. The objective is to understand the evolution of the associated dual variable λ_j within that interval. In other words, we want to know what variation in λ_j may be expected as a reaction to a variation in y_j. We take a rather practical approach this time to gain intuition on the question. However, the reader may find in [Boy03, Sec. 5.6.3] a more formal analysis under the topic of *local sensitivity analysis*.

Define $\boldsymbol{x}_j^*(y_j)$ as the optimal solution of the primal subproblem in (3.62) and allow y_j to be in the range $[y_j^1, y_j^2]$. Then, x_j^* describes a curve in the domain of the subproblem as y_j moves. Figure 3.6 exemplifies the situation. In darkest line, there is the curve $x_j^*(y_j)$ between y_j^1 and y_j^2. Moreover, we have depicted in dotted lines the contour plots for the objective function and in solid lines the constraints $h(\boldsymbol{x}_j) = y_j^1$ and $h(\boldsymbol{x}_j) = y_j^2$. Finally, the subset $\mathcal{X}_j$ is represented using an arbitrary number of constraints $g_j^l(\boldsymbol{x}_j) \leq 0$.

Primal subproblems are now redefined as one-dimensional optimization problems making use of the previously defined optimal curve, $\boldsymbol{x}_j^*(t_j)$ with $t_j \in [y_j^1, y_j^2]$, and assuming that the constraint is active as

$$\begin{array}{ll} \min\limits_{t_j} & f_j(\boldsymbol{x}_j^*(t_j)) \\ s.t. & h_j(\boldsymbol{x}_j^*(t_j)) \leq y_j. \end{array} \tag{3.72}$$

Note that the set of constraints $\boldsymbol{x}_j \in \mathcal{X}_j$ in (3.62) is not necessary now as that information is implicitly included in the curve $\boldsymbol{x}_j^*(t_j)$. Moreover, the optimal value of (3.72) function of y_j forms a convex function with convex domain, as can be extracted from the discussion in (3.28) and (3.29).

If the Lagrangian of (3.72) is differentiated with respect to t_j, it holds that

$$\frac{\partial L(t_j, \lambda_j)}{\partial t_j} = \frac{\partial f_j(\boldsymbol{x}_j^*(t_j))}{\partial t_j} + \lambda_j \frac{\partial h_j(\boldsymbol{x}_j^*(t_j))}{\partial t_j} = 0 \tag{3.73}$$

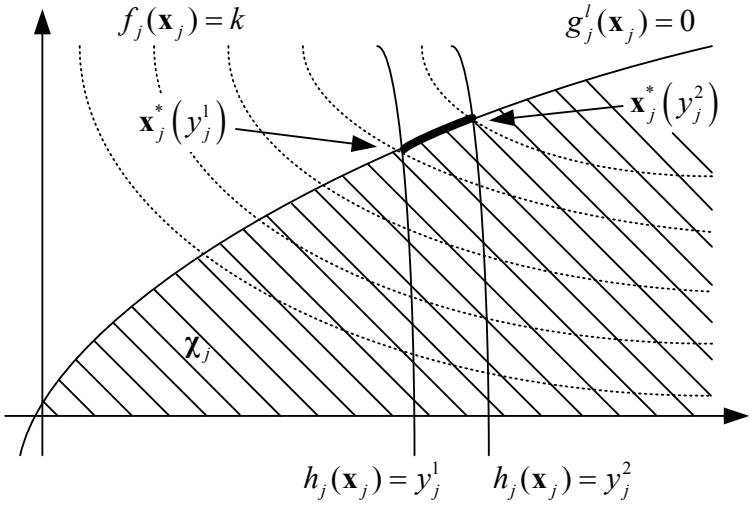

Figure 3.6: Interpretation of the relationship between y_j and the Lagrange multiplier λ_j.

and since $h_j(\boldsymbol{x}_j^*(t_j)) = t_j$, it is verified that

$$\frac{\partial f_j(\boldsymbol{x}_j^*(t_j))}{\partial t_j} = -\lambda_j. \tag{3.74}$$

Note that the optimal solution of (3.72) is attained at $t_j = y_j$. This result is in accordance with the results in [Boy03, Sec. 5.6.3] (fixing $y_j = 0$) and the previously found result in (3.32). This can be seen in Figure 3.7, where we represent the functions $f_j(\boldsymbol{x}_j^*(t_j))$ and $h_j(\boldsymbol{x}_j^*(t_j))$. Fixing $t_j = y_j = y_j^1$, the equilibrium equation imposed by the partial of the Lagrangian with respect to t_j in (3.73) forces to choose an adequate value of λ_j such that the slopes of $f_j(\boldsymbol{x}_j^*(t_j))$ and $h_j(\boldsymbol{x}_j^*(t_j))$ compensate one each other. For a greater value of t_j such as $t_j = y_j^2$ and given that $f_j(\boldsymbol{x}_j^*(t_j))$ is a convex function of t_j (see Lemma 1), it is clear that, in order to restore equilibrium in the slopes of the functions, a lower value of λ_j is required. Therefore, we can conclude that λ_j is a decreasing function of y_j.

This result is summarized in the following Lemma.

Lemma 2 *Primal and dual subproblems in (3.62) and (3.67) have a relationship through primal and dual variables y_j and λ_j (assuming that the local constraints in $\mathcal{Y}_j$ are not active). It holds that*

- *An increase (decrease) on the primal value y_j implies a decrease (increase) on the dual variable λ_j, although not linear.*
- *An increase (decrease) on the dual value λ_j implies a decrease (increase) on the primal variable y_j, although not linear.*

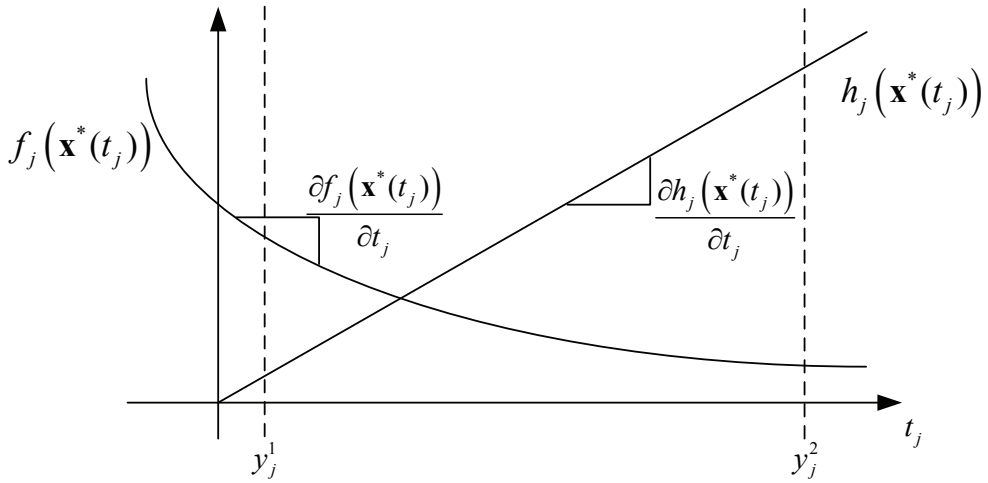

Figure 3.7: Graphical representation of the problem in (3.72).

Coordination between Subproblems. How Coupling is Managed.

We focus now on the original problem in (3.61). The objective is to embed primal and dual subproblems in a procedure to find the global solution of the problem. This implies the optimization over $\boldsymbol{y}$ and its dual $\boldsymbol{\lambda}$, which are not taken account in the subproblems. Let us rewrite the full Lagrangian of the problem as

$$\begin{array}{rl} L(\{\boldsymbol{x}_j, \boldsymbol{v}_j, \boldsymbol{\xi}_j\}, \boldsymbol{y}, \boldsymbol{\lambda}, \boldsymbol{\mu}) & = \sum_{j=1}^{J} f_j(\boldsymbol{x}_j) + \sum_{j=1}^{J} \lambda_j (h_j(\boldsymbol{x}_j) - y_j) + \boldsymbol{\mu}^T(\boldsymbol{A}\boldsymbol{y} - \boldsymbol{c}) \\ & + \sum_{j=1}^{J} \boldsymbol{v}_j^T \boldsymbol{g}_j(\boldsymbol{x}_j) + \sum_{j=1}^{J} \boldsymbol{\xi}_j^T \boldsymbol{r}_j(y_j) \end{array} \tag{3.75}$$

where the functions $\{\boldsymbol{r}_j(y_j)\}$ represent an arbitrary number of constraints on the coupling variable $\boldsymbol{y}$ that define the convex subset $\mathcal{Y}$. Rcall that it is possible to uncouple those constraints (depending only on y_j) as $\mathcal{Y}$ is the cartesian product of J one-dimensional subsets, $\mathcal{Y}_j$. Typically, $K_j = 2$, since in one-dimensional optimization only lateral constraints are meaningful. Similarly, the set of constraints $\boldsymbol{g}_j(\boldsymbol{x}_j) = [g_1(\boldsymbol{x}_j), \ldots, g_{K_j}(\boldsymbol{x}_j)]^T$ define the convex subsets $\mathcal{X}_j$.

Among the KKT conditions for optimality of the solution, the focus is now on the ones related with the coupling variable $\boldsymbol{y}$, either from the primal or dual point of view. In the optimal values $\boldsymbol{x}_j^*$, $\boldsymbol{y}^*$, $\boldsymbol{\lambda}^*$ and $\boldsymbol{\mu}^*$, it holds

$$\begin{array}{rcl} \nabla_{\boldsymbol{y}} L(\{\boldsymbol{x}_j^*\}, \boldsymbol{y}^*, \boldsymbol{\lambda}^*, \boldsymbol{\mu}^*) & = & \boldsymbol{A}^T\boldsymbol{\mu}^* - \boldsymbol{\lambda}^* + \sum_{j,k} \xi_j^k \nabla_{\boldsymbol{y}} \{r_j^k(y_j)\} = \boldsymbol{0} \\ \boldsymbol{\mu}^{*T}(\boldsymbol{A}\boldsymbol{y}^* - \boldsymbol{c}) & = & \boldsymbol{0} \\ \boldsymbol{A}\boldsymbol{y}^* & \leq & \boldsymbol{c} \\ \boldsymbol{y}^* & \in & \mathcal{Y} \end{array} \tag{3.76}$$

Two important conclusions can be extracted to guide primal and dual subproblems towards the optimal solution of the coupled problem. They are:

- If $\mu_k > 0$, then $\boldsymbol{a}_k^T \boldsymbol{y} = c_k$ due to the slackness constraint. The converse applies when $\boldsymbol{a}_k^T \boldsymbol{y} < c_k$ and then it is required that $\mu_k = 0$.

- As stated before (in Lemma 2), it is verified that $\lambda_j = [\boldsymbol{A}^T]_j \, \boldsymbol{\mu}$ when the local constraints in $\mathcal{Y}_j$ are not active. If any of the local constraints is active, i.e $r_j^k = 0$, then the optimality condition $\frac{\partial}{\partial y_j} L(\{\boldsymbol{x}_j^*, \boldsymbol{\upsilon}_j^*, \boldsymbol{\xi}_j^*\}, \boldsymbol{y}^*, \boldsymbol{\lambda}^*, \boldsymbol{\mu}^*) = 0$ can be attained by means of many different values of λ_j adjusting the value of the multiplier $\xi_j^k \geq 0$, which is fully uncoupled from the other optimality conditions $\frac{\partial}{\partial y_k} L(\{\boldsymbol{x}_j^*, \boldsymbol{\upsilon}_j^*, \boldsymbol{\xi}_j^*\}, \boldsymbol{y}^*, \boldsymbol{\lambda}^*, \boldsymbol{\mu}^*) = 0$ with $j \neq k$. Therefore, in such a case the condition is not useful to relate $\boldsymbol{\lambda}$ with $\boldsymbol{\mu}$.

With those observations, we have provided sufficient conditions to interconnect primal and dual subproblems. Next we use these to derive the primal and the dual projections of the method.

From Dual Subproblems to Primal Subproblems: the Primal Projection

First, consider the simplest connection, from dual subproblems to primal subproblems. Given the dual variables $\boldsymbol{\mu}$, the dual subproblems in (3.67) obtain the values of the primal variables y_j and $\boldsymbol{x}_j$. However, there is no guarantee to accomplish the necessary condition $\boldsymbol{A}\boldsymbol{y} \leq \boldsymbol{c}$. Moreover, note that once fixed the values of $\boldsymbol{\mu}$, it is implicitly assumed (using slackness) that for each $\mu_k > 0$, $\boldsymbol{a}_k^T \boldsymbol{y} = c_k$. Again, this is not necessarily attained in dual subproblems. To correct those primal unfeasibilities, dual subproblems are connected to the primal subproblems with the primal projection for the method, which solves the following optimization problem

$$\begin{array}{lll} \min\limits_{\hat{\boldsymbol{y}}} & \|\boldsymbol{y}_0 - \hat{\boldsymbol{y}}\|_2^2 & \\ s.t. & \boldsymbol{a}_k^T \hat{\boldsymbol{y}} = c_k, & k \big| \mu_k > 0 \\ & \boldsymbol{a}_k^T \hat{\boldsymbol{y}} \leq c_k, & \text{other } k \\ & \hat{\boldsymbol{y}} \in \mathcal{Y} & \end{array} \tag{3.77}$$

where $\boldsymbol{y}_0$ is the output of the dual subproblems.

The primal projection takes the role of the primal master in pure primal decomposition and performs a projection to the feasible subset. However, the projection is this time conditioned to the values of $\boldsymbol{\mu}$, which force additional equality constraints. Disregarding this subtle difference, the idea is the same as in gradient projected methods, where unfeasible updates are in this way corrected. Moreover, the new point $\hat{\boldsymbol{y}}$ is the one that, lying in the feasible set, is closer to the given point $\boldsymbol{y}_0$. Note that such procedure guarantees primal feasibility by moving the solution away from $\boldsymbol{y}_0$ by the minimum possible distance. Later on, we define the dual converse of primal projection, the dual projection, and the same idea holds. This establishes a connection between both projections.

Consider now the following Lemma.

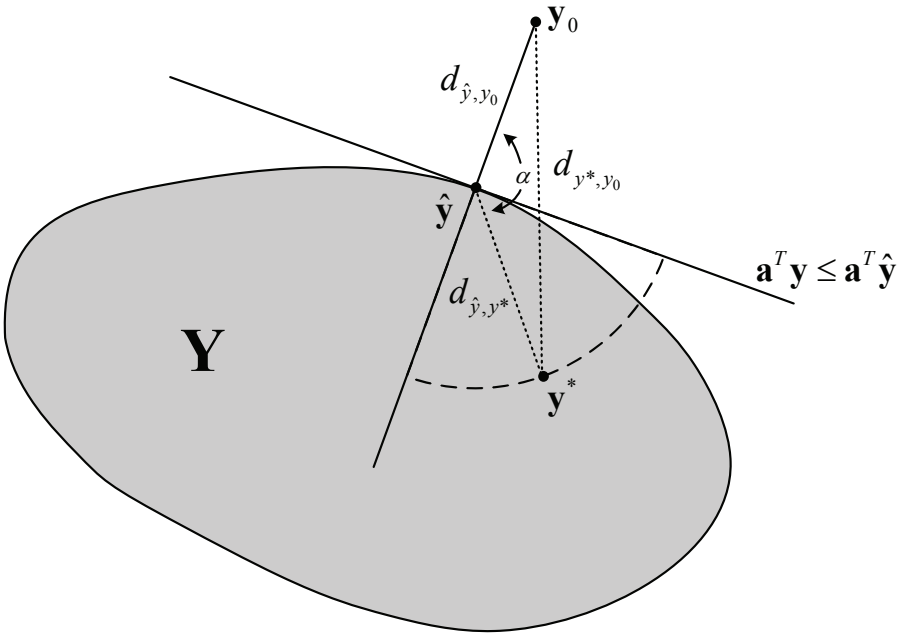

Figure 3.8: Supporting hyperplane.

Lemma 3 *Assuming that the feasible set (with respect to to $\boldsymbol{y}$) of (3.61) coincides with the feasible set of (3.77), the solution to the primal projection, $\hat{\boldsymbol{y}}$, verifies that it is not farther to the optimal solution of (3.61) than $\boldsymbol{y}_0$.*

Proof. First, note that the feasible set of the primal projection problem is a convex subset, since it is the intersection of the convex subset $\mathcal{Y}$ with linear equalities and inequalities [Boy03, Sec. 2.3.1]. If $\boldsymbol{y}_0 \in \mathcal{Y}$, then we have $\hat{\boldsymbol{y}} = \boldsymbol{y}_0$ and the property holds. If $\boldsymbol{y}_0 \notin \mathcal{Y}$, then the solution $\hat{\boldsymbol{y}}$ must be in the boundary of $\mathcal{Y}$ (otherwise $\hat{\boldsymbol{y}}$ would be even farther from $\boldsymbol{y}_0$). It is possible to define a supporting hyperplane [Boy03, Sec. 2.5.2] to the set at the point $\hat{\boldsymbol{y}}$ (the hypothetic solution) since it is on the boundary of the set (which is convex and compact). A supporting hyperplane of $\mathcal{Y}$ at the point $\hat{\boldsymbol{y}}$ is an hyperplane which verifies that all the points within the subset are contained by it. In other words, it is defined as $HP = \{\boldsymbol{y} | \boldsymbol{p}^T\boldsymbol{y} = \boldsymbol{p}^T\hat{\boldsymbol{y}}\}$, with $\boldsymbol{p} \neq \boldsymbol{0}$, and satisfies that, for every $\hat{\boldsymbol{y}}' \in \mathcal{Y}$, it holds

$$\boldsymbol{p}^T\hat{\boldsymbol{y}}' \leq \boldsymbol{p}^T\hat{\boldsymbol{y}}. \tag{3.78}$$

See this graphically in Figure 3.8. Note that $\hat{\boldsymbol{y}}$ is the orthogonal projection of $\boldsymbol{y}_0$ to the described hyperplane. Now, let us write the distance between two points a and b as $d_{a,b}$. Then, for any $\boldsymbol{y}_0$, $\hat{\boldsymbol{y}}$ and $\boldsymbol{y}^* \in \mathcal{Y}$, the application of the cosine theorem attains

$$d_{\boldsymbol{y}_0,\boldsymbol{y}^*} = \sqrt{d^2_{\hat{\boldsymbol{y}},\boldsymbol{y}_0} + d^2_{\hat{\boldsymbol{y}},\boldsymbol{y}^*} - 2d_{\hat{\boldsymbol{y}},\boldsymbol{y}^*}d_{\hat{\boldsymbol{y}},\boldsymbol{y}^*}\cos\alpha} \tag{3.79}$$

where α is the angle defined by the segment lines from $\hat{\boldsymbol{y}}$ to $\boldsymbol{y}_0$ and from $\hat{\boldsymbol{y}}$ to $\boldsymbol{y}^*$, respectively. Finally, noting that $\alpha \in [\frac{\pi}{2}, \frac{3\pi}{2}]$, it is confirmed that $d_{\boldsymbol{y}_0,\boldsymbol{y}^*} \geq d_{\hat{\boldsymbol{y}},\boldsymbol{y}^*}$. ■

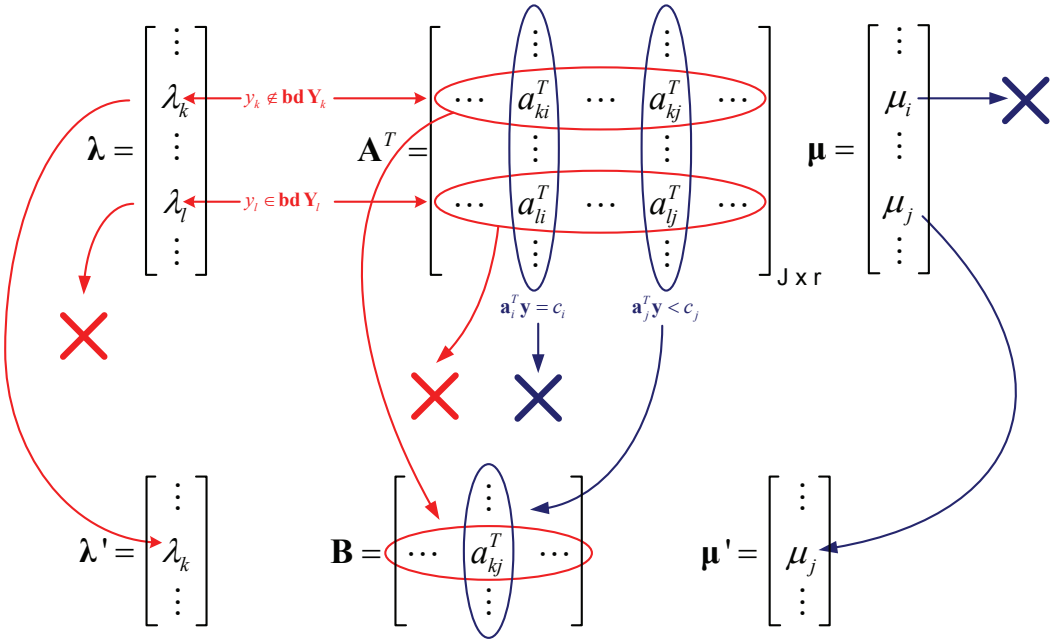

Figure 3.9: Construction of the linear system $\boldsymbol{\lambda}'_0 = \boldsymbol{B}\boldsymbol{\mu}'$ used in the dual projection of the method.

From Primal Subproblems to Dual Suproblems: the Dual Projection

Consider now the link from primal subproblems to dual subproblems or equivalently, how the values in $\boldsymbol{\lambda}_0 = [\lambda_{0_1}, \ldots, \lambda_{0_J}]^T$ (from now on the output of the primal subproblems) are transformed to the values $\boldsymbol{\mu}$ (the input of the dual subproblems). In this case, two of the previous observations are used: i) if $\boldsymbol{a}_k^T\boldsymbol{y} < c_k$, then $\mu_k = 0$ and ii) the fact that $\lambda_{0_j} = [\boldsymbol{A}^T]_j\,\boldsymbol{\mu}$ for those y_j not in the boundary of $\mathcal{Y}_j$. First, we construct the new matrix $\boldsymbol{B}$ by selecting the k^{th} column of $\boldsymbol{A}^T$ if $\boldsymbol{a}_k^T\boldsymbol{y} = c_k$ and discarding it if $\boldsymbol{a}_k^T\boldsymbol{y} < c_k$. If the k^{th} column is eliminated, then immediately $\mu_k = 0$. Accordingly, a new $\boldsymbol{\mu}'$ vector is defined with the non-zero values. Similarly, the files in $\boldsymbol{A}^T$ whose associated $y_j \in \text{bd } \mathcal{Y}_j$ are discarded in $\boldsymbol{B}$ and not included in the new vector $\boldsymbol{\lambda}'_0$. See it graphically in Figure 3.9. In this way, the linear system $\boldsymbol{\lambda}'_0 = \boldsymbol{B}\boldsymbol{\mu}'$ collects the equations that are useful for the obtention of a new $\boldsymbol{\mu}$ from the given $\boldsymbol{\lambda}_0$ values (output of the primal subproblems). Note that the KKT optimality conditions associated to the coupling variables that have been relaxed in primal and dual subproblems (hence not taken into account therein) are now considered.

The linear system $\boldsymbol{\lambda}'_0 = \boldsymbol{B}\boldsymbol{\mu}'$ is in general overdetermined or, in some cases, determined. In order to verify it, take a feasible primal point $\boldsymbol{y}$ and let a subset $\mathcal{M}$ of the constraints $\boldsymbol{a}_i^T\boldsymbol{y} \leq c_i$ in (3.61) attain equality if $i \in \mathcal{M}$. With that subset of affine equalities, define the linear system of equations $\boldsymbol{A}^{\mathcal{M}}\boldsymbol{y} = \boldsymbol{c}^{\mathcal{M}}$. Note that by construction, card $\{\mathcal{M}\}$ equals the number of elements in $\boldsymbol{\mu}'$. Since $\boldsymbol{A}$ is assumed to be a full rank matrix, we have rank $\boldsymbol{A}^{\mathcal{M}}$ = card $\{\mathcal{M}\}$. And since

the matrix $\boldsymbol{A}^{\mathcal{M}}$ is a flat matrix, the matrix $(\boldsymbol{A}^{\mathcal{M}})^T$ is tall. Finally, it holds that the number of variables y_j such that $y_j \notin \mathcal{Y}_j$ is at least equal to card $\{\mathcal{M}\}$ (otherwise there is a contradiction in the definition of the coupling system $\boldsymbol{A}^{\mathcal{M}}\boldsymbol{y} = \boldsymbol{c}^{\mathcal{M}}$) and therefore it is verified that the system of equations[5] $\boldsymbol{\lambda}'_0 = \boldsymbol{B}\boldsymbol{\mu}'$ is determined or overdetermined.

The completion of the dual projection requires the previous values of $\boldsymbol{\mu}$, called $\boldsymbol{\mu}^t$, to obtain $\boldsymbol{\mu}^{t+1}$. The objective in dual projection is to provide dual feasible values $\boldsymbol{\lambda}^{t+1} = \boldsymbol{A}^T\boldsymbol{\mu}^{t+1}$ such that the relative position to $\boldsymbol{\lambda}^*$ is preserved (if possible) when updating from $\boldsymbol{\lambda}^t$ to $\boldsymbol{\lambda}^{t+1}$. That is, if $\lambda_k^t < \lambda_k^*$ ($\lambda_k^t > \lambda_k^*$), then we want that $\lambda_k^{t+1} < \lambda_k^*$ ($\lambda_k^{t+1} > \lambda_k^*$) – if it is possible given the $\boldsymbol{\lambda}_0$ values from the primal subproblems –. Also, we want to take advantage of the approaching updates in primal projection ($\hat{\boldsymbol{y}}$ is closer to $\boldsymbol{y}^*$ than $\boldsymbol{y}_0$) and use the information in $\hat{\boldsymbol{y}}$ (which is available at the output of the primal subproblems, $\boldsymbol{\lambda}_0$, when $\hat{\boldsymbol{y}}$ is the input to them).

The logic in the previous discussion is to try to keep the successives updates of the dual subproblems within the same zone (a zone is defined as the subset of points $\boldsymbol{y}_0$ that have the same relative position with respect to the constraints in $\boldsymbol{A}\boldsymbol{y}_0 = \boldsymbol{c}$) and approaching to the optimal value $\boldsymbol{y}^*$, while the constraints in $\boldsymbol{A}\boldsymbol{y} \preceq \boldsymbol{c}$ are taken into account. This forces primal projections to have similar directions in successive updates and avoids abrupt changes of zone (it is also discussed later), as shown in the following example. Consider, for instance, that $\boldsymbol{\lambda}^t = \boldsymbol{A}^T\boldsymbol{\mu}^t \prec \boldsymbol{\lambda}^*$. When this $\boldsymbol{\lambda}^t$ is used as the input of the dual subproblems, the output $\boldsymbol{y}_0$ attains $\boldsymbol{A}\boldsymbol{y}_0 \succ \boldsymbol{c}$ (recall the relationship between primal and dual variables in the subproblems in Lemma 2). If primal projection is applied to the point $\boldsymbol{y}_0$, then the resulting $\hat{\boldsymbol{y}}$ is closer to $\boldsymbol{y}^*$ (as already shown in Lemma 3). For the sake of simplicity, assume now that all constraints keep active in the iterations considered. Finally, if dual projection achieves $\boldsymbol{\lambda}^{t+1} = \boldsymbol{A}^T\boldsymbol{\mu}^{t+1} \prec \boldsymbol{\lambda}^*$, then the update on $\boldsymbol{y}_0$ will also attain $\boldsymbol{A}\boldsymbol{y}_0 \succ \boldsymbol{c}$. Moreover, it will be closer to the optimal solution since the dual projection has used updated information from the primal subproblems when $\hat{\boldsymbol{y}}$ was the input of those. In general, the subset of active constraints evolves with successive updates until the optimal subset is found. The algorithm we propose is capable of discovering that optimal subset and therefore to define the zone from where to reach the optimal solution (where the $\boldsymbol{y}_0$ points of primal projection lie), as discussed later.

Using the arguments above and taking again the problem $\boldsymbol{\lambda}'_0 = \boldsymbol{B}\boldsymbol{\mu}'$ (that implicitly includes optimality conditions for the primal and dual coupling variables), note that the intuitive solution (and in some sense dual converse of the primal projection) that is found as the argument of the following least squares problem

$$\begin{array}{ll} \min\limits_{\boldsymbol{\mu}'} & \|\boldsymbol{\lambda}'_0 - \boldsymbol{B}\boldsymbol{\mu}'\|^2 \\ s.t. & \boldsymbol{\mu}' \succeq \boldsymbol{0} \end{array} \tag{3.80}$$

does not meet the previous requirements. Note that such strategy has no control on where new

[5] $\boldsymbol{B}$ is a selection of the equations defined by the matrix $(\boldsymbol{A}^{\mathcal{M}})^T$ since, due to the construction process in Figure 3.9, some of the remaining equations in $\boldsymbol{B}$ may contain only zero entries and they are eliminated.

updates are placed (relative to $\boldsymbol{\lambda}^*$).

Our proposal to perform the dual projection checks the distances between the proposed $\boldsymbol{\lambda}_0$ values (from the primal subproblems) and the previous feasible values derived from $\boldsymbol{\mu}^t$ as $\boldsymbol{\lambda}^t = \boldsymbol{A}^T\boldsymbol{\mu}^t$. The distance vector $\boldsymbol{d}$ is readily given as

$$\boldsymbol{d} = diag\left((\boldsymbol{\lambda}^t - \boldsymbol{\lambda}_0)(\boldsymbol{\lambda}^t - \boldsymbol{\lambda}_0)^T\right) = diag\left((\boldsymbol{A}^T\boldsymbol{\mu}^t - \boldsymbol{\lambda}_0)(\boldsymbol{A}^T\boldsymbol{\mu}^t - \boldsymbol{\lambda}_0)^T\right) \tag{3.81}$$

Now, since the subsystem of interest is $\boldsymbol{\lambda}'_0 = \boldsymbol{B}\boldsymbol{\mu}'$, we accordingly define $\boldsymbol{d}'$ by collecting the values d_k where k is such that $y_k \notin \text{bd } \mathcal{Y}_k$. To finally obtain $\boldsymbol{\mu}'$, we take from the subsystem $\boldsymbol{\lambda}'_0 = \boldsymbol{B}\boldsymbol{\mu}'$ the minimum subset of equations that are linearly independent and that have the minimum possible values in $\boldsymbol{d}'$. The indices of the equations selected are grouped in the integer subset $\mathcal{D}$ and the corresponding linear systems of equations is $\boldsymbol{\lambda}'_{0\mathcal{D}} = \boldsymbol{B}_{\mathcal{D}}\boldsymbol{\mu}'$. A simple algorithm to obtain the subset is:

---

set $\mathcal{D} = \{\oslash\}$, $\mathcal{K} = \{1, \ldots, length(\boldsymbol{\lambda}'_0)\}$ and do

1. search the minimum value d'_k with $k \in \mathcal{K}$
2. set $\mathcal{D}^{\triangleright} = \mathcal{D} \cup k$
3. if $rank(\boldsymbol{B}_{\mathcal{D}^{\triangleright}}) > rank(\boldsymbol{B}_{\mathcal{D}})$, then $\mathcal{D} = \mathcal{D}^{\triangleright}$
4. $\mathcal{K} = \mathcal{K} \setminus k$

repeat until $rank(\boldsymbol{B}_{\mathcal{D}}) = length(\boldsymbol{\mu}')$

Once given $\mathcal{D}$, the output of the dual projection must take into account the optimality condition $\boldsymbol{\mu} \succeq \boldsymbol{0}$. It is obtained as the argument of the following quadratic optimization problem,

$$\begin{array}{ll} \min\limits_{\boldsymbol{\mu}'} & \|\boldsymbol{\lambda}'_{0\mathcal{D}} - \boldsymbol{B}_{\mathcal{D}}\boldsymbol{\mu}'\|^2 \\ s.t. & \boldsymbol{\mu}' \succeq \boldsymbol{0} \end{array} \tag{3.82}$$

From the value of $\boldsymbol{\mu}'$, the output values $\boldsymbol{\mu}^{t+1}$ are readily obtained by adding zero elements into the corresponding positions, i.e. $\mu_k^{t+1} = 0$ if the corresponding primal value $y_k \in \text{bd } \mathcal{Y}_k$.

As an example to illustrate what dual projection performs, consider the situation in Figure 3.10, where we graphically obtain $\boldsymbol{\lambda}^{t+1}$ from $\boldsymbol{\lambda}^t$ and the output of the subproblems ($\boldsymbol{\lambda}_0$). For simplicity reasons, assume that all $\boldsymbol{\lambda}_0$ and $\boldsymbol{\mu}$ values are active, so the system of equations $\boldsymbol{\lambda}'_0 = \boldsymbol{B}\boldsymbol{\mu}'$ is for this particular case equivalent to the linear system $\boldsymbol{\lambda} = \boldsymbol{A}^T\boldsymbol{\mu}^t$. In the figure, we have depicted the two-dimensional subspace generated by $\boldsymbol{\mu}$ inside the subspace $\mathbb{R}^3_+$ of $\boldsymbol{\lambda}$. The following equations relate both subspaces

$$\begin{array}{rcl} \lambda_1 &=& \mu_1 \\ \lambda_2 &=& \mu_2 \\ \lambda_3 &=& \mu_1 + \mu_2 \end{array} \quad . \tag{3.83}$$

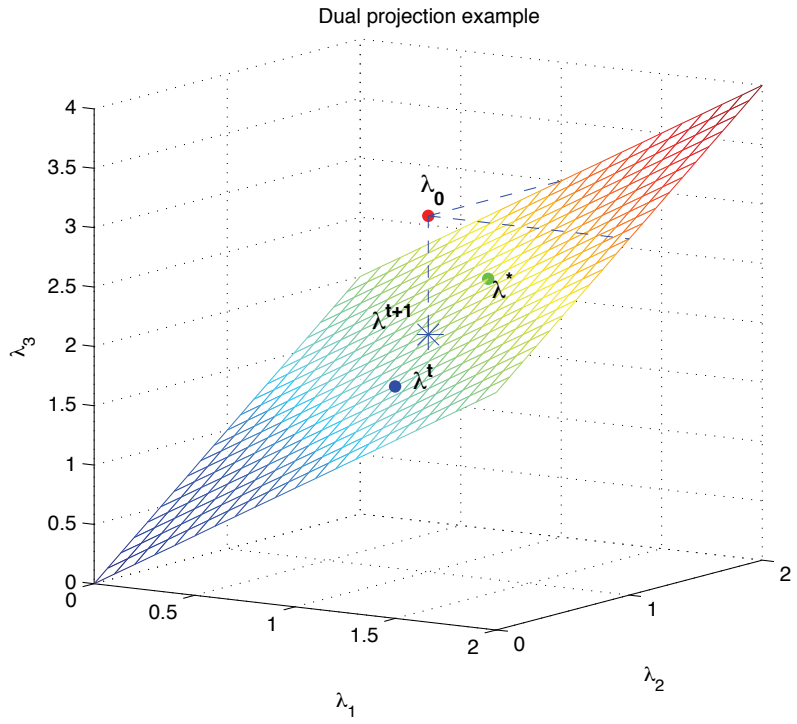

Figure 3.10: A dual projection example.

In dashed lines, there are the three possible projections into the subset of $\boldsymbol{\mu}$ from the given point $\boldsymbol{\lambda}_0$. Note that they are found by solving the previous system by selecting 2 out of 3 equations. The point $\boldsymbol{\lambda}^{t+1}$ is the selected projection. Note that it keeps the relative position with respect to $\boldsymbol{\lambda}^*$ at the same time it gets closer to the optimal value.

If we calculate the distance $\|\boldsymbol{\lambda}'^{t+1} - \boldsymbol{\lambda}'^{t}\|^2$ in a general case (consider $\boldsymbol{\lambda}'^{t+1} = \boldsymbol{B}\boldsymbol{\mu}'^{t+1}$), we have that

$$\|\boldsymbol{\lambda}'^{t+1} - \boldsymbol{\lambda}'^{t}\|^2 = \sum_i (\lambda_i'^{t+1} - \lambda_i'^{t})^2. \tag{3.84}$$

Assuming that the solution to the reduced linear system of equations $\boldsymbol{\lambda}'_{\mathcal{D}} = \boldsymbol{B}_{\mathcal{D}}\boldsymbol{\mu}'$ attains $\boldsymbol{\mu}' \succeq \mathbf{0}$, we have

$$\|\boldsymbol{\lambda}'^{t+1} - \boldsymbol{\lambda}'^{t}\|^2 = \sum_{i\in\mathcal{D}} d'_i + \sum_{i\notin\mathcal{D}} (\lambda_i'^{t+1} - \lambda_i'^{t})^2, \tag{3.85}$$

because for each $i \in \mathcal{D}$, it holds that $\lambda_i'^{t+1} = \lambda'_{0_i}$. Furthermore, the quantities $\lambda_i'^{t+1}$ and $\lambda_i'^{t}$ can be expressed, for each $i \notin \mathcal{D}$, as a linear combination of the values $\lambda_i'^{t+1}$ and $\lambda_i'^{t}$ with $i \in \mathcal{D}$, respectively. With that observation, we can write

$$\|\boldsymbol{\lambda}'^{t+1} - \boldsymbol{\lambda}'^{t}\|^2 = \sum_{i\in\mathcal{D}} d'_i + \sum_{i\notin\mathcal{D}} \left(f_i \left(\sqrt{d'_{j\in\mathcal{D}}} \right) \right)^2, \tag{3.86}$$

where $f_i\left(\sqrt{d'_{j\in\mathcal{D}}}\right)$ is a certain linear combination of the square root of the elements in $\boldsymbol{d}'$ that belong to the subset $\mathcal{D}$. The equation in (3.86) justifies the method employed in the dual projection. In other words, by selecting the equations whose d'_i values are the smallest available, we hope that the output of the dual projection $\boldsymbol{\lambda}^{t+1} = \boldsymbol{A}^T\boldsymbol{\mu}^{t+1}$ is close to the previous $\boldsymbol{\lambda}^t$ value (always conditioned to the values of $\boldsymbol{\lambda}_0$, implicitly obtained from the primal projection through primal subproblems), although not necessarily the closest one.

At this point, we have introduced all the elements that are required to construct the proposed coupled-decomposition method. The reader would have noticed that primal and dual subproblems, as well as primal projection, can be perfectly isolated and so they have been explained. Against, dual decomposition and the motivation behind suggests to interact with primal projection using primal and dual subproblems as translators between primal and dual domains. The algorithm we propose can then be summarized as follows:

---

initialize $\boldsymbol{\mu}^t = \boldsymbol{\mu}^0$ (e.g. $\boldsymbol{\mu}^0 = \mathbf{0}$)

repeat

1. Set $\boldsymbol{\lambda}^t = \boldsymbol{A}^T\boldsymbol{\mu}^t$ and compute the dual subproblems using (3.67). Store $\boldsymbol{y}_0^t, \{\boldsymbol{x}_j\}^t$.
2. Use $\boldsymbol{y}_0^t$ and $\boldsymbol{\mu}^t$ in the primal projection (3.77) and obtain $\hat{\boldsymbol{y}}^t$.
3. Input $\hat{\boldsymbol{y}}^t$ in the primal subproblems (3.62) and get the dual candidates $\boldsymbol{\lambda}_0^t$.
4. Using $\boldsymbol{\lambda}_0^t$ and $\hat{\boldsymbol{y}}^t$, update $\boldsymbol{\lambda}^{t+1} = \boldsymbol{A}^T\boldsymbol{\mu}^{t+1}$ by performing dual projection (3.82).

until stopping criteria are accomplished

To finally complete the solution, an adequate stopping criterion must be defined for the algorithm. In the review of interior point methods, it has been said that typical stopping criteria in most algorithms fix a threshold to the relative variation of the objective value, to the solution attained, or both. In other words, for a given threshold $\epsilon > 0$, numerical methods can be stopped at a certain iteration if $\frac{|f_0(\boldsymbol{x}^{n+1}) - f_0(\boldsymbol{x}^n)|}{|f_0(\boldsymbol{x}^{n+1})|} < \epsilon$ or $\frac{||\boldsymbol{x}^{n+1} - \boldsymbol{x}^n||}{||\boldsymbol{x}^{n+1}||} < \epsilon$, or both. In the MVC decomposition method, the difference between the current value of the primal subproblem and the dual subproblem was used, since when both are evaluated in the optimal primal and dual values, the difference vanishes (strong duality holds).

The stopping criterion we propose for the coupled-decomposition method checks the following differences in primal and dual domains,

$$\frac{\|\hat{\boldsymbol{y}}^t - \boldsymbol{y}_0^t\|^2}{\|\hat{\boldsymbol{y}}^t\|^2} \leq \epsilon \qquad \text{and} \qquad \frac{\|\boldsymbol{\lambda}_0'^t - \boldsymbol{B}^t\boldsymbol{\mu}'^t\|^2}{\|\boldsymbol{B}^t\boldsymbol{\mu}'^t\|^2} < \epsilon. \tag{3.87}$$

When the optimal solution of the problem is attained in primal and dual domains, i.e. $\hat{\boldsymbol{y}}^t$ and $\boldsymbol{\mu}^t$ with $t \longrightarrow \infty$, both numerators vanish. It is not difficult to check that under the assumptions

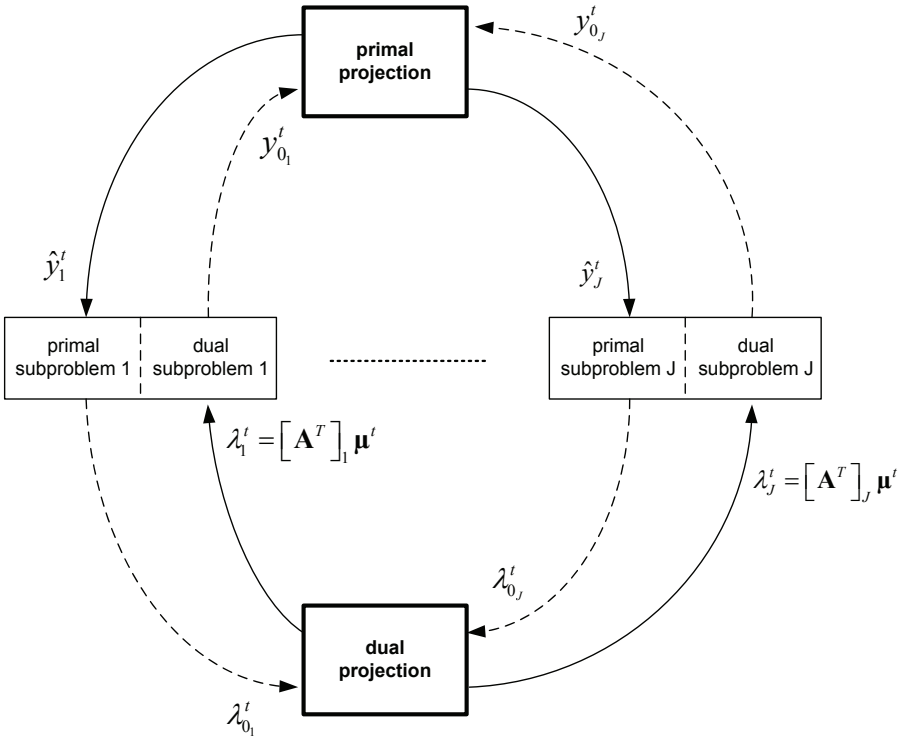

Figure 3.11: Block diagram of the coupled-decomposition method.

made in the problem statement, all KKT conditions of the global problem can be fulfilled using the values obtained. Therefore, the solution is optimal and the stopping criterion is well established.

The reader can find again in Figure 3.11 the block diagram representation of the method. Primal and dual subproblems are linked to primal and dual projections with arrows that represent, in a distributed implementation of the method, the message passing that is required.

3.3.2 Resource-Price Interpretation

It is possible to give an economic interpretation to convex problems by relating primal variables to resources employed and dual variables to the prices that have to be paid for using such resources. For that purpose, let us rewrite again the primal subproblem in (3.62) as

$$\begin{array}{ll} \min\limits_{\boldsymbol{x}} & f(\boldsymbol{x}) \\ s.t. & \boldsymbol{x} \in \mathcal{X}, \\ & h(\boldsymbol{x}) \leq y \end{array} \tag{3.88}$$

and call λ the dual Lagrange variable associated to the constraint $h(\boldsymbol{x}) \leq y$. While studying the relationship between primal an dual subproblems, it has been shown that an increase in λ implies a decrease in y and viceversa. Therefore, we can interpret that if the price of the

resource increases, less resources are used in order to optimize the revenue, which is $f(\boldsymbol{x})$. On the contrary, if the price is reduced, the revenue is optimized by employing more resources.

However, we are mostly interested in the extension of the interpretation of the subproblems to the general problem formulation in (3.61) and the algorithm proposed to solve it. The variables involved are the primal and dual candidates of the subproblems, i.e. $\boldsymbol{y}_0$ and $\boldsymbol{\lambda}_0$, and the primal and dual corrections performed by the projections, i.e. $\hat{\boldsymbol{y}}$ and $\boldsymbol{\lambda} = \boldsymbol{A}^T\boldsymbol{\mu}$. Note that the price that the j^{th} subproblem is willing to pay, i.e. $\lambda_j = [\boldsymbol{A}^T]_j\,\boldsymbol{\mu}$, is obtained as the sum of the prices of the constraints (grouped in vector $\boldsymbol{\mu}$) where j^{th} subproblem competes for the allocation of that resource. As an example, consider the scenario proposed in (3.83). Therein, subproblem 1 and subproblem 3 compete to allocate $y_1 + y_3 \leq c_1$, whereas subproblem 2 and subproblem 3 do their part with $y_2 + y_3 \leq c_2$.

Under this economic perspective, the method we propose can be interpreted as follows. Once fixed the prices to pay in order to make use of a shared resource (the values in $\boldsymbol{\mu}$), the dual subproblems compute the price they have to pay (in $\boldsymbol{\lambda}$) and take the quantities of resource (grouped in $\boldsymbol{y}_0$) that maximize their own revenue (by properly allocating its internal resources $\boldsymbol{x}_j$). However, these may not be feasible and primal projection corrects the values to the nearest feasible ones. Again, these may not be feasible, now from the dual (price) point of view. In other words, some of the subproblems pay more than others for the same resources. The dual projection is in charge of reaching a consensus on the price of the shared resources (in $\boldsymbol{\mu}$). From that point of view, dual projection updates the prices in $\boldsymbol{\mu}$ trying to avoid sudden increases or decreases in the price that the subproblems will pay in $\boldsymbol{\lambda} = \boldsymbol{A}^T\boldsymbol{\mu}$. Hence, dual projection imposes the constraints that the prices should satisfy. Note that if the price is abruptly too expensive or too cheap, in both cases the dual subproblems will fix $y_j \in \text{bd}\ \mathcal{Y}_j$ and they will be not prepared to pay anything for them. This will definitively difficult the consensus among parts.

The key issues of the method are: i) the relation between primal and dual variables in the subproblems (see Lemma 2); ii) the primal projection, which assures to get closer to the optimal solution (see Lemma 3) and iii) the dual projection, which imposes the constraints that the prices must verify ($\boldsymbol{\lambda} = \boldsymbol{A}^T\boldsymbol{\mu}$). Note that the method is able to discover which coupling constraints within $\boldsymbol{A}\boldsymbol{y} \preceq \boldsymbol{c}$ are active (i.e. attained with equality), which implies that the corresponding values within $\boldsymbol{\mu}$ satisfy $\mu_k > 0$. This is done in primal and dual projections as follows. On one hand, a μ_k value enters the active subset of $\boldsymbol{\mu}$ values when the constraint $\boldsymbol{a}_k^T\boldsymbol{y} \leq c_k$ becomes active (i.e. attained with equality) after the primal projection. On the other hand, an active μ_k value leaves the active subset when the dual projection forces $\mu_k = 0$. Finally, we want to remark that both primal and dual projections can be efficiently computed using numerical methods (since they are QP problems) and that there is no combinatorial process throughout the whole method.

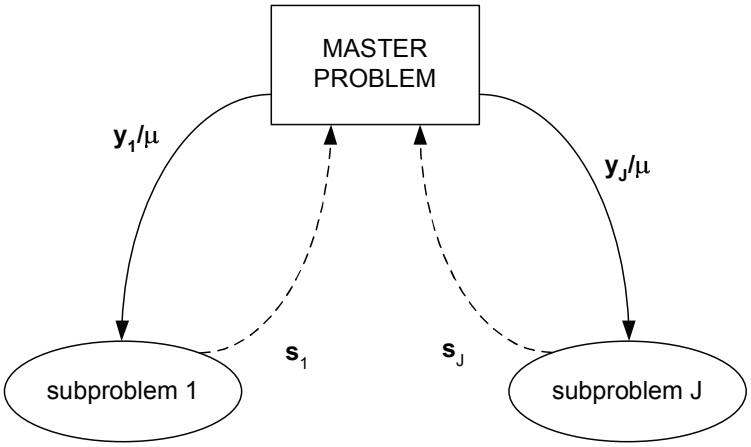

Figure 3.12: Block diagram in pure primal/dual decomposition.

3.3.3 Comparison with Previous Approaches

After the description of the method and the final summary in block diagram representation, the coupled-decomposition method is compared to the pure primal and dual decomposition approaches and to the MVC decomposition method from an architecture point of view.

Consider first the block diagram of a pure primal/dual decomposition method (as described in Sections 3.2.1 and 3.2.2) and depicted in Figure 3.12. It is clearly noted that the way the problem is split is comparable to the coupled-decomposition method because several subproblems are taken into account, though signalling is simpler. The master problem sends to the subproblems the variables that couple the subproblems through the constraints (these are $\boldsymbol{y}_i$ in the primal case and $\boldsymbol{\mu}$ in the dual case). With these values, the subproblems optimize their local variables and compute the subgradients $\boldsymbol{s}_i$. These indicate to the master problem what the updates of $\boldsymbol{y}_i$ and $\boldsymbol{\mu}$ should be so as to optimize their local subproblems. That information allows the master problems to decide the best strategy to reach global optimality. In terms of the time required to reach a solution, we want to remark that both approaches may require many iterations to converge, which can be in part justified by the problem of having a user-defined step-size in the master problems (as previously discussed in the corresponding sections).

Note that in the coupled-decomposition method, the master problems play the role of primal and dual projections. However, the philosophy in the computation is different (we do not use the subgradient concept) and so they actually are the projections. The method is able to combine both primal and dual decompositions in a unified approach.

If we consider now a block diagram picture of the MVC decomposition method as described in Section 3.2.3 (see Figure 3.13), we first realize that the problem is split into only two subproblems, primal subproblem and dual subproblem. Moreover, there is no dual or primal master as it

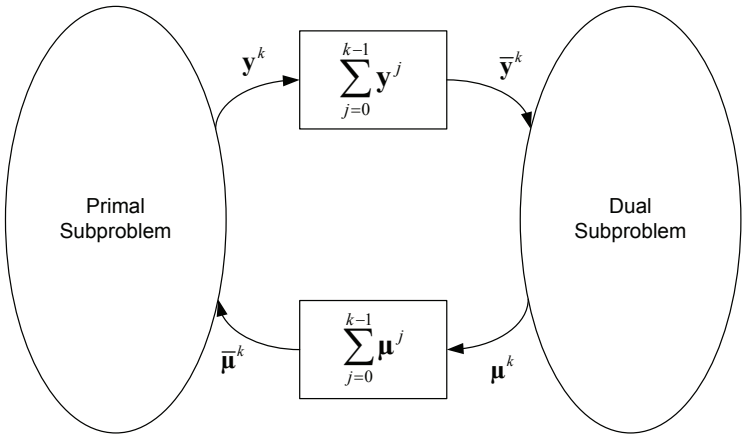

Figure 3.13: Block diagram in MVC decomposition.

happens to be with the rest of the methods. The idea of *projection* is no further used but a time-average of the outputs of primal and dual subproblems is required to guarantee the convergence of the algorithm. In practical terms, this reduces significantly the speed of convergence of the algorithms, as we will show later with an example.

Finally, we summarize the results of the comparison among methods in Table 3.1.

3.3.4 Geometric Interpretation

Consider now the following optimization problem

$$\begin{array}{lll} \min\limits_{x_1,x_2,y_1,y_2} & -p_1\log x_1 - p_2 \log x_2 & \\ s.t. & m_i \leq x_i \leq d_i, & i=1,2 \\ & x_i \leq y_i & i=1,2 \\ & y_1+y_2 \leq c & \\ & m_i \leq y_i \leq d_i, & i=1,2 \end{array} , \tag{3.89}$$

which is adequately written to suit a coupled-decomposition strategy. In this case, we have λ_1 and λ_2 as dual variables associated to the constraints $x_i \leq y_i$ and μ as the dual variable associated to the coupling constraint $y_1 + y_2 \leq c$.

Method	Number of subproblems	Primal treatment	Dual treatment	Algorithm step-size
Primal Decomposition	Several	✓	×	User-defined
Dual Decomposition	Several	×	✓	User-defined
MVC Decomposition	2	✓	✓	Time-average
Coupled-decomposition	Several	✓	✓	×

Table 3.1: Comparison among methods.

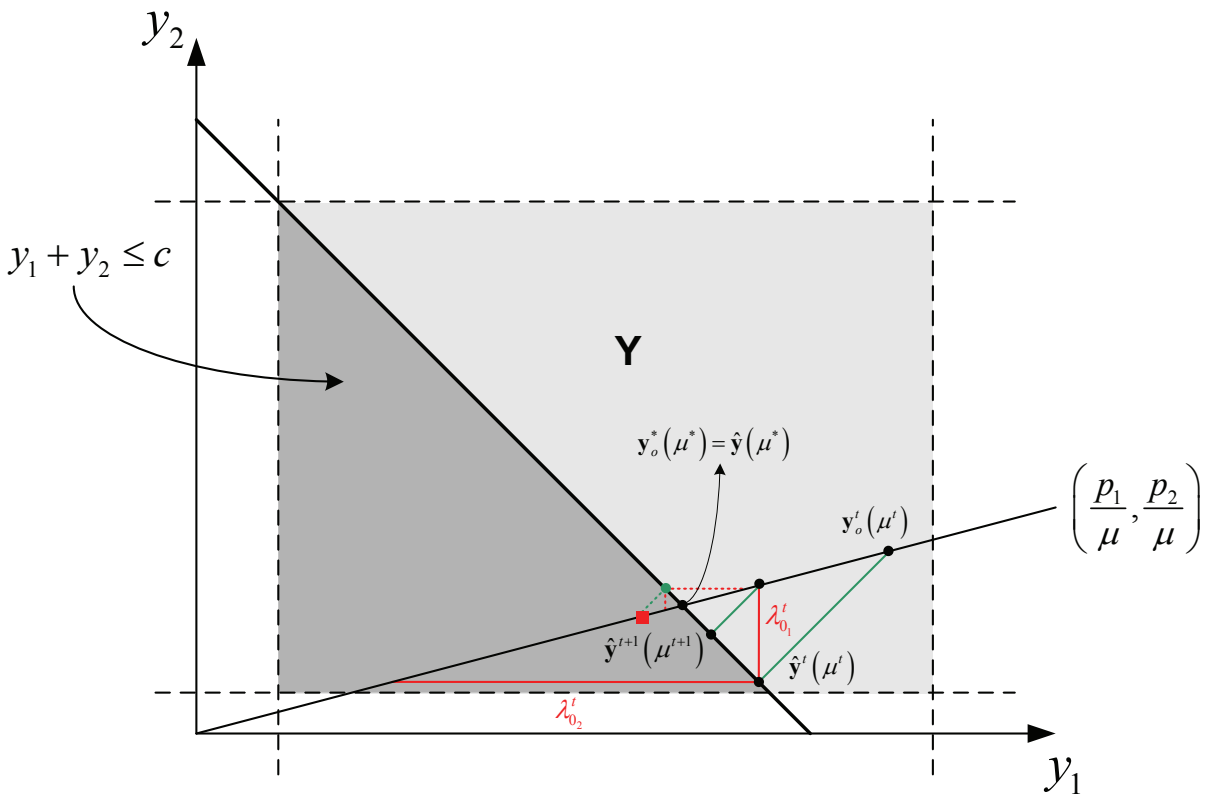

Figure 3.14: Geometric interpretation of the proposed method.

The primal subproblems are

$$\begin{array}{ll} \min\limits_{x_i} & -p_i \log x_i \\ s.t. & m_i \leq x_i \leq d_i \\ & x_i \leq y_i \end{array} \tag{3.90}$$

and can be solved analytically using the KKT conditions of the problem. The optimal value x_i is readily given as

$$\boldsymbol{x}_i = \frac{p_i}{\lambda_i}\Big]_{m_i}^{d_i} \tag{3.91}$$

where

$$a\Big]_{A_1}^{A_2} = \begin{cases} A_2, & a > A_2 \\ a, & A_1 \leq a \leq A_2 \\ A_1, & a < A_1 \end{cases} \tag{3.92}$$

The same relation would be obtained if we study the dual subproblems and hence, the relationship between dual and primal variables in subproblems (Lemma 2) is confirmed in this example.

Another known result applied to this problem is that, if $m_i < y_i < d_i$, then it holds $\lambda_i = [\boldsymbol{A}^T]_i\,\mu$, so when variables $\{y_1, y_2\}$ do not saturate to the lateral constraints, it is verified that

$$\mu = \lambda_1, \qquad \text{and} \qquad \mu = \lambda_2 \tag{3.93}$$

and therefore it is also true that for a given μ that accomplishes the considerations above, we have

$$\boldsymbol{x}(\mu) = \boldsymbol{y}(\mu) = \left[\frac{p_1}{\mu}, \frac{p_2}{\mu}\right]^T. \tag{3.94}$$

The previous results allow us to give a geometrical interpretation of the way the method operates and intuitively show how it converges to the optimal solution of the problem. For that purpose, consider Figure 3.14. The zone shaded in light grey and labelled as $\mathcal{Y}$ represents the lateral constraints $m_i \leq y_i \leq d_i$. If we intersect that zone with the half-space $y_1 + y_2 \leq c$ we get the zone shaded in darker grey, which is the feasible set of the problem. A line represents the values that the variables y_i take depending on the value of μ, accordingly to (3.94). Note that the slope of the line depends on the values of p_1 and p_2.

Assume that at a certain iteration of the proposed algorithm, the value μ^t is found. Using dual subproblems, we get $\boldsymbol{y}_0^t$, which is unfeasible for the problem. Thanks to primal projection (represented with a line), we reach $\hat{\boldsymbol{y}}^t$, which is feasible but diverges from the subspace generated by μ (a line in this case, too). From $\hat{\boldsymbol{y}}^t$, the primal subproblems emit their candidates for the dual variables $\boldsymbol{\lambda}$, i.e. the values $\lambda_{0_1}^t$ and $\lambda_{0_2}^t$. The red lines in the figure (vertical and horizontal departing from $\boldsymbol{y}_0^t$) represent the next value of $\hat{\boldsymbol{y}}_0^{t+1}$ when the equation $\lambda_{0_1}^t = \mu^{t+1}$ or the equation $\lambda_{0_2}^t = \mu^{t+1}$ is selected in the dual projection. If λ_{0_1} is used, which gives the closest possible value of μ^{t+1} to μ^t, we realize that the algorithm finds new values of $\boldsymbol{y}_0^{t+1}$ and $\hat{\boldsymbol{y}}^{t+1}$ that evolve towards the optimal value $\boldsymbol{y}_0^*(\mu^*) = \hat{\boldsymbol{y}}^*(\mu^*)$. Note that the algorithm forces $\boldsymbol{y}_0^t(\mu^t) \succ \boldsymbol{y}_0^*(\mu^*)$.

Imagine now that the strategy in the dual projection is to update the value of μ in a least-squares approach. For the problem under study this implies to solve the following problem

$$\begin{array}{cc} \min\limits_{\mu} & \|\boldsymbol{\lambda}_0 - \mathbf{1}\mu\|^2 \\ s.t. & \mu \geq 0 \end{array} \tag{3.95}$$

with solution $\mu = \frac{\lambda_{0_1}+\lambda_{0_2}}{2}$. The red square in Figure 3.14 approximately represents $\boldsymbol{y}_0^{t+1}$ for this particular dual projection. In this case, $\boldsymbol{y}_0^t(\mu^{t+1}) \prec \boldsymbol{y}_0^*(\mu^*)$ and we change the zone from where we perform primal projection: at iteration t we had $\boldsymbol{y}_0^t$ in the half-space $y_1 + y_2 > c$, whereas at iteration $t+1$, the update lies in $y_1 + y_2 < c$. Note in the figure that such strategy may not converge depending on the particular parameters of the problem, since it is possible to find an example where iterates keep jumping from one half-space to the other.

3.3.5 Examples and Performance

In this section we evaluate the performance of the coupled-decomposition method in two different scenarios and, at the same time, we take the opportunity to compare it through simulations with the other decomposition approaches described in the chapter.

Example 1

First, consider the following minimization problem

$$\begin{array}{ccc} \min\limits_{\boldsymbol{x}} & -\sum_{i=1}^{20} p_i \log x_i & \\ s.t. & m_i \leq x_i \leq d_i, & i = 1, \ldots, 20 \\ & \boldsymbol{A}\boldsymbol{x} \leq \boldsymbol{c} & \end{array} \tag{3.96}$$

where the values of $\boldsymbol{c}$, $\boldsymbol{m}$, $\boldsymbol{d}$ and $\boldsymbol{p}$ have been randomly chosen using distinct uniform probability density functions (p.d.f.). For the problem we simulate now, we have

$$\begin{aligned} \boldsymbol{c} &= [78.064, 342.67, 144.95, 60.464, 388.53, 353.98, 113.22]^T \\ \boldsymbol{m} &= [4.63, 0.58, 3.66, 1.04, 2.69, 4.32, 0.48, 1.65, 3.24, 2.16, \ldots \\ &\quad \ldots, 0.78, 1.97, 2.47, 0.65, 1.35, 1.63, 4.76, 4.34, 4.56, 3.47]^T \\ \boldsymbol{d} &= [38.48, 29.51, 33.83, 29.33, 57.56, 32.40, 20.57, 19.82, 32.23, 8.76, \ldots \\ &\quad \ldots, 38.04, 51.56, 45.19, 11.80, 46.46, 39.73, 35.09, 10.15, 59.96, 4.54]^T \end{aligned} \tag{3.97}$$

The matrix A has also been randomly generated with i.i.d (independent and identically distributed) Bernoulli variables of probability $p = 0.5$. Furthermore, $\boldsymbol{A}$ is discarded if it is not a

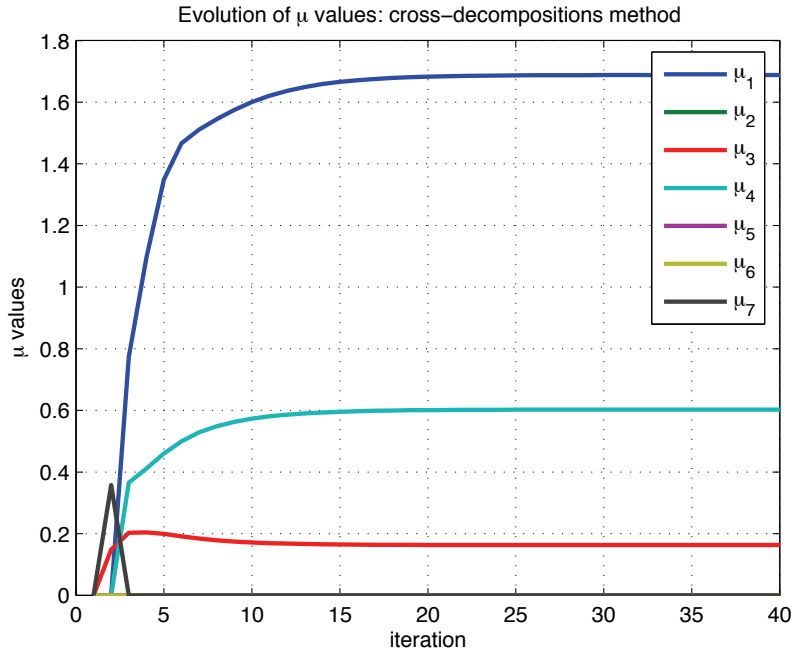

Figure 3.15: Evolution of dual variables $\boldsymbol{\mu}$ for problem (3.96) using the coupled-decomposition method.

full rank matrix. For the problem under study, we have

$$\boldsymbol{A} = \begin{bmatrix} 1 & 0 & 1 & 1 & 0 & 0 & 1 & 1 & 0 & 0 & 0 & 0 & 1 & 0 & 0 & 1 & 1 & 1 & 1 & 0 \\ 1 & 1 & 0 & 0 & 0 & 0 & 0 & 0 & 0 & 1 & 1 & 1 & 0 & 1 & 0 & 0 & 1 & 0 & 0 & 1 \\ 0 & 1 & 0 & 0 & 0 & 0 & 0 & 1 & 0 & 0 & 1 & 1 & 0 & 1 & 1 & 1 & 0 & 0 & 1 & 1 \\ 0 & 0 & 0 & 0 & 0 & 0 & 0 & 1 & 0 & 1 & 1 & 1 & 0 & 0 & 0 & 1 & 0 & 0 & 0 & 0 \\ 1 & 1 & 0 & 0 & 1 & 1 & 1 & 0 & 0 & 1 & 1 & 0 & 1 & 0 & 0 & 0 & 0 & 1 & 0 & 1 \\ 0 & 1 & 1 & 1 & 1 & 0 & 0 & 0 & 0 & 0 & 0 & 1 & 0 & 0 & 0 & 1 & 1 & 0 & 0 & 1 \\ 1 & 0 & 0 & 0 & 0 & 0 & 1 & 1 & 1 & 0 & 0 & 1 & 1 & 0 & 0 & 1 & 0 & 1 & 1 & 1 \end{bmatrix}. \tag{3.98}$$

Using the proposed coupled-decomposition method, we finally get the following optimal value:

$$\begin{aligned} \boldsymbol{x}^* = [&4.63, 20.07, 9.06, 5.63, 57.56, 32.40, 11.06, 6.56, 32.23, 8.76, \ldots \\ &\ldots, 18.88, 20.17, 3.89, 11.80, 46.46, 6.07, 10.59, 10.15, 10.38, 4.54]^T. \end{aligned} \tag{3.99}$$

We have checked that it is the optimal value of the by computing the solution with general non-linear constrained optimization methods. The evolution of the dual values $\boldsymbol{\mu}$ is depicted in Figure 3.15. Note that μ_1, μ_3 and μ_4 are the ones with non-zero values and thus constraints 1, 3 and 4 are attained with equality. Note also that initially μ_7 is considered active for the problem but discarded afterwards. Hence, the algorithm has found out the correct set of active constraints of the problem. If we take a look at the successive values of the constraints of the problem, i.e. the values $\boldsymbol{a}_i^T\boldsymbol{x} - c_i$, we confirm the statement above. See it in Figure 3.16. Furthermore, it can be observed that before reaching the optimal value $\boldsymbol{x}^*$, the constraints that are active at the

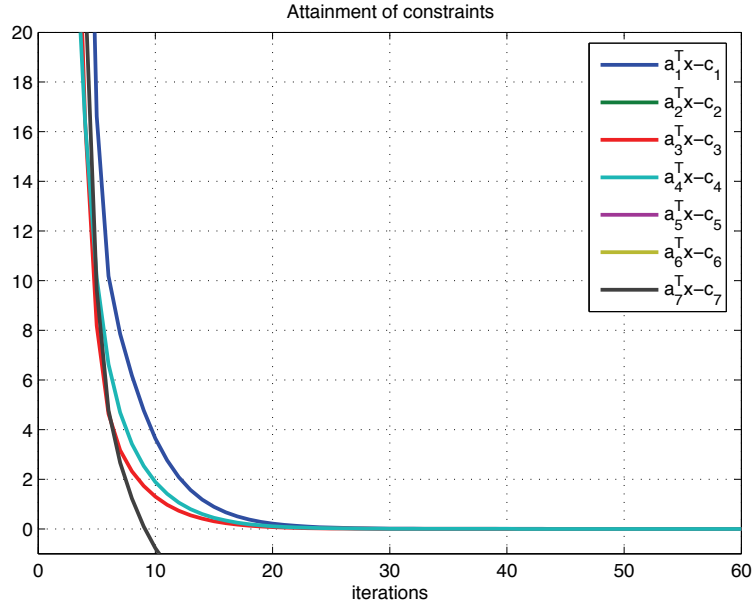

Figure 3.16: Evolution of the quantities $\boldsymbol{a}_i^T\boldsymbol{x} - c_i$ for problem (3.96) using the coupled-decomposition method.

optimal solution, violate these at all the iterations, which is coherent with the fact that the initial values of $\boldsymbol{\mu}$ are set to zero. Therefore, it holds that near the optimum, the projections of the values $\boldsymbol{y}_0^t(\boldsymbol{\mu}^t)$ onto the feasible set always depart from the same zone. The zone is the intersection of the half-spaces $\boldsymbol{a}_i^T\boldsymbol{x} > c_i$ for the active constraints of the problem in the optimal solution and the half-paces $\boldsymbol{a}_i^T\boldsymbol{x} < c_i$ for the other constraints.

Now we can compare the performance of the proposed coupled-decomposition method with the other reviewed decomposition approaches. More exactly, we compare our solution to the MVC decomposition approach in Section 3.2.3 and to a pure dual decomposition strategy (reviewed in Section 3.2.2). Both performance comparisons are also useful to check the consistency of the results.

In Figure 3.17, the reader can find the evolution of the primal variables $\bar{\boldsymbol{y}}^k$ of the MVC decomposition method (see Section 3.2.3) applied to solve (3.96). The first thing to note is that the method reaches approximately the same solution $\boldsymbol{x}^*$ attained with the proposed method, so results are coherent. However, the most remarkable issue in the MVC decomposition from the performance point of view is how time averaging (which is done both in primal and dual domains) influences the evolution of the variables. In the problem under study, it is clear that the method evolves smoothly towards the optimal solution and thus, the method we shows faster convergence.

The previous result relating the MVC decomposition method to our proposed technique

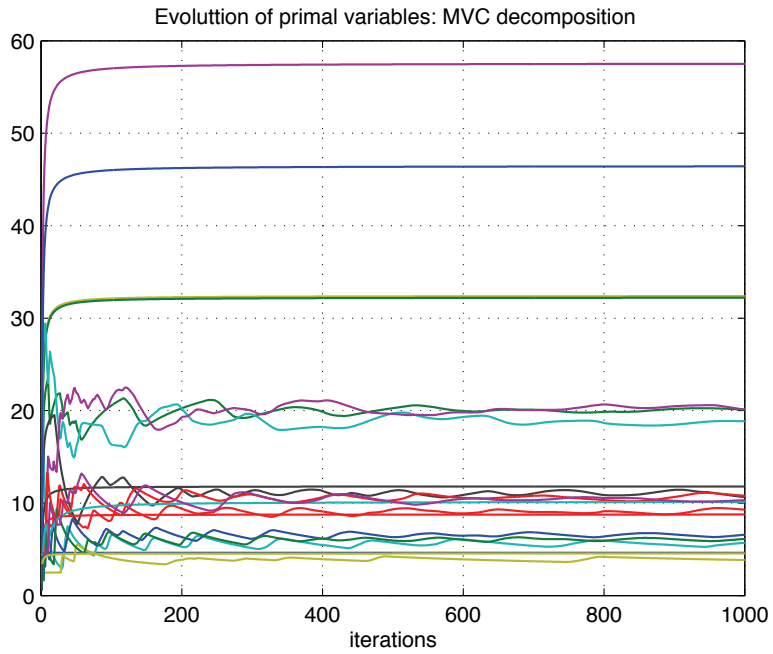

Figure 3.17: Evolution of the primal variables $\bar{\boldsymbol{y}}^k$ for the problem in (3.96) using the MVC decomposition method.

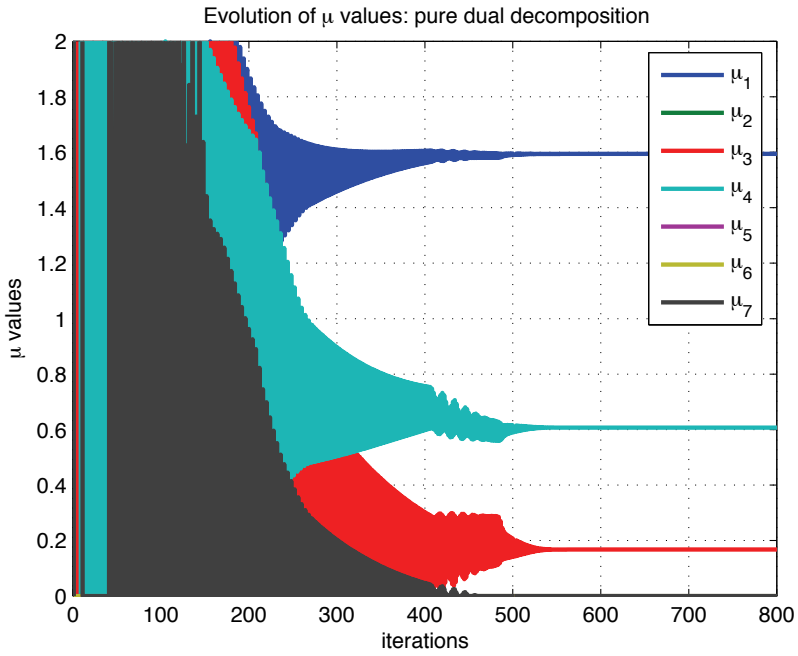

Figure 3.18: Evolution of the $\boldsymbol{\mu}$ values for problem (3.96) using a pure dual decomposition approach with diminishing step-size $\alpha = \frac{5}{k}$.

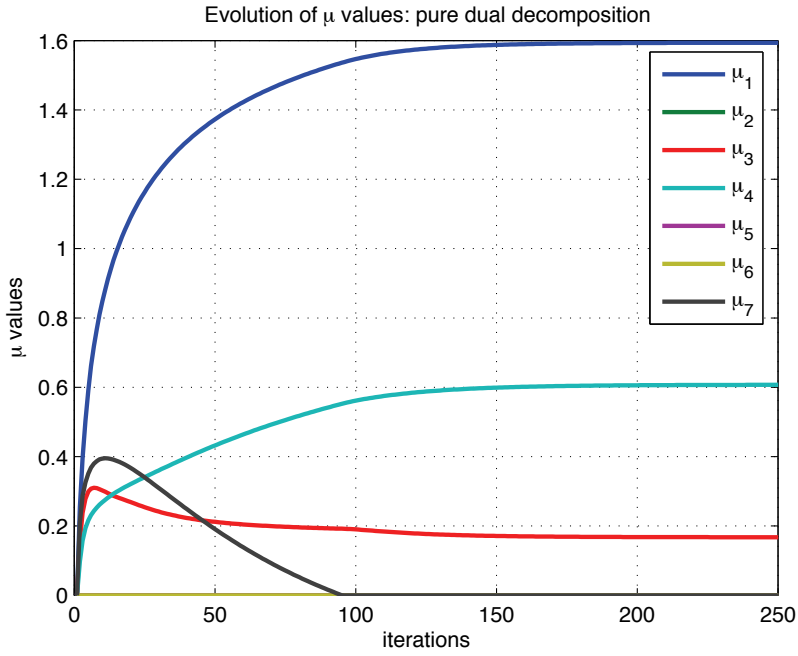

Figure 3.19: Evolution of the $\boldsymbol{\mu}$ values for problem (3.96) using a pure dual decomposition approach with constant step-size $\alpha = 0.001$.

can be extended also to the classical decomposition solutions. In this case, we compare with a pure dual decomposition approach with two different settings of the step-size α. In the first case, we set a coarse value of 5 but it is modified using a diminishing step-size approach, so α is calculated at each iteration k as $\alpha(k) = \frac{5}{k}$. Doing so, the optimal solution is well attained though the initial value is not adequate for the problem. In a second setting of the parameter, we set up a manually-tuned constant step-size of 0.001. The results of the iterations of the algorithm, plotted as the evolution of the dual values $\boldsymbol{\mu}$, are found in Figures 3.18 and 3.19. The reader can check again in this occasion that both results coincide with the results in the coupled-decomposition method (see Figure 3.15).

Aided by the previous figures, we want to remark graphically the inconvenience of the step-size in classical decomposition strategies. Note that a coarse adjustment of the parameter produces oscillations in the variables until a proper value is found. Globally, the algorithm requires many iterations to find out a solution. Setting a proper value of α improves the result and reduces significantly the time to converge. Still, the convergence of the proposed coupled-decomposition method is significantly better in terms of the number of iterations required to reach the optimal solution. Note that in many applications, it is difficult to perform a continuous tuning of the step-size and it becomes a shortcoming of classical approaches.

Example 2

In the second scenario, we change both the objective function and the type of coupling constraints. In the objective function we replace logarithms with square roots and the linear coupling constraints are modified by quadratic functions on the variables. The aspect of the problem is now

$$\begin{array}{ll} \min\limits_{\boldsymbol{x}} & -\sum_{i=1}^{20} p_i\sqrt{x_i} \\ s.t. & m_i \leq x_i \leq d_i, \quad i = 1,\ldots,20 \\ & \boldsymbol{A}\boldsymbol{h}(\boldsymbol{x}) \leq \boldsymbol{c} \end{array} \tag{3.100}$$

where $\boldsymbol{h}(\boldsymbol{x}) = [x_1^2,\ldots,x_N^2]^T$.

As in the previous example, we take random values for the parameters of the problem, which in this case are

$$\begin{array}{c} \boldsymbol{c} = [686.28, 441.12, 423.45, 319.79, 679.60, 671.36, 152.86]^T \\ \\ \boldsymbol{m} = [3.19, 2.15, 2.93, 1.57, 1.30, 4.99, 1.98, 2.38, 1.86, 4.70, \ldots \\ \ldots, 2.52, 4.70, 4.92, 1.78, 1.76, 4.20, 4.16, 2.22, 4.22, 2.40]^T \\ \\ \boldsymbol{d} = [5.24, 39.83, 39.58, 15.61, 40.93, 18.66, 8.77, 40.83, 5.61, 25.94, \ldots \\ \ldots, 23.77, 42.00, 9.18, 21.48, 32.58, 14.38, 15.13, 43.32, 40.05, 8.08]^T \end{array} \tag{3.101}$$

and

$$\boldsymbol{A} = \begin{bmatrix} 1 & 0 & 0 & 1 & 1 & 1 & 1 & 1 & 1 & 0 & 0 & 0 & 0 & 0 & 0 & 0 & 0 & 0 & 0 & 0 \\ 1 & 1 & 1 & 0 & 0 & 0 & 1 & 1 & 1 & 1 & 1 & 1 & 1 & 1 & 0 & 1 & 1 & 0 & 1 & 1 \\ 0 & 1 & 0 & 0 & 0 & 0 & 1 & 0 & 1 & 1 & 0 & 1 & 1 & 1 & 0 & 1 & 0 & 1 & 1 & 1 \\ 1 & 0 & 1 & 1 & 1 & 1 & 0 & 1 & 0 & 0 & 1 & 0 & 0 & 1 & 1 & 1 & 1 & 0 & 1 & 0 \\ 1 & 0 & 0 & 1 & 0 & 0 & 1 & 1 & 0 & 1 & 0 & 1 & 0 & 0 & 1 & 0 & 0 & 0 & 1 & 1 \\ 0 & 1 & 1 & 0 & 0 & 0 & 1 & 1 & 1 & 1 & 1 & 0 & 0 & 1 & 1 & 0 & 1 & 1 & 1 & 0 \\ 0 & 0 & 1 & 0 & 0 & 1 & 1 & 0 & 0 & 0 & 1 & 1 & 0 & 1 & 0 & 0 & 0 & 0 & 0 & 0 \end{bmatrix}. \tag{3.102}$$

Figure 3.20 plots the evolution of the dual variables $\boldsymbol{\mu}$. As in the previous example, note that the proposed method gets the optimal solution after performing a few iterates of the algorithm. In Figure 3.21 the two stopping criteria used in the method are plotted versus the iteration number. It can be checked that both quantities tend to zero as the optimal solution is approached. In the first subplot (top) we have the quadratic Euclidean distance between the output of the dual subproblems $\boldsymbol{\lambda}_0^t$ and the correction made by the primal projection $\hat{\boldsymbol{y}}^t$. Therefore, for the optimal values of $\boldsymbol{\mu}$, i.e. $\boldsymbol{\mu}^*$, we check that no correction is required since the translation of these to the primal domain attains also the primal optimal solution $\boldsymbol{y}^*$. Something similar can be extracted from the second subplot (bottom), where the difference (in absolute value) between the dual candidates proposed by primal subproblems $\boldsymbol{\lambda}_0^t$ and the correction made by the dual projection $\boldsymbol{\lambda}^{t+1} = \boldsymbol{A}^T\boldsymbol{\mu}^{t+1}$ is plotted. Again, an optimal primal value $\boldsymbol{y}_0^t = \boldsymbol{y}^*$ requires no correction when it is translated to a dual domain by the primal subproblems.

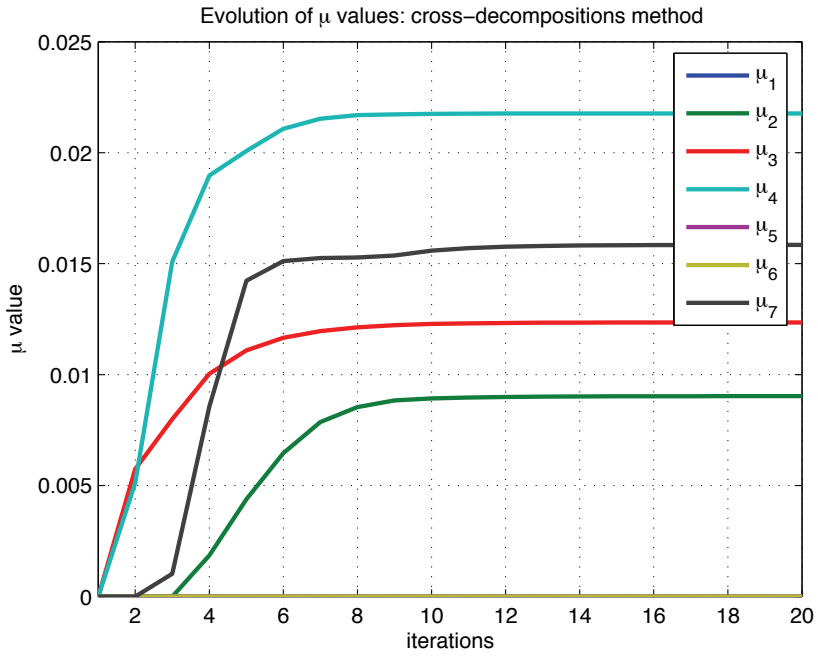

Figure 3.20: Evolution of dual variables $\boldsymbol{\mu}$ for the problem (3.100) using the coupled-decomposition method.

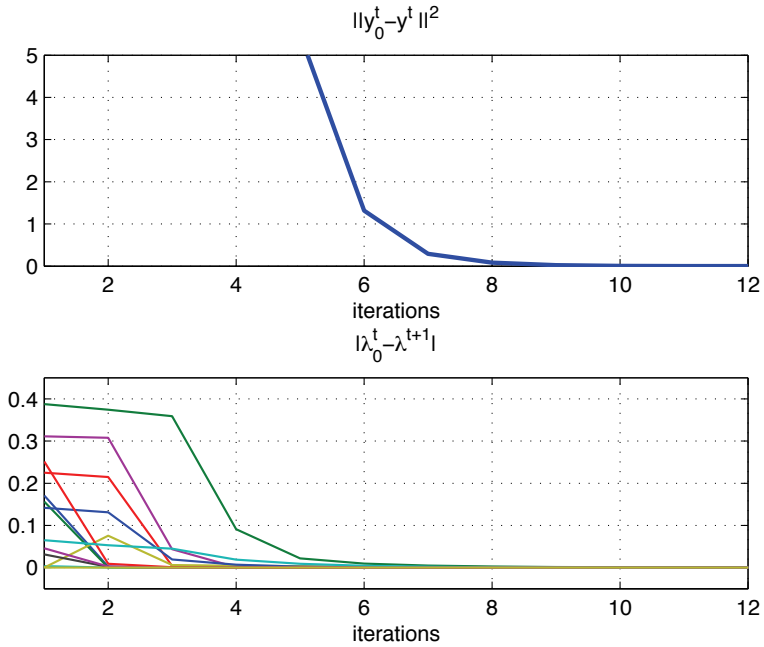

Figure 3.21: Attainment of the stopping criteria proposed for the coupled-decomposition method.

3.3.6 Formal Proof of the Method for a Single Coupling Constraint

Up to this point we have introduced the method that we propose and we have shown its good performance in terms of speed of convergence (in comparison with known decomposition approaches in the literature) through simulation examples. We have justified and interpreted every step of the method. Still, a formal proof is required for a full comprehension and further refinement (if possible). The conclusions extracted from a huge number of random scenarios simulated and correctly solved are full of promise. However, we are not yet able to provide a complete proof of the general case presented and it remains as further work in an open research line. At this moment, we can contribute with a proof for a reduced version of the problem when we consider only one coupling constraint.

Consider throughout this section the following problem formulation

$$\begin{array}{lll} \min\limits_{\{\boldsymbol{x}_j\},\boldsymbol{y}} & \sum_{j=1}^{J} f_j(\boldsymbol{x}_j) & \\ s.t. & \boldsymbol{x}_j \in \mathcal{X}_j, & j=1,\ldots,J \\ & h_j(\boldsymbol{x}_j) \leq y_j, & j=1,\ldots,J \\ & \mathbf{1}^T\boldsymbol{y} \leq c & \\ & \boldsymbol{y} \in \mathcal{Y}, & \mathcal{Y} = \mathcal{Y}_1 \times \ldots \times \mathcal{Y}_J \end{array} \tag{3.103}$$

where $\mathbf{1}$ is a column vector with J unity entries. Let μ be the dual variable associated to the coupling constraint $\mathbf{1}^T\boldsymbol{y} \leq c$.

We have basically two options to prove the convergence of the algorithm to the optimal solution. From the primal point of view, we can prove that

$$\hat{\boldsymbol{y}}^t \overset{t\to\infty}{\longrightarrow} \boldsymbol{y}^* \tag{3.104}$$

or alternatively, form the dual domain, we can prove that

$$\boldsymbol{\lambda}^t = \mathbf{1}\,\mu \overset{t\to\infty}{\longrightarrow} \boldsymbol{\lambda}^* = \mathbf{1}\,\mu^* \tag{3.105}$$

Since strong duality holds, both options are equivalent. We choose to prove the second statement for simplicity.

Note that primal and dual projections are rather simple for problem (3.103). In the dual projection, we only need to fix the value of μ to the value in $\lambda_0'^t$ with minimum distance to the previous values $\boldsymbol{\lambda}'^t = \mathbf{1}\,\mu^t$. The primal projection is, in this case, the projection to the half-space $\mathbf{1}^T\boldsymbol{y} \leq c$ with the additional constraint $\boldsymbol{y} \in \mathcal{Y}$. However, we prove that for the one constraint problem, it is not necessary to take this additional constraint into account and the algorithm still converges. Anyway, as in the general case, we construct the vector $\boldsymbol{\lambda}'^t$ by taking into account only the elements in $\boldsymbol{\lambda}_0^t$ whose associated values $\boldsymbol{y}_0^t$ belong to $\operatorname{int}\mathcal{Y}$. Under this prmise, primal projection can be analytically computed as [Boy03, Sec. 8.1]

$$\hat{\boldsymbol{y}^t} = \begin{cases} \boldsymbol{y}_0^t + \frac{(c-\mathbf{1}^T\boldsymbol{y}_0^t)\mathbf{1}}{J} & \mathbf{1}^T\boldsymbol{y}_0^t > c \\ \boldsymbol{y}_0^t & \mathbf{1}^T\boldsymbol{y}_0^t < c \end{cases} \tag{3.106}$$

Assume now that at instant t we have

$$\mu^t < \mu^*. \tag{3.107}$$

Applying $\lambda^t = \mathbf{1}\,\mu^t$ to the dual subproblems and given the relationship between primal and dual variables in the subproblems, it is true that

$$y_{0_i}^t \geq y_i^*, \qquad \forall i \tag{3.108}$$

where equality is attained only when $y_i^* \in \text{bd } \mathcal{Y}_i$.

In the primal projection, it is verified that

$$\hat{y}_i = y_{0_i} - k_i,\ k_i \geq 0, \qquad \forall i \tag{3.109}$$

thanks to the lemma below.

Lemma 4 *Given the optimization problem*

$$\begin{array}{ll} \min\limits_{\hat{\boldsymbol{y}}} & \|\boldsymbol{y}_0 - \hat{\boldsymbol{y}}\|^2 \\ s.t. & \mathbf{1}^T\hat{\boldsymbol{y}} \leq c \\ & \hat{\boldsymbol{y}} \in \mathcal{Y} \end{array} \tag{3.110}$$

where $\mathcal{Y} = \mathcal{Y}_1 \times \ldots \times \mathcal{Y}_J$ and given $\boldsymbol{y}_0$ such that $\mathbf{1}^T\boldsymbol{y}_0 > c$ and $\boldsymbol{y}_0 \in \mathcal{Y}$, then the optimal solution of the problem can be expressed as

$$\hat{\boldsymbol{y}}^* = \boldsymbol{y}_0 - \boldsymbol{k} \tag{3.111}$$

with $\boldsymbol{k} \succeq \mathbf{0}$.

Proof. First, note that a point $\hat{\boldsymbol{y}} = \boldsymbol{y}_0 - \boldsymbol{k}$ with $\boldsymbol{k} \succeq \mathbf{0}$ can be feasible since it may attain both $\mathbf{1}^T\hat{\boldsymbol{y}} \leq c$ and $\hat{\boldsymbol{y}} \in \mathcal{Y}$ (assuming that the intersection is not empty). The former holds because $\mathbf{1}^T\boldsymbol{y}_0 > c$ and since $\boldsymbol{y}_0 \in \mathcal{Y}$, a point $\hat{\boldsymbol{y}}$ arbitrarily close to $\boldsymbol{y}_0$ satisfies also the latter. Then, we have to prove that a point that does not accomplish the equation $\hat{\boldsymbol{y}} = \boldsymbol{y}_0 - \boldsymbol{k}$ for positive values in $\boldsymbol{k}$ can not be optimal for problem (3.110).

We prove this last result by induction. Assume a certain vector $\boldsymbol{k}$, called $\boldsymbol{k}^\triangleright$ that attains $\mathbf{1}^T(\boldsymbol{y}_0 - \boldsymbol{k}^\triangleright) = c$ and $\boldsymbol{k}^\triangleright \succeq \mathbf{0}$. Construct now a new vector $\boldsymbol{k}^\dagger$ from $\boldsymbol{k}^\triangleright$ by fixing its l^{th} element $k_l^\dagger = -a$ with $a > 0$ and distributing the difference $|k_l^\triangleright - k_l^\dagger|$ among the rest of elements in $\boldsymbol{k}^\dagger$ so as to attain the equality coupling constraint. In other words,

$$\begin{array}{c} k_i^\dagger = \left\{ \begin{array}{ll} -a, & i = l \\ k_i^\triangleright + \epsilon_i, & i \neq l, \epsilon_i > 0 \end{array} \right. \\ \sum_i k_i^\dagger = \mathbf{1}^T\boldsymbol{y}_0 - c \end{array} \tag{3.112}$$

We introduce some results from majorization theory [Mar79] that we need to complete the proof. First, let the components of $\boldsymbol{x} \in \mathbb{R}^n$ be ordered in decreasing order and express it as

$$x_{[1]} \geq \ldots \geq x_{[n]}. \tag{3.113}$$

Then, it is said [Mar79, 1.A.1] that a vector $\boldsymbol{y}$ majorizes a vector $\boldsymbol{x}$ (which we denote by $\boldsymbol{y} \succ^M \boldsymbol{x}$), $\boldsymbol{x}, \boldsymbol{y} \in \mathbb{R}^n$ if

$$\begin{array}{l} \sum_{i=1}^{k} x_{[i]} \leq \sum_{i=1}^{k} y_{[i]}, \quad k = 1, \ldots, n-1 \\ \sum_{i=1}^{n} x_{[i]} = \sum_{i=1}^{n} y_{[i]} \end{array} \tag{3.114}$$

From the definition above and the construction process of $\boldsymbol{k}^\dagger$, we can state that $\boldsymbol{k}^\dagger \succ^M \boldsymbol{k}^\triangleright$.

Second, a real-valued function ϕ on a set $\mathcal{A} \subseteq \mathbb{R}^n$ is called Schur-convex if [Mar79, 3.A.1]

$$\boldsymbol{y} \succ^M \boldsymbol{x} \text{ on } \mathcal{A} \Rightarrow \phi(\boldsymbol{y}) \geq \phi(\boldsymbol{x}). \tag{3.115}$$

And third, a function

$$\phi(\boldsymbol{x}) = \sum_i g(x_i) \tag{3.116}$$

where g is convex, is Schur-convex [Pal03, Corollary 3.1].

With those results in hand, we want to compare $\|\boldsymbol{y}_0 - \hat{\boldsymbol{y}}\|^2$ for $\boldsymbol{k} = \boldsymbol{k}^\triangleright$ and $\boldsymbol{k} = \boldsymbol{k}^\dagger$. Let us rewrite the quadratic norm as

$$\|\boldsymbol{y}_0 - \hat{\boldsymbol{y}}\|^2 = \|\boldsymbol{y}_0 - \boldsymbol{y}_0 + \boldsymbol{k}\|^2 = \sum_i k_i^2 \tag{3.117}$$

and consider $\phi(\boldsymbol{k}) = \sum k_i^2$, which is a Schur-convex function. Finally, since $\boldsymbol{k}^\dagger \succ^M \boldsymbol{k}^\triangleright$, we have

$$\|\boldsymbol{k}^\dagger\|^2 \geq \|\boldsymbol{k}^\triangleright\|^2 \tag{3.118}$$

and thus, any solution where one element of $\boldsymbol{k}$ is negative is not optimal (since the problem is convex and has a single solution). The proof ends by induction of this result to an arbitrary number of negative elements in $\boldsymbol{k}$.

It is known [Mar79, p. 7] that a vector with equal entries is majorized for all other vectors that have the same total-sum value. Note that this is in accordance with the primal projection in (3.106), where the constraint $\hat{\boldsymbol{y}} \in \mathcal{Y}$ is not considered. ■

Apply now the relationship between primal and dual subproblems (see Lemma 2) to the values $\hat{\boldsymbol{y}}^t$ that result after computing the dual projection. Either if it has been computed taking into account $\hat{\boldsymbol{y}} \in \mathcal{Y}$ or not, we know that

$$\lambda_{0_i}^t \geq \lambda_i^t, \qquad \forall i \tag{3.119}$$

Furthermore, if $\hat{\boldsymbol{y}}^t$ is not the optimal value, it is verified that there are some of the $\lambda_{0_i}^t$ values that attain $\lambda_{0_i}^t \leq \lambda_i^*$ whereas the rest attain $\lambda_{0_i}^t \geq \lambda_i^*$, since it holds that $\mathbf{1}^T \hat{\boldsymbol{y}} = c$ and therefore, some

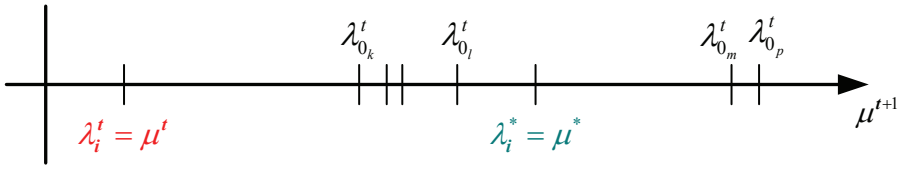

Figure 3.22: Example of the situation before performing dual projection.

of the $\hat{y}_i$ values attain $\hat{y}_i \geq y_i^*$ and the rest attain $\hat{y}_i \leq y_i^*$. Applying the relationship between primal variables and dual variables in the subproblems, the previous statement is readily found. An example of the situation that we expect before computing the dual projection is depicted in Figure 3.22.

Note that not all the $\lambda_{0_i}^t$ are useful in the obtention of μ^{t+1} since we discarded the values whose associated $\hat{y}_i$ values attained $\hat{y}_i \in \text{bd } \mathcal{Y}_i$. The valid values form the vector $\boldsymbol{\lambda}_0^{'t}$ and in the dual projection we manage the system of equations $\boldsymbol{\lambda}_0^{'t} = \mathbf{1}\mu^{t+1}$. In the worst case, the vector $\boldsymbol{\lambda}_0^{'t}$ may contain just a single value. We want to remark that no value is not possible since we assume that the coupling constraint is active. Otherwise, $\mu = 0$ and the global problem is readily optimized by just solving the subproblems. In order to consider the situation where $\boldsymbol{\lambda}_0^{'t}$ contains only one element, we have the following lemma.

Lemma 5 *Let a primal point $\hat{\boldsymbol{y}}$ attain $\mathbf{1}^T\hat{\boldsymbol{y}} = c$ and $\hat{\boldsymbol{y}} \in \mathcal{Y}$. Let also $\boldsymbol{\lambda}_0'$ be a vector containing the dual translation (computed by primal subproblems) of the values in $\hat{\boldsymbol{y}}$ that attain $\hat{\boldsymbol{y}} \in \text{int } \mathcal{Y}$. Then, if $\boldsymbol{\lambda}_0'$ (which contains all the possible μ^{t+1} candidates) is an scalar λ_0' (i.e. we have only one candidate), then it holds*

$$\lambda_0' \leq \lambda^{'*} \tag{3.120}$$

where $\lambda^{'*}$ is the optimum value of $\boldsymbol{\lambda}$ for the selected position in λ_0' (equal to μ^*).

Proof. From Lemma 4, we know that $\hat{\boldsymbol{y}} = \boldsymbol{y}_0 - \boldsymbol{k}$, $\boldsymbol{k} \succeq \mathbf{0}$ if $\mathbf{1}^T\boldsymbol{y}_0 > c$ and $\boldsymbol{y}_0 \in \mathcal{Y}$. In the case under study, only one value in $\hat{\boldsymbol{y}}$, take $\hat{y}_i$, attains $\hat{y}_i \in \text{int } \mathcal{Y}$. The other values are reduced by a certain quantity $k_j > 0$ unless it is verified that $\hat{y}_j = \inf \mathcal{Y}_j$. From the discussion above, if all $\hat{y}_j = \inf \mathcal{Y}_j$ except $\hat{y}_i$ and $\hat{\boldsymbol{y}}$ is not optimal, then it holds

$$\hat{y}_i \geq y_i^* \tag{3.121}$$

since $\mathbf{1}^T\hat{\boldsymbol{y}} = c$. Note that the same reasoning applies in the case where primal projection takes into account only the constraint $\mathbf{1}^T\boldsymbol{y} \leq c$. In that case, the same quantity is extracted to all the values in $\boldsymbol{y}_0$ attaining $\mathbf{1}^T\hat{\boldsymbol{y}} = c$, indistinctly if $\hat{y}_j < \inf \mathcal{Y}_j$ or not. Therefore, the same result holds for the value $\hat{y}_i \in \text{int } \mathcal{Y}_i$. ■

Finally, in the dual projection we choose μ^{t+1} as the $\lambda_{0_i}^{'t}$ value that has the minimum distance with μ^t as

$$\mu^{t+1} = \arg \left\{ \begin{array}{cc} \min\limits_{\mu^{t+1}} & (\mu^{t+1} - \mu^t)^2 \\ s.t. & \mu^{t+1} \in \{\lambda_{0_1}^{'t}, \ldots, \lambda_{0_M}^{'t}\} \end{array} \right\} \tag{3.122}$$

Collecting the results obtained before, we have

$$\mu^{t+1} > \mu^t \tag{3.123}$$

since every value in $\boldsymbol{\lambda}_0^{'t}$ verifies $\lambda_{0_i}^{'t} > \mu^t$. Furthermore, it is also true that

$$\mu^{t+1} < \mu^* \tag{3.124}$$

since the value $\lambda_{0_i}^{'t}$ closer to μ^t accomplishes $\lambda_{0_i}^{'t} < \lambda_i^{'*} \leq \mu^*$, which is derived from Lemma 5 and the first equation in (3.76). See also a graphical explanation in Figure 3.22. So we can finally conclude that

$$\mu^t < \mu^{t+1} < \mu^*. \tag{3.125}$$

This result reveals that the successive iterates of μ^t increase in value and that they are upper-bounded by μ^*. To end the proof, it is required to show that $\mu^t \overset{t\to\infty}{\longrightarrow} \mu^*$. This is done by contradiction. Assume that there exists a value $\mu^{\triangleright}$ where successive iterates converge. Then $\mu^{\triangleright}$ is an stationary point of the method. In other words, a complete iteration of the method starting from $\mu^{\triangleright}$ returns exactly the same value. This enforces in primal projection that $\hat{\boldsymbol{y}} = \boldsymbol{y}_0(\mu^{\triangleright})$, otherwise the values in $\boldsymbol{\lambda}_0'$ increase and so the update in μ (dual projection). Given the relationship between primal and dual subproblems, we see that the previous equation is only attained if $\mu^{\triangleright} = \mu^*$ since a lower value $\mu^{\triangleright} < \mu^*$ will obtain a primal point $\boldsymbol{y}_0(\mu^{\triangleright})$ from dual subproblems such that $\mathbf{1}^T \boldsymbol{y}_0(\mu^{\triangleright}) > c$.

Note that the dual projection in the single constraint problem is equivalent to selecting the minimum of the values in $\boldsymbol{\lambda}_0^{'t}$ if $\mu^t < \mu^*$. In other words, (3.122) is equivalent to

$$\mu^{t+1} = \min(\boldsymbol{\lambda}_0^{'t}). \tag{3.126}$$

Setting $\mu^0 = 0$ we guarantee that $\mu^0 < \mu^*$ and that $\mu^t < \mu^*$ in the next iterations of the algorithm. In case $\mu^t > \mu^*$, the dual projection is equivalent to the selection of the maximum value in $\boldsymbol{\lambda}_0^{'t}$ and therefore, (3.122) turns into

$$\mu^{t+1} = \max(\boldsymbol{\lambda}_0^{'t}). \tag{3.127}$$

It can be easily proved then that the successive updates of μ attain

$$\mu^t > \mu^{t+1} > \mu^* \tag{3.128}$$

and that the algorithm also converges to the optimum value (the proof is analogous to the previous case).

Furthermore, if we make use of the maximum or minimum functions in the dual projection and the initial hypothesis is not accomplished, i.e. $\mu^t > \mu^*$ for the minimum or $\mu^t < \mu^*$ for the maximum, the algorithm still converges. It can be easily seen from the example in Figure 3.22 that if the maximum function is used in that situation of the figure, then $\mu^{t+1} > \mu^*$ and in the iteration $t+1$, all the requirements to converge with the max function are fulfilled.

3.4 Summary

This chapter contributes to the field of decomposition techniques applied to convex programs. We begin with a brief review of general convex optimization theory. Thereafter, we revisit the known decomposition techniques that exist in the literature, namely: i) primal decomposition; ii) dual decomposition and iii) MVC decomposition. All these strategies are used to separate a given convex optimization problem into smaller problems, termed the subproblems. Depending on the strategy used, these are coordinated in different ways, always leading to the same global optimal solution. In particular, primal and dual decompositions use a subgradient-driven approach that optimizes either the primal or the dual version of the problem. A different approach is derived in the MVC decomposition method, where one primal and one dual subproblems are defined. The technique alternates the computation of both subproblems (that exchange primal and dual variables) in order to attain the optimal value of the problem.

After the initial literature review, we propose a novel decomposition technique, the coupled-decomposition method. It is a generalization of the MVC decomposition one since it intertwines primal and dual variables of multiple primal and dual subproblems. An extensive description of the method is provided, as well as the logic in the procedure, a comparison with the existing methods and a geometric interpretation. We shall remark that the results obtained show a significant gain in terms of convergence speed with respect to the other mechanisms. Finally, a formal convergence proof for a reduced case (considering a single constraint) is provided.

Chapter 4

Cross-Layer Dynamic Bandwidth Allocation in DVB-RCS

This chapter is devoted to the design of bandwidth allocation mechanisms in the Digital Video Broadcasting - Return Channel Satellite (DVB-RCS) system using the convex decompositions perspective described in Chapter 3. The specific multiple access of the system, which assigns bandwidth to users subject to what they have previously requested, makes it particularly suitable to the mentioned approach. In this chapter, we contribute with a specialized framework for the problem that attains fairness among users, the potential incorporation of quality of service (QoS) policies and efficiency in the allocation.

4.1 Introduction to DVB-RCS

A comprehensive introduction about the return channel over satellite of the DVB requires first a brief introduction to Digital Video Broadcasting - Satellite (DVB-S) and to Digital Video Broadcasting - Second Generation Satellite (DVB-S2). The oldest DVB standard in the satellite field, the DVB-S [ETS97], is a widely accepted standard in the forward link of broadband satellite communications. There are nowadays many satellites and a huge number of ground receivers using that technology to receive digital broadcast television. The natural evolution of DVB-S is DVB-S2 [ETS05b] and allows for a more flexible usage of the satellite capacity. A redefined physical layer with adaptive modulation and coding (ACM) is one of the key improvements in DVB-S2. Thus modulation and coding are adjusted depending on the channel quality of each satellite-ground link and the goal is to operate always as close as possible to the varying channel capacity.

In parallel to the evolution of DVB over satellite systems, the development of the actual knowledge society has been intensively related to new technologies that enable interaction among people. Two classical examples are the growth and penetration of internet services and mobile

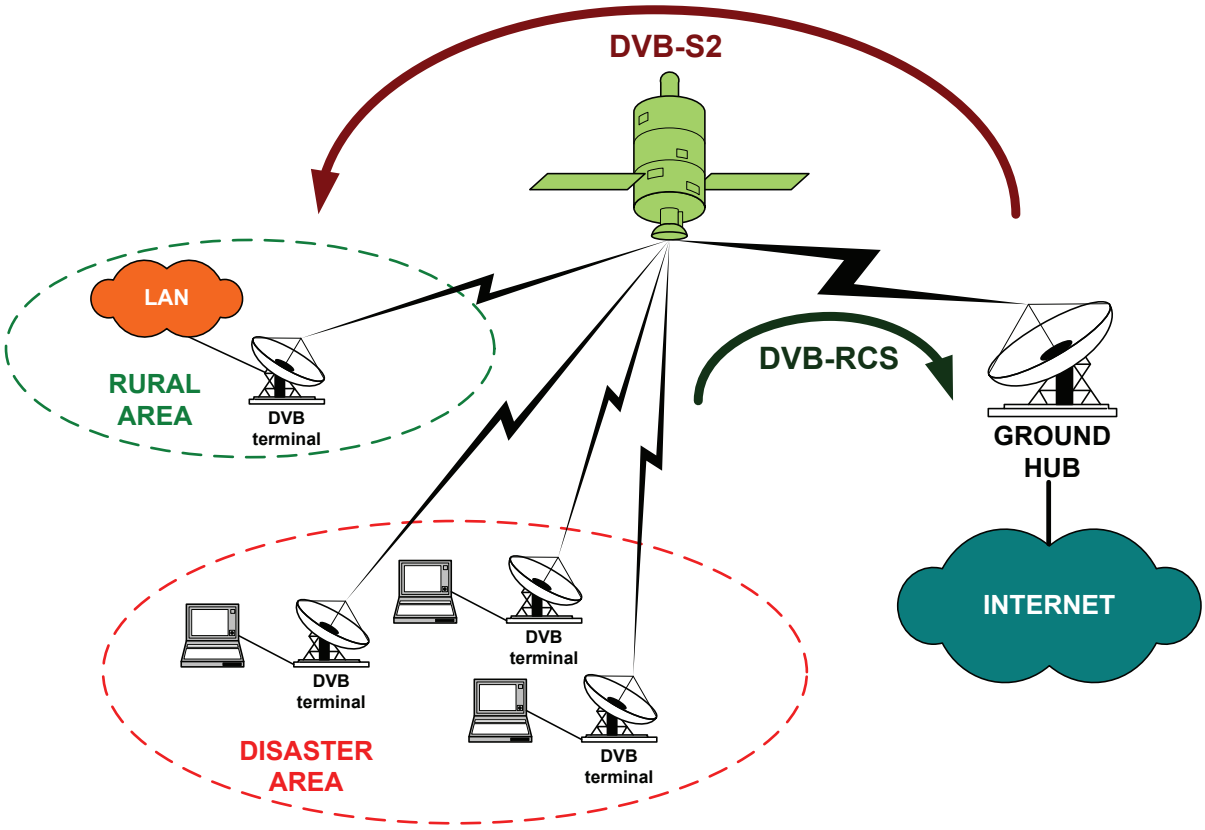

Figure 4.1: DVB-S2/DVB-RCS scenario.

communications among the population. The actual trend is to merge a variety of systems in a single terminal that will allow the end user to get closer to a an infinity of multimedia contents. Satellite DVB is also aware of the outlook and has designed its second generation to accommodate, besides TV contents, also broadband interactive multimedia services [LN01], which can be multicast or unicast. The list of services is long, from classical web browsing, mail or file transfer protocol (ftp) applications to more demanding ones such as video-conferences, virtual meetings or Voice over Internet Protocol (VoIP) services [Ski05].

These wide system possibilities of DVB-S2 require interactivity. It is sometimes achieved using ground networks, but this is not always a valid solution. A return link over the satellite is mandatory since a single terrestrial option for a return link would limit the expansion of DVB-S2 to certain areas. Consider, for example, remote places (as the ones in rural zones), disaster areas, etc. The current counterpart of DVB-S2 for the return link is the DVB-RCS standard [ETS05a, ETS03c]. We focus our work on unicast services for which ACM has been made mandatory in the DVB-S2 standard while adaptive coding is allowed in the DVB-RCS standard. To our knowledge, while the adaptive nature of the forward link is attracting increasing interest [Rin04, Alb05], the adaptive nature of the DVB-RCS still requires research effort in order

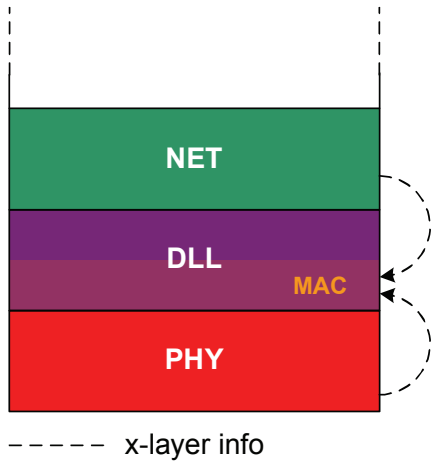

Figure 4.2: Cross-layer signalling in the OSI protocol stack.

to optimize the system performance. Some previous works on the subject include [Chi04a] and [Got06]. A possible DVB-S2/DVB-RCS scenario is depicted in Figure 4.1 with two different network configurations. In one hand, the satellite subnetwork provides coverage to a rural area and thus, a local area subnetwork is behind the DVB terminal. In the other hand, a disaster zone is depicted and different equipments (maybe operated by rescue agents, police, firemen, army, etc.) directly connected to portable DVB terminals are used to coordinate the operations in the area.

The work we present along this chapter is devoted to the multiple access part of the system that runs, given the Open Systems Interconnection (OSI) model [Zim80], at the Medium Access Control (MAC) sublayer of the Data Link Layer (DLL). The goal is to adequately distribute the transmission resources of the satellite so as to obtain maximum revenue or utility (later on, we define this concept mathematically). Our approach considers not only local information available at MAC layer (for example, the length of MAC queues) but also PHY layer and Network (NET) layer information. From the PHY layer, the channel quality of each RCS Terminal (RCST) is taken into account in the resource distribution. As far as the NET layer is concerned, we require to be able to distinguish the variety of services carried by Internet Protocol (IP) packets and to reflect so with more or less transmission opportunities. The idea underneath is to merge the satellite subnetwork in a QoS-based IP environment and make it as transparent as possible to the whole network. The argumentation above justifies the words cross-layer in the chapter title as far as certain flows of information from one layer to another are foreseen (see Figure 4.2).

In the next section we perform a detailed description of the Dynamic Bandwidth Allocation (DBA) mechanisms in DVB-RCS. Nevertheless, let us end this introduction with a brief comment on the multiplex of the DVB-RCS or, in other words, on how radio resources are planned in order to allow several RCSTs to transmit simultaneously. The multiple access of DVB-RCS

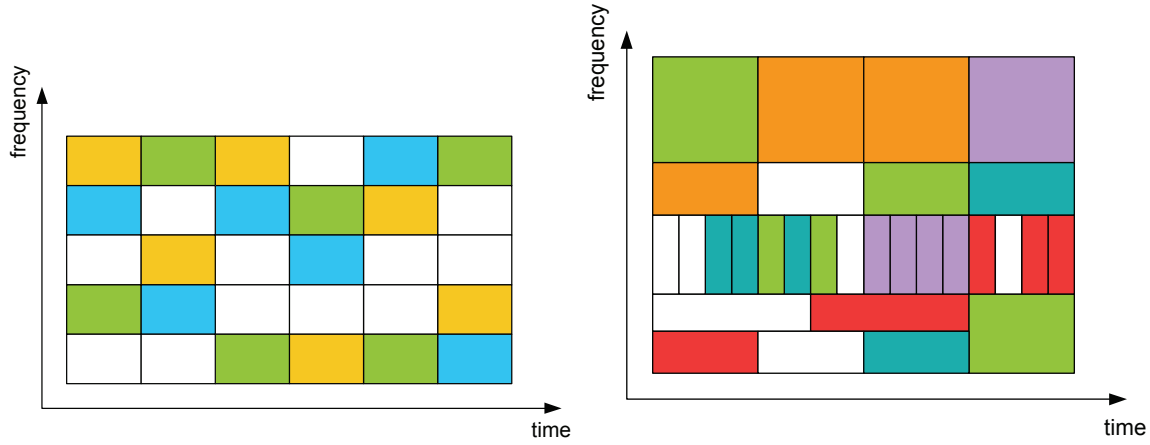

Figure 4.3: Examples of Fixed MF-TDMA (left) and Dynamic MF-TDMA (right).

is a Multi-Frequency Time Division Multiple Access (MF-TDMA), which results in a hybrid combination of Time Division Multiple Access (TDMA) and Frequency Division Multiple Access (FDMA). According to the standard [ETS05a, Sec. 6.7], two options are possible: Fixed MF-TDMA (mandatory) and Dynamic MF-TDMA (optional). In the fixed version, the available satellite bandwidth is divided into several subcarriers of the same bandwidth and time-slots are defined in each subcarrier. All time-slots are identical. The time-slots assigned to a certain RCST can belong to different subcarriers and thus, DVB-RCS equipments must support frequency hoping, which improves system performance thanks to the frequency diversity. An example of fixed MF-TDMA can be seen in Figure 4.3 (left), where time-slots are colored depending on the RCST that transmits on them. In the Dynamic MF-TDMA situation, time-slots are more flexible in the sense that different bandwidths and durations are allowed. In this situation, the available time-frequency resources on the satellite create an infinite number of options on how to share them. An example of Dynamic MF-TDMA is plotted in Figure 4.3 (right).

Our contribution considers a dynamic MF-TDMA basis, which is more interesting from the design point of view since there are many degrees of freedom to be exploited in order to improve system performance. However, an infinite number of possibilities in defining and allocating time-slots appears. This fact implies solving combinatorial problems if a fully flexible strategy is envisaged, which can not be accomplished in polynomial time. Since we are interested in practical solutions (in terms of computation time), we propose an optimization framework that fixes some structure to the problem and allows the use of time-efficient algorithms. Note the implicit tradeoff between performance and usability.

After introducing the generalities that will be developed along this chapter, the next section deals with a specific description of the DBA part in DVB-RCS.

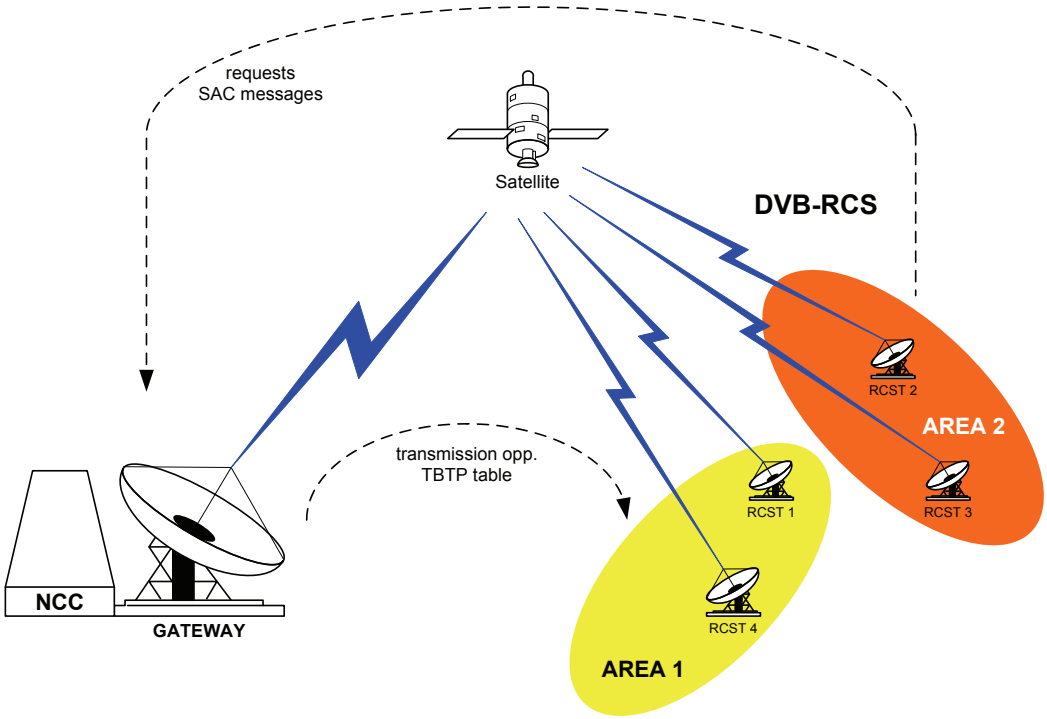

Figure 4.4: DVB-RCS system overview.

4.2 Dynamic Bandwidth Allocation in DVB-RCS

Consider a transparent satellite network as depicted in Figure 4.4, where we take into account only the return link of the general system in Figure 4.1. A significant part of the system under study is the process carried out by the Network Control Center (NCC), which is attached to the ground hub and has a key role in the multiple access part of the system. The NCC is in charge of collecting the traffic demands [Aça99, Aça02, Pri04] of the RCSTs and running adequate DBA algorithms trying to maximize the benefit that RCSTs get from the available radio resources. The output of the DBA algorithms is sent back to the terminals and informs them about their transmission opportunities. In short, the NCC informs each RCST about the time-slots assigned and their corresponding parameters (position in the time-frequency axes, bandwidth, time duration, etc.).

Bandwidth allocation techniques allowed by the standard belong to the class called resource reservation on-demand [Iuo05] or Demand-Assignment Multiple Access (DAMA) because users get resources only when they ask for them. Though the final allocation is centralized at the NCC, there is a big difference with classical centralized networks (connection-oriented) since there is no guarantee to get the desired resources if lots of users access the system. Bandwidth reservation messages are sent from the RCSTs to the NCC and a scheduler applies the DBA

algorithms. The resulting allocation is sent back to the RCSTs at least one Round Trip Time (RTT) after the request was sent. This parameter has to be taken into account in DVB-RCS since it is relatively high (specially if we compare it to the values in terrestrial networks) and directly affects the latency of the system.

RCSTs capacity requests can be emitted every RTT; however, not all the stations will request bandwidth continuously. It will depend in general on the queued traffic at the MAC queues of each terminal and requests are sent using the standard-defined SAC (Satellite Access Control) messages [ETS05a, Sec. 6.6]. At its turn, the time-slot allocation is sent form the NCC to RCSTs using the Terminal Burst Time Plan (TBTP) [ETS05a, Sec. 6.7]. See Figure 4.4. It is important to note here the challenging allocation problem: while the IP traffic is inherently connectionless, DAMA algorithms actually set up a connection over the DVB-RCS air interface [Lee04]. At its turn, the time-slot allocation is sent form the NCC to RCSTs using the Terminal Burst Time Plan (TBTP) [ETS05a, Sec. 6.7]. See Figure 4.4.

There are three main types of capacity requests defined in the DVB-RCS standard [ETS05a, Sec. 6.8]. From highest to lowest priority, these are:

- Constant Rate Assignment (CRA): the RCST requires a constant rate to transmit during all the time. Only the most critical services will be requested under this option.
- Rate-Based Dynamic Capacity (RBDC): a bandwidth request (made in terms of rate capacity) remains effective until it is updated or timed out. In contrast to CRA, a RBDC strategy allows statistical multiplexing among many RCSTs, resulting in a more efficient use of the satellite bandwidth. Services that suit such request type are, for example, VoIP and video-conference.
- Volume-Based Dynamic Capacity (VBDC): it requires a certain amount of volume capacity to transmit information regardless the way it is done (no constant rate is needed). These type of requests are cumulative in the sense that new requests add to the previous ones. For example, services matching such type of request are ftp and web browsing.

Additionally, the standard defines the Absolute VBDC (AVBDC) and the Free Capacity Assignment (FCA) [Nea01]. The former requests volume capacity as in VBDC but this time in absolute terms. That is, when a RCST emits an AVBDC request, all the previous VBDC ones are omitted. The motivation is to replace previous VBDC requests when the RCST senses that these may have been lost. The latter (FCA) is not really a capacity request since it may be granted by the NCC but not requested by the RCSTs. It falls in the volume capacity category and it has been designed to distribute unused capacity of the satellite to the terminals.

Finally, let us define the MF-TDMA structure in DVB-RCS. The highest level of division is constituted by the Superframe (SF) and is a portion of time and bandwidth in the return

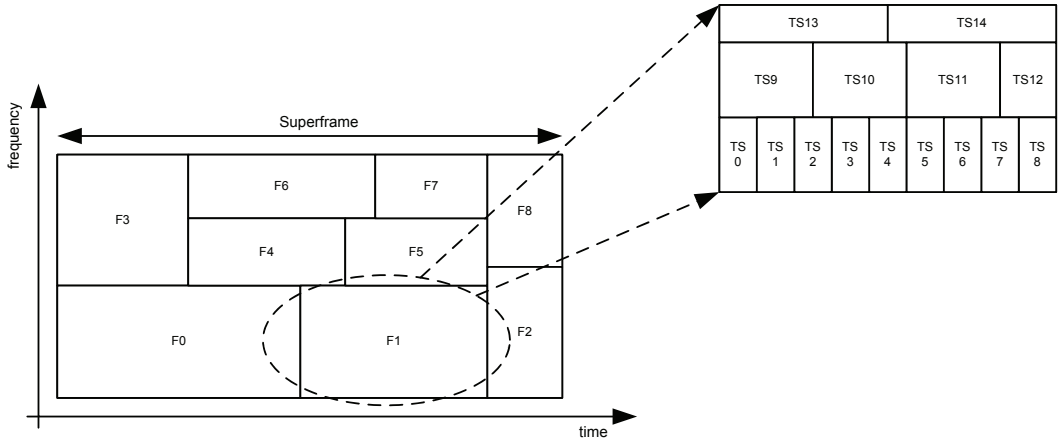

Figure 4.5: Possible Superframe configuration.

link. Each SF contains a number frames (32 at most) that constitute an intermediate level of organization between the time-slots and the SF, justified by signalling reasons. The frames may have arbitrary bandwidth and time duration. Inside each frame there are the time-slots, the last subdivision of the satellite capacity. Each frame contains at most 2048 time-slots with arbitrary bandwidth and duration. Whatever the division in frames and time-slots is, it is specified and signalled from the NCC to the RCSTs in the Frame Composition Table (FCT) and the Timeslot Composition Table (TCT), respectively. In the TCT the type of time-slot (i.e, different traffic TS, synchronization TS, etc.) is also specified. A picture showing a possible structure in the SF is drawn in Figure 4.5.

In summary, the requests generated by all terminals in a beam constitute the inputs of the allocation problem. It is not considered here how terminals generate them, but it is an important part to be considered jointly with the DBA. In our work, we assume that terminals request for just what they need using the appropriate capacity request type. Note also that due to the latency of the system (about half a second of round trip time in geostationary orbit), traffic prediction may also play an important role. Then, for each bandwidth allocation update, the NCC signals a TBTP to the RCSTs, where it points out which timeslots in the MF-TDMA are assigned to each terminal. With that information, the terminal schedules the traffic stored in the MAC queues. In the next section, we provide our proposed DBA framework in DVB-RCS. As discussed above, our approach fixes some structure to the MF-TDMA since a combinatorial solution is not practical in terms of computational time.

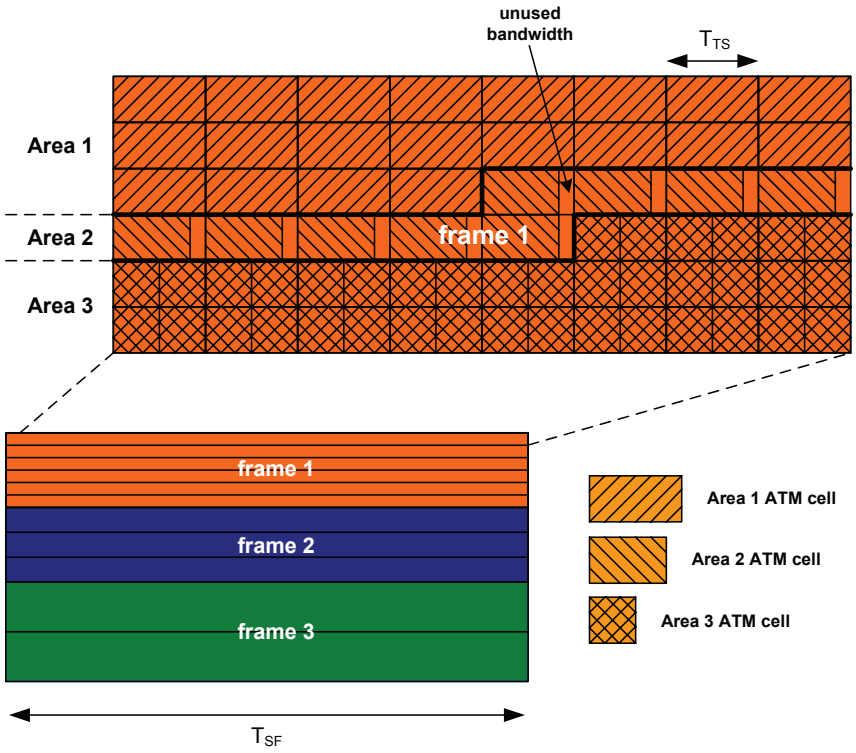

Figure 4.6: Proposed allocation framework.

4.3 Proposed Cross-Layer Framework

In the design of the proposed framework it is possible to distinguish two differentiated parts, which are actually highly coupled:

- Structure imposed to the MF-TDMA.
- The DBA procedure itself (i.e. the allocation algorithm used).

Note that the performance and the design of the DBA algorithm strongly depends on the particular configuration of the Superframe. In other words, if the Superframe is defined with a structure that has few degrees of freedom (an extreme case would be the fixed MF-TDMA), less performance can be expected in terms of bandwidth utilization or the total rate conducted through the satellite. In order to illustrate the question, imagine that no structure is imposed to the transmission and therefore, each RCST is allowed to transmit with an arbitrary time-slot (with distinct bandwidths and/or time durations). This is in principle a good option since it is possible to fulfill the whole Superframe. However, the organization of such a collection of time-slots with different shapes in the MF-TDMA may be difficult. Indeed, all the possible relative positions (with respect to the others in the SF) and shapes of the time-slots should be checked

to get the optimum. Concerning only the relative positions of the time-slots, it is required to search over a combinatorial number of possibilities and this makes the problem not solvable in polynomial time. Therefore, it is actually meaningful to impose some structure on the MF-TDMA. We deal with such imposed structure issues in this section, whereas the allocation itself is the subject of the next section.

Let us consider that the Superframe is divided into N_F frames that span the entire time duration and share the satellite bandwidth as in Figure 4.6 (bottom). This division of the Superframe has been already considered in the DVB-RCS guidelines document [ETS03c]. We further assume that each frame is divided into several subcarriers of the same bandwidth but not necessarily equal to the bandwidth of the subcarriers in other frames. This distinction intends to accommodate different users accounting for different Service Level Agreements (SLAs), terminal equipment or location, so that an RCST uses only one type of carrier. Under these assumptions, the global allocation problem is decoupled into N_F smaller and independent subproblems.

Fix now just one of the subproblems. The task therein is to multiplex N users into C carriers of BW bandwidth that transmit during T_{SF} seconds (see Figure 4.6, top). Let us introduce at this point the concept of *area* in the DVB-RCS environment. Terminals in DVB-RCS can adapt to the channel link quality as it happens with the ACM technique in DVB-S2 but with the difference that only the coding rate of RCSTs is allowed to change. In this occasion, we talk about Adaptive Coding (AC). According to the ETSI technical specification [ETS05c], an area is formed by the subset of RCSTs that transmit with the same symbol and coding rate. A terminal must belong only to one area. In our framework, all terminals in a frame coincide in symbol rate since all the subcarriers in it use the same bandwidth. Therefore, terminals are grouped into areas depending only on their coding rate. The channel quality in DVB-RCS strongly depends on meteorological issues such as rain or snow. Since those events are usually manifested in cells, we can interpret that the previously defined areas will correspond to the zones in the earth surface where propagation conditions are similar. See this interpretation in Figure 4.4.

The question now is how to fix the time-slot duration inside each DVB-RCS frame. Note that information is already quantized in MAC queues, where we have MAC frames in general. For the particular case of DVB-RCS, Asynchronous Transfer Mode (ATM) cells of 53 bytes or Moving Picture Experts Group (MPEG) containers of 188 bytes are considered. We introduce now the key aspect of the proposed framework, which establishes the tradeoff choice between complexity and optimality. A time-slot of duration T_{TS} is fixed common to all areas at each frame. However, the time-slot duration may change in subsequent Superframes depending on the traffic demands and the distribution of terminals into areas. In Figure 4.6 the idea is depicted with three areas. Inside each time-slot we transmit as many complete MAC frames as possible and thus, it may happen that part of the time-slot remains unused. Moreover, part of the frame may be not occupied by any time-slot. The time duration of a MAC frame transmission depends

on the coding rate of the RCST or, equivalently, on the area where the RCST is attached to. For a fixed time-slot duration and a fixed coding-rate, we can define the bandwidth efficiency of the time-slot as the percentage of time it is used to transmit. It is common to all the time-slots that are assigned to RCSTs in a given area and thus, it is meaningful to group all the RCSTs in the frame depending on their area as in Figure 4.6. Transmission of multiple MAC frames in a single time-slot already exists in the standard, where the allowed values are 1, 2 and 4.

Once the proposed Superframe organization is defined, let us discuss how cross-layer information interacts with the proposed framework. From the PHY layer of terminals we get at the NCC the coding rates of the RCSTs and we use this information to set up the best possible DVB-RCS frame configuration, which depends only on the time-slot duration and the aggregate requests from each area. For example, in the hypothetic situation where all RCSTs are in good propagation conditions and belong to the same area, it is possible to set up a time-slot duration that gets 100% bandwidth efficiency in all the time-slots of the frame. The goal is to achieve maximum frame efficiency for all distributions of users among areas and we study this in Section 4.5.

Interaction with the upper layers is more tricky since the NCC does not know the QoS requirements of the enqueued traffic at the MAC queues of the RCSTs that have caused the emission of capacity requests. In this case it is necessary to explicitly signal the information. Assuming that a transparent transponder is used, the field *Channel_ID* of the SAC messages is not used. It has 4 bits available that we can use to distinguish the QoS that each traffic requires, even when resources are asked under the same type of capacity request. If we think of an IP environment, it is desirable to be able to prioritize some services over the others with the final objective of having a satellite sub-network as transparent as possible.

Further interesting features of our model are signalling reduction and higher robustness to changes in the quality of the radio links in the satellite network. With respect to signalling, the advantage is to have many time-slots with exactly the same characteristics (duration, bandwidth, etc.) as is depicted in Figure 4.6. It is then possible to define the time-slot once at the beginning of the subcarrier and indicate how many times it is repeated, reducing the signalling in FCT and TCT tables. The reader can find in [VC05, Lee04], different approaches that consider changing continuously the time-slot duration as a function of the coding rate of the area. With respect to robustness, note that once a time-slot has been allocated to a RCST, the terminal may use it with a different coding rate (keeping within the time-slot limits) without interfering other transmissions. Advantages and disadvantages of different approaches have to be read from the complexity-performance trade-off already discussed.

Finally, we include the hierarchical bandwidth allocation concept defined in [ETS05c], which is also compatible with our approach. The motivation is to guarantee some minimum resources to Service Providers (SPs) as an extra mechanism to grant Quality of Service (QoS) to their

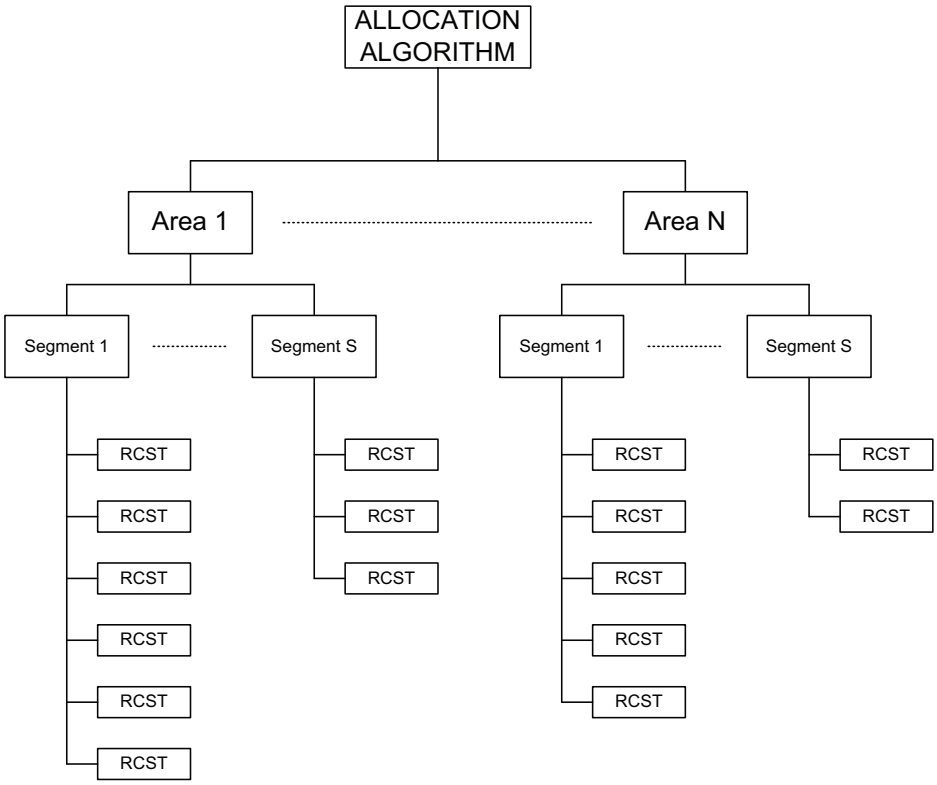

Figure 4.7: Bandwidth allocation hierarchy in DVB-RCS.

attached RCSTs. Note that not all the RCSTs attached to a certain SP see necessarily the same channel conditions and thus, they do not belong to the same area in general. It is then adequate to define the segment concept [ETS05c]. A segment is the subset of RCSTs in the network that have contracted their services with a particular SP and may intersect in general with the subsets that define the areas in the system. Figure 4.7 depicts the situation. In general, satellite resources must be distributed among areas, segments and finally among RCSTs. It can be done step by step by distributing resources through the entities on the hierarchy (i.e. distribute first among areas, then among segments in the areas and finally among RCSTs), or globally. This is discussed in the following section.

4.4 Cross-Layer Dynamic Bandwidth Allocation Algorithms

In this section, we develop practical algorithms that have to be able to operate in real-time [Lee04]. In the DVB-RCS scenario, algorithms must compute the allocation in tens of milliseconds, which is small compared to the RTT. Beyond the time limit, a good distribution of resources makes the most efficient use of the satellite bandwidth and maximizes the total rate conducted by the transponder. If we only take these considerations into account, the optimal

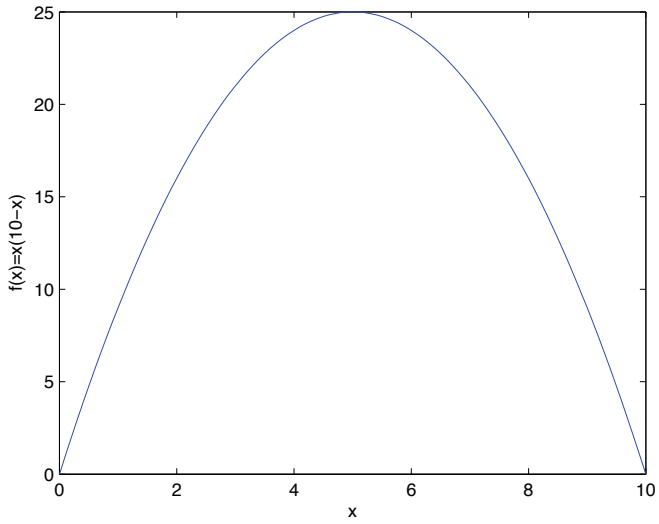

Figure 4.8: Simple fairness example.

solution is to allocate resources to RCSTs with the best coding rates, which corresponds to an opportunistic design. However, users with permanent bad propagation conditions are delayed until other users release their resources. It may not be a problem if the system works far from the saturation point but it is terribly unfair otherwise. This situation is avoided including fairness among users in the design and it is done using known results from game theory or resource allocation strategies [Mut99, Yaï00].

It is known that a fair distribution of a quantity P of resources among N entities is achieved if the product of the resources allocated to them is maximized [Maz91]. We use entity as a generic concept here. It can stand for RCST, user or even connection depending on the granularity of the solution. In other words, we can talk about connections when it is necessary to distinguish distinct services of the same user or we can use RCSTs if all the users and connections behind the terminals are equally treated. Consider the following simple example: 10 units of some material have to be shared among two persons. One gets x and the other one gets $10 - x$. The product of both, $f(x) = x(10 - x)$, is plotted in Figure 4.8. We immediately realize that the maximum of the function is achieved when both get 5 units of product, which intuitively shows the way fairness can be obtained with product forms.

Therefore, the allocation problem is mathematically described in the following maximization problem,

$$\begin{array}{ll} \max\limits_{x_1,\ldots,x_N} & \prod_{i=1}^{N} x_i^{p_i} \\ s.t. & \sum_{i=1}^{N} x_i \leq P \\ & m_i \leq x_i \leq d_i \end{array} \quad . \tag{4.1}$$

where m_i is the minimum amount of resources that must be granted to entity i and d_i stands

for its request. Finally, p_i is a weighting factor that represents the importance or priority of that entity (over the whole). It can be proved that the resolution of (4.1) achieves an asymmetric (due to the weighting parameters) proportional fair solution, which is a particular definition of fairness introduced by Kelly et al. [Kel98]. We consider this formulation for DBA in the DVB-RCS, but other applicability examples include scheduling in the DVB-S2 or rate allocation in terrestrial links [Pal07]. If we had considered the sum of x_i as the the objective function of the problem, then the solution is interpreted under the perspective of opportunistic designs: the non-served entity with highest priority reaches its demand or gets all the remaining resources.

The problem in (4.1) can be easily converted to a convex optimization problem [Boy03] by transforming the objective function with the natural logarithm since both the objective function and the constraints are convex functions of the variables (for further details, see Section 3.1). The optimal objective value of the transformed problem is not the same but it is attained at the same optimal point. That happens because the logarithm function is an strictly increasing function for positive values and thus, the position of maxima and minima of any positive function are not altered when composed with the logarithm. The equivalent formulation coincides then with the Network Utility Maximization (NUM) formulation in [Pal07] or [Lee06a] among others,

$$\begin{array}{cc} \max\limits_{x_1,\ldots,x_N} & \sum_{i=1}^{N} p_i \cdot \log x_i \\ s.t. & \sum_{i=1}^{N} x_i \leq P \\ & m_i \leq x_i \leq d_i \end{array} \quad . \tag{4.2}$$

In the previous formulation, the utility that each user gets from a quantity x_i of resources is measured as its natural logarithm. In terms of "utility", the interpretation is that extra resources are more useful when few or no resources are available. On the other side, more resources do not excessively increase utility if we have a lot of them. The resulting problem is semi-analytically solved applying KKT conditions [Boy03], with the solution

$$x_i = \left\lceil \frac{p_i}{\lambda} \right\rceil_{m_i}^{d_i} \triangleq \begin{cases} \frac{p_i}{\lambda}, & m_i \leq \frac{p_i}{\lambda} \leq d_i \\ m_i, & \frac{p_i}{\lambda} \leq m_i \\ d_i, & \frac{p_i}{\lambda} \geq d_i \end{cases} \quad . \tag{4.3}$$

where λ is a positive value such that $\sum_{i=1}^{N} x_i = P$. This value is usually obtained applying the bisection method [Rek83]. However, as the number of entities grows, the method may require excessive computation time [Gir00] (remember that in DVB-RCS the problem has to be solved in tens of milliseconds). From another perspective, the faster the allocation is computed, the highest is the number of users the system can manage. Our proposed coupled-decomposition method in Section 3.3 is applied to this particular problem and we show that we can improve the performance of the bisection method. In practical terms, the more users can be managed in the satellite sub-network, the more connections can be distinguished.

A graphical interpretation of the solution is found by filling a multiple-column recipient shaped accordingly with the demands, guaranteed resources and priorities of the entities with a

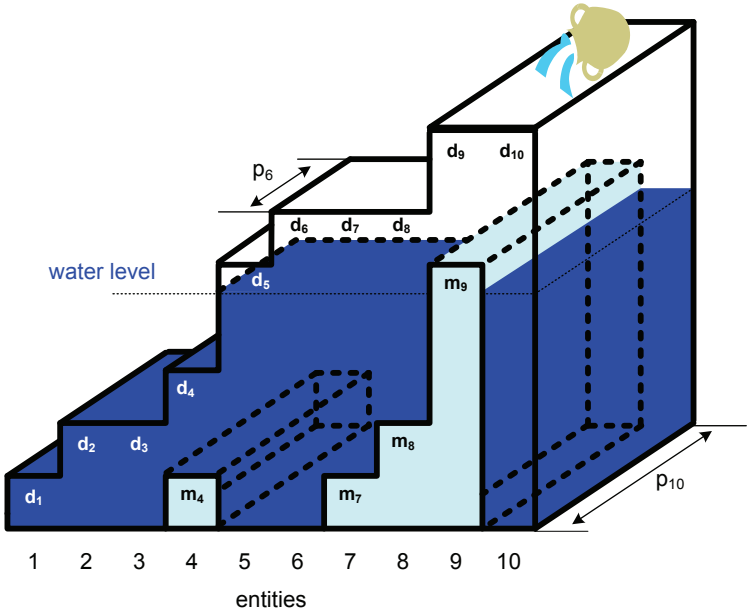

Figure 4.9: Graphical fair resource distribution.

quantity P of water [Pal05]. See Figure 4.9. Each column represents an entity, where the height is the amount of resources requested (d_i) and the depth is the priority of the entity (p_i). Each column has to be filled at least to the water-level defined by m_i. As it can be appreciated, the solution first fulfils the m_i water-levels ("pale water") and "equally" distributes the remaining water ("strong water") among the columns. The common water-level is $\frac{1}{\lambda}$, so entities with requests below the water-level get exactly the resources they have asked but not more while the others fairly share the resources in the system.

4.4.1 Global DBA Optimization Problem

Let us slightly modify the problem in (4.1) to precisely model the resource allocation in the proposed DVB-RCS framework. The formulation is

$$\begin{array}{ll} \max\limits_{\{x_{i,j}\}} & \prod_{i,j} (x_{i,j} \cdot K_i)^{p_{i,j}} \\ s.t. & \sum_{i,j} x_{i,j} \leq P \\ & \lceil \frac{m_{i,j}}{K_i} \rceil \leq x_{i,j} \leq \lceil \frac{d_{i,j}}{K_i} \rceil, \quad \forall i,j \end{array} , \tag{4.4}$$

where P is the total number of time-slots in the frame, $x_{i,j}$ stands for the amount of time-slots assigned to RCST i with request j and $p_{i,j}$ defines the priority of RCST i in j^{th} connection. As before, $d_{i,j}$ and $m_{i,j}$ stand for demands and minimum guaranteed resources (now expressed in number of ATM cells or MPEG containers). Assume, in accordance with [ETS05c], that each SP decides how to distribute the minimum amount of resources that it has contracted among the RCSTs attached to it, so that $\sum_{i \in S_k, j} m_{i,j} = M_k$, where M_k is the minimum guaranteed

resources to the terminals in segment k, S_k.

For the sake of simplicity, we base further considerations on a system using ATM cells at its MAC layer. However, these can be substituted for MPEG containers or any defined MAC frame type without affecting the following discussions. Finally, K_i establishes the number of ATM cells that RCST i can transmit in a time-slot. This value depends on the time-slot duration in the frame and on the time required by the RCST to transmit an ATM cell, which depends on the coding rate of the terminal. Remember that the coding rate is established by the AC technique of DVB-RCS and it is a function of the channel quality. We use $\lceil a \rceil$ to represent the ceil function, which returns the nearest integer that is bigger or equal than a. On the opposite side, $\lfloor b \rfloor$ corresponds to the floor function and returns the nearest integer lower or equal to b.

The formulation in (4.4) is a relaxation of the real bandwidth allocation problem since we do not restrict the quantities $x_{i,j}$ to be integer values. The final solution can then be obtained by simple down-rounding or it can be further refined by distributing the remaining resources (after rounding down the result of the optimization process) using some simple heuristic criteria. For example, a meaningful strategy is to perform a round-robin allocation to RCSTs or connections ordered by $p_{i,j}$ (from highest to lowest). Another option is to use variable threshold rounding [Xia03] instead of down-rounding and get a final allocation that is closer to the available frame capacity. It consists in fixing a threshold v between 0 and 1 and perform the rounding operation as

$$[c]_v = \begin{cases} \lceil c \rceil, & c - \lfloor c \rfloor > v \\ \lfloor c \rfloor, & c - \lfloor c \rfloor \leq v \end{cases} . \tag{4.5}$$

If $v = 0$, we have the floor function and if $v = 1$ we have the ceil function. Note that rounding up the real-valued solution may not be a feasible solution for the DBA problem since we may exceed the available capacity. By setting v properly, it is possible to adjust the final solution to the frame capacity. However, we expect to have in general few degradation as far as RCSTs manage a big number of ATM cells. In that situation, the remaining capacity after down-rounding will be small in relative terms.

4.4.2 Global DBA Optimization Algorithm

In order to efficiently solve the DBA optimization problem under study, the coupled-decomposition method developed in Section 3.3 is now applied to (4.4). In the following, we identify the subproblems (primal and dual) and the projections (primal and dual) of the method and we propose analytical solutions for them. Previously, the problem has to be transformed to a convex optimization problem suitable to the proposed method. By transforming the objective

function with the natural logarithm and adding new variables $y_{i,j}$ we get

$$\begin{array}{ll} \min\limits_{\{x_{i,j},y_{i,j}\}} & -\sum_{i,j} p_{i,j}\log x_{i,j} - \sum_{i,j} p_{i,j}\log K_i \\ s.t. & \lceil \frac{m_{i,j}}{K_i} \rceil \leq x_{i,j} \leq \lceil \frac{d_{i,j}}{K_i} \rceil, \qquad \forall i,j \\ & \lceil \frac{m_{i,j}}{K_i} \rceil \leq y_{i,j} \leq \lceil \frac{d_{i,j}}{K_i} \rceil, \qquad \forall i,j \\ & x_{i,j} \leq y_{i,j}, \qquad \forall i,j \\ & \sum_{i,j} y_{i,j} \leq P \end{array} . \tag{4.6}$$

Note that the term $-\sum_{i,j} p_{i,j}\log K_i$ affects the objective value of the problem but not the optimal solution and thus, it may be obviated for allocation purposes.

Primal and dual subproblems

Consider fixed values for variables $y_{i,j}$ that are feasible for (4.6). Then the joint program can be solved individually optimizing each of the primal subproblems, since (4.6) fully decouples. For the j^{th} connection on the i^{th} RCST, the primal subproblem is

$$\begin{array}{ll} \min\limits_{x_{i,j}} & -\sum_{i,j} p_{i,j}\log x_{i,j} \\ s.t. & \lceil \frac{m_{i,j}}{K_i} \rceil \leq x_{i,j} \leq \lceil \frac{d_{i,j}}{K_i} \rceil \\ & x_{i,j} \leq y_{i,j} \end{array} . \tag{4.7}$$

It is possible to solve it analytically using the KKT conditions with the following result

$$x_{i,j} = y_{i,j}\Big]_{\lceil \frac{m_{i,j}}{K_i} \rceil}^{\lceil \frac{d_{i,j}}{K_i} \rceil}, \qquad \lambda_{i,j} = \begin{cases} \frac{p_{i,j}}{x_{i,j}}, & y_{i,j} < \lceil \frac{d_{i,j}}{K_i} \rceil \\ 0, & y_{i,j} \geq \lceil \frac{d_{i,j}}{K_i} \rceil \end{cases} \tag{4.8}$$

where $\lambda_{i,j}$ is the Lagrange dual variable associated to the constraint $x_{i,j} \leq y_{i,j}$.

Dual subproblems are derived when the Lagrange multiplier associated to the coupling constraint $\sum_{i,j} y_{i,j} \leq P$, which we call μ, is fixed. Then the joint problem decouples in the dual domain and the problem can be solved individually optimizing the following dual subproblems

$$\begin{array}{ll} \min\limits_{x_{i,j},y_{i,j}} & -\sum_{i,j} p_{i,j}\log x_{i,j} + \mu \cdot y_{i,j} \\ s.t. & \lceil \frac{m_{i,j}}{K_i} \rceil \leq x_{i,j} \leq \lceil \frac{d_{i,j}}{K_i} \rceil \\ & x_{i,j} \leq y_{i,j} \end{array} . \tag{4.9}$$

As in primal subproblems, an analytical solution to (4.9) is readily found using KKT conditions. The result is

$$x_{i,j} = \frac{p_{i,j}}{\mu}\Big]_{\lceil \frac{m_{i,j}}{K_i} \rceil}^{\lceil \frac{d_{i,j}}{K_i} \rceil}, \qquad y_{i,j} = x_{i,j}. \tag{4.10}$$

In the following, we describe primal and dual projections for problem (4.6). As it happens with primal and dual subproblems, simple analytical solutions arise and thus, the computational load at each iteration of the coupled-decomposition method applied to the DVB-RCS scenario is relatively low.

Primal and dual projections

The mission of the primal projection is to correct, if necessary, the result of the dual subproblems. Since the main interest of the problem is on managing the coupling among the subproblems, i.e. on finding the optimal distribution of resources, we can assume $\mu > 0$ in general. If resources are not scarce, i.e. if P exceeds the sum of the demands of the terminals, then $\mu = 0$ and all connections in all terminals get what they request. A positive value of μ forces the coupling constraint to be attained with equality. Let us collect the output of all the dual subproblems for a given value of μ, i.e. the values $y_{i,j}$ for all i and j, in the vector $\boldsymbol{y}(\mu)$. Given the relationship between primal and dual subproblems in Section 3.3.1, it is clear that if $\mu > \mu^*$, then $y_{i,j} < y^*_{i,j}$ for all i and j and thus $\sum_{i,j} y_{i,j} < P$. Conversely, if $\mu < \mu^*$ we have $\sum_{i,j} y_{i,j} > P$. The correction made by primal projection (in vector $\hat{\boldsymbol{y}}$) results from the computation of the following convex program,

$$\begin{array}{ll} \min\limits_{\hat{\boldsymbol{y}}} & \|\boldsymbol{y} - \hat{\boldsymbol{y}}\|^2 \\ s.t. & \lceil \frac{m_{i,j}}{K_i} \rceil \leq \hat{y}_{i,j} \leq \lceil \frac{d_{i,j}}{K_i} \rceil, \quad \forall i,j \\ & \sum_{i,j} \hat{y}_{i,j} = P \end{array} \tag{4.11}$$

which is the projection of $\boldsymbol{y}$ to the hyperplane $\sum_{i,j} \hat{y}_{i,j} = P$, taking additionally into account the lateral constraints represented by $\lceil \frac{m_{i,j}}{K_i} \rceil \leq \hat{y}_{i,j} \leq \lceil \frac{d_{i,j}}{K_i} \rceil$. However, as discussed in Section 3.3.6, it is possible to omit the lateral constraints in the single coupling constraint problem without affecting the convergence of the method to the optimal solution, so in this case primal projection can be easily computed by just projecting the vector $\hat{\boldsymbol{y}}$ to the hyperplane $\sum_{i,j} \hat{y}_{i,j} = P$. The problem has the following analytical solution

$$\hat{\boldsymbol{y}} = \boldsymbol{y} + \frac{(P - \mathbf{1}^T \boldsymbol{y})}{\mathbf{1}^T \mathbf{1}} \tag{4.12}$$

where $\mathbf{1}$ is a vector with all entries equal to one and the appropiate size.

Dual projection works with the values inside the vector $\hat{\boldsymbol{y}}$ that we get from primal projection but transformed to the dual domain using the primal subproblems. These values are the dual variables $\lambda_{0_{i,j}}$. The goal is to reach a consensus on the value of the dual variable μ (associated to the coupling constraint) using the candidate values $\lambda_{0_{i,j}}$. As shown in Section 3.3.6, the value of μ can be easily obtained in the single coupling constraint situation as

$$\mu = \min(\boldsymbol{\lambda}') \tag{4.13}$$

where the vector $\boldsymbol{\lambda}'$ contains all the $\lambda_{i,j}$ values whose corresponding $y_{i,j}$ (output and input to the primal subproblems, respectively) fulfill $\lceil \frac{m_{i,j}}{K_i} \rceil < \hat{y}_{i,j} < \lceil \frac{d_{i,j}}{K_i} \rceil$. Another possibility is to use the max function instead of the minimum, but once any of them is selected, it must be not changed.

Having defined both the subproblems and the projections, the coupled-decomposition method is fully described and can be applied to the DVB-RCS allocation problem. However, we propose

to improve the performance of the technique thanks to a redefinition of the stopping criterion. We show that, under some circumstances, it is possible to stop the iterations of the coupled-decomposition algorithm before it converges but still find the optimal solution.

Stopping criterion

Consider now a more detailed convergence analysis of the proposed method explicitly applied to problem (4.6), which studies the evolution of the successive values of μ through the quantity

$$\left|\frac{1}{\mu^{t+1}} - \frac{1}{\mu^*}\right|. \tag{4.14}$$

Since convergence of μ to the optimal value μ^* has been established in Section 3.3.6, we consider here the analysis on the convergence speed of the technique. For the sake of simplicity and without loss of generality, the subsequent analysis is done assuming a single index i for the variables in $\boldsymbol{y}$ (of dimension N).

First, let us write the optimal values of variables y_i as

$$y_i^* = \begin{cases} \frac{p_i}{\mu^*}, & i \in \bar{\mathcal{S}}^* \\ m_i, & i \in \mathcal{M}^* \\ d_i, & i \in \mathcal{D}^* \end{cases}, \tag{4.15}$$

where $\bar{\mathcal{S}}^*$ is the subset of terminals with optimal solution $y_i \in (m_i, d_i)$, $\mathcal{M}^*$ defines the terminals with solution $y_i = m_i$ and $\mathcal{D}^*$ includes terminals with solution $y_i = d_i$. Since in the optimal solution it holds $\sum y_i = P$, the optimal water-level is derived as

$$\frac{1}{\mu^*} = \frac{P - \sum_{i\in\mathcal{D}^*} d_i - \sum_{i\in\mathcal{M}^*} m_i}{\sum_{i\in\bar{\mathcal{S}}^*} p_i}. \tag{4.16}$$

The next step revisits a complete iteration of the algorithm in order to derive $\frac{1}{\mu^{t+1}}$ from $\frac{1}{\mu^t}$, where t indexes the iterations. Given μ^t, the primal variables y_i^t are computed using the dual subproblems as

$$y_i = \begin{cases} \frac{p_i}{\mu^t}, & i \in \bar{\mathcal{S}}^t \\ m_i, & i \in \mathcal{M}^t \\ d_i, & i \in \mathcal{D}^t \end{cases} \tag{4.17}$$

where $\bar{\mathcal{S}}^t$, $\mathcal{M}^t$ and $\mathcal{D}^t$ are the counterpart of $\bar{\mathcal{S}}^*$, $\mathcal{M}^*$ and $\mathcal{D}^*$ in (4.15) at iteration t when μ^* is replaced by μ^t.

The corrected primal variables after the primal projection are

$$\hat{y}_i = y_i - \frac{\sum_i y_i - P}{N} = y_i - k \tag{4.18}$$

where $k > 0$ if we assume that the water-level at t (i.e. $\frac{1}{\mu^t}$) is over the optimum, i.e. $\mu^t < \mu^*$. See Section 3.3.6 for further details.

Accordingly, the candidates (λ_i) that the primal subproblems propose for the dual coupling variable μ are

$$\frac{1}{\lambda_i} = \frac{\hat{y}_i]_{m_i}^{d_i}}{p_i} = \begin{cases} \frac{1}{\mu^t} - \frac{k}{p_i}, & i \in \bar{\mathcal{S}}^{t'} \\ \frac{m_i}{p_i}, & i \in \mathcal{M}^{t'} \\ \frac{d_i}{p_i}, & i \in \mathcal{D}^{t'} \end{cases} . \tag{4.19}$$

Note that $\bar{\mathcal{S}}^{t'}$ does not necessarily coincide with $\bar{\mathcal{S}}^t$. The same is verified for $\mathcal{M}^{t'}$ and $\mathcal{D}^{t'}$.

Finally, μ is updated thanks to the dual projection

$$\frac{1}{\mu^{t+1}} = \frac{1}{\min\{\boldsymbol{\lambda}'\}} = \frac{1}{\mu_t} - \frac{k}{p_{max}} \tag{4.20}$$

with $p_{max} = \max_{i \in \bar{\mathcal{S}}^{t'}}\{p_i\}$. Note that the assumption $k > 0$ is coherent with the usage of the min function in the dual projection (see Section 3.3.6).

In the light of the previous result, we can expand (4.14) into

$$\left| \frac{1}{\mu^{t+1}} - \frac{1}{\mu^*} \right| = \left| \frac{1}{\mu^t} - \frac{1}{\mu^*} - \frac{k}{p_{max}} \right|, \tag{4.21}$$

where k can be substituted by

$$k = \frac{\sum_{i \in \bar{\mathcal{S}}^t} \frac{p_i}{\mu^t} + \sum_{i \in \mathcal{M}^t} d_i + \sum_{i \in \mathcal{D}^t} D_i - P}{N}, \tag{4.22}$$

which results after the combination of (4.17), (4.18) and the fact that $\sum \hat{y}_i = P$. Note that since $k > 0$, the solutions computed by the dual subproblems in (4.17) exceed the optimal ones if they do not saturate. Furthermore, since $\mu^t < \mu^*$ (see Section 3.3.6), the following statements hold at the t^{th} iteration

$$\begin{aligned} \mathcal{D}^t &= \mathcal{D}^* \cup \mathcal{D}^{extra} \\ \bar{\mathcal{S}}^* &= \bar{\mathcal{S}}^t \cup \bar{\mathcal{S}}^{extra} \\ \mathcal{M}^* &= \mathcal{M}^t \cup \mathcal{M}^{extra} \end{aligned} \tag{4.23}$$

where the definition of $\mathcal{D}^{extra}$, $\bar{\mathcal{S}}^{extra}$ and $\mathcal{M}^{extra}$ is implicit within the formulation. Note that these sets are empty when the solution is optimal.

Introduce the previous subsets definitions in equation (4.22) and identify therein the definition of $\frac{1}{\mu^*}$ from (4.16). It is possible to conclude then

$$k = \frac{\sum_{i \in \bar{\mathcal{S}}^*} p_i}{N} \left[\frac{1}{\mu^t} - \frac{1}{\mu^*} \right] + \frac{1}{N} \left[\sum_{i \in \mathcal{D}^{extra}} D_i - \sum_{i \in \bar{\mathcal{S}}^{extra}} \frac{p_i}{\mu^t} - \sum_{i \in \mathcal{M}^{extra}} d_i \right] \tag{4.24}$$

Since the algorithm converges, it holds that from a certain iteration $t^{\triangleright}$ the extra subsets attain $\bar{\mathcal{S}}^{extra} = \mathcal{M}^{extra} = \mathcal{D}^{extra} = \{\emptyset\}$. We say then that the algorithm has entered the optimal zone

(i.e. $t \geq t^{\triangleright}$) because the extra subsets remain empty as in the optimal solution. In that zone,

$$k = \frac{\sum\limits_{i \in \bar{\mathcal{S}}^*} p_i}{N} \left[\frac{1}{\mu^t} - \frac{1}{\mu^*} \right] \tag{4.25}$$

and the combination of that result with (4.21) shows the speed of convergence of the algorithm in the optimal zone,

$$\left| \frac{1}{\mu^{t+1}} - \frac{1}{\mu^*} \right| = \left| \frac{1}{\mu^t} - \frac{1}{\mu^*} \right| - \frac{\sum\limits_{i \in \bar{\mathcal{S}}^*} p_i}{p_{max} \cdot N} \left| \frac{1}{\mu^t} - \frac{1}{\mu^*} \right| = \left| \frac{1}{\mu^t} - \frac{1}{\mu^*} \right| \cdot \left(1 - \frac{\sum\limits_{i \in \bar{\mathcal{S}}^*} p_i}{p_{max} \cdot N} \right) \tag{4.26}$$

In the case where $\mu^t > \mu^*$, a similar discussion conducts to the same convergence results if the maximum function is used in dual projection.

Some intuition about the performance of the method is gained with the analysis of the particular case where $p_i = 1$ for all i. Equation (4.26) is then rewritten as

$$\left| \frac{1}{\mu^{t+1}} - \frac{1}{\mu^*} \right| = \frac{n_s}{N} \left| \frac{1}{\mu^t} - \frac{1}{\mu^*} \right| \tag{4.27}$$

where n_s is the number of terminals with solution $x_i = m_i$ or $x_i = d_i$. Assume that no user saturates. We read from the previous result that the optimum is then found in just one iteration. This is verified since the primal projection exactly computes that optimum. On the contrary, when nearly all users saturate, the convergence of the algorithm is much slower.

The results above are useful to determine when the iterates of the algorithm belong to the optimal zone. It is very useful since it allows to stop iterating and to calculate analytically the optimal solution. Consider the following function of three consecutive updates of the algorithm

$$B^t = \frac{\frac{1}{\mu^{t+1}} - \frac{1}{\mu^t}}{\frac{1}{\mu^t} - \frac{1}{\mu^{t-1}}} \tag{4.28}$$

It can be verified that when the algorithm reaches the optimal zone, the value of B^t is the same for iterations t and $t+1$. Call B_c to that value, whose expression is

$$B_c = 1 - \frac{\sum\limits_{i \in \bar{\mathcal{S}}^*} p_i}{p_{max} \cdot N} \,. \tag{4.29}$$

Once the condition holds, i.e. we are in the optimal zone ($t \geq t^{\triangleright}$), the exact solution to the problem is found in a single step as

$$\mu^* = \frac{\sum\limits_{i \in \bar{\mathcal{S}}^*} p_i}{P'}, \qquad y_i = \frac{p_i}{\mu^*}, \tag{4.30}$$

where $P' = P - \sum_{i \in \mathcal{D}^*} d_i - \sum_{i \in \mathcal{M}^*} m_i$ is the quantity of resources that are distributed among the entities that do not have a saturated solution.

Complete algorithm

To end the section, we summarize the proposed method. The reader can also find a flow chart of the iterative method in Figure 4.10.

Take initial guess $\mu^0 = 0.5 \cdot [\frac{N}{P-\sum m_{i,j}} + \frac{1}{\max\{d_{i,j}\}}]$ and repeat

1. Allocate resources using μ^t and obtain $y_{i,j}(\mu^t)$ as in (4.10).
2. Project the previous solution to the capacity limit, $\sum_{i,j} \hat{y}_{i,j} = P$ and get $\hat{y}_{i,j} = y_{i,j} + \frac{P-\sum_{i,j} y_{i,j}}{\mathbf{1}^T\mathbf{1}}$ (primal projection).
3. Construct the vector $\boldsymbol{\lambda}'$ collecting the estimates $\lambda_{0_{i,j}} = \frac{p_{i,j}}{\hat{y}_{i,j}}$ where the values $\hat{y}_{i,j}$ attain $\lceil\frac{m_{i,j}}{K_i}\rceil < \hat{y}_{i,j} < \lceil\frac{d_{i,j}}{K_i}\rceil$.
4. Update μ^{t+1} with the lowest value in the vector (dual projection).
5. Compute the value $B^t = \frac{\frac{1}{\mu^{t+1}} - \frac{1}{\mu^t}}{\frac{1}{\mu^t} - \frac{1}{\mu^{t-1}}}$.

until $|B^t - B^{t-1}| < \epsilon$ (step 6 in Figure 4.10). Then compute the optimal solution as

7. Calculate the current solution (with μ^{t+1}) using (4.10).
8. Obtain the set $\mathcal{S} = \mathcal{D}^* \cup \mathcal{M}^* = \left\{i,j | x_{i,j} = \lceil\frac{m_{i,j}}{K_i}\rceil \text{ or } x_{i,j} = \lceil\frac{d_{i,j}}{K_i}\rceil\right\}$.
9. Calculate the remaining resources P' as $P' = P - \sum_{i,j\in\mathcal{S}} x_{i,j}$.
10. Modify the solution found in step 7 only at the entities that do not belong to $\mathcal{S}$ as $x_{i,j} = \frac{P' p_{i,j}}{\sum_{i,j\notin\mathcal{S}} p_{i,j}}$.

Cross-layer information

Cross-layer information is included in the original formulation (4.4) thanks to the parameters K_i and $p_{i,j}$. The first one implicitly takes into account that the RCSTs in the frame may have different coding rates. Note that the time required to transmit an ATM cell depends on the specific coding rate of the terminal and therefore, the number of MAC frames that fit in a time-slot (the parameter K_i) is function of that value. We include in this way PHY-layer information. To convey QoS information from the upper-layers (e.g. IP-DiffServ) we have the parameters $p_{i,j}$, which allow to balance or prioritize the resource allocation towards the RCSTs or services with higher values. There are many ways to select the values of the parameters that depend on the policy we take. In general, if we are interested to provide a satellite sub-network as transparent as possible to IP QoS, the design of $p_{i,j}$ will depend on the type of capacity request emitted (MAC layer) and/or on the service underneath this request (IP layer). However, the formulation

proposed in this section is flexible enough to incorporate also other types of policies. Some hypothetic examples are:

- prioritize the areas with higher coding rates to achieve a higher sum rate in the satellite,
- prioritize the segments of the system depending on the QoS policy that each SP has contracted or
- distinguish individual RCSTs if they pay for distinct QoS levels.

4.4.3 Hierarchical DBA Optimization Algorithm

In the previous section we have formulated the DBA problem for DVB-RCS as a convex optimization problem and we have detailed the method to compute the allocation efficiently. In the results section we compare the performance of the method with other known solutions and we show the advantage in terms of computational time. We want to remark that it is an important issue in DVB-RCS since it may be a limiting factor on the number of users or connections routed through the satellite. Using the global allocation discussed up to this point, we allocate resources to areas, segments and RCSTs in a single step. It is the more accurate allocation we can do since decisions are taken at the lowest possible level, even distinguishing connections that belong to the same terminal.

A more practical approach is possible if we split the joint allocation in some steps of resource distribution, at the expenses of some optimality loss. Note that in our framework this degradation implies a less fair solution. It is then adequate to make use of the bandwidth allocation hierarchy defined in [ETS05c] and summarized in Figure 4.7. The idea is pretty simple: allocate resources at each level in the hierarchy, namely: areas, segments and terminals. The same formulation is employed to solve each distribution process but the number of variables to manage reduces significantly and so the time to optimize them. Moreover, the allocation of resources to services or connections can be done at the RCSTs and not at the NCC, reducing the computational load of the later.

In the first phase of the hierarchical approach, the overall demands and guaranteed resources per area are computed. These constitute the inputs of the DBA algorithm to obtain the allocation per area. Inside each area, the same procedure is done with segments in a second phase and again, inside each segment with RCSTs in the third and last phase. This is graphically expressed in Figure 4.11, where N_i is the aggregated demand on area i and S_{ij} is the aggregated demand on segment j (operated by SP j) inside area i. Note that we can use the priority values $p_{i,j}$ at each phase of the hierarchical algorithm with different purposes that depend on what is managed at each stage. In the first phase, we can treat areas differently. For example, we can balance

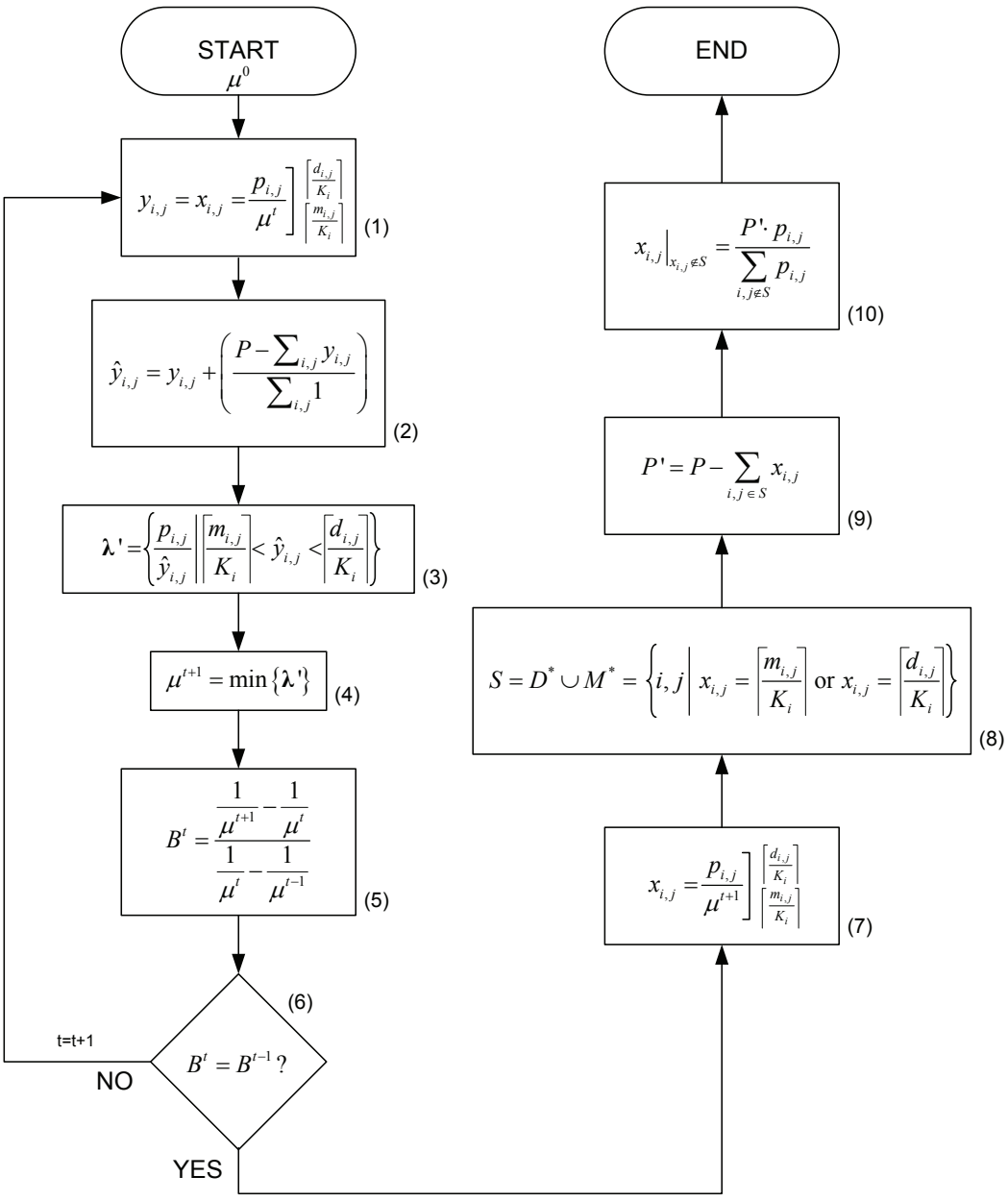

Figure 4.10: Joint DBA algorithm.

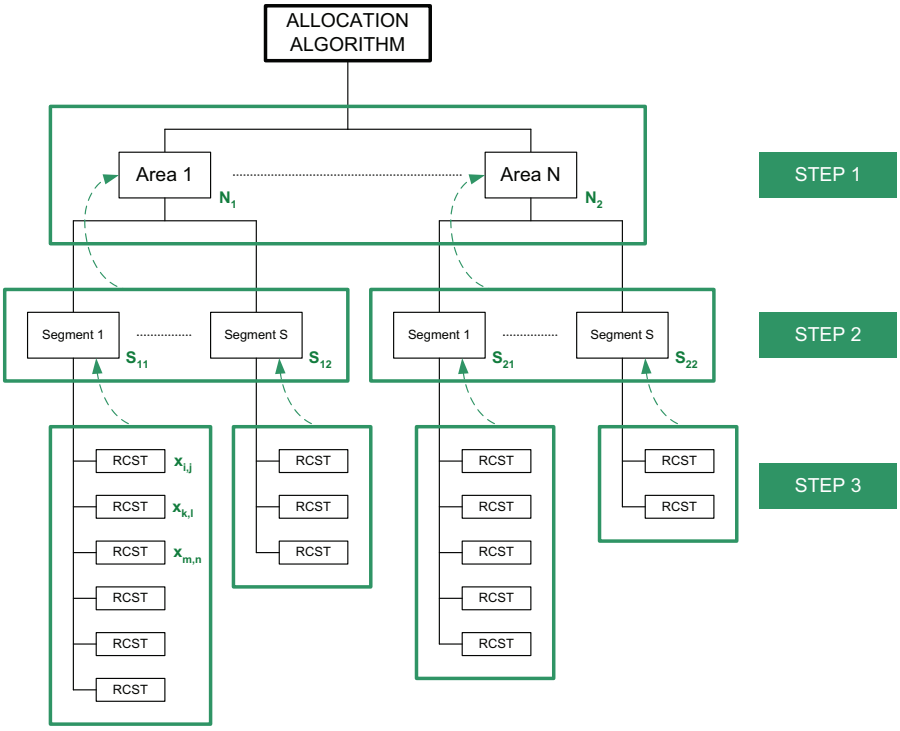

Figure 4.11: Hierarchical DBA algorithm.

the allocation towards the RCSTs with higher coding rates. In the second phase, the distinction can be based on the QoS guarantees that each SP has contracted for its segment. In the third phase, the SPs may have interest in serving terminals with different quality levels. Finally, each RCST can manage its resources according to the services that pass through it. Note that a potential scenario of application of DVB-RCS considers a Local Area Network (LAN) attached to a RCST.

4.4.4 Free Capacity Assignment

We have assumed throughout this chapter that the system is overloaded in the sense that the requested resources exceed the available ones. It is the most interesting situation from the engineering point of view since reasonable decisions on the distribution of the scarce resources are essential to have a system working properly. This has motivated our work in the chapter. However, it is possible to face the opposite situation, where the available resources exceed the requests. The allocation is then pretty simple: assign each RCST what it has requested.

In that situation, it seems reasonable to allocate the remaining resources or part of them to the terminals. This is called the free capacity assignment [Nea01]. Note that the latency in a geostationary satellite communications system is about half a second and thus, it is probable

that the current allocation (which is a reaction to the capacity requests emitted at least one RTT before) no longer fits the current traffic requirements. Free capacity assignment working jointly with traffic prediction palliates this satellite drawback and thus, a new allocation problem exists. Fortunately, the problem can be formulated as in (4.4) setting the requests to a very high value, i.e. $d_{i,j} = \infty$ for all i, j, and the minima to 0, i.e. $m_{i,j} = 0$ for all i, j. Priority values $p_{i,j}$ may be used now to balance traffic towards the terminals that may require more resources in the immediate future as foreseen by prediction techniques.

Up to this point, we have described our DBA framework in DVB-RCS divided in two parts, namely: i) structure of the frame and, ii) cross-layer DBA algorithm. While all the details about the latter have already been discussed, there is still room to optimize system performance if the time-slot duration is properly adjusted to the characteristics of the frame. We do this in the next section. Since we make use of the coding rates of the RCSTs in the frame, the approach is cross-layer.

4.5 Cross-Layer Timeslot Optimization: Joint DBA and Frame Design

Let us consider the original DBA problem in (4.4) and explicitly introduce the dependence of the problem on the time-slot duration T_{TS} as

$$\begin{array}{c} \max\limits_{T_{TS},\{x_{i,j}\}} \\ s.t. \end{array} \begin{array}{c} \prod_{i,j} \left(x_{i,j} \cdot K(T_{TS}, t_{a(i)})\right)^{p_{i,j}} \\ \sum_{i,j} x_{i,j} \leq P(C, T_F, T_{TS}) \\ \lceil \frac{m_{i,j}}{K(T_{TS}, t_{a(i)})} \rceil \leq x_{i,j} \leq \lceil \frac{d_{i,j}}{K(T_{TS}, t_{a(i)})} \rceil \\ T_{min} \leq T_{TS} \leq T_{max} \end{array}, \tag{4.31}$$

where C is the number of carriers in the frame, T_F is the frame duration and $t_{a(i)}$ is the time duration of an ATM cell transmitted by the i^{th} RCST ($a(i)$ denotes the area of the RCST i). Note the relation between $t_{a(i)}$ and the coding rate of the i^{th} terminal.

If we take the following expressions for $K(T_{TS}, t_{a(i)})$ and $P(C, T_F, T_{TS})$,

$$K(T_{TS}, t_{a(i)}) = \lfloor \frac{T_{TS}}{t_{a(i)}} \rfloor, \qquad P(C, T_F, T_{TS}) = \lfloor \frac{T_F}{T_{TS}} \rfloor, \tag{4.32}$$

being $\lfloor \cdot \rfloor$ the floor function, then we can rewrite the joint DBA problem as

$$\begin{array}{c} \max\limits_{T_{TS},\{x_{i,j}\}} \\ s.t. \end{array} \begin{array}{c} \prod_{i,j} \left(x_{i,j} \cdot \lfloor \frac{T_{TS}}{t_{a(i)}} \rfloor\right)^{p_{i,j}} \\ \sum_{i,j} x_{i,j} \leq C \cdot \lfloor \frac{T_F}{T_{TS}} \rfloor \\ \lceil \frac{m_{i,j}}{\lfloor \frac{T_{TS}}{t_{a(i)}} \rfloor} \rceil \leq x_{i,j} \leq \lceil \frac{d_{i,j}}{\lfloor \frac{T_{TS}}{t_{a(i)}} \rfloor} \rceil \\ T_{min} \leq T_{TS} \leq T_{max} \end{array}. \tag{4.33}$$

The joint problem in $\{x_{i,j}\}$ and T_{TS} is non-convex, which is readily concluded by the non-convex dependance on T_{TS} imposed by the floor function. Note that $\lfloor \frac{T_{TS}}{t_{a(i)}} \rfloor$ is an staggered function of T_{TS} and that it is not difficult to find a counter-example not attaining the definition of a convex function (see Section 3.1). However, we have yet established convexity of the problem for a fixed T_{TS} or equivalently, for fixed values of K_i and P.

Let us assume that we can adjust the time-slot duration between T_{min} and T_{max} as it is formulated in (4.33) and consider Lemma 6 to certify that it is not necessary to search over the whole range of the variable to find the optimal solution to the problem.

Lemma 6 *Starting from a feasible value of T_{TS} and increasing it, this can only reduce the value of the objective function till a value multiple of some of the $t_{a(i)}$'s is used.*

Proof. Start with $T_{TS} = T_{min}$ and increase T_{TS}. Stop when a multiple of any of the $t_{a(i)}$'s is attained. Call this value T^1_{mult}. Then, it is clear that the K_i values do not change in the interval $[T_{min}, T^1_{mult})$. However, it is also true that $P(T^1_{mult}) \leq P(T_{min})$. Therefore, the optimal solution of the global problem can not improve until (possibly) $T_{TS} = T^1_{mult}$. The same argumentation holds for $T_{TS} \in [T^1_{mult}, T^2_{mult})$ (where T^2_{mult} is the next multiple of any of the $t_{a(i)}$ values). Iterating this procedure, it can also be verified for the whole range of the time-slot duration, i.e. $T_{TS} \in [T_{min}, T_{max}]$. ■

Lemma 6 states that the optimal value of the problem in (4.33) is attained at a time-slot duration that is a multiple of the time required to transmit an ATM cell in one of the areas, i.e. $t_{a(i)}$. So a practical way to solve the problem is to fix the value of T_{TS} to each of the meaningful candidates and to solve thereafter the allocation problem, which is efficiently solved using the results in the previous section. Note that in the DVB-RCS situation, the number of areas is very low. Thus, we can expect the same about the list of candidates T^k_{mult}. It is feasible then to solve the joint problem with an exhaustive small search over T_{TS}. Moreover, the list of candidates is further reduced as we can discard equal proposed values that are computed as multiples of different values of $t_{a(i)}$. Note that the approach is valid for the joint DBA algorithm as well as for the hierarchical approach.

The algorithm to solve the joint DBA and TS selection is summarized as:

---

1. Construct the list of candidate values to T_{TS} (i.e. all multiples of $t_{a(i)}$, $i = 1, \ldots, N$, between T_{min} and T_{max}).
2. Reduce the list by suppressing equal values coming from multiples of different $t_{a(i)}$'s.
3. Solve the allocation problem for each of the possible values of T_{TS}.

4. Finally, select the T_{TS} with best objective value in (4.31).

Finally, we want to mention that in a practical situation it is not necessary to compute the value of T_{TS} at each frame since the time-slot duration depends on the area parameters and we can assume that these vary slowly in time because an area is an aggregation of many RCSTs. The most relevant parameter is how the traffic transported by the satellite is distributed among areas. In the next section, we show the impact of a time-slot duration maladjustment in performance.

4.6 Results and Discussion

The section starts with a discussion on operational aspects of the proposed framework, which are exemplified by means of a small DBA example. It shows the benefits of taking into account cross-layer messages coming from the upper layers, which allow us to balance the resulting allocation in a QoS-oriented perspective. Next, we perform a study with a relatively large system, with many terminals populating each of the areas. The study will reveal the advantages of adapting the time-slot duration to the traffic load thanks to PHY cross-layer information. Finally, computational complexity and signalling overhead issues are discussed. We show the impact of our algorithm in time requirements and we establish a comparison between the signalling needs of the framework we propose and a non-structured one.

4.6.1 Operational Aspects

Let us assume now a reduced allocation problem involving 24 RCSTs that share 100 time-slots. Note that the results derived in this analysis can be extrapolated to a larger system with more terminals and resources since the problem will be similar in relative terms. The scenario under consideration is summarized in Tables 4.1 and 4.2. In Table4.1 we define the parameters of interest of each RCST, namely: i) assigned area; ii) number of ATM cells per time-slot that the terminal can transmit; iii) the RCSTs' requests; iv) the RCSTs' minimum guaranteed resources and v) the priority of each request. Table 4.2 relates terminals to segments (we consider just two segments for simplicity reasons). Finally, Table 4.3 proposes a potential association between services, the type of request used to enter the satellite network and the corresponding priority. Note that we have assumed a single service or connection running at each RCST, which may not be the case in real life. Fortunately, this simplification does not subtract generality to the problem at the same time that offers a better understanding of it. The conclusions drawn here are valid also for a multi-connection scenario.

Using the hypotheses summarized in the previous tables, we compute the allocation with

Area	RCST	ATM cells per TS	Requests	Minimums	Priorities
1	1-2	1	$[15, 16]$	$[2, 0]$	$[1.75, 1.25]$
2	3-6	1	$[9, 19, 14, 5]$	$[0, 1, 2, 0]$	$[1.5, 2, 1.25, 1.75]$
3	7-13	2	$[17, 13, 4, 5, 13, 13, 8]$	$[1, 2, 2, 2, 0, 1, 1]$	$[1.75, 2, 1.5, 2, 1.25, 1.5, 1.25]$
4	14-20	2	$[12, 10, 2, 2, 7, 1, 8]$	$[1, 0, 2, 2, 2, 1, 2]$	$[1.5, 1.5, 1.75, 1.75, 2, 1.25, 1]$
5	21-24	2	$[14, 3, 2, 13]$	$[0, 1, 2, 3]$	$[1.5, 2, 1, 1.75]$

Table 4.1: RCSTs definition.

Segment identifier	Attached RCSTs
1	$[1, 3, 4, 7, 8, 9, 14, 15, 16, 17, 21, 22]$
2	$[2, 5, 6, 10, 11, 12, 13, 18, 19, 20, 23, 24]$

Table 4.2: Assignment of RCSTs to segments.

Requested QoS	Associated priorities	Request type
VoIP	2	RBDC
Video streaming	1.75	RBDC
Telnet, gaming	1.5	VBDC
Web browsing	1.25	VBDC
FTP, SMTP	1	VBDC

Table 4.3: Types of request.

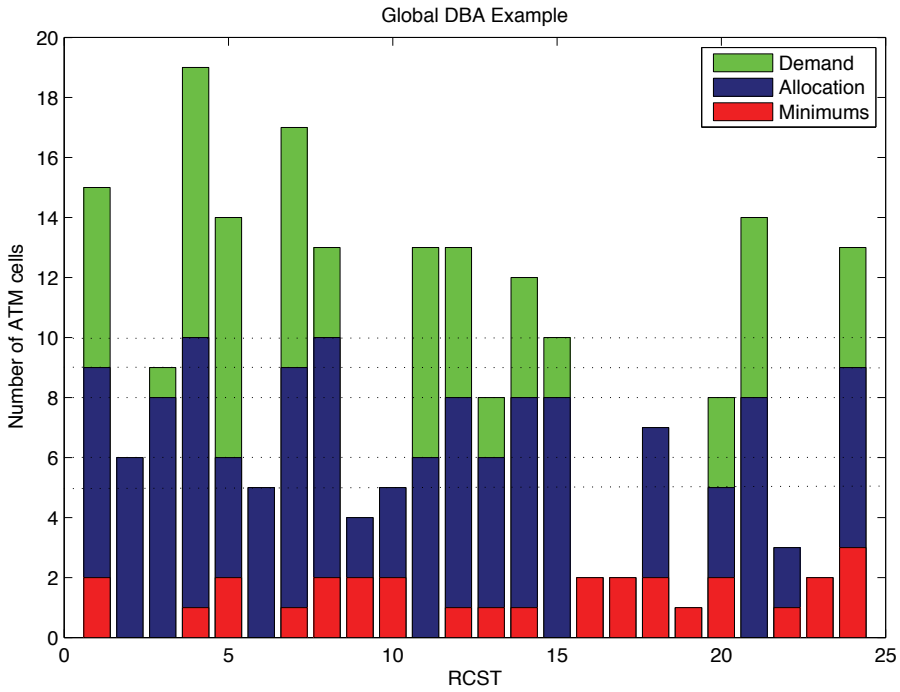

Figure 4.12: Global DBA example.

both the global DBA and the hierarchical algorithms. The resulting resource distribution from the global method is depicted in Figure 4.12 in form of a bar diagram (one bar for each terminal). The reader may appreciate the final allocation (in number of ATM cells) in blue whereas the requests and minimum guaranteed resources of each terminal are plotted in green and red, respectively. In this case, we have obtained the real-valued solution to the problem and it has been rounded down to fit the DVB-RCS situation. It is important to notice in Figure 4.12 the balancing of the allocation towards the terminals with highest priorities. The dotted horizontal lines show the water-levels fixed by each of the distinct priority values. For requests exceeding those water-level values, that depend on the available system resources, a terminal with higher priority receives always a higher allocation. On the contrary, an RCSTs never receives extra resources when it reaches its own request, independently of its priority. As an example, compare RCSTs 12 and 11. The former receives a larger allocation thanks to its larger priority despite they have requested the same amount of resources. RCST 12 transports streaming video, a priority service, whereas RCST 11 does simply web browsing. Compare now RCSTs 21 and 22. The former has lowest priority but receives the highest allocation. This is because the request of the latter is below the water-level that it has been fixed for the former (which is actually attained).

We compare now the global and hierarchical DBA algorithms maintaining the same scenario.

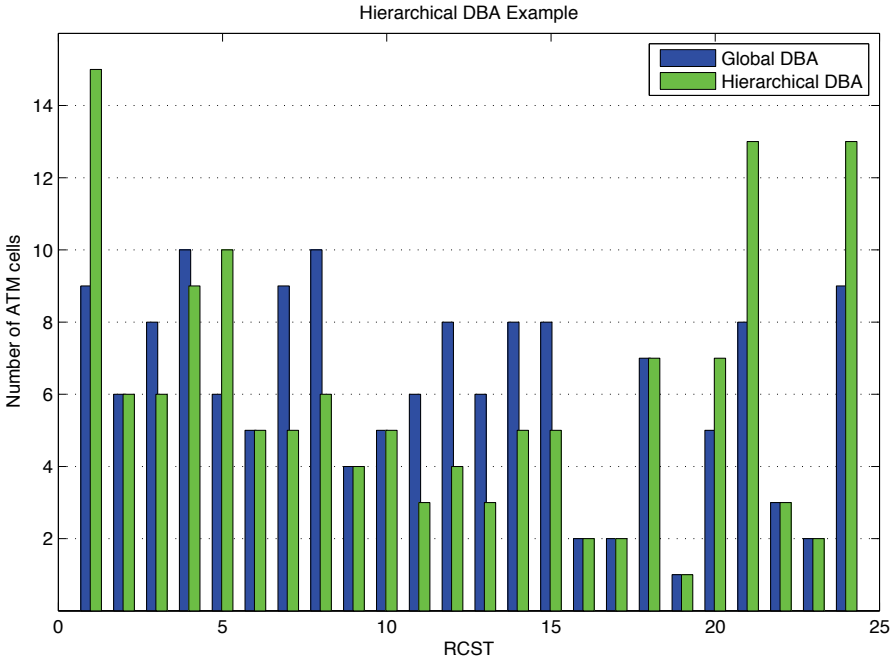

Figure 4.13: Hierarchical vs. global DBA.

The final allocation for both designs is depicted in Figure 4.13. The blue bars correspond to the global DBA and the green ones to the hierarchical approach. The result clearly illustrates the differences between both methods. If we want to quantize it, one possibility is to measure the value of the objective function attained for both approaches. Another possibility is to use the Fairness Index definition from [Jai84] as a measure of the fairness achieved. It departs from a known solution which is assumed to be the fairest one. In our case, it corresponds to the one obtained with the global DBA procedure. Let us call it $\{x^*_{i,j}\}$ in general. Then it constructs a new set of variables $\{y_{i,j}\}$ that depends both on the fairest solution $\{x^*_{i,j}\}$ and the one to be checked $\{x_{i,j}\}$ as

$$y_{i,j} = \frac{x_{i,j}}{x^*_{i,j}}, \qquad \forall i, j. \tag{4.34}$$

Finally, the Fairness Index (FI) is computed as

$$FI = \frac{(\sum_{i,j} y_{i,j})^2}{Y \sum_{i,j} y^2_{i,j}}, \tag{4.35}$$

where $Y = \sum_{i,j} 1$ is the total number of connections taking into account all RCSTs. We can give a geometric interpretation to the FI if we compare a vector $\boldsymbol{y}$ (which is the vertical stack of the values in $\{y_{i,j}\}$) with an all-ones vector of the same dimension using the scalar product. See the plot in Figure 4.14, where θ is the angle between vectors. Note that we can rewrite (4.35) as

$$FI = \frac{(\boldsymbol{y} \times \mathbf{1})^2}{Y\|\boldsymbol{y}\|^2} = \frac{(\|\boldsymbol{y}\|\,\|\mathbf{1}\|\,\cos\theta)^2}{\|\mathbf{1}\|^2\|\boldsymbol{y}\|^2} = \cos^2\theta \tag{4.36}$$

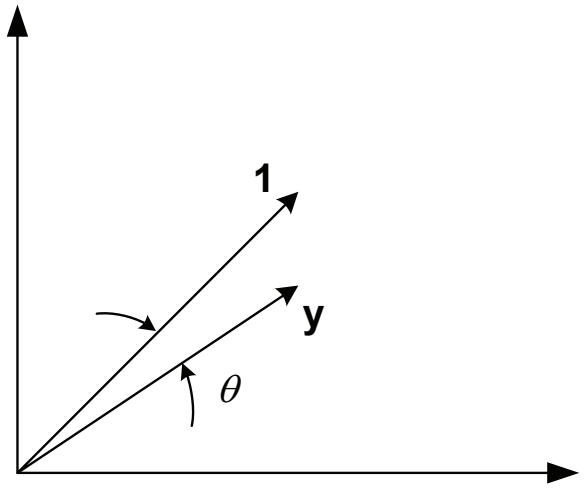

Figure 4.14: Geometric interpretation of the FI.

so that the FI is an implicit measure on the angle between the most fair solution (the vector $\mathbf{1}$ in the space of $\boldsymbol{y}$) and any other solution $\boldsymbol{y}$.

Figure 4.15 depicts the performance differences between the global and the hierarchical approach. Both the optimal value attained in (4.6) and the Fairness Index in (4.35) are depicted. Looking at the first measure, a slight reduction is perceived. However, since the objective function is logarithmic, it is difficult to establish how significant the improvement is. In terms of the FI, a reduction of about 12% is achieved and it allows a more comprehensive interpretation. Look now in a service per service basis: if the allocation is $x_{i,j} = x^*_{i,j}$, we are 100% fair ($FI = 1$) with that service. On the other hand, if the allocation is $x_{i,j} = 0$ with $x^*_{i,j} > 0$, we are totally unfair ($FI = 0$). So the hierarchical strategy is in mean about 12% unfair.

Finally, we want to illustrate the advantage of a proper balance of the resource distribution thanks to the defined priorities. Table 4.4 compares the amount of traffic (in number of ATM cells) dedicated to each application or service (as defined in Table 4.3) when priorities are considered and when not (fixing all $p_{i,j} = 1$). The result confirms the desired increased allocation at the most stringent applications, proving the interest in the proposed cross-layer mechanism established with the upper-layers of the system.

4.6.2 Global System Performance

In this part we simulate a bigger satellite sub-system and the main objective now is to analyze the benefits of cross-layer interaction with the PHY layer of the system using the joint DBA and frame design developed in Section 4.5. For that purpose, assume a frame duration of 26.5ms and consider the allocation of users among 111 carriers of 540kHz each, spanning 60MHz in total.

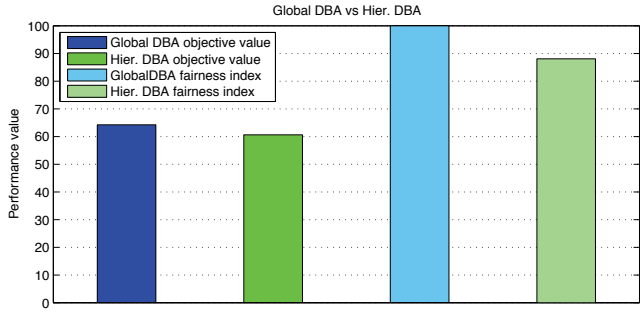

Figure 4.15: DBA algorithms performance

Traffic type	With priorities	Without priorities	Opportunistic allocation
VoIP	35	31	47
Video streaming	36	33	54
Telnet, gaming	44	44	48
Web browsing	25	31	0
FTP, SMTP	7	10	0

Table 4.4: Traffic (in number of ATM cells) with/without priorities.

We study a PHY layer with AC where five possible coding rates are feasible. This assumption is in accordance with the DVB-RCS standard when convolutional coding is used. As discussed before, users are grouped into areas depending on their transmitting rate. We have summarized in Table 4.5 the key area parameters, namely: i) the coding rate employed and ii) the time duration of an ATM cell in the area. Our simulation assumes a Quadrature Phase Shift Keying (QPSK) modulation using a raised cosine pulse with a roll-off factor of 0.35. Furthermore, the time-slot duration is limited between $T_{min} = t_1$ and $T_{max} = 3t_1$.

Define $\boldsymbol{v}$ as the vector whose k^{th} component contains the mean number of terminals in area k. A stochastic realization of the number of RCSTs in each area is then computed using uniform

Area identifier	Coding rate	ATM cell duration
1	$r_1 = 1/2$	$t_1 = 1.06ms$
2	$r_2 = 2/3$	$t_2 = 0.795ms$
3	$r_3 = 3/4$	$t_3 = 0.707ms$
4	$r_4 = 5/6$	$t_4 = 0.636ms$
5	$r_5 = 7/8$	$t_5 = 0.606ms$

Table 4.5: Areas definition.

probability density functions (pdf) as

$$\mathcal{V}_k \sim \mathcal{U}[0, 2 \cdot v_k], \qquad k = 1, \ldots, 5, \tag{4.37}$$

where $\mathcal{U}[a, b]$ is the integer uniform pdf with values between a and b, so that $\boldsymbol{\mathcal{V}} = [\mathcal{V}_1, \ldots, \mathcal{V}_5]^T$ defines a random scenario with a mean terminal distribution as in $\boldsymbol{v}$. Within each stochastic scenario (a realization of $\boldsymbol{\mathcal{V}}$), the requests emitted by each RCST are also randomly generated as

$$d_i \sim \mathcal{U}[0, 2\frac{D_{tot}}{\mathbf{1}^T \boldsymbol{v}}], \qquad \forall i, \tag{4.38}$$

where $\mathbf{1}^T \boldsymbol{v}$ is the mean number of RCSTs in the system and D_{tot} is the load offered to the system in number of ATM cells . In other words, it is the total amount of traffic requested to the satellite, even if it could not be allocated. Note that this model assumes equal expected number of requests per terminal but allows us to adjust the distribution of terminals among the areas. Furthermore, as far as we are interested in the macro system behavior, we assume for simplicity reasons that no minimum resources need to be allocated and that the priority of all terminals and connections equals one, so that we do not distinguish different connections at the same RCST (the subindex j is dropped).

Let us define the Aggregated Data Rate (ADR) transported by the satellite subnetwork as the sum rate of the system for a certain allocation of resources $\{x_i\}$

$$ADR = \frac{\sum_i \min\left(K_i x_i, d_i\right) \cdot 53bytes}{26.5ms}. \tag{4.39}$$

The min function takes into account the case where the terminal can potentially transmit more ATM cells in the assigned time-slots than what it really does due to rounding. As an example of the situation, consider a terminal that allocates 2 ATM cells per time-slot and its request is 9 cells. If it receives 5 time-slots from the DBA algorithm, then it sends 9 ATM cells to the satellite instead of 10. The maximum possible ADR is achieved when the whole frame is fulfilled with ATM cells of the highest coding rate area using the best time-slot configuration. With the values assumed in our simulation it is possible to transmit 4662 cells that finally correspond to 74.59Mbps of ADR. This value is taken as the reference value ADR_{ref}.

We run Monte Carlo simulations that show the mean value of ADR as a function of the load offered to the system D_{tot} for a fixed distribution of users $\boldsymbol{v}$. The simulated range of D_{tot} goes from 500 to 6000 ATM cells in steps of 500 cells. The results obtained with the proposed DBA mechanisms are compared to the ones attained by the optimal solution to the problem, which is combinatorial. In this case, the time-slot duration is not fixed. Instead, it exactly fits the duration required to transmit an ATM cell and thus, it depends on the coding rate of the terminal. The goal is to find the best possible ordering of time-slots, that is, the one that uses the time in the subcarriers to the maximum extent. To compute (approximately) the optimal solution, we first fix the lowest possible water-level (using the minimum request of all terminals)

and we generate random permutations (each permutation defines a different ordering of the time-slots of the active users within the subcarrier/s) in order to select the most efficient one (the one that leaves less free-space in the subcarrier/s). Then, the water-level is fixed to the second lowest request and the procedure is repeated until all the subcarriers are used or all the requests are allocated. In practice, we have used 50 random orderings at each stage observing that minor or no gains are reported by the last trials, which assures to fairly approximate the real optimum.

In Figure 4.16 we plot the ADR in the system using either the proposed technique or the optimum allocation for a user distribution $\boldsymbol{v} = [5, 10, 10, 30, 45]$, which assumes that most users are in rather good propagation conditions (it is a realistic hypothesis). The proposed method is computed with three different choices of TS duration, namely: i) the optimal value; ii) the minimum feasible value $T_{TS} = t_1$, and iii) $T_{TS} = 4t_4$, which is a value that suits the current load and user distribution (not necessarily the optimum). Note that the election $T_{TS} = t_1$ is the natural one without considering multiple MAC frames in a time-slot. The reader may appreciate significant gains comparing the rates obtained with the optimal time-slot duration to the ones achieved with $T_{TS} = t_1$. Furthermore, the distance with the optimal allocation is considerably reduced. Note also that the election $T_{TS} = 4t_4$ attains nearly the same performance as the optimal T_{TS}, proving that it is not necessary to adjust the value at each bandwidth allocation process. This robust behavior is very interesting in practical systems. We confirm it by simulating a drastic change in the user distribution to $\boldsymbol{v} = [20, 20, 20, 20, 20]$ in Figure 4.17. We assume now that there is a rain event and many users lower the coding rain to adapt to the new bad propagation conditions. Still, the value $T_{TS} = 4t_4$ exhibits acceptable rates, close to the ones obtained with the optimal value.

Figure 4.18 evaluates the efficiency in terms of frame occupation. For this purpose, we plot the Bandwidth Occupation (BO), computed as

$$BO = \frac{\sum_i \min\left(K_i \cdot x_i, d_i\right) \cdot t_{a(i)} \cdot 540kHz}{C \cdot 540kHz \cdot 26.5ms} \tag{4.40}$$

as a function of $\frac{ASD}{ADR_{ref}}$. ASD stands for Aggregated System Demand and it is the total sum of requests in the satellite sub-network in number of ATM cells, i.e. $ASD = \sum_i d_i$. The reference value ASD_{ref} is, as before, the maximum number of ATM cells transmitted in the system (at the highest coding rate), i.e. 4662 ATM cells in our simulation. Therefore, the BO is the percentage of the frame (interpreted as a time-frequency zone) being used by the satellite. We compare the proposed method with an opportunistic allocation, which corresponds to the solution of (4.31) when the objective function is replaced by $\sum_{i,j} \left(x_{i,j} \cdot K(T_{TS}, t_{a(i)})\right)^{p_{i,j}}$. Opportunistic approaches are known to be terribly unfair since the goal is to maximize global benefits (the sum-rate in this case) without considering the way it is achieved. Assuming $p_{i,j} = 1$, the opportunistic solution allocates first the users with highest coding rates since the benefit is higher

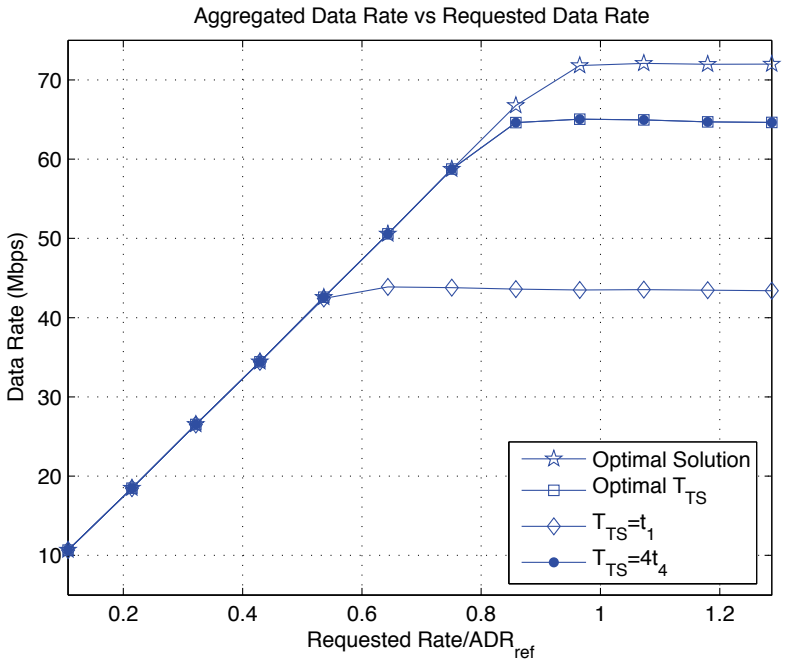

Figure 4.16: Aggregated Data Rate (good conditions).

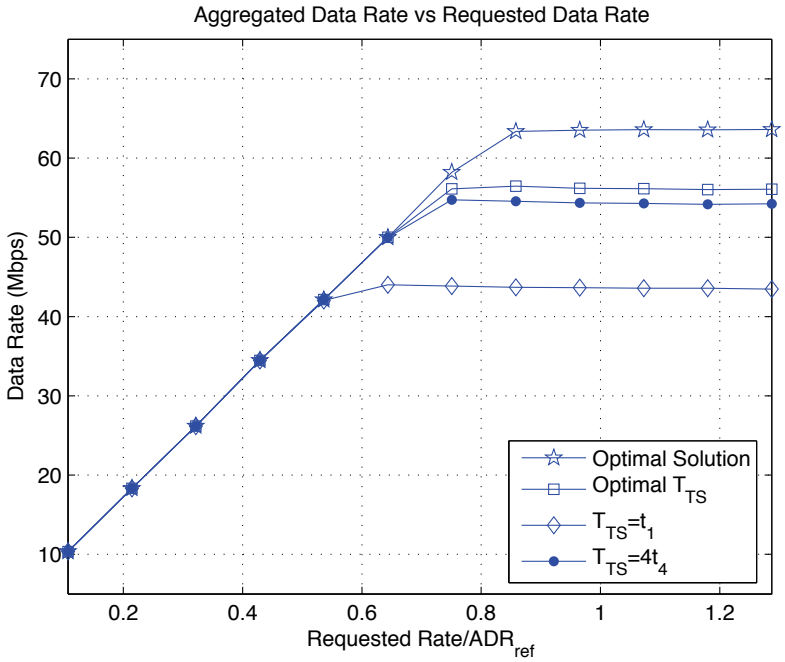

Figure 4.17: Aggregated Data Rate (bad conditions).

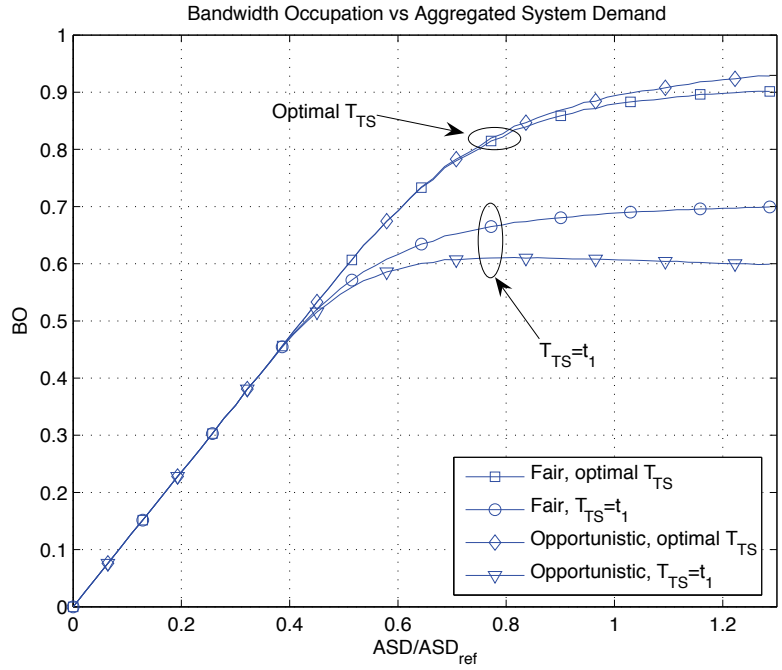

Figure 4.18: Bandwidth occupation.

(more ATM cells fit in the frame). Remaining resources are then distributed among RCSTs that use the second highest rate and so on. The procedure is clearly detrimental to terminals with low coding rates since they get fewer opportunities or even none. Both methods are computed with optimal time-slot selection and $T_{TS} = t_1$. Results show that optimizing T_{TS} improves significantly the occupation for both fair and opportunistic strategies while it reduces the bandwidth occupation differences between the two designs. The optimal (combinatorial) allocation (not plotted) saturates to a value close to 1 when the load of the system allows to use all the frame.

Additional insight into the bandwidth allocation issue is gained with the following analysis.

Bandwidth Occupation

area/T_{TS}	t_1	$2t_5$	$2t_4$	$2t_3$	$2t_2$	$3t_5$	$3t_4$	$3t_3$	$3t_2$	$4t_5$	$4t_4$	$4t_3$	$5t_5$
1	**1,00**	0,87	0,83	0,75	0,66	0,58	0,54	**1,00**	0,83	0,83	0,83	0,75	0,66
2	0,75	0,65	0,62	0,56	**1,00**	0,87	0,81	0,75	0,62	0,93	0,93	0,84	0,75
3	0,66	0,58	0,55	**1,00**	0,89	0,77	0,72	**1,00**	0,83	0,83	0,83	**1,00**	0,89
4	0,60	0,52	**1,00**	0,90	0,80	0,70	0,97	0,90	0,75	0,75	**1,00**	0,90	0,80
5	0,57	**1,00**	0,95	0,85	0,76	**1,00**	0,93	0,85	0,71	0,95	0,95	0,85	0,95
mean	0,71	0,73	0,79	0,81	0,82	0,78	0,79	0,90	0,75	0,86	**0,91**	0,87	0,81

Table 4.6: System occupation analysis.

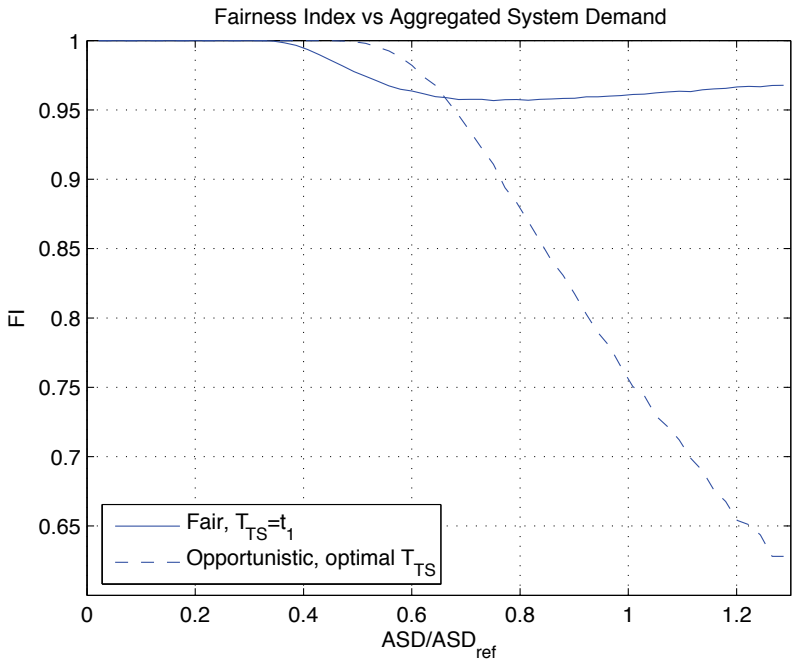

Figure 4.19: Fairness study.

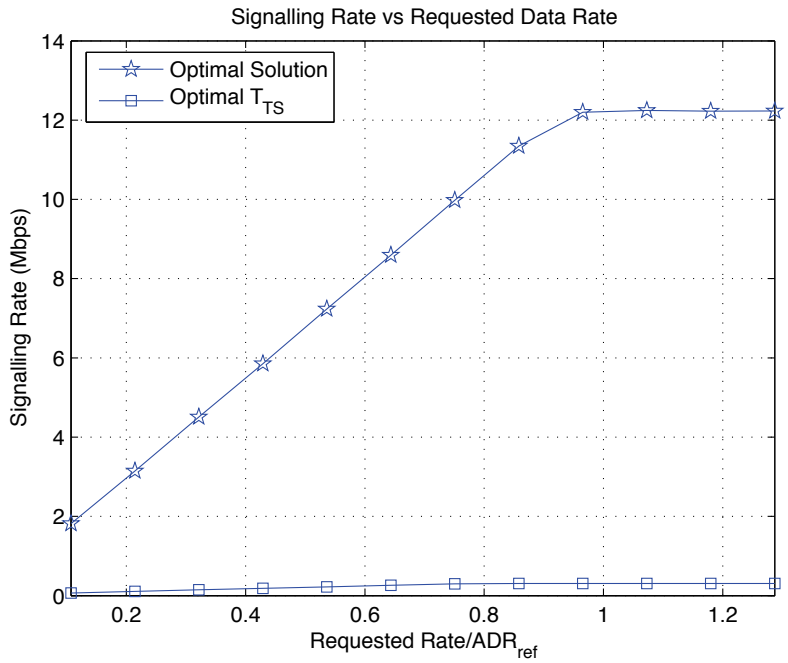

Figure 4.20: Signalling Rate (good conditions).

Assume the hypothetic scenario where all terminals belong to one area and transmit with a single coding rate. Further assume that the total amount of traffic requested in the area is fairly above the system limit, so that all the available resources in the frame are employed. Finally, compute the BO for the described situation and for all the meaningful candidates of T_{TS}. The results of the previous analysis for the five areas considered is found in Table 4.6. Note that in case that the expected distribution of users into areas $\boldsymbol{v}$ is known, it is possible to approximate the BO of the system as a function of the time-slot duration as

$$BO(T_{TS}) \approx \frac{\sum_i v_i BO_i^{T_{TS}}}{\sum_i v_i} \tag{4.41}$$

where $BO_i^{T_{TS}}$ is the bandwidth occupation of the system when all RCSTs belong to the i^{th} area and the time-slot duration is T_{TS}. Therefore, it is possible to adjust the T_{TS} off-line given the frame parameters and an estimation of $\boldsymbol{v}$. Even with no information on the distribution it is possible to adjust the value in the max-min sense. In other words, we can choose the time-slot duration that maximizes the BO when the unknown distribution $\boldsymbol{v}$ appears to be the worst possible. In our example, the max-min T_{TS} is $T_{TS} = 4t_4$ (marked in yellow). If some information is available, for example, if we know that most of the traffic is in areas 3 and 4, the best choices for T_{TS} are $T_{TS} = 2t_3$, $T_{TS} = 3t_3$ or $T_{TS} = 4t_3$. This table further justifies that it is not necessary to update T_{TS} at every allocation cycle.

Finally, Figure 4.19 studies how is fairness affected by: i) a non-optimal time-slot duration $T_{TS} = t_1$ in the proposed global DBA method and ii) an opportunistic strategy with optimized time-slot duration. As before, we make use of the fairness index introduced in [Jai84] and formulated in (4.35). To obtain it, we assume that the most fair solution is the one attained with the fair approach and optimal time-slot duration. Note that T_{TS} for the fair solution does not necessarily coincide with the optimal value for the opportunistic approach. The result in the figure confirms that the fair strategy sustains fairness even when the time-slot duration is far from the optimal one. On the contrary, the opportunistic solution tends to be more unfair as the total demand in the system increases because the terminals with lowest rates are discarded to benefit the ones with better propagation conditions.

4.6.3 Computational Complexity and Signalling

The last part of this section is dedicated to show the advantages of the proposed framework in terms of signalling efficiency and reduced computational complexity. To begin with, consider the amount of information required to signal the frame structure in the proposed framework and in the optimal (combinatorial) solution. Since no frame structure is imposed in the second option, it is mandatory (according to the standard) to indicate the position of each time-slot in the frame, which is done at the Frame Composition Table (FCT) [ETS05a, Sec. 8.5]. In numbers, we need $(174 + N_{TS} \cdot 72)$bits to transmit the FCT, where N_{TS} is the number of

time-slots[1] allocated in the frame. It takes 26.5ms in our simulation. On the contrary, the use of the proposed frame structure reduces this quantity to $(174 + C_u \cdot 72)$bits, where C_u is the number of carriers employed to transmit, because it is possible to signal the time-slot at the beginning of the frame and indicate the number of repetitions. Figure 4.20 plots these quantities in form of signalling rate (i.e. divided by 26.5ms) as a function of the normalized requested rate in the system when $\boldsymbol{v} = [5, 10, 10, 30, 45]$. The result clearly shows the advantage of the structured option with a reduction of about 12Mbps devoted to signalling in a loaded system. Note in Figure 4.16 that the increase in transmitted data rate in the same conditions in a more structured frame is around 8Mbps and therefore, an structured option is meaningful.

In addition, our design facilitates the computation of a fair and time-efficient solution, which is imperative in practical systems. To exemplify it, we solve the allocation problem using our DBA algorithm and the bisection method, which is known to suit practical implementations [Pal05], applied to (4.2) in a Pentium®-Mobile processor running at 1.73GHz. The inputs to both algorithms are discrete (integer) uniform random variables with different thresholds: i) $d_i \sim \mathcal{U}[1, 20]$; ii) $m_i \sim \mathcal{U}[0, 3]$ and iii) $K_i \sim \mathcal{U}[1, 2]$. Priorities are also discrete, $p_i \sim \mathcal{U}[1, 2]$, but with a step of 0.25 (i.e. $p_i \in \{1, 1.25, 1.5, 1.75, 2\}$). We run Monte-Carlo simulations to extract the mean computation time function of the number of terminals. The results are depicted in Figure 4.21. The reader may appreciate that the proposed global DBA algorithm solves the problem in half the time required by the bisection method. Translating the result in the context of DVB-RCS (assuming 100ms of available time to compute the allocation), it is equivalent to say that the bisection method is able to manage 8500 users whereas our method would manage 18000.

4.7 Summary

The main contributions of this chapter are the design of an optimized framework to work with the dynamic allocation procedure in the DVB-RCS standard together with fair and time-efficient DBA algorithms that take into account cross-layer information both from the lower layer (PHY layer) and the upper layers (IP layer in our example). The proposed algorithm is derived using the convex duality and decomposition results in Chapter 3.

Our approach is compliant with the DVB-RCS standard. Unlike other approaches, our contribution fixes some structure, the time-slot, common to all areas (i.e., coding rates). This results in reduced signalling, increased robustness to PHY-layer changes and reduced complexity of the subsequent resource allocation. Then, depending on the spectral efficiency of the RCSTs within a given area, one or more ATM cells per time-slot can be transmitted. The time-slot is optimized

[1]Recall that each time-slot fits exactly one ATM cell in the optimal case whereas it can allocate more than one ATM cell in our proposed framework.

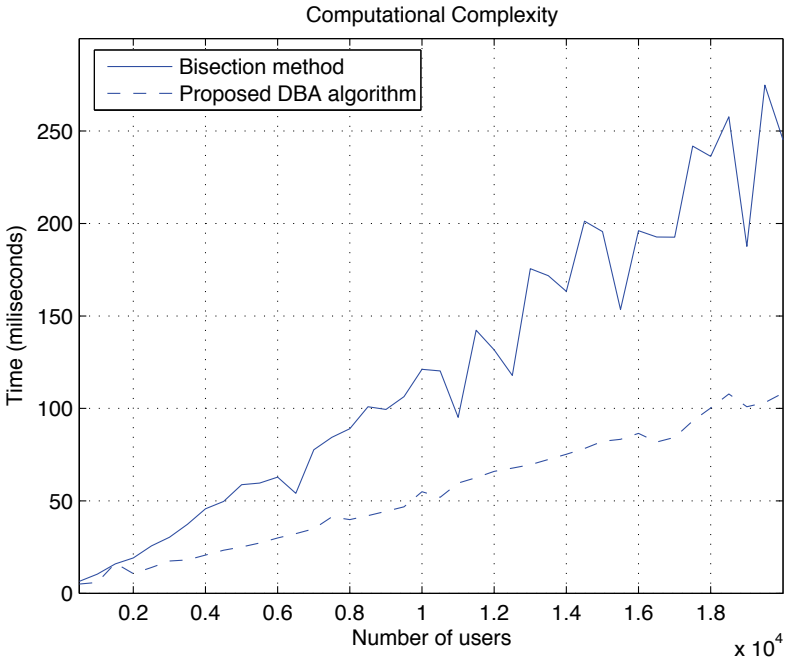

Figure 4.21: Computational time (global DBA and bisection method).

either for each allocation cycle or in a max-min sense. Results show that the MAC cross-layer design enabled by an adaptive PHY layer reports significant gains.

Thereafter, time-efficient algorithms have been presented for the allocation of bandwidths to RCSTs (in global and hierarchical approaches). Both algorithms are able to find the exact solution to their respective problems with less than half the time that the widely used bisection method would need. We have exemplified the algorithms, showing the sub-optimality of the hierarchical approach. This makes even more important to solve the global allocation with little complexity.

Finally, the use of priorities at MAC-layer gives continuity to the QoS requirements defined at upper layers, such as IP layer. Priorities can be explicitly signalled to the NCC or alternatively, the NCC can extract this information from the traffic.

Chapter 5

Distributed Algorithm for Uplink Scheduling in WiMAX Networks

We propose in this chapter another application of the decomposition strategies exposed in Chapter 3, this time focusing on the scheduling aspects at the uplink of the Worldwide Interoperability for Microwave Access (WiMAX) system from a MAC-layer point of view. Resource allocation in the WiMAX uplink falls into the DAMA-type of approaches. The different services managed by a terminal (and mapped to MAC-layer logical connections) request transmission opportunities that are granted in a terminal basis. We address in this chapter the scheduling formulation and computation under a generic NUM approach that is particularized to a proportional fairness strategy, like in DVB-RCS. The design is suitable for PMP and tree-deployed mesh network configurations, which may have application in WiMAX used as the backhaul network. In both cases, the network is optimized centrally from the Base Station (BS). However, the solution is computed in a distributed manner without requiring explicit communication from all terminals to the BS.

5.1 Introduction to WiMAX

The wireless community has recently directed much attention onto a variety of topics related to WiMAX technologies as a broadband solution. Two different standards are under this commercial nomenclature: the IEEE 802.16 [IEE04], with its extension to mobile scenarios IEEE 802.16e [IEE06], and the ETSI HiperMAN [ETS03b, ETS03a]. Operating mainly in the range of 2GHz to 11GHz, WiMAX enables fast deployment of the broadband network even in remote locations with low coverage of wired technologies, such as the DSL (Digital Subscriber Loop) family. WiMAX extends the widely-used WLAN (Wireless Local Area Network) coverage to tens of kilometers, and thus the interest to use such platform to bring internet access to rural and isolated places is logical.

Four different PHY layers have been defined in the IEEE 802.16 standards [IEE04, IEE06]. These are:

- Wireless Metropolitan Area Network (WirelessMAN) Single Carrier (SC): it is devoted to operation frequencies beyond 11GHz and requires Line of Sight (LOS) propagation.
- WirelessMAN SCa (access): a single carrier system for frequencies between 2GHz and 11GHz and designed for point-to-multipoint (PMP) operation.
- WirelessMAN Orthogonal Frequency Division Multiplexing (OFDM): designed to operate in the range between 2GHz and 11GHz in non-LOS (NLOS) propagation conditions. It uses 256 subcarriers and it has been accepted as the reference PHY layer for fixed deployments, being also referred to as fixed WiMAX.
- WirelessMAN Orthogonal Frequency Division Multiple Access (OFDMA): uses 2048 subcarriers and it is devoted to PMP with NLOS propagation. Operates in the range between 2GHz and 11GHz. This PHY layer has been modified in [IEE06] to an Scalable OFDMA (SOFDMA) where 128, 512, 1024 and 2048 subcarriers can be configured. The motivation of such scalability is to adapt it to the nature of the mobile channel and thus, this PHY layer has been accepted for mobile operation, being also referred to as mobile WiMAX.

Typically, terminals use OFDM as the modulation technique in mobile scenarios and also in fixed WiMAX. Regarding the multiple access strategy, fixed terminals employ mainly TDMA whereas mobile units use an OFDMA approach. Generally speaking, the PHY layer in WiMAX allows many degrees of adaptation to the channel conditions of the terminals thanks to adaptive coding and modulation (ACM), power control and subchannelization in the OFDM mode. A subchannel is a logical collection of subcarriers that depends on the subcarrier permutation mode. A data block is then sent over one or multiple subchannels. In summary, PHY layer flexibility allows to set up a transmission at many different points in the multi-user capacity region of the system and it is a courageous task to set it up in the best possible way given channel and traffic load conditions. Our contribution considers a given PHY set up and the goal is to distribute the available resources (link rates) among the services that require them. Future work will consider also PHY layer aspects.

The MAC layer in WiMAX can be divided in three parts: the service-specific Convergence Sublayer (CS), the common-part sublayer and the security sublayer [And07]. The CS is the interface with the IP layer and manages data packets to and from this layer, also known as Service Data Units (SDUs). Among its inter-layer adaptation tasks, we can find header compression and address mapping. The common-part sublayer performs most of the MAC-layer tasks, such as fragmentation and concatenation of SDUs into MAC Packet Data Units (PDUs), MAC man-

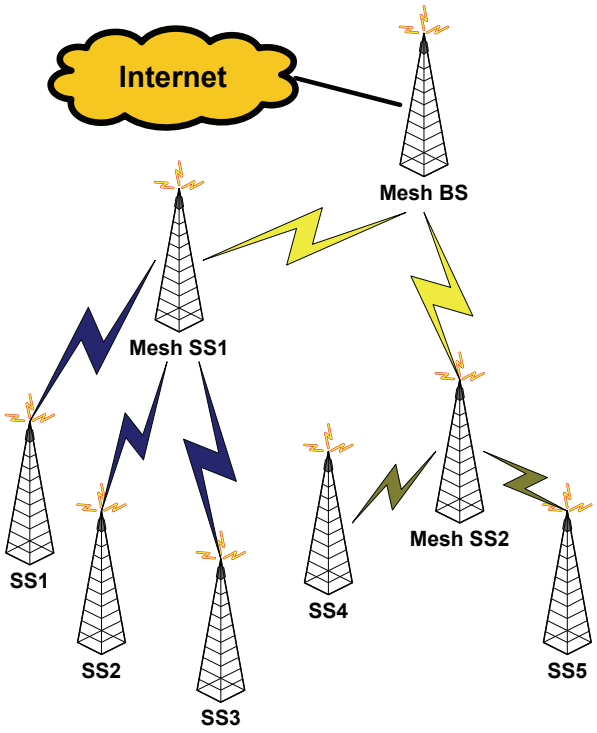

Figure 5.1: WiMAX mesh network.

agement, QoS control, scheduling, ARQ, etc. Our work is focused on this sublayer. Finally, the security sublayer is mainly in charge of encryption and authorization tasks.

Let us now discuss about network topologies. There are two possible architectures in WiMAX, namely: i) PMP and ii) mesh. In PMP mode, one Base Station (BS) serves a certain amount of Subscriber Stations (SSs) using direct links like in traditional cellular networks, whereas in mesh mode, SSs can be linked directly to the BS or routed through other SSs in the network. In Figure 5.1 there is a mesh topology example. Note that it is a particular case of a mesh network since it is tree-deployed. It is possible to identify 3 PMP clusters within. At the top of the tree a PMP network is formed by MeshSS1, MeshSS2 and the MeshBS. Below, there are two other PMP clusters: one headed by MeshSS1 and another one headed by MeshSS2. We will consider in this work either PMP or tree-deployed mesh networks. The practical motivation is that under such circumstances it is possible to compute the scheduling in a distributed way and thus reduce the signalling compared to the one that would be required if the necessary information to calculate the scheduling had to be gathered at a central node in the network. Moreover, the request/allocation mechanism envisaged in the standard document for centralized scheduling suggests the implementation of such topology since requests at one node have to be aggregated to the requests performed at the nodes below.

In the uplink of the system, the SSs request resources in terms of bytes of information and

they do so for each connection at the SS. Roughly speaking, we can associate connections with services (further details are given in the next section). However, the result of the allocation is given on a terminal basis and it is the SS that is in charge of distributing the allocation among the services within; therefore, from a scheduling point of view, the tree-topology interpretation makes sense even in the PMP case. In this situation, we may consider two allocation levels: at the highest, the distribution of the BS resources among the SSs; and at the lowest, the allocation of the SS grants to the services underneath. In the mesh mode the standard defines two types of transmission scheduling, namely: i) centralized and ii) distributed, which shall not be confused in the distributed nature of the computation of the allocation that we propose. In centralized scheduling the allocation is conducted by the Mesh BS as outlined some lines above, whereas in distributed scheduling, some parts of the network are allocated separately. Note that we propose to perform centralized scheduling with the signalling advantages of a distributed strategy (not distributed scheduling) since thanks to decomposition ideas, the bandwidth allocation may be computed in a distributed way.

Previous works related to resource allocation in WiMAX networks address a variety of scenarios, from PMP to mesh, from TDMA to OFDMA access types, and distinguishing single channel or multi-channel networks, most of them from a physical (PHY) layer perspective, where the goal is to properly configure the transmission parameters. At the best of our knowledge, two main approaches are found in the literature, namely: i) formulate the problem in a mathematical optimization framework and ii) develop heuristic algorithms. In the sequel, we briefly review some of the works (more details can be found in Section 2.4.2). In [Mak07], the authors propose an heuristic solution for the case of a single cell OFDMA WiMAX network that maximizes the network sum-rate under some fairness considerations. The authors in [Wei05] analyze how concurrent transmissions boost performance in mesh-type networks by proposing an interference-aware routing and scheduling mechanism. In [Du07], one can find a discussion about the advantages of a multi-channel network. Finally, [Sol06] contributes with a mathematical optimization solution that falls into the NUM framework, where a distributed optimal solution to the established NUM problem is obtained using a convex decomposition approach [Pal07]. It combines PHY and MAC scheduling aspects.

In this work we concentrate on the scheduling design of the uplink of a WiMAX network from a MAC layer perspective, which considers a DAMA approach. We assume either a PMP or a tree-deployed mesh network, which is useful when WiMAX is employed as the backhaul network [Lee06b]. Our solution can be included in the class of proportionally fair schedulers [Kel98] and it is formulated as a NUM problem. The objective is to fairly allocate all the connections or services in the system depending on the mid-term transmission resources provided by the PHY layer. The proposed solution is distributed in the sense that it allows us to jointly optimize the entire network without the need of a central node (and subsequent signalling requirements), and

provides faster convergence than other known distributed techniques. Next section details the procedure for requesting and allocating bandwidth in WiMAX.

5.2 Bandwidth Request and Allocation in the WiMAX Uplink

As introduced in the previous section, each WiMAX SS may support many connections and each one is described by a Connection Identifier (CID). There is a primary CID (which is in charge of MAC messaging) and several secondary CIDs, all devoted to different services. The exact mapping between services and connections is not specified in the standard, but the underlying motivation is to group services that have similar QoS requirements under the same logical connection. QoS requirements are characterized by means of a set of attributes [IEE04, Sec. 6.14], all of them related to each service flow thanks to the Service Flow Identifier (SFID). All CIDs in the system use a three-way handshake in which they request uplink bandwidth, wait for the BS to compute the allocation and get their grants using the Uplink (UL) MAP messages.

Requests are made in terms of bytes of information and can be incremental (if they add to the previous ones) or aggregate (if they replace them). The way the SSs ask for resources is either using a specific bandwidth-request MAC Packet Data Unit (PDU) or piggybacking on a generic MAC PDU. The UL MAP also defines the dedicated or shared UL resources that the SSs can use to emit their bandwidth requests. This mechanism is known as polling in the WiMAX context. If there are enough available resources to poll each SS separately, then we have unicast polling. On the contrary, a subset of terminals or even all terminals enter in a contention process and we have multicast/broadcast polling. Remember that resources are granted in WiMAX in a SS basis and it is the SS that distributes these among the attached CIDs and therefore, distributed solutions benefit from reduced signalling in a joint network optimization strategy.

In order to provide Quality of Service (QoS), five different scheduling services are defined in the WiMAX standards:

- The Unsolicited Grant Service (UGS): it is devoted to real-time service flows that generate packets of constant size on a periodic time basis, as it is the case in VoIP. UGS grants a fixed-size allocation without explicit bandwidth requests in order to reduce the associated system overhead and the latency in scheduling.

- The real-time Polling Services (rtPS): accommodates real-time services that generate data packets of variable size on a periodic time basis, as it happens with MPEG video. The BS provides polling opportunities to the SS with an adequate rate to fit the latency requirements of the services. The goal is to have a more efficient system able to compensate the signalling overhead derived from the request and allocation process.

- The non-real-time Polling Services (nrtPS) is similar to rtPS but contention-based polling is used in addition to the unicast version, where request opportunities are less frequent than in rtPS.

- The Best-Effort service (BE) is designed for services with low QoS requirements so that the scheduling process prioritizes all other services. In this case requests are emitted using only the contention-based polling mechanism.

- The extended real-time Polling Service (ertPS) was introduced in the mobile WiMAX [IEE06] and it lies in between the UGS and the rtPS. In this case the periodic resources allocated to the SS can be used either for transmitting data or for requesting additional bandwidth and therefore, this service suits traffic types whose bandwidth requirements change with time.

Services flows are explicitly described in terms of QoS related parameters, such as latency, jitter, throughput and packet error rate. The components of a service flow are:

- Service flow ID (SFID): a 32-bit identifier.

- Connection ID (CID): a 16-bit identifier of the connection that carries the service.

- Provisioned QoS parameter set: it contains the recommended QoS settings for the service and is usually provided by the higher layers.

- Admitted QoS parameter set: the QoS parameters that can be actually satisfied with the current MAC/PHY layer configuration. It may be a subset of the provisioned QoS parameter set when the BS is not able to attain all QoS requirements.

- Active QoS parameter set: it is the subset of QoS parameters that are provided to the service flow at a given time.

- Authorization module: a logical BS function that verifies every potential change to the QoS parameters and classifiers related with a service flow.

Service flows are usually grouped into service classes with similar QoS requirements. This fact enables that requests at any point in the network are globally consistent from a higher-layer perspective. However, the way service flows are grouped into service classes is left as an open issue in the WiMAX standard.

Up to this point, we have reviewed the most significative aspects of the scheduling issues that appear in the uplink of WiMAX. The interested reader can find a good explanation on the standard and related aspects in [And07]. We propose now a mathematical optimization approach

to deal with the depicted situation and we do it using the framework of NUM. Let us formulate the scheduling as

$$\begin{array}{ll} \max\limits_{\{\boldsymbol{r}_i\}} & \sum_{i=1}^{N} U_i(\boldsymbol{r}_i) \\ s.t. & \boldsymbol{r}_i \in \mathcal{R}_i, \qquad i = 1 \dots N \\ & \sum_{i=1}^{N} h_i(\boldsymbol{r}_i) \leq c \end{array} \tag{5.1}$$

where $U_i(\boldsymbol{r}_i)$ is the utility function perceived at entity i that depends on the granted rates $\boldsymbol{r}_i$. Given the network topology assumed, entity i can be (from top to bottom) the Mesh BS, a Mesh SS, a SS and finally, a CID. In general, $U_i(\boldsymbol{r}_i)$ is the result of a convex optimization problem of the same nature as (5.1). Later on, we will provide an example to illustrate our mathematical framework. The functions $h_i(\boldsymbol{r}_i)$ are convex functions of the rates $\boldsymbol{r}_i$ and c is the total amount of available resources. We assume that c is a parameter of the problem that is given by the specific PHY layer configuration as the mid term capacity. The convex subsets $\mathcal{R}_i$ are cartesian products that define the maximum and minimum values that the rates in $\boldsymbol{r}_i$ can take.

Let us consider now the network configuration in Figure 5.1 and assume that it is possible to map the different services and their requests to certain utility functions and subsets $\mathcal{R}_i$. Note that the specific choice of those functions defines the nature of the solutions. As we have done in the DVB-RCS case in Chapter 4, we use weighted logarithmic utility functions of the granted rates to attain an asymmetric proportionally fair solution [Kel98]. However, the decomposition approach is valid for any convex function given the specified tree network topology. Consider first the allocation of resources performed at the Mesh BS among Mesh SS1 and Mesh SS2. We formulate the problem as

$$\begin{array}{ll} \max\limits_{\boldsymbol{r}^1, \boldsymbol{r}^1} & U^1(\boldsymbol{r}^1) + U^2(\boldsymbol{r}^2) \\ s.t. & \boldsymbol{r}^i \in \mathcal{R}^i, \qquad i = 1, 2 \\ & \sum_{i=1}^{2} \mathbf{1}^T \boldsymbol{r}^i \leq c \end{array} \tag{5.2}$$

where $\boldsymbol{r}^1 = [\boldsymbol{r}_1^T, \boldsymbol{r}_2^T, \boldsymbol{r}_3^T]^T$, $\boldsymbol{r}^2 = [\boldsymbol{r}_4^T, \boldsymbol{r}_5^T]^T$ and c is the amount of resources available at the Mesh BS to transmit to the core network. For the sake of simplicity, superscripts are now related to Mesh SSs whereas subscripts are associated to SSs. Note that $\boldsymbol{r}^1$ aggregates all the rates at SSs 1 to 3, i.e. $\boldsymbol{r}_1$ to $\boldsymbol{r}_3$. Furthermore, each $\boldsymbol{r}_i$ is a vector that contains the rates of all the CIDs attached to SSi.

The allocation at a level below, i.e. from Mesh SS1 to SSs 1 to 3 and from Mesh SS2 to SSs 4 to 5, is then implicit in the functions $U^1(\boldsymbol{r}^1)$ and $U^2(\boldsymbol{r}^1)$, respectively. In the first case, the explicit formulation is

$$U^1(\boldsymbol{r}^1) = \begin{array}{ll} \max\limits_{\boldsymbol{r}_1, \boldsymbol{r}_2, \boldsymbol{r}_3} & U_1(\boldsymbol{r}_1) + U_2(\boldsymbol{r}_2) + U_3(\boldsymbol{r}_3) \\ s.t. & \boldsymbol{r}_i \in \mathcal{R}_i, \qquad i = 1, 2, 3 \\ & \sum_{i=1}^{3} \mathbf{1}^T \boldsymbol{r}_i \leq c^1 \end{array} , \tag{5.3}$$

where c^1 is the rate capacity of the link between the Mesh SS1 and the Mesh BS. Similarly, we can write the optimization problem that models $U^2(\boldsymbol{r}^2)$. Note that $U^i(\boldsymbol{r}^i)$ are concave functions

on the variables $\boldsymbol{r}^i$ (given the functions $U_i(\boldsymbol{r}_i)$ are concave) since they are the result of a convex optimization problem (expressed in maximization form), as discussed in Chapter 3.

Finally, the allocation of resources to CIDs attached to i^{th} SS is done by solving the following allocation problems that result from the explicit expressions of $U_i(\boldsymbol{r}_i)$,

$$U_i(\boldsymbol{r}_i) = \begin{array}{ll} \max\limits_{\{r_{i,j}\}} & \sum_j U_{i,j}(r_{i,j}) \\ s.t. & r_{i,j} \in \mathcal{R}_{i,j}, \qquad \forall j \\ & \sum_j r_{i,j} \leq c_i \end{array} , \tag{5.4}$$

where c_i is the rate capacity of the link between the i^{th} SS and the Mesh SS where it is attached to and $r_{i,j}$ is the granted rate to j^{th} CID at the i^{th} SS. The functions $U_{i,j}$ are no longer expressed as convex optimization problems in the last allocation level. Instead, they are represented through analytical expressions, such as the weighted logarithm of the granted rates in a proportionally fair design. The subsets $\mathcal{R}_{i,j}$ define now the requested rate of the CID or $d_{i,j}$ (in its maximum value) and the guaranteed rate or $m_{i,j}$ (in the minimum value). Note that the subsets $\mathcal{R}^i$ and $\mathcal{R}_i$ in the previous allocation phases are formed by union of the one dimensional subsets $\mathcal{R}_{i,j}$ in the multi-dimensional space, as well as vectors $\boldsymbol{r}^i$ and $\boldsymbol{r}_i$ are formed by stacking together the elements $r_{i,j}$.

From the scheduling problems (5.2) to (5.4), the reader may appreciate that the global allocation is divided into several smaller resource distribution problems of PMP type. Regarding signalling issues, as it will be discussed in the next section, each entity or node in the network negotiates a total amount of resources (i.e. the sum of the rates allocated at the node) with the nodes above and it is the node that distributes the granted amount among the nodes or connections below, whatever the situation is. Remember that the standard enforces, at the lowest allocation level, that the SSs distribute their granted resources among the connections attached to them, so the architecture we propose is in accordance with the IEEE 802.16 definitions. Both issues, signalling and PMP-wise scheduling, are graphically depicted in Figure 5.2. It is an example of a two-level tree-deployed network and does not coincide with the example depicted in Figure 5.1.

The next section is devoted to the application of known decomposition techniques (primal and dual) to the previous scheduling formulation in order to compute the joint resource allocation in a multi-level decompositions approach. It is also possible to perform such multi-level decomposition using the proposed coupled-decomposition method described in Chapter 3 with the subsequent benefits in terms of convergence speed, as it is discussed in the following. All the strategies are distributively computed in the way described in Figure 5.2.

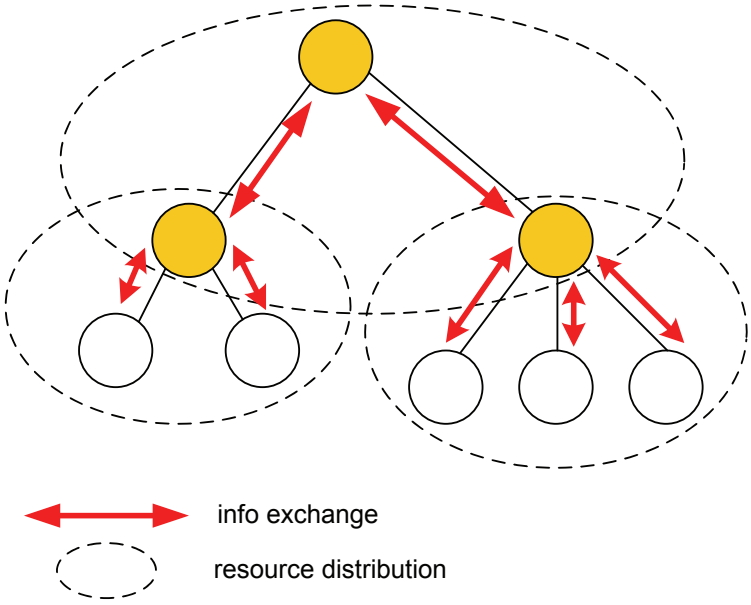

Figure 5.2: Proposed distributed bandwidth allocation.

5.3 Distributed Scheduling Using Convex Decompositions

Consider again (5.1) as the basic scheduling piece in our architecture, which formulates a PMP resource allocation, and let us solve it in terms of a primal, dual or a coupled-decomposition approach. Moreover, in this section we include a detailed description of the quantities that need to be signalled between network nodes to cope with a tree-deployed network topology using the three approaches.

5.3.1 Primal Decomposition

Problem (5.1) is adequate to perform a dual decomposition since it has a coupling constraint. In order to attain a primal decomposition, we include the coupling variables $\{y_i\}$ and write (5.1) equivalently as

$$\begin{array}{ll} \max\limits_{\{\boldsymbol{r}_i, y_i\}} & \sum_{i=1}^{N} U_i(\boldsymbol{r}_i) \\ s.t. & \boldsymbol{r}_i \in \mathcal{R}_i, \quad i = 1, \ldots, N \\ & h_i(\boldsymbol{r}_i) \leq y_i, \quad i = 1, \ldots, N \\ & \sum_{i=1}^{N} y_i \leq c \end{array} . \tag{5.5}$$

Following the results in Chapter 3, it is possible to define the primal master problem and

the primal subproblems. The subproblems are defined for fixed values of $\{y_i\}$ as

$$U_i^P(y_i) = \begin{array}{c} \max \\ \{\boldsymbol{r}_i\} \\ \boldsymbol{r}_i \in \mathcal{R}_i \\ h_i(\boldsymbol{r}_i) \leq y_i \end{array} \quad U_i(\boldsymbol{r}_i) \tag{5.6}$$

and it is known that for fixed i, $U_i^P(y_i)$ is a concave function of y_i. Note that the maximization of a concave function is equivalent to the minimization of a convex one and thus the previous statement is easily verified from the results in Lemma 2 at Chapter 3. Using $U_i^P(y_i)$ we define the primal master problem as

$$\begin{array}{ll} \max\limits_{\{y_i\}} & \sum_{i=1}^N U_i^P(y_i) \\ s.t. & \sum_{i=1}^N y_i \leq c \end{array} . \tag{5.7}$$

The master problem is solved using the subgradient method (see details in Section 3.2.1). A subgradient (conceptually equivalent to the gradient) of $U_i^P(y_i)$ at the point y_i, $s_i(y_i)$ is readily found from the solution of (5.6) as

$$s_i = \lambda_i^*(y_i) \tag{5.8}$$

where λ_i^* is the optimal value of the Lagrange multiplier associated to the constraint $h_i(\boldsymbol{r}_i) \leq y_i$ for a given value y_i. The completion of the method is attained with the following update of the coupling variables

$$y_i^{t+1} = \left[y_i^t + \alpha(t) \cdot s_i(y_i^t) \right]^P , \tag{5.9}$$

where t indexes iterations, $\alpha(t)$ is the user-defined step-size of the method and $[\cdot]^P$ denotes the projection onto the half-space $\sum_{i=1}^N y_i \leq c$, that can be analytically computed [Boy03, Sec. 8.1].

In Figure 5.3 we detail the allocation process of the network depicted in Figure 5.2 using primal decomposition. Note that we assume just two scheduling levels for simplicity but the procedure can be extended to an arbitrary number of layers. We have indexed in the figure the variables related to the allocation at the highest level with a superscript and the variables related to the lowest level distribution with a subscript. The highest node (the BS in the WiMAX context) is labelled as MP as it computes only a master problem. Similarly, the lowest nodes (the CIDs in WiMAX) are labelled as SP since they only perform the function of the subproblems. On the contrary, the intermediate nodes compute both master problems (for the nodes below) and subproblems (for the node above). Red arrows signal the allocated resources to the nodes below whereas blue arrows signal the subgradients to nodes above.

The global solution is distributively attained in the following way: Start from a feasible distribution of resources y^1 and y^2 such that $y^1 + y^2 = c$, where c is the rate capacity from the BS to the core network. The next step requires computation of the subgradients s^1 and s^2 and thus, solving the corresponding subproblems. Each of the subproblems can be solved using a primal decomposition and we can apply the subgradient method again. For example, we perform

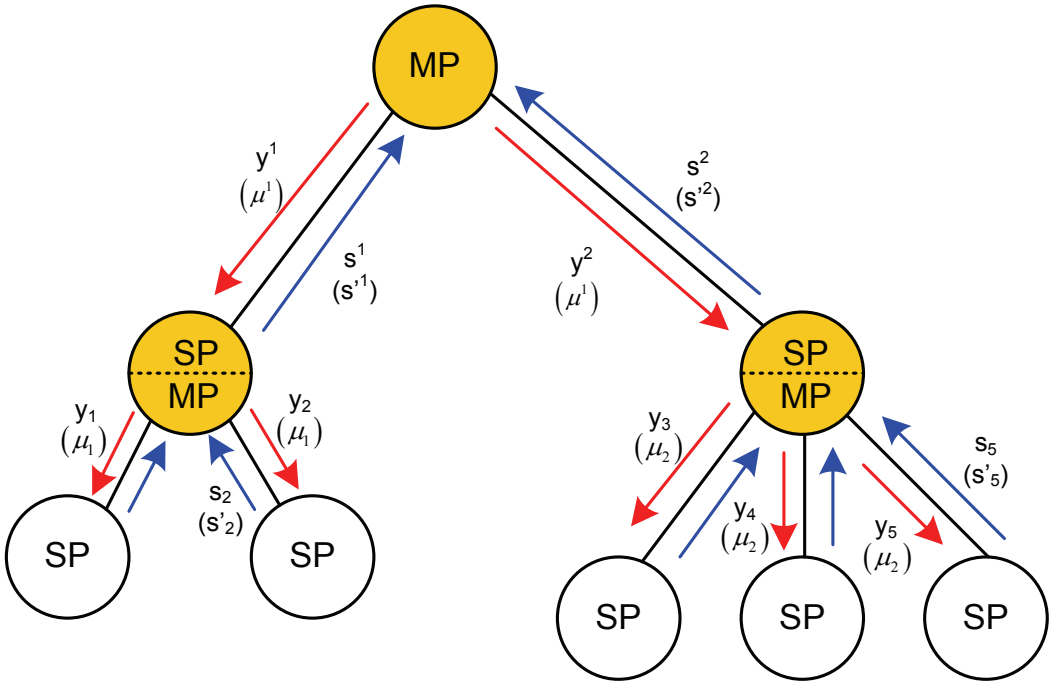

Figure 5.3: System view of a 2-level primal (dual) decomposition.

the inner iterations and exchange the variables y_3, y_4 and y_5 and the corresponding subgradients s_3, s_4 and s_5 to be able to compute s^2. Note that the subgradients are related in this inner case to the constraints $r_i \leq y_i$ and that the master problem enforces $y_3+y_4+y_5 \leq y^2$ (imposed by the first decomposition) and also $y_3 + y_4 + y_5 \leq c^2$ (imposed by the second decomposition), where c^2 is the rate capacity between the BS and the SS (a system parameter). Once the solution is available, s^2 is computed (related to $y_3 + y_4 + y_5 \leq y^2$) and it is used to update the higher-layer allocation together with s^1. The procedure is repeated until it converges. Note that at each outer iteration, a solution to the subproblems is needed and thus the scheduling procedures work with different updating rates.

5.3.2 Dual Decomposition

A dual decomposition of (5.1) is attained when we construct a partial Lagrangian relaxing only the coupling constraint, which allows to rewrite the original problem as

$$\begin{array}{lll} \min\limits_{\mu} \max\limits_{\{\boldsymbol{r}_i\}} & \sum_{i=1}^{N} U_i(\boldsymbol{r}_i) - \mu(\sum_{i=1}^{N} h_i(\boldsymbol{r}_i) - c) & \\ s.t. & \boldsymbol{r}_i \in \mathcal{R}_i, & i = 1, \ldots, N \\ & \mu \geq 0 & \end{array} , \tag{5.10}$$

where μ is the Lagrange multiplier associated to the coupling constraint.

Let us rewrite the previous result as

$$\begin{array}{cc} \min\limits_{\mu} & \sum_{i=1}^{N} U_i^D(\mu) + \mu\, c \\ s.t. & \mu \geq 0 \end{array}, \tag{5.11}$$

where

$$U_i^D(\mu) = \left\{ \begin{array}{cc} \max\limits_{\boldsymbol{r}_i} & U_i(\boldsymbol{r}_i) - \mu\, h_i(\boldsymbol{r}_i) \\ s.t. & \boldsymbol{r}_i \in \mathcal{R}_i \end{array} \right. . \tag{5.12}$$

Now $U_i^D(\mu)$ are the dual subproblems and (5.11) is the dual master problem. Note that the coupling is driven in dual decomposition by the variable μ. In other words, for the optimal value μ^* the dual subproblems could compute the optimal allocation in a fully decoupled manner.

As discussed in Chapter 3, the subgradient method is also used to solve the dual master problem and a subgradient of U_i^D at μ, $s_i'(\mu)$, is readily found as

$$s_i' = -h_i(\boldsymbol{r}_i^*(\mu)), \tag{5.13}$$

where $\boldsymbol{r}_i^*(\mu)$ is the optimal value of the primal variables in the dual subproblem when a value of μ is given. The following iterations are then applied to find the optimal value of the dual variable,

$$\mu^{t+1} = \left[\mu^t + \alpha(t) \cdot \left(c - \sum_{i=1}^{N} h_i\left(\boldsymbol{r}_i^*(\mu^t)\right) \right) \right]^+ \tag{5.14}$$

where t indexes iterations, $\alpha(t)$ is the user-defined step-size of the method and $[\cdot]^+$ is the projection to the non-negative orthant in order to grant the accomplishment of the constraint $\mu \geq 0$ in the master dual problem. See further details on dual decomposition in Section 3.2.2.

The architecture of dual decomposition in terms of signalling is pretty similar to the one described for primal decomposition. Again, let us review the scheduling process in the network example of Figure 5.2, this time using a two-level dual decomposition. However, note that the results here are general as they can be extended to an arbitrary number of layers or scheduling stages. The specific signalling required is described by Figure 5.3 substituting s^i and s_i by s'^i and s_i', respectively, and $\{y^1, y^2\}$, $\{y_1, y_2\}$ and $\{y_3, y_4, y_5\}$ by μ^1, μ_1 and μ_2, respectively. In other words, the BS (at top) first sends to the SSs (intermediate nodes) the values of the dual variable μ^1, which is the same for both SSs. With that μ^1 value the dual subproblems in (5.12) are defined. The computation of the dual subproblems can be done by performing a second dual decomposition since

$$U_i^D(\boldsymbol{r}_i) = \left\{ \begin{array}{cc} \max\limits_{\boldsymbol{r}_i} & U_i(\boldsymbol{r}_i) - \mu\, h_i(\boldsymbol{r}_i) \\ s.t. & \boldsymbol{r}_i \in \mathcal{R}_i \end{array} \right. = \left\{ \begin{array}{cc} \max\limits_{\boldsymbol{r}_i} & \sum_j U_{i,j}(r_{i,j}) - \mu \sum_j h_{i,j}(r_{i,j}) \\ s.t. & r_{i,j} \in \mathcal{R}_{i,j} \\ & \sum_j h_{i,j}(r_{i,j}) \leq c^i \end{array} \right. \tag{5.15}$$

where j indexes the nodes at the lowest level (i.e. CIDs) and c^i is the rate capacity seen at the i^{th} SS to the BS (a system parameter). Note in (5.15) the substitution of $U_i(\boldsymbol{r}_i)$ by its optimization

problem form including the scheduling at the lower level and also the substitution of $h_i(\boldsymbol{r}_i)$ in terms of the variables managed at the lowest layer. Given this second dual decomposition, a subgradient method approach requires the exchange of the dual variables μ_1 and μ_2 along with the corresponding subgradients s_i'. Once the solution of U_i^D is attained at μ^1, the subgradients s'^1 and s'^2 are readily found and μ^1 is updated. As it happens with primal decomposition, different update rates are given at each layer since an update in an upper layer requires convergence of the solution at the stages below.

5.3.3 Coupled-Decomposition

Let us consider the problem formulation in (5.5), which is adequate both for a primal decomposition and also for a dual decomposition [Pal07] when the constraint $\sum_{i=1}^{N} y_i \leq c$ is relaxed in the Lagrangian. The coupled-decomposition method intertwines both approaches in a single method and boosts the convergence speed of the algorithm significantly. In the sequel, we review the strategy applied to the specific case of WiMAX scheduling. The details of the method can be found in Section 3.3.

Given a value for the dual variable associated to the coupling constraint μ, the dual subproblems compute the amount of resources y_i dedicated to the i^{th} subnetwork (with rates in $\boldsymbol{r}_i$) as

$$y_i(\mu) = \arg_{y_i} \quad \max_{\substack{\boldsymbol{r}_i, y_i \\ \boldsymbol{r}_i \in \mathcal{R}_i \\ h_i(\boldsymbol{r}_i) \leq y_i}} \quad U_i(\boldsymbol{r}_i) - \mu \cdot y_i \tag{5.16}$$

If we explicitly formulate the scheduling within the subnetworks (indexed by j) that integrate the i^{th} subnetwork, the problem is

$$\begin{array}{ll} \max\limits_{\{\boldsymbol{r}_{i,j}, y_{i,j}\}} & \sum_j U_{i,j}(\boldsymbol{r}_{i,j}) - \mu \sum_j y_{i,j} \\ s.t. & \boldsymbol{r}_{i,j} \in \mathcal{R}_{i,j} \\ & h_{i,j}(\boldsymbol{r}_{i,j}) \leq y_{i,j} \\ & \sum_j y_{i,j} \leq c^i \end{array} \tag{5.17}$$

where $y_i = \sum_j y_{i,j}$ and c^i is the maximum rate capacity (a system parameter) from the i^{th} PMP subnetwork to the node above it. The problem decomposes again and may be solved using a coupled-decomposition strategy. In practice, we have found that (5.17) may be approximately solved if we obviate the constraint $\sum_j y_{i,j} \leq c^i$ without affecting the global convergence of the method (the constraint is taken into account in the following steps). In that case, the dual value μ propagates to all the PMP subnetworks below. It is then used in the lowest level to compute the allocation at a CID basis and group allocations are propagated backwards and added to finally obtain y_i. See the idea of the first step of the method in Figure 5.4.

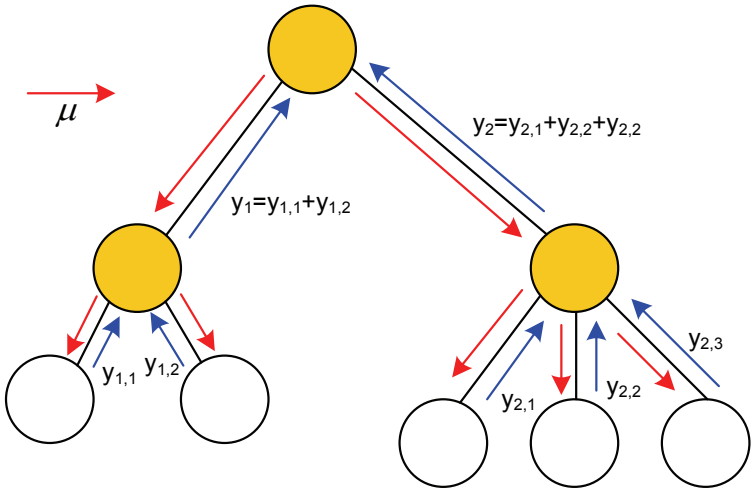

Figure 5.4: Approximate resolution of dual subproblems in the coupled-decomposition method.

Once the values $\{y_i\}$ are available, primal projection prevents them from exceeding the rate capacity limits of the network. It finds the new allocation values $\{\hat{y}_i\}$ by means of solving the following quadratic minimization problem,

$$\begin{array}{ll} \min\limits_{\{\hat{y}_i\}} & \sum_i (\hat{y}_i - y_i)^2 \\ s.t. & m_i \leq \hat{y}_i \leq \min(d_i, c^i) \\ & \sum_i \hat{y}_i = c \end{array} \tag{5.18}$$

where m_i and d_i are the sum of the minimum guaranteed resources and the aggregated demand in the i^{th} subnetwork. Note that we consider in primal projection the constraint $\sum_j y_{i,j} \leq c^i$ (equivalently $\hat{y}_i \leq c^i$), obviated in the dual subproblems.

In the next step, subnetworks obtain their μ candidates λ_i after the computation of the following primal subproblems,

$$\begin{array}{ll} \max\limits_{\boldsymbol{r}_i} & U_i(\boldsymbol{r}_i) \\ s.t. & \boldsymbol{r}_i \in \mathcal{R}_i \\ & h_i(\boldsymbol{r}_i) \leq \hat{y}_i \end{array} \tag{5.19}$$

where λ_i is implicitly achieved as it is the dual variable associated to the constraint $h_i(\boldsymbol{r}_i) \leq \hat{y}_i$. Due to the decoupled structure of $U_i(\boldsymbol{r}_i)$ and $h_i(\boldsymbol{r}_i)$, primal subproblems resemble to the original problem in 5.1. Therefore, they can be iteratively solved using the coupled-decomposition method that works this time with a reduced problem.

Finally, dual projection decides the μ update from the candidates λ_i. As discussed in Section 3.3, not all the λ_i values are valid for this computation and we select only the ones that are found with an input $\hat{y}_i$ to the primal subproblem that verifies $m_i \leq \hat{y}_i \leq \min(c^i, d_i)$. Let us group all these valid dual candidates (from the valid subproblem subset) in the vector $\boldsymbol{\lambda}'$. Then,

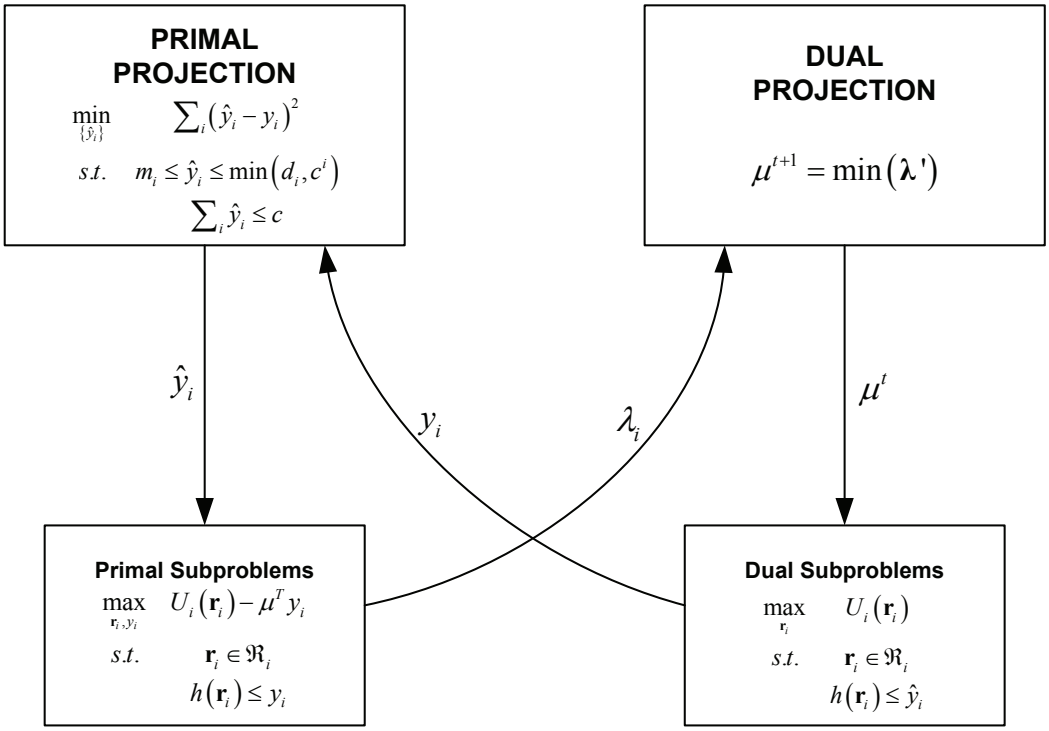

Figure 5.5: Flow diagram of the coupled-decomposition method.

dual projection computes the μ update as

$$\mu = \min_{\lambda_i} \boldsymbol{\lambda}'. \tag{5.20}$$

See in Figure 5.5 a flow diagram of the method that shows the connections among primal and dual projections and subproblems, where the variable t indexes iterations.

As we have done with primal and dual decompositions, we review now the signalling required to attain the solution in the network example of Figure 5.2 in a distributed manner using the coupled-decomposition algorithm. After that, we briefly discuss the situation with mare than two levels in the network. The following steps, depicted and specified in Figure 5.6, obtain the optimal scheduling in the network:

1. The dual variable μ^t is spread through the network.

2. The end-nodes transmit the allocation computed with μ^t to the nodes above. Intermediate nodes obtain their allocation as the sum of the ones below.

3. The highest node corrects the previous allocations to attain the rate capacity towards the core network, i.e. c, and taking also into account the rate capacities to the nodes below, i.e. c^i.

4. The corrected allocations are used by the intermediate nodes to perform new iterations of the coupled-decomposition method and obtain the dual variable candidates λ_i.

5. Finally, the highest node in the network updates the value of the dual variable to μ^{t+1} using dual projection.

In case of considering three scheduling levels, the algorithm would first spread the μ value (step 1) from the top of the network to the end-nodes. After that, steps 2 and 3 (obtention of the primal variables and the primal projection) would be applied to the lowest two levels (as in the previous example) and once again to the highest two levels. At the top level, each SS would start new iterations of the coupled-decomposition method (step 4) to obtain all the μ candidates. Note in this case that one iteration requires the computation of new inner iterations (of the complete method, exactly as in the previous example) at the two levels below (in order to optimize those subnetworks underneath). When the μ candidates are available, dual projection is solved (step 5) and another highest level iteration can be done. This is repeated until the solution converges to the optimal one. Therefore, one iteration at the lowest level takes more time than one iteration at the highest one because, at the highest level, it is necessary to wait for the updates at the levels in between.

To end this section, let us briefly interpret the operation of our joint and distributed scheduling proposal. The key idea is to reach a consensus on the price μ to be paid to use the network resources. Within our PMP or tree-deployed topology, it is natural to negotiate prices and allocated resources at the end-nodes depending on the QoS requirements of the connections and therefore, the global price is propagated to the whole network. In this way, all the connections are equally treated by the highest network node. However, it may happen that a certain μ is not valid for a given subnetwork, either because it implies exceeding the capacity of the subnetwork or because it does not attain the minimum grants. In such occasions, the subnetwork computes its own price (λ_i in the previous example) to satisfy the constraints. Note, from the point of view of the KKT optimality conditions of the problem, that such constraints attained with equality make feasible a non-zero value of the associated Lagrange multipliers λ_i, which are common to all the connections in the subnetwork below and play the role of μ inside it. Therefore, each subnetwork defines its own price when it is necessary (it may differ from μ) and KKT conditions can be attained to obtain the optimal bandwidth allocation or scheduling.

5.4 PMP Scheduling Example

In this section, we test the decomposition techniques (dual decomposition and coupled-decomposition) in a small PMP network example and we compare both results to a non-distributed computation performed with the MVC decomposition method, reviewed in Section

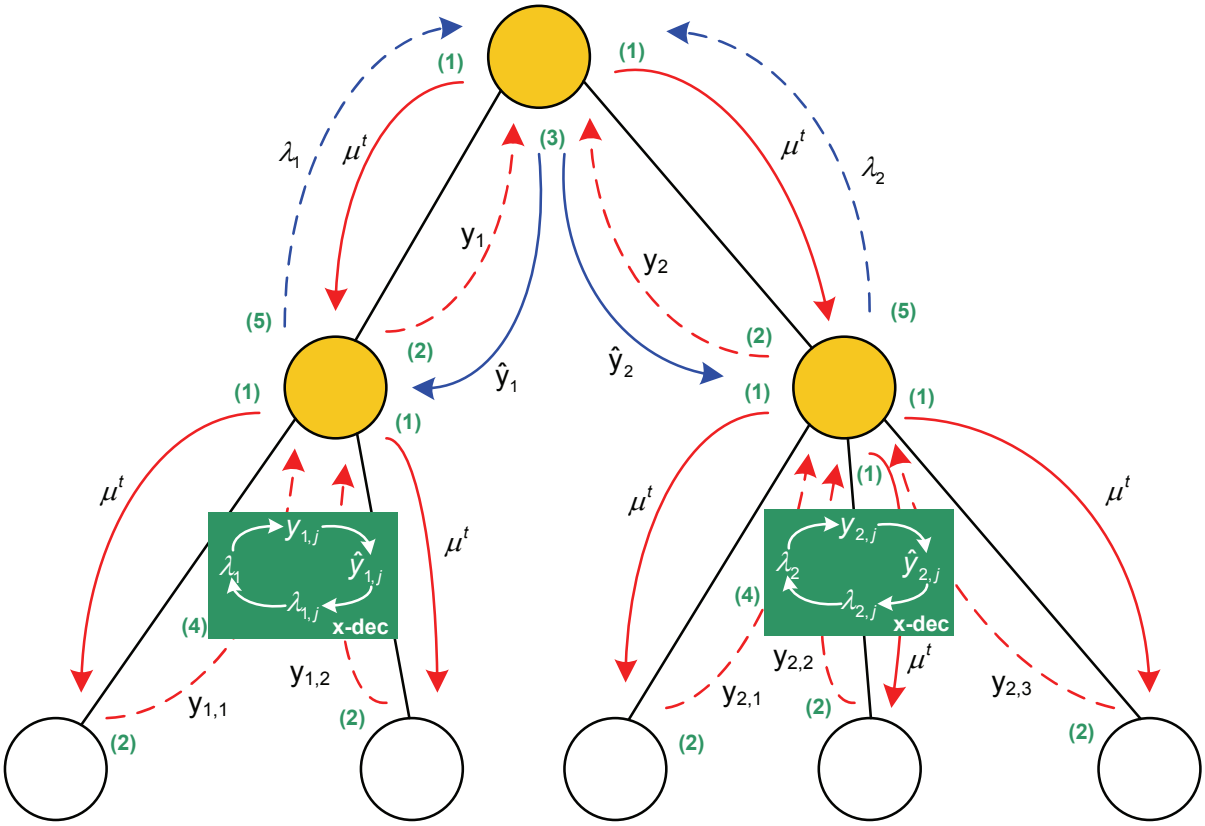

Figure 5.6: Signalling in coupled-decomposition.

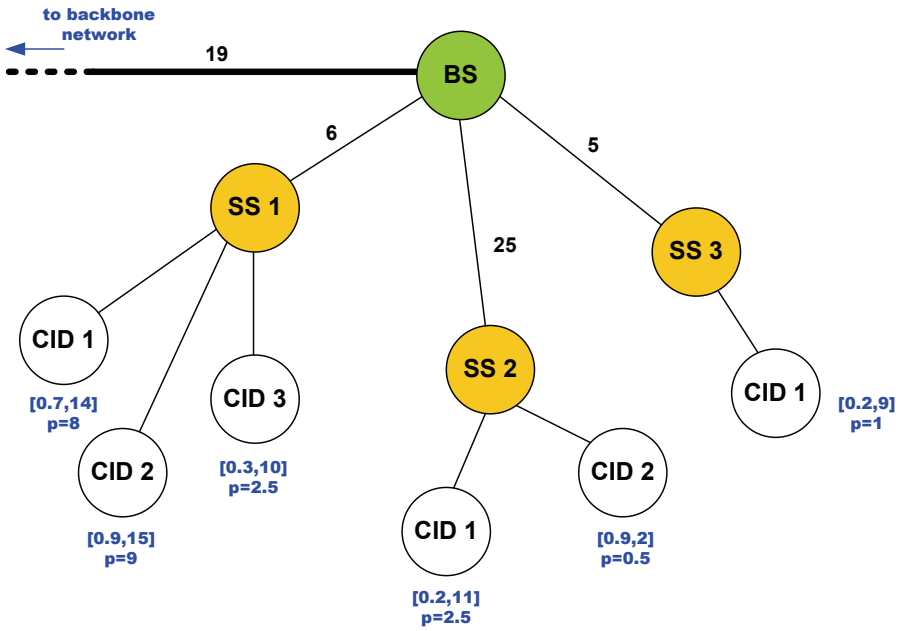

Figure 5.7: Network example under test.

3.2.3. Let us consider the network topology depicted in Figure 5.7, where three SSs manage six CIDs. Each CID is assumed to be mapped to a service with independent QoS requirements. The links are labelled with their rate capacity, given by the PHY layer configuration of each of them. Two scheduling levels can be identified in the figure, namely: i) from the SSs to the BS at the high level and ii) from the CIDs to the corresponding SS at low level. The former is mathematically defined as in (5.1) with

$$U_i(\boldsymbol{r}_i) = \left\{ \begin{array}{ll} \max\limits_{\boldsymbol{r}_i} & \sum_j U_{i,j}(r_{i,j}) \\ s.t. & \sum_j r_{i,j} \leq c^i \end{array} \right\}, \quad h_i(\boldsymbol{r}_i) = \sum_j r_{i,j}, \tag{5.21}$$

where $r_{i,j}$ is the transmission rate of CIDj at SSi and c^i is the rate capacity from SSi to the BS. At the lowest level, problem (5.1) is solved for the i^{th} SS using

$$U_{i,j} = p_{i,j} \log r_{i,j}, \qquad h_{i,j}(r_{i,j}) = r_{i,j}. \tag{5.22}$$

In both cases, the subsets $\mathcal{R}_i$ and $\mathcal{R}_{i,j}$ contain the maximum and minimum rate values of the CIDs within them. However, note that at the highest level and from a practical point of view, we need to know only the sum of maxima and minima since these two values are enough to iterate the variables $\{y_i\}$, $\{\hat{y}_i\}$, $\{\lambda_i\}$ and μ of the proposed algorithm. The specific quantities per CID, i.e. $\mathcal{R}_{i,j}$, are only required at the lowest level to obtain the scheduling of CIDs.

Recall that the election of logarithmic functions of the rates responds to a proportional fair criterion as it is discussed in [Kel98], but other utility functions can be used. We further use the priority values $p_{i,j}$, as in the DVB-RCS case in Chapter 4, to balance the scheduling towards some services depending on the specific QoS policy and thus the solution is asymmetric proportionally fair. These values are depicted in blue in Figure 5.7 at each CID. The max and min values in $\mathcal{R}_{i,j}$ (in brackets in the figure) define the requested and minimum granted rates of each service, respectively. In WiMAX, the UGS can be requested with a minimum granted rate regardless the value of $p_{i,j}$ whereas the ertPS can be requested with the minimum grant plus the request of extra resources modulated by an adequate priority value. The other service types can be configured with adequate priority values as well. Note that the original requests in terms of bytes of information can be transformed to rates taking into account the time basis of the requests.

We assess now the convergence speed terms of the following solutions, namely:

- A two-level dual decomposition approach.
- A MVC decomposition approach.
- A coupled-decomposition strategy.

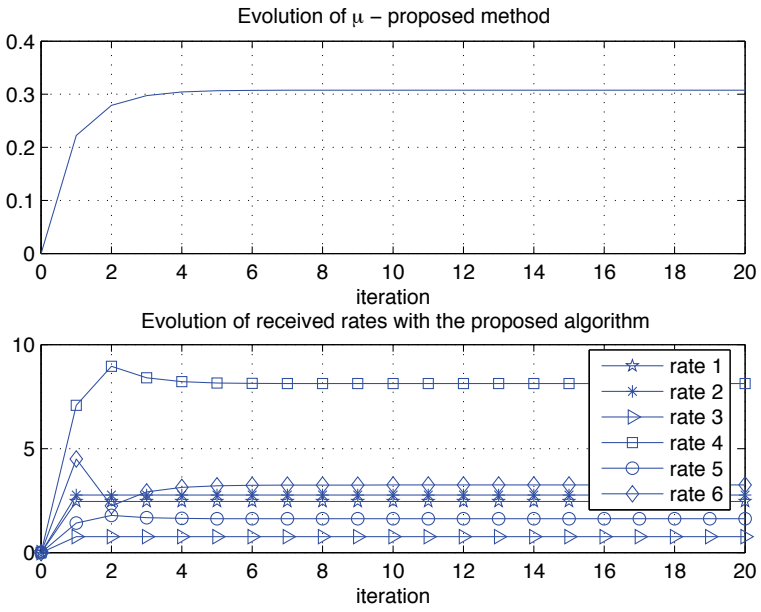

Figure 5.8: Evolution of rates and dual variable μ with the coupled-decomposition method.

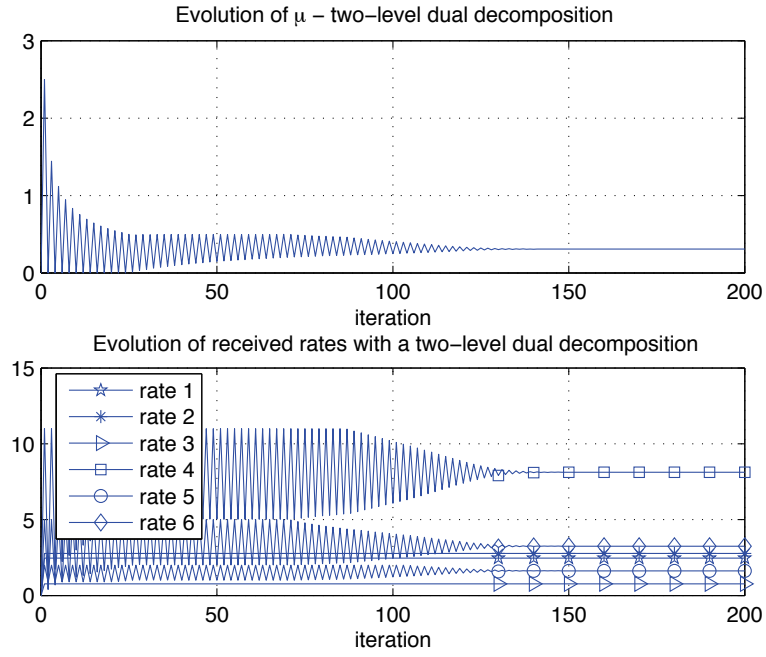

Figure 5.9: Evolution of rates and dual variable μ using a two-level dual decomposition approach.

The results of the proposed method are depicted in Figure 5.8. The first subplot contains the evolution of the dual variable at the highest allocation level and the second subplot shows the evolution of the allocated rates at the CIDs (rates are ordered from left to right according to the CIDs in Figure 5.7). The same results with a two-level dual decomposition approach are plotted in Figure 5.9. Dual or primal decompositions require a user-defined adaptation step and in this case we choose a diminishing step size of the form $\alpha(t) = \frac{\alpha_0}{\sqrt{t}}$ with $\alpha_0 = 0.5$. Note that the coupled-decomposition method does not have this undesired feature. In both cases, at each iteration of the highest level, it is required to attain the solution at each CID at the lowest scheduling level, so that convergence properties should be more important as more scheduling levels are considered. In other words, assuming that I iterations are required at each level before converging to a solution and that the network has l levels, then the BS finds the optimal allocation with an equivalent number of iterations[1] equal to I^l. In the light of the results, it is clear that the coupled-decomposition solution provides more than one order of magnitude of advantage in terms of iterations of the algorithm.

For the sake of completeness, we compare the previous results with the MVC decomposition method, which is described in [Hol06] and reviewed in Section 3.2.3. It is not distributed but uses also the idea of combining primal and dual decompositions of the problem in a single approach. Results are plotted in Figure 5.10 and again the coupled-decomposition method converges to the optimal solution much faster. Therefore, it is a good candidate to cope with the uplink scheduling in WiMAX, either in PMP networks or in tree-deployed backhaul applications.

5.5 Summary

In this chapter we have applied the coupled-decomposition method to the design of the scheduling in the uplink of WiMAX networks. The network topology considered is the basic Point to Multipoint in WiMAX and can be extended to a tree-deployed network that has its application, for example, in backhaul system deployments. The problem is formulated as a NUM problem and thanks to the proposed decomposition techniques, the optimal solution is computed in a distributed manner, as enforced by the WiMAX standard: each SS schedules its own CIDs with the granted resources. In general, the whole network optimization is broken into several PMP scheduling levels in a top-bottom design, where each terminal interchanges resource allocation and prices with the node above. The goal is to reach a consensus on the global price, which may differ from one subnetwork to another depending on the constraints of the problem. Those constraints include the rate limitations imposed by the specific physical layer configuration, the accomplishment of all requests in the subnetworks and the non-attainment (given the global price, not the price in the subnetwork) of the minimum guaranteed resources.

[1] We define the equivalent number of iterations as the number of them that would be required in a single level network.

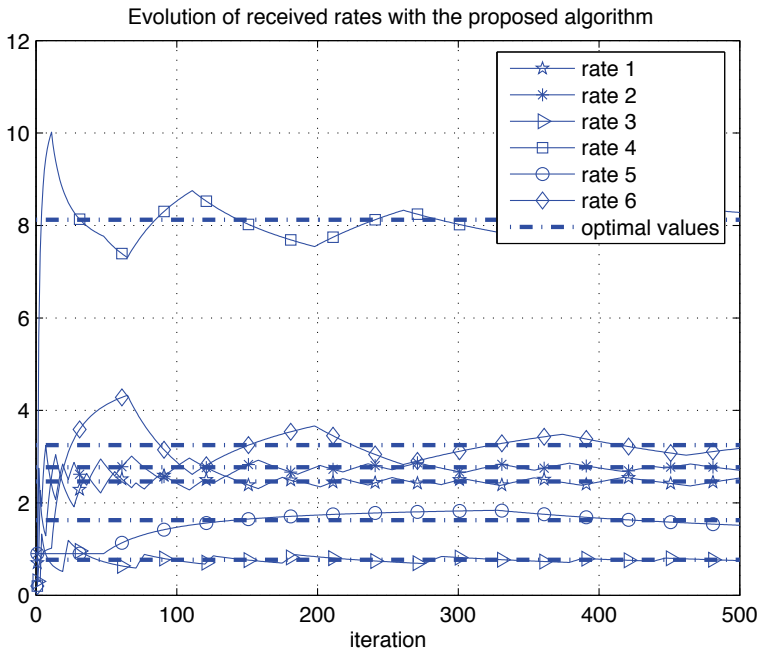

Figure 5.10: Evolution of rates using a MVC decomposition approach.

We have shown that the NUM framework is suitable for WiMAX scenarios since an adequate selection of utility functions allows us to attain fair solutions or to sustain QoS definitions (from the higher layers). Finally, simulation results show that the coupled-decomposition algorithm converges much faster than other approaches in the literature, which is specially relevant as the number of scheduling levels grows.

Chapter 6

Conclusions and Future Work

This Ph.D. dissertation has explored Dynamic Bandwidth Allocation (DBA) solutions applied to the multiple access techniques of multimedia and QoS-enabled systems. Mathematically speaking, all the work has been based in the Network Utility Maximization (NUM) framework and in the convex decomposition techniques that make a distributed solution be possible. Since the DBA philosophy may involve procedures and protocols in several layers of the OSI protocol stack, it is mandatory to define adequate cross-layer interactions in order to optimize a common system performance metric. Once again, decomposition techniques provide the mathematical framework needed to define such interactions (message passing) and to attain the optimal solution. Multiple access strategies formulated as NUM problems have been set up throughout this work with a common fairness perspective and balancing resources as a function of the desired QoS. In the following, we draw the conclusions of this thesis and some open issues to be addressed as future work.

6.1 Conclusions

In Chapter 2 we have introduced some of the key topics that have been used throughout this dissertation. Specifically, we have revisited the concepts of Network Utility Maximization and the various mathematical representations of fairness. Furthermore, cross-layer philosophy as well as the importance of decomposition architectures in relation with NUM for the development of future network protocols have been reviewed. Finally, we have made a survey of state-of-the-art DBA solutions in the DVB-RCS and WiMAX standards.

Chapter 3 has first revisited some basics in convex optimization theory. Thereafter, we have reviewed the most popular decomposition techniques in the network community, namely: primal and dual decompositions. In the NUM context, dual decomposition is usually the preferred strategy because it involves less signalling. Notwithstanding, primal and dual decompositions

are not the only possibilities that one can consider when trying to decompose an optimization problem. Recently, some works have proposed the use of the Mean Value Cross decomposition method and thus, we have also reviewed this alternative solution. The idea is to combine both primal and dual representations of a convex optimization problem in a single algorithm. In MVC decomposition, the problem is conceptually split into a primal and a dual subproblem whereas in primal/dual decomposition, there may be an arbitrary number of subproblems and a master problem that coordinates them. After that, we have developed a novel decomposition technique, which we call coupled-decomposition method and which is the major theoretical contribution of this dissertation. This new method combines ideas from both primal/dual decompositions and the MVC decomposition method. It proposes a novel manner to intertwine primal and dual subproblems using novel blocks in the decomposition, which are the primal projection and the dual projection. In some sense, the MVC decomposition method is improved and generalized to support an arbitrary number of subproblems. As a result, we achieve big advantage in terms of computational time and thus, algorithm efficiency. Our solution reaches the optimal solution with a reduced number of iterations and furthermore, it is not necessary to tune any user-defined parameter, as it happens with the primal/dual decompositions.

In Chapter 4 we have applied the results in Chapter 3 in order to solve the problem of DBA in the Demand Assignment Multiple Access mechanism of the DVB-RCS standard. Although given that the satellite sub-network is point to multipoint and that the optimization process is conducted at a central node in the network, we show that using the coupled-decomposition method we decrease the time of computation of the number of time-slots per terminal by a factor of two with respect to the classical approach. Since the amount of time available to obtain each allocation is limited, the efficiency of the algorithm limits the number of users in the system. Therefore, our technique doubles the number of potential users. Furthermore, we have shown that thanks to our choice of utility functions in the NUM framework, we attain a fair resource distribution that can also prioritize the final allocation towards the most stringent traffic flows (in terms of QoS requirements). The required information, available at the upper layers of the system, needs to be communicated to the MAC layer, that runs the allocation algorithm, and thus, our approach is cross-layer. That interaction is possible in a transparent satellite DVB-RCS network by means of reutilizing signalling fields that are planned for non-transparent networks. Finally, we have also contributed with a proposal to structure the resources in the Multi-Frequency-TDMA frame of the system. Since the requests of users can be potentially multiplexed within the frame having a combinatorial number of options (as specified in the standard) and this is not practical from an implementation perspective (it is a problem that is non-solvable in polynomial time), we optimize the frame structure as a function of the coding rate that users employ in the transmission. Note that DVB-RCS employs adaptive coding to adapt to the variations on the quality of the channel. Taking into account the transmission rate of each terminal, which is cross-layer information that flows from PHY to MAC layers, we

achieve a frame utilization that is close to the optimal one.

Finally, in chapter 5 we consider the DBA design of the DAMA mechanism that has been envisaged for the uplink of WiMAX. The standard defines a basic point to multipoint network topology and also a mesh mode. In mesh mode, each Subscriber Station can connect directly to the Base Station or through other terminals, the Mesh Base Stations. In this chapter, we concentrate on DBA at the MAC layer, thus providing the mechanism to achieve an efficient balance of traffic flows. We consider a tree-deployed network that can be used, for example, when WiMAX implements the backhaul transport network. Note that a particular case of that topology is the point to multipoint, as in the DVB-RCS case. The goal is to fairly allocate bandwidth among all the traffic flows accessing the network. For that purpose, we use the NUM framework developed in Chapter 4 and extend it to the new topology. Furthermore, we want to achieve a good balance between signalling and computation time while we maintain the philosophy defined in the standard document for centralized scheduling. Essentially, terminals must request resources in an aggregate basis (including the requests of all the nodes below) and allocate sum-grants accordingly. Under those circumstances, we show that the coupled-decomposition strategy suits perfectly the requirements and that it attains the optimal solution with a significant reduction of iterations with respect to other strategies, which also implies reducing the amount of signalling in the network. In summary, global optimal flow control is efficiently achieved without spreading requests and grants throughout the whole access network, as described in the standard document. Instead, signalling is confined within each of the point to multipoint sub-pieces in the tree.

This Ph.D. thesis has explored the universe of decomposition possibilities in convex programming and it has contributed with a novel decomposition architecture. Furthermore, two examples have demonstrated the benefits of the new approach in two practical cases. Before ending the conclusions of the work, let us emphasize the importance of decomposition techniques as a guide on how to or how not to divide (vertically within a network element and horizontally among several elements) future networks and protocols in layers. Fortunately, there is still much work to be done and we identify some of those open issues in the next section.

6.2 Future Work

In the following we detail some of the questions that should be addressed in future extensions of this dissertation. In Chapter 3 some of the possibilities are:

- To formally prove the convergence of the coupled-decomposition method for the case of an arbitrary number of constraints and, if possible, to refine the method accordingly. Special attention must be given to the definition and computation of the dual projection.

- To exploit the special structure of the constraint matrix (that has either one or zero values) in order to compute primal and dual projections more efficiently.
- To characterize, if possible, the speed of convergence of the algorithm as a function of the problem size.
- Finally, to explore the applicability of the coupled-decomposition method to more general problem formulations. In particular, it would be interesting to explore how the method (or an extended version of it) could be implemented in non-structured or ad-hoc networks.

In Chapter 4 we consider the following extensions:

- To investigate simple strategies that allow to tune the priority values in the utility functions and thus achieving the desired degree of QoS at each connection.
- To test the proposed algorithm in more realistic scenarios. For example, a nice job would be to include the proposed algorithm in a DVB-RCS system simulator with more realistic traffic and request patterns.
- To focus the joint design of the request/allocation process. In other words, to integrate the request process with the allocation algorithm with the objective of attaining an efficient bandwidth utilization and sustaining the QoS constraints.
- To study the impact of mobility and channel variations to the proposed schemes and to modify them accordingly, maybe reformulating the NUM problem in order to be able to manage statistical information.

Last but not least, the research lines that continue the work in Chapter 5 are:

- To explore how useful can be other network topologies in the WiMAX context and to provide the most adequate decomposition strategies therein.
- And finally, since WiMAX has considered adaptive physical layers that allow to adapt the rate capacity of the links between nodes, there is a huge work in developing algorithms and protocols that jointly tune the physical layer parameters and allocate the service flows. Within those PHY layer parameters, one can consider power control, adaptive coding and modulation or subcarrier allocation among others.

Bibliography

[Ada02] D. Adami, R.G. Garroppo, and S. Giordano, "Resource Management and QoS Architectures in DAMA Satellite Access Networks", *IEEE International Conf. on Communications, Vol. 5, pp. 2978-2982*, May 2002.

[Alb05] G. Albertazzi, S. Cioni, G.E. Corazza, M. Neri, R. Pedone, P. Salmi, A. Vanelli-Coralli, and M. Villanti, "On the adaptive DVB-S2 physical layer: design and performance", *IEEE Wireless Communications, Vol. 12, No. 6, pp. 62 - 68*, Dec 2005.

[Ale08] S. P. Alex, and L. M. A. Jalloul, "Performance Evaluation of MIMO in IEEE802.16e/WiMAX", *IEEE Journal of Selected Topics in Signal Processing, Vol. 2, No. 2, pp. 181-190*, Apr 2008.

[Alo05] S. Alouf, E. Altman, J. Galtier, J.-F. Lalande, and C. Touati, "Quasi-Optimal Bandwidth Allocation for Multi-Spot MFTDMA Satellites", *Proceedings IEEE INFOCOM, Vol. 1, pp. 560-571*, Mar 2005.

[And73] L.G. Anderson, "A Simulation Study of Some Dynamic Channel Assignment Algorithms in a High Capacity Mobile Telecommunications System", *IEEE Transactions on Vehicular Technology , Vol. 22, No. 4, pp. 210-217*, Nov 1973.

[And07] J.G. Andrews, A. Ghosh, and R. Muhamed, *Fundamentals of WiMAX: Understanding Broadband Wireless Networking*, Prentice-Hall, 2007.

[AY07] T. Ali-Yahiya, A.-L. Beylot, and G. Pujolle, "Radio Resource Allocation in Mobile WiMax Networks using Service Flows", *Proceedings of the IEEE Int. Symposium on Personal, Indoor and Mobile Radio Communications (PIMRC), pp. 1-5*, Sep 2007.

[Aça99] G. Açar, and C. Rosenberg, "Algorithms to compute for Bandwidth on Demand Requests in a Satellite Access Unit", *Proceedings of 5th Ka Band Utilization Conference, Taormina, Italy*, Oct 1999.

[Aça02] G. Açar, and C. Rosenberg, "Weighted fair bandwidth-on-demand (WFBoD) for geostationary satellite networks with on-board processing", *Computer Networks, Vol. 39, No. 1, pp. 5-20*, May 2002.

[Ber87] D. Bertsekas, and R. Gallager, *Data Networks*, Prentice-Hall, 1987.

[Ber93] C. Berrou, A. Glavieux, and P. Thitimajshima, "Near Shannon limit error-correcting coding and decoding: Turbo-codes", *IEEE Int. Conf. on Comm. (ICC), Vol. 2, pp. 1064-1070*, May 1993.

[Ber99] D.P. Bertsekas, *Nonlinear Programming*, Belmont, MA, USA: Athena Scientific, 1999.

[Ber04] R.A. Berry, and E.M. Yeh, "Cross-layer Wireless Resource Allocation", *IEEE Signal Processing Magazine, pp. 59-68*, Sep 2004.

[Boy03] L. Boyd, and S. Vandenberghe, *Convex optimization*, Cambridge University Press, 2003.

[Cel03] N. Celandroni, F. Davoli, and E. Ferro, "Static and Dynamic Resource Allocation in a Multiservice Satellite Network with Fading", *Int. J. Satell. Commun. Network., Vol. 21, No. 4-5, pp. 469-487*, July-Oct 2003.

[Cel06] N. Celandroni, F. Davoli, E. Ferro, and A. Gotta, "Adaptive Cross-Layer Bandwidth Allocation in a Rain-Faded Satellite Environment", *International Journal of Communication Systems, Vol. 19, No. 5, pp. 509-530*, Jun 2006.

[Cer78] V.G. Cerf, and P.T. Kirstein, "Issues in Packet-Network Interconnection", *Proceedings of the IEEE, Vol. 66, No. 11, pp. 1386-1408*, Nov 1978.

[Chi04a] L. Chisci, R. Fantacci, F. Francioli, and T. Pecorella, "Dynamic bandwidth allocation via distributed predictive control in satellite networks", *First Int. Symp. on Control, Comm. and Signal Processing, pp. 373-376*, Mar 2004.

[Chi04b] L. Chisci, R. Fantacci, and T. Pecorella, "Predictive Bandwidth Control for GEO Satellite Networks", *IEEE International Conference on Communications, Vol. 7, pp. 3958-3962*, Jun 2004.

[Chi07] M. Chiang, S.H. Low, A.R. Calderbank, and J.C. Doyle, "Layering as Optimization Decomposition: A Mathematical Theory of Network Architectures", *Proceedings of the IEEE, Vol. 95, No. 1, pp. 255-312*, Jan 2007.

[Cov91] T.M. Cover, and J.A. Thomas, *Elements of Information Theory*, John Wiley & Sons, Inc., 1991.

[Dat99] B.N. Datta, *Applied and Computational Control, Signals and Circuits: Volume 1*, 1st edtion, Birkhäuser Boston, 1999.

[Den83] J.E. Dennis, and R.B. Schnabel, *Numerical methods for unconstrained optimization and nonlinear equations*, Prentice-Hall Series in Computational Mathematics, 1983.

[Du07] P. Du, W. Jia, L. Huang, and W. Lu, "Centralized Scheduling and Channel Assignment in Multi-Channel Single-Transceiver WiMax Mesh Network", *in proc. IEEE Wireless Comm. and Net. Conf (WCNC), Hong Kong (China)*, Mar 2007.

[Erw06] L. Erwu, S. Gang, Z. Wei, and J. Shan, "Bandwidth Allocation for 3-Sector Base Station in 802.16 Single-Hop Self-Backhaul Networks", *IEEE Vehicular Technology Conference, pp. 1-5*, Sep 2006.

[ETS97] ETSI, "Digital Video Broadcasting (DVB); Framing structure, channel coding and modulation for 11/12 GHz satellite services", *ETSI EN 300 421*, Aug 1997.

[ETS03a] ETSI, "Broadband Radio Access Networks (BRAN); HIPERMAN; Data Link Control (DLC) Layer.", *ETSI TS 102 178*, Mar 2003.

[ETS03b] ETSI, "Broadband Radio Access Networks (BRAN); HIPERMAN; Physical (PHY) Layer.", *ETSI TS 102 177*, Feb 2003.

[ETS03c] ETSI, "Digital Video Broadcasting (DVB); Interaction channel for Satellite Distribution Systems; Guidelines for the use of EN 301 790", *ETSI TR 101 790*, Jan 2003.

[ETS05a] ETSI, "Digital Video Broadcasting (DVB); Interaction Channel for Satellite Distribution Systems", *ETSI EN 301 790*, Apr 2005.

[ETS05b] ETSI, "Digital Video Broadcasting (DVB); Second generation framing structure, channel coding and modulation systems for Broadcasting, Interactive Services, News Gathering and other broadband satellite applications", *ETSI EN 302 307*, Mar 2005.

[ETS05c] ETSI, "Satellite Earth Stations and Systems (SES); Broadband Satellite Multimedia (BSM) Services and Architectures: QoS Functional Architecture", *ETSI TS 102 462*, Dec 2005.

[Fle80] R. Fletcher, *Practical Methods of Optimization*, Wiley, 1980.

[Ger05] A.B. Gershman, and N.D. Sidiropoulos, *Space-time Processing for MIMO Communications*, John Wiley & Sons, 2005.

[Gia06] G. Giambene, and S. Kota, "Cross-Layer Protocol Optimization for Satellite Communications Networks: A Survey", *International Journal of Satellite Communications and Networking, Vol. 24, No. 5, pp. 323-341*, Sep 2006.

[Gir00] A. Girard, C. Rosenberg, and M. Khemiri, "Fairness and Aggregation: A Primal Decomposition Study", *Networking 2000, Lecture Notes in Computer Science 1815, Springer-Verlag, pp. 667-678*, May 2000.

[Gol05] A. Goldsmith, *Wireless Communications*, Cmbridge University Press, 2005.

[Got06] F. Gotta, A. Portoti, and R. Sechhi, "Dynamic bandwidth allocation via distributed predictive control in satellite networks", *Proc. from the 2006 workshop on ns-2: the IP network simulator*, Oct 2006.

[Hac00] A. Hac, and Boon Ling Chew, "Demand Assignment Multiple Access Protocols for Wireless ATM Networks", *IEEE Vehicular Technology Conference-Fall VTC 2000, Vol. 1, pp. 237-241*, Sep 2000.

[Hay96] S. Haykin, *Adaptive Filter Theory*, 3rd edtion, Prentice-Hall, 1996.

[Hin07] R. Hincapie, J. Sierra, and R. Bustamante, "Remote Locations Coverage Analysis with Wireless Mesh Networks Based on IEEE 802.16 Standard", *IEEE Communications Magazine, Vol. 45, No. 1, pp. 120-127*, Jan 2007.

[Hol92] K. Holmberg, "Linear Mean Value Cross Decomposition: a Generalization of the Kornai-Liptak Method", *European Journal of Operational Research , Vol. 62, pp. 55-73*, Oct 1992.

[Hol97] K. Holmberg, "Mean Value Cross Decomposition Applied to Integer Programming Problems", *European Journal of Operational Research , Vol. 97, pp. 124-138*, Feb 1997.

[Hol06] K. Holmberg, and K.C. Kiwiel, "Mean Value Cross Decomposition for Nonlinear Convex Problems", *Optimization Methods and Software, Vol. 21, No. 3, pp. 401-417*, Jun 2006.

[Ibn04] M. Ibnkahla, Q.M. Rahman, A.I. Sulyman, H.A. Al-Asady, Jun Yuan, and Safwat, "High-Speed Satellite Mobile Communications: Technologies and Challenges", *Proceedings of the IEEE, Vol. 92, No. 2, pp. 312-339*, Feb 2004.

[IEE04] IEEE, "Air Interface for Fixed Broadband Wireless Access Systems", *IEEE Standards*, Oct 2004.

[IEE06] IEEE, "Air Interface for Fixed and Mobile Broadband Wireless Access Systems; Amendment 2: Physical and Medium Access Control Layers for Combined Fixed and Mobile Operation in Licensed Band and Corrigendum 1", *IEEE Standards*, Feb 2006.

[Iuo05] N. Iuoras, and L.-N. Tho, "Dynamic capacity allocation for quality-of-service support in IP-based satellite networks", *IEEE Wireless Communications, Vol. 12, No. 5, pp. 14-20*, Oct 2005.

[Jai84] R. Jain, D. Chiu, and W. Hawe, "A Quantitative Measure of Fairness and Discrimination for Resource Allocation in Shared Systems", *Tech. Rep. DEC TR-301, Digital Equipment Corp.*, Sep 1984.

[Joh06] B. Johansson, P. Soldati, and M. Johansson, "Mathematical Decomposition Techniques for Distributed Cross-Layer Optimization of Data Networks", *IEEE Journal on Selected Areas in Communications, Vol. 24, No. 8, pp. 1535-1547*, Aug 2006.

[Kel97] F. Kelly, "Charging and Rate Control for Elastic Traffic", *European Transaction on Telecommunications, Vol. 8, No. 1, pp. 33-37*, Jan 1997.

[Kel98] F.P. Kelly, A. Maulloo, and D. Tan, "Rate control for communication networks: shadow prices, proportional fairness and stability", *Journal of Operations Research Society, Vol. 49, No. 3, pp. 237-252*, Mar 1998.

[Kiv03] D. Kivanc, G. Li, and H. Liu, "Computationally Efficient Bandwidth Allocation and Power Control for OFDMA", *IEEE Transactions on Wireless Communications, Vol. 2, No. 6, pp. 1150-1158*, Nov 2003.

[Kifl06] C. Kiflling, "Efficient Resource Management strategies for MF-TDMA satellite reverse links with Fade Mitigation Techniques", *Advanced Satellite Mobile Systems (ASMS)*, May 2006.

[Kno95] R. Knopp, and P.A. Humblet, "Information Capacity and Power Control in Single-Cell Multiuser Communications", *IEEE International Conf. on Communications, Vol. 1, pp. 331-335*, Jun 1995.

[Kof02] I. Koffman, and V. Roman, "Broadband Wireless Access Solutions Based on OFDM Access in IEEE 802.16", *IEEE Communications Magazine, Vol. 40, No. 4, pp. 96-103*, Apr 2002.

[Kun03] S. Kunniyur, and R. Srikant, "End-to-End Congestion Control Schemes: Utility Functions, Random Losses and ECN Marks", *IEEE/ACM Transactions on Networking, Vol. 11, No. 5, pp. 689-702*, Oct 2003.

[La02] R.J. La, and V. Anantharam, "Utility-based Rate Control in the Internet for Elastic Traffic", *IEEE/ACM Trans. Networking, Vol. 9, No. 2, pp. 272-286*, Apr 2002.

[Las02] L.S. Lasdon, *Optimization Theory for Large Systems*, Dover Publications, 2002.

[Lee04] K.-D. Lee, and K.-N. Chang, "A real-time algorithm for timeslot assignment in multirate return channels of interactive satellite multimedia networks", *IEEE Journal on Sel. Areas in Comm., Vol. 22, No. 3, pp. 518-528*, Apr 2004.

[Lee06a] J.W. Lee, M. Chiang, and A.R. Calderbank, "Network Utility Maximization and Price-Based Distributed Algorithms for Rate-Reliability Tradeoff", *in Proc. IEEE Infocom, Barcelona, Spain*, Apr 2006.

[Lee06b] S. Lee, G. Narlikar, M. P·l, G. Wilfong, and L. Zhang, "Admission Control for Multihop Wireless Backhaul Networks with QoS Support", *in proc. IEEE Wireless Comm. and Net. Conf (WCNC), Las Vegas (USA)*, Apr 2006.

[Lin84] S. Lin, D. Costello, and M. Miller, "Automatic-Repeat-Request Error-Control Schemes", *IEEE Communications Magazine, Vol. 22, No. 12, pp. 5-17*, Dec 1984.

[LN01] T. Le-Ngoc, and T. Elshabrawy, "Broadband Satellite Access for Interactive Multimedia Services", *Space Commun.*, vol. 17, pp. 35–48, 2001.

[Low99] S.H. Low, and D.E. Lapsely, "Optimization Flow Control, I: Basic Algorithm and Convergence", *IEEE/ACM Trans. Networking, Vol. 7, No. 6, pp. 861-874*, Dec 1999.

[Low03] S.H. Low, "A Duality Model of TCP and Queue Management Algorithms", *IEEE/ACM Trans. Networking, Vol. 11, No. 4, pp. 525-536*, Aug 2003.

[Mak07] B. Makarevitch, "Adaptive Resource Allocation for WiMAX", *Proceedings of the IEEE Int. Symposium on Personal, Indoor and Mobile Radio Communications (PIMRC), pp. 1-6*, Sep 2007.

[Mar79] A.W. Marshall, and I. Olkin, *Inequalities: Theory of Majorization and Its Applications*, Academic Press, New York, 1979.

[Maz91] R. Mazumdar, L.G. Mason, and C. Douligeris, "Fairness in network optimal flow control: optimality of product forms", *IEEE Trans. on Comm., Vol. 39, No. 5, pp. 775-782*, May 1991.

[Mo00] J. Mo, and J. Walrand, "Fair End-to-end Window-based Congestion Control", *IEEE/ACM Trans. Networking, Vol. 8, No. 5, pp. 556-567*, Oct 2000.

[Mut99] A. Muthoo, *Bargaining Theory with Applications*, Cambridge University Press, 1999.

[Nea01] J. Neale, and A.K. Mohsen, "Impact of CF-DAMA on TCP via satellite performance", *Proc. of Global Telecommunications Conference, GLOBECOM'01, Vol. 4, pp. 2687-2691*, Nov 2001.

[Nes94] Y. Nesterov, and A. Nemirovsky, "Interior-point polynomial methods for convex programming", *Studies in Applied Mathematics, SIAM, Vol. 13*, 1994.

[Niy07] D. Niyato, and E. Hossain, "Integration of IEEE 802.11 WLANs with IEEE 802.16-Based Multihop Infrastructure Mesh/Relay Networks: A Game-Theoretic Approach to Radio Resource Management", *IEEE Network, Vol. 21, No. 3, pp. 6-14*, May 2007.

[Pal03] D.P. Palomar, *A Unified Framework for Communications through MIMO Channels*, Technical University of Catalonia (UPC), 2003.

[Pal05] D.P. Palomar, and J. Fonollosa, "Practical Algorithms for a Family of Waterfilling Solutions", *IEEE Trans. on Signal Processing, Vol. 53, No. 2, pp. 686-695*, Feb 2005.

[Pal06] D.P. Palomar, and M. Chiang, "A Tutorial on Decomposition Methods for Network Utility Maximization", *IEEE Journal on Selected Areas in Communications, Vol. 24, No. 8, pp. 1439-1451*, Aug 2006.

[Pal07] D.P. Palomar, and M. Chiang, "Alternative Decompositions for Distributed Maximization of Network Utility: Framework and Applications", *in IEEE Tran. on Automatic Control, Vol. 52, No. 12, pp. 2254-2269*, Dec 2007.

[Pau97] A.J. Paulraj, and C.B. Papadias, "Space-Time Processing for Wireless Communications", *IEEE Signal Processing Magazine, Vol. 14, No. 6, pp. 49-83*, Nov 1997.

[Pic82] R. Pickholtz, D. Schilling, and L. Milstein, "Theory of Spread-Spectrum Communications - A Tutorial", *IEEE Transactions on Communications, Vol. 30, No. 5, pp. 855-884*, May 1982.

[Pie05] A. Pietrabissa, T. Inzerilli, O. Alphand, P. Berthou, T. Gayraud, M. Mazzella, E. Fromentin, and F. Lucas, "Validation of a QoS Architecture for DVB-RCS Satellite Networks Via the SATIP6 Demonstration Platform", *Computer Networks, Vol. 49, No. 6, pp. 797-815*, Dec 2005.

[Pri04] F.D. Priscoli, and A. Pietrabissa, "Design of a bandwidth-on-demand (BoD) protocol for satellite networks modelled as time-delay systems", *Automatica, Vol. 40, No. 5, pp. 729-741*, May 2004.

[Rap79] S. Rappaport, "Demand Assigned Multiple Access Systems Using Collision Type Request Channels: Traffic Capacity Comparisons", *IEEE Transactions on Communications, Vol. 27, No. 9, pp. 1325-1331*, Sep 1979.

[Rek83] G.V. Reklaitis, A. Ravindran, and K.M. Ragsdell, *Engineering Optimization: Methods and Applications*, Wiley-Interscience, 1983.

[Rin04] M.A. Rinaldo, R. Vázquez-Castro, and A. Morello, "DVBS2 ACM modes for IP and MPEG unicast applications", *International Journal of Satellite Communications, Vol. 22(3), pp. 367-399*, May-Jun 2004.

[Ros06] L. Rosati, and G. Reali, "Jointly Optimal Routing and Resource Allocation in Hybrid Satellite/Terrestrial Networks", *International Workshop on Satellite and Space Communications, pp. 29-33*, Sep 2006.

[Sai97] H. Saito, "Dynamic Resource Allocation in ATM Networks", *IEEE Communications Magazine, Vol. 35, No. 5, pp. 146-153*, May 1997.

[Sha48] C.E. Shannon, "A Mathemathical Theory of Communication", *Bell Syst. Tech. Journal, Vol. 27*, Jul 1948.

[Sha03] S. Shakkotai, T.S. Rappaport, and P. Karlsson, "Cross-layer Design for Wireless Networks", *IEEE Comm. Mag., Vol. 41, No. 10*, Oct 2003.

[Ski05] H. Skinnemoen, A. Vermesan, A. Iuoras, G. Adams, and X. Lobao, "VoIP over DVB-RCS with QoS and bandwidth on demand", *IEEE Wireless Communications, Vol. 12, No. 5, pp. 46-53*, Oct 2005.

[Sol06] P. Soldati, B. Johansson, and M. Johansson, "Distributed Optimization of End-to-End Rates and Radio Resources in WiMax Single-Carrier Networks", *in proc. IEEE Global Telecomm. Conf. (GLOBECOM), San Francisco (USA)*, Nov 2006.

[Tao05] J. Tao, F. Liu, Z. Zeng, and Z. Lin, "Throughput Enhancement in WiMax Mesh Networks Using Concurrent Transmission", *Proceedings of the Int. Conference on Wireless Communications, Networking and Mobile Computing (WCNC), Vol. 2, pp. 871-874*, Sep 2005.

[Tia05] Y. Tian, K. Xu, and N. Ansari, "TCP in Wireless Environments: Problems and Solutions", *IEEE Communications Magazine, Vol. 43, No. 3, pp. S27-S32*, Mar 2005.

[VC05] M.A. Vázquez-Castro, M. Ruggiano, L.S. Ronga, and M. Werner, "Uplink Capacity Limits for DVB-RCS Systems with Dynamic Framing and Adaptive Coding", *Proc.* 23^{rd} *In. Com. Sat. Sys. Conf., Rome*, Sep 2005.

[VR83] T.J. Van Roy, "Cross Decomposition for Mixed Integer Programming", *Mathematical Programming , Vol. 25, No. 1, pp. 46-63*, Jan 1983.

[Wei05] H.Y Wei, S. Ganguly, R. Izmailov, and Z.J. Hass, "Interference-Aware IEEE 802.16 WiMax Mesh Networks", *in proc. IEEE Vehicular Tech. Conf (VTC'05 Spring), Stockholm (Sweden)*, May 2005.

[Won99] C.Y. Wong, R.S. Cheng, K.B. Letaief, and R.D. Murch, "Multiuser OFDM with Adaptive Subcarrier, Bit, and Power Allocation", *IEEE Journal on Selected Areas in Communications, Vol. 17, No. 10, pp. 1747-1758*, Oct 1999.

[Xia03] L. Xiao, X. Johansson, H. Hindi, S. Boyd, and A. Goldsmith, "Joint Optimization of Communication Rates and Linear Systems", *IEEE Trans. on Autom. Control, Vol. 48, No. 1, pp. 148-153*, Jan 2003.

[Xia04] L. Xiao, M. Johansson, and S. Boyd, "Simulatenous Routing and Resource Allocation via Dual Decomposition", *IEEE Trans. Comm., Vol. 52, No. 7, pp. 1136-1144*, Jul 2004.

[Xyl99] G. Xylomenos, and G.C. Polyzos, "Internet Protocol Performance over Networks with Wireless Links", *IEEE Network, Vol. 13, No. 4, pp. 55-63*, Jul 1999.

[Yaï00] H. Yaïche, R.R. Mazumdar, and C. Rosenberg, "A game theoretic framework for bandwidth allocation and pricing in broadband networks", *IEEE/ACM Trans. on Networking, Vol. 8, No. 5, pp. 667-678*, Oct 2000.

[Zan97] J. Zander, "Radio Resource Management in Future Wireless Networks: Requirements and Limitation", *IEEE Comm. Magazine*, Aug 1997.

[Zha06] J. Zhang, and D. Zheng, "A Stochastic Primal-Dual Algorithm for Joint Flow Control and MAC Design in Multi-hop Wireless Networks", *40th Annual Conference on Information Sciences and Systems, pp.339-344*, Mar 2006.

[Zim80] H. Zimmermann, "OSI Reference Model - The ISO Model of Architecture for Open Systems Interconnection", *IEEE Trans. on Communications, Vol. 28, No. 4, pp. 425-432*, Apr 1980.